

Investigation on Transformation of Carbon Black to Carbon Nanotube using Arc Discharge Method

THESIS

Submitted in the partial fulfillment
of the requirements for the degree of

DOCTOR OF PHILOSOPHY

by

NEHA ARORA
[2012PHXF423P]

Under the Supervision of

PROF. NITI NIPUN SHARMA
Department of Mechanical Engineering
School of Automobile, Mechanical & Mechatronics Engineering
Manipal University, Jaipur – 303 007

Co- Supervision

PROF. S. S. ISLAM
Solid state Electronics Research Laboratory
Jamia Millia Islamia (A Central University), New Delhi – 110 025



BITS Pilani
Pilani | Dubai | Goa | Hyderabad

BIRLA INSTITUTE OF TECHNOLOGY & SCIENCE
PILANI – 333 031 (RAJASTHAN) INDIA

2017



**BIRLA INSTITUTE OF TECHNOLOGY & SCIENCE
PILANI – 333 031 (RAJASTHAN) INDIA**

CERTIFICATE

This is to certify that the thesis entitled “**Investigation on Transformation of Carbon Black to Carbon Nanotube using Arc Discharge Method**” submitted by Neha Arora, ID.No. 2012PHXF423P for award of Ph.D. Degree of the institute embodies original work done by her under my supervision.

Signature in full of the Supervisor _____

Name : **Dr. NITI NIPUN SHARMA**

Designation : Professor, Dean FOE

Department of Mechanical Engineering

School of Automobile, Mechanical & Mechatronics Engineering

Manipal University, JAIPUR

Date : _____

Acknowledgement

This thesis would not have been possible without the support of many people. Many thanks to my supervisor, Prof. N N Sharma, for the guidance and support he has provided throughout the course of this research. His advices have been inspiring and motivating, and his words of encouragement have always been a strong support especially in difficult moments.

I am immensely thankful to Prof. Souvik Bhattacharyya, Vice-Chancellor, BITS-Pilani; Prof. Ashoke Kumar Sarkar, Director, BITS-Pilani, Pilani Campus. I express my gratitude to Prof. Sanjay Kumar Verma (Dean, Academic Research Division); Prof. Hemant Ramanlal Jadhav (Associate Dean, Academic Research Division) BITS-Pilani, Pilani Campus for their constant and official support and encouragement.

My sincere thanks to Prof. P Srinivasan (Head of the Department, Mechanical Engineering) for his support during completion of the research work. I am grateful to the entire faculty and staff of Mechanical Engineering Department for their kind support and assistance.

I thanks Prof. Mani Sankar Dasgupta (Chief, Central Placement Unit); Prof. B K Rout (Associate Dean, Academic Registration & Counseling Division); Doctoral Research Committee (DRC); Prof. Anshuman Dalvi and Dr. Sharad Shrivastava my Doctoral Advisory Committee (DAC) members; Dr. Jitendra Singh Rathore and Dr. Sachin Ulhas Belgamwar; who gave their precious time to provide suggestions that immensely helped in improving the quality of my PhD thesis.

I would also like to express my gratitude to all the technical staff, especially to Sh. Yadav and Sh. Ashok for providing me the electrical equipment and support and special thanks to Sh. Vinod for providing help in drilling of electrodes.

I would also like to thanks Dr. Kanupriya Sachdev, MNIT, Jaipur, Prof. S.S Islam, Jamia Millia Islamia, New Delhi, Prof. Sushil Mishra, IIT Bombay and Prof. Manish Hooda, SCL, Chandigarh for providing me the FESEM and TEM facility for analysis of collected samples.

My endless thanks to my friends Ms. Paridhi Puri, Ms. Shivani Nain, Ms. Tamalika, Ms. Ritika Sharma, Ms. Vidushi Asati, Ms. Zaiba Khan, Ms. Chetna Sangwan, Mr. Rahul Singh Kotesa, Mr. Chaitanya K.N.K., Mr. Bhawani Shankar, Mr. Madhu Seetharaman and Dr. Vijay Kumar and my aunty Mrs. Neelam Bhatia who endured this long process with me, always offering support and care. I would like to thanks Mr. Santosh Kumar Saini (Academic Registration & Counseling Division) for his help in assembling of my thesis.

Finally, I would like to thanks my lovable family, my niece Tiya Arora and my in-laws specially my father in-law for their everlasting support and care through my life. In particular I must acknowledge my husband Tarun a deepest gratitude for his understanding, endless patience and encouragement for completion of my thesis.

Neha Arora

Over the last two decades, Researchers have proposed different routes to synthesize high quality carbon nanotubes. The most popular and widely used synthesis techniques are Arc discharge, Chemical vapor deposition and Laser ablation. Among various synthesis routes, arc discharge is regarded as the best technique to produce high quality carbon nanotubes. Though this technique has been in used for the long time but the effect of several parameters like arc current, applied voltage, arc temperature and type of carbon precursors has not been much explored. Researchers have mainly used graphite as carbon precursor. The aim of this research was to investigate the effect of carbon black on synthesis of CNT. Carbon black is an amorphous form of carbon which has a high surface-area-to volume ratio and easily available material on earth. To achieve the objective of proposed research, the thesis is divided into six chapters. Some of the salient features of these chapters are as follows:

Chapter 1 Introduces carbon, its allotrope and methods to synthesize carbon nanotube. Various precursors used in synthesis of CNTs as reported in published scientific literature are briefed. The motivation of this research is also discussed at the end of the chapter.

In Chapter 2, we have discussed about the literature available for synthesis of CNTs using arc discharge method and we observe that Literature lacks correlation between growth conditions and synthesized product. We have discussed growth mechanism of carbon nanotubes in arc discharge. The effects of several arc parameters such as power supply, environment, pressure, electrode geometry, catalyst and temperature and their corresponding physics has been detailed. We have reviewed and presented various carbon precursors used in synthesis of CNTs using arc discharge. At the end we have identified the gaps in research and defined the scope of the present work.

In Chapter 3, we have discussed the various design of arc chamber available in literature. We have designed the arc discharge chamber by considering mechanical design and electrical circuit design of the custom built arc chamber.

In Chapter 4, we have briefly discussed about carbon black, its basic chemistry, morphology and surface activity. We have introduced about different grades of carbon black used in literature. In addition, we have investigated the amenability of different grades of furnace carbon black in conversion to CNTs using DC arc discharge method.

In Chapter 5, using designed arc discharge set up, we have synthesized MWCNTs at an arc current ranging from 25 to 40 A using DC arc discharge setup. Field emission Scanning electron microscopy, transmission electron microscopy and TGA were carried out for ensuring the formation of MWCNTs. Temperature profiles of the arc were recorded and observed micrographs and corresponding arc temperature profiles it became evident that a critical temperature range of 1400-1600°C is necessary for synthesis of MWCNTs using arc discharge. If the temperature is outside the range of 1400-1600°C, then very few or no CNTs are observed. We did TGA analysis to measure the thermal stability in the synthesized CNT samples and observed that the thermal stability of as synthesized MWCNTs is much higher as compared to typical MWCNTs stability reported in literature.

Moreover, the role of applying pulse arc in comparison to application of DC arc discharge needs another investigation. We have also investigated the effect of arc current variation from 22 A to 40 A with the step of 4 A with respect to time using pulse arc discharge method. It was observed that the nanoparticle merged into multilayer sheet with scattered flower type structure distributed on top layer and converted into tube like structure of different diameter at 40 A for 60 sec.

In Chapter 6, we present the overall conclusions and future scope of the present study.

CONTENTS	Page No.
<i>Acknowledgement</i>	i-ii
<i>Abstract</i>	iii-iv
<i>Table of Contents</i>	v-vii
<i>List of Tables</i>	viii
<i>List of Figures</i>	ix-xi
Chapter 1 Introduction	1-14
1.1 Allotropes of Carbon	1
1.2 Methods to Synthesize CNTs	4
1.3 Precursors for CNTs Synthesis	7
1.4 Motivation	9
1.5 Summary	10
<i>References</i>	11
Chapter 2 Literature Review	15-72
2.1 Introduction	15
2.2 Nanotube Growth in Arc Discharge	17
2.2.1 Arc Discharge Setup	17
2.2.2 Growth Mechanism of Carbon Nanotubes in Arc Discharge	18
2.2.2.1 Vapor phase growth	20
2.2.2.2 Liquid phase growth	21
2.2.2.3 Solid phase growth	21
2.3 Arc discharge Parameters	22
2.3.1 Effect of Power Supply	22
2.3.1.1 Type of power supply	22
2.3.1.2 Effect of voltage	33
2.3.1.3 Effect of arc current	34
2.3.1.4 Frequency	36
2.3.1.5 Effect of grain size	36
2.3.1.6 Role of catalyst	37

CONTENTS	Page No.
2.3.1.7 <i>Role of atmosphere</i>	40
2.3.1.8 <i>Effect of pressure</i>	43
2.3.1.9 <i>Role of temperature</i>	44
2.3.1.10 <i>Effect of setup modification</i>	45
2.3.1.11 <i>Effect of cathode shape</i>	46
2.3.1.12 <i>Size and yield of CNT in arc discharge</i>	47
2.4 Carbon Precursors in Arc Discharge	48
2.5 Summary	52
<i>References</i>	54
Chapter 3 Design of Experimental Set Up	73-94
3.1 Introduction	73
3.2 Arc Discharge Setup Design	73
3.2.1 Mechanical Design	76
3.2.2 Design of Electrical Circuit	85
3.2.2.1 <i>DC power supply</i>	86
3.2.2.2 <i>Pulsed power supply</i>	87
3.3 Conclusion	91
<i>References</i>	92
Chapter 4 Experiments with Different Grades of Carbon Black	95-112
4.1 Introduction	95
4.2 Morphology of Carbon Black	97
4.3 Experiment with Different Carbon Black Grades	102
4.3.1 Experimental Setup	102
4.4 Conclusion	109
<i>References</i>	111

CONTENTS		Page No.
Chapter 5	Role of Parameters in Synthesis of CNTs from Carbon Black	113-140
5.1	Introduction	113
5.2	Role of Arc Current	114
5.2.1	Characterization	115
5.3	Role of Temperature	125
5.3.1	Characterization	125
5.4	Role of Pulse Arc Discharge	134
5.5	Conclusion	137
	<i>References</i>	139
Chapter 6	Overall Conclusion and Future Scope	141-143
6.1	Overall Conclusion	141
6.2	Future Scope of the Work	142
	<i>Appendices (A1,A2,A3,A4)</i>	A1-A24
	<i>List of Publications</i>	B1
	<i>Brief biography of the Candidate</i>	B2
	<i>Brief biography of the Supervisor</i>	B3
	<i>Brief biography of the Co-Supervisor</i>	B4

List of Tables

Table No.	Title	Page No.
2.1	Arc discharge synthesis of CNT using DC power supply	25
2.2	Arc discharge synthesis of CNT using AC power supply	32
2.3	Arc discharge synthesis of CNT using pulsed DC power supply	33
2.4	Effect of catalyst on CNT formation	39
2.5	Effect of different environment on CNT formation	42
2.6	Effect of different growth parameters on size and yield of CNT	47
4.1	First digit assignment by ASTM in carbon black nomenclature system	98
4.2	Details of various grades of carbon black	100
5.1	Quantitative analysis of deposited sample from carbon black	115

List of Figures

Figure No.	Title	Page No.
1.1	Allotropes of carbon	2
1.2	Method used for synthesis of CNTs	4
2.1	Bar graph showing papers published on arc discharge synthesis of CNT	15
2.2	Schematic of an arc discharge setup	17
2.3	Schematic showing the formation of CNTs using different power supplies	23
2.4	Pie chart showing percentage of papers published on arc discharge synthesis of CNT	24
2.5	Variation in current values used in literature to synthesize CNTs using arc discharge	35
2.6	Role of catalyst in growth of CNTs	37
2.7	Pie chart showing percentage of papers on synthesis of CNT using arc discharge method under different atmosphere	41
2.8	Bar graph showing number of papers published at different range of pressure	44
2.9	Pie chart showing percentage of papers using various carbon precursors for nanotube formation	49
3.1	Schematic diagram of set up modification of electrodes (a) Six electrodes are mounted on a wheel at an equal distance; (b) Rotating cathode; (c) Plasma rotating electrode; (d) Cathode inclined at an angle 30° with anode	75
3.2	Two electrodes mounted horizontally	76
3.3	Shows holding screw giving proper gripping to the electrodes	76
3.4	Copper pipe attached to the electrodes	77
3.5	Bellow flange assembly	77
3.6	Teflon guide and Teflon push fit part	78
3.7	Nut, washer and support Patti part	78
3.8	Three studs, motor mounting plate, bearing plate and Nema 23 stepper motor	79
3.9	Coupler and linear bearing part	79
3.10	Push fit 1-8 inch part	80

Figure No.	Title	Page No.
3.11	CF-35 part	80
3.12	Feed through and feed through nut part	81
3.13	Support Patti, washer and nut part to cathode side	81
3.14	Delrin and push fit part	81
3.15	Chamber pipe	82
3.16	Window cover with door glass	82
3.17	Thermal imaging camera i.e. fitted to arc discharge set up	83
3.18	Water cooled jacket	84
3.19	ISO-Flange and two 1-4 base coupling part	84
3.20	Leg assembly	85
3.21	Flow chart diagram of DC power supply	86
3.22	DC arc discharge setup	87
3.23	Schematic diagram of the pulsed power supply	89
3.24	Shows gate driver IC2113 and optocoupler 6N137	90
4.1	Shows primary particle, aggregate and agglomerate	97
4.2	Furnace and thermal black particle size comparison	98
4.3	Schematic of carbon black surface adsorption sites	101
4.4(a)	Schematic of an arc discharge setup	103
4.4(b)	Front view of setup consist of arc discharge chamber with automatic controller	104
4.4(c)	Back view has thermal imaging camera i.e. fitted to arc discharge set up	104
4.5	Sample preparation	105
4.6	Shows granular structure of carbon black FESEM and TEM image	106
4.7	Shows the FESEM images on the left side of sample A [Tread *A (non-ASTM)] at 40 A for 60 sec and TEM image on the right side	106
4.8	Shows the FESEM images on the left side of sample B (N134) at 40 A for 60 sec and TEM image on the right side	107
4.9	Shows the SEM images on the left side of sample C (N121) at 40 A for 60 sec and TEM image on the right side	107
4.10	Shows the FESEM images on the left side of sample D (N660) at 40 A for 60 sec and TEM image on the right side	108
4.11	Shows the FESEM images on the left side of sample E (N330) at 40 A for 60 sec and TEM image on the right side	108

Figure No.	Title	Page No.
5.1	FESEM Micrographs showing MWCNTs formed at different arc current levels and their corresponding temperature profiles.	119
5.2	Shows the FESEM Micrographs and their arc temperature (a) at 35A which results in poor formation of CNTs due to Unstable arc temperature (b) Shows formation of Carbon Nano rods at 40 A	121
5.3	Thermo gravimetric analysis of as synthesized MWCNTs	124
5.4	Effect of arc temperature on arc discharge products for a constant arc current of 40 A.	131
5.5	TEM Micrographs of (a) As synthesized MWCNTs at 1800°C (b) Typical MWCNTs formed at 40 A with Temperature of 1400-1600°C	132
5.6	FESEM image of (a) At arc current of 22 A for 60 sec (b) At 26 A (c) At 28A (d) At 30 A (e) At 32 A (f) At 35 A (g) At 37 A (h) CNTs at 40 A	135
5.7	FESEM Images of various samples of experiment conducted under different conditions(1) For fixed arc current(40 A) & variable time durations(30s,60s) (a) Carbon black (b) Sample after 30s (c) Sample after 60s (2) For different arc current & fixed time durations(30s): (d) Sample when arc current is 30 A (e) Sample when arc current is 40 A. (3)For different arc current & fixed time duration (60s): Sample when arc current is 20 A (g) Sample when arc current is 30 A (h) Sample when arc current is 40 A. (i) CNT of diameter 58.56 nm	137

CHAPTER 1

Introduction

Carbon is all pervading and is an essential element for all known form of life on earth. Not only live but a bulk of non-living material attributes their existence and properties to carbon so much so that a separate study is established for carbon and its different compound and allotropes. The name 'carbon' comes from the Latin word carbo which means coal or charcoal. The importance of carbon is obvious from the fact that most basic transducer of energy quintessential for survival of life in any form i.e. plants have carbon as the most important element. Without carbon the plant would not exist and plants being originating component of food chain, its non-existence means every animal on earth will face challenge of survival.

Carbon has various formations useful for industrial applications for example when carbon combines with another element it appears with extraordinary different properties like carbonates (CaCO_3) which appears in the form of limestone, marble and chalk; in combination with hydrogen it forms hydrocarbon which is present in deposits of fossils fuels i.e. natural gas, petroleum and coal; in environment carbon is present in the form of carbon dioxide taken in by plants which undergo the process of photosynthesis and also used in fire extinguisher.

The allotropes of carbon are equally an interesting subject matter of investigation. In non- living matter, carbon exists as compounds and different allotropic forms. The later spans the range from hardest material like diamond to most amorphous material like Carbon black (CB). In next section allotropes of carbon are detailed which is relevant to understanding the background of investigation in this thesis.

1.1 Allotropes of Carbon

Elemental carbon exists in several forms, each of which has its own physical and chemical characteristics known as allotropes of carbon. Few allotropes of carbon which are important in context to usage in day to day life are shown in Figure 1.1.



Figure 1.1: Allotropes of carbon (a) Diamond [1] (b) Graphite [2] (c) Fullerenes [3] (d) CNTs [4] (e) Coke [5] (f) Charcoal [6] (g) Carbon Black [7]

Carbon exists in two allotropic forms crystalline and amorphous. Amorphous carbon is the name of carbon that does not have any crystalline structure. On macroscopic scale, amorphous carbon has no definite structure but on Nano microscopic scale we can see it is made up of regularly arranged carbon atoms. Coal is formed in nature by carbonization of wood i.e. conversion of wood to coal under the influence of high temperature, high

pressure but in the absence of air. Wood Charcoal is a black, porous and brittle solid formed when wood is heated strongly in a very limited supply of air. Carbon black is formed when a natural gas is burnt in limited supply of air.

Crystalline form of carbon include graphite, diamond, fullerenes and CNTs .Graphite is one of the softest substances, used in many industrial applications in the form of coke, in the production of steel and as writing material in the form of lead for pencils. Graphite is an electrical conductor due to delocalization of pi bond electrons above and below the planes of carbon atoms. These electrons are free to move and so are able to conduct electricity.

Diamond is another allotrope of carbon, whose hardness and high dispersion of light make it useful for industrial applications and jewelry. Apart from this, diamonds are also used as a cutting tool because of its hardness.

Fullerene is a molecule of carbon that exists in the form of hollow sphere and tubes. Spherical fullerene known as buckminsterfullerene's resemble to the soccer ball and cylindrical fullerenes are called carbon nanotubes. It is similar to that of graphite, which is composed of stacked graphene sheets of hexagonal rings that are linked together but fullerene may also contain the pentagonal rings.

Carbon nanotubes (CNTs) are one of the strongest materials in nature. CNTs are long hollow cylinders of graphene. The discovery of carbon nanotubes (CNT) by Iijima in 1991 [8] opened the new era in material science that have incredible number of potential uses in the field of electronic, mechanical, thermal, optical etc. The structure of carbon nanotube is formed by rolling the single sheet of graphite i.e. graphene. CNTs typically have a diameter ranging from lesser than 1nm to around 50nm. Nanotubes can have a single outer wall of carbon or they can be made of multiple walls (cylinders inside other cylinders of carbon).

CNTs are gaining importance because of its extraordinary properties which can revolutionize the material applications in human support. All out efforts by scientists are perused to synthesize CNTs from various precursors and by various methods. In next section, we briefly present different methods to synthesize CNTs that have been reported in published scientific literature.

1.2 Methods to Synthesize CNTs

Carbon nanotubes were first discovered by Iijima [8] in 1991. The synthesis of carbon nanotubes has attracted researchers for over 20 years, who have proposed and observed insightful studies that have led to better understanding of the growth mechanism of carbon nanotubes. Over these two decades, researchers have used different routes to synthesize CNTs most used of which are Arc discharge, Chemical Vapor Deposition, Laser Ablation, Hydro-thermal synthesis, Electrolysis, Ball milling, Flame synthesis and are shown as schematic in Figure 1.2.

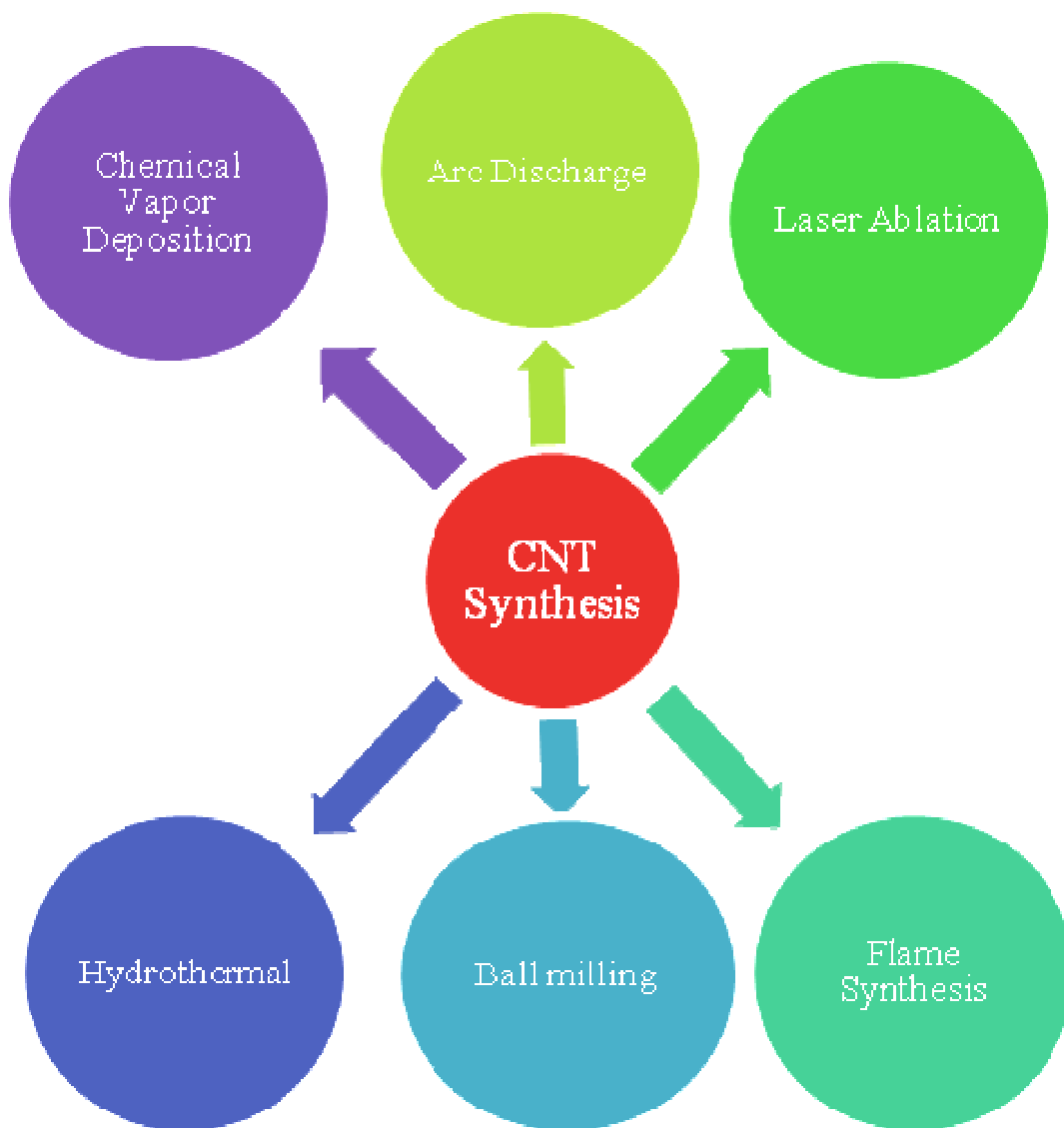


Figure 1.2: Methods used for synthesis of CNTs

An arc discharge synthesis of carbon nanotubes consists of graphite electrodes containing a carbon precursor, which are sublimed in an inert atmosphere using an electric current. The carbon arc provides a convenient and traditional tool for generating the high temperatures needed to vaporize carbon atoms into plasma. Some of the phenomenal work in arc discharge synthesis includes Ebbesen and Ajayan [9] who reported large scale synthesis of CNTs in helium atmosphere in 1992. In 1995, Wang et al. [10] produced Multiwalled carbon nanotubes(MWCNTs) in hydrogen atmosphere using arc discharge. In 1997, Journet et al. [11] demonstrated large scale synthesis of Singlewalled carbon nanotubes(SWCNTs) in Helium atmosphere. Shi et al. [12] in 1999 demonstrated bulk synthesis of SWCNTs in high pressure helium atmosphere. The arc discharge process is dependent on several parameters like power supply, chamber pressure, electrode geometry, catalyst etc. that influence the nature of the CNT produced.

Another efficient route for the synthesis of bundles of SWCNTs is the laser ablation technique. In this method, a piece of graphite target is vaporized by laser irradiation under high temperature in an inert atmosphere. The quality and yield of these products have been found to depend on the reaction temperature. The best quality is obtained at reaction temperature of 1200°C [13]. The pulsed laser-ablation process for the production of SWCNTs was developed in 1995 by Guo et al. [14] at Rice University. A laser beam (532 nm), was focused onto a metal-graphite composite target which was placed in a high-temperature (1200°C) furnace. The laser beam ablates the graphite target and the soot produced is swept by the flowing argon gas and deposited onto a water-cooled copper collector positioned downstream just outside the furnace. In 1996, Thess et al. [15] successfully developed a laser ablation method for the mass production of SWCNTs. In 1997 Rao et al. [16] used double beam laser to improve the laser ablation process. Nanotubes produced by laser ablation have higher purity and their structure is better graphitized. However, the laser ablation technique favors the growth of SWCNTs. The disadvantage of this method is the high power input and less CNTs deposition.

Selective production of nanotubes with predefined properties can be achieved by chemical vapor deposition (CVD) [17][18] which is the most economic process for large scale CNTs production [18]. In this process, catalytic decomposition of hydrocarbon or

carbon monoxide feedstock occurs with the aid of supported transition metal catalyst in a flow furnace at atmospheric pressure. It was first devised in 1993 by Yacamàn et al. [19] who synthesized carbon nanotubes by catalytic decomposition of acetylene over iron particles at 700°C. The choice of catalyst is one of the most important parameters affecting the CNTs growth in this process. As compared to arc-discharge and laser-ablation methods, CVD is a simple and economic technique for synthesizing CNTs at low temperature and ambient pressure. In yield and purity, CVD beats the arc discharge and laser ablation methods but it is not suitable for synthesis of CNTs from powdered carbon precursors like graphite and carbon black.

Apart from above mentioned widely used synthesis methods, several other methods have been proposed by researchers. However, they have not been extensively used owing to their drawbacks and limitations. In 2002, Gogotsi et al [20] devised a hydrothermal technique for synthesis of CNTs. They synthesized Multiwall open-end and closed carbon nanotubes with the wall thickness from several to more than 100 carbon layers using polyethylene/water mixtures in the presence of nickel at 700–800°C under 60-100 MPa pressure. Manafi et al [21] in 2008 used hydrothermal techniques to prepare large quantity of carbon nanotubes using NaOH, aqueous solution of dichloromethane, CCl₂ and metallic Lithium at 150-160°C for 24 h. This process has many advantages in comparison with other methods such as easy availability of raw materials and it is a low temperature process (about 150-180°C). This method is environmentally benign and inexpensive.

Electrolysis is a less common method for CNT production which was developed by Hsu et al. in 1995 [22]. In this process electro spinning of alkali (Li, K, Na) or alkaline-earth (Mg, Ca) metals from their chloride salts on a graphite cathode is followed by the formation of carbon nanotubes by the interaction of the metal being deposited with the cathode. After the electrolysis the carbonaceous material is extracted by dissolving the ionic salt in distilled water. The cathode erodes during the electrolysis and the electrolytic products are a mixture of CNTs and a large proportion of carbon nanoparticles of different structures. The nanotubes produced are usually multi-walled; however, Bai et al. have grown SWCNTs [23] using electrolysis. They prepared nanotubes by electrolytic conversion of graphite to carbon nanotubes in fused NaCl at 810°C using Argon as inert gas.

CNT synthesis through concentrated solar light was proposed by Laplaze et al. [24] in 1998. The advantage of the solar method is the use of light as in laser ablation to induce the vaporization of the target and the possibility to control each synthesis parameter independently. The carbon and catalyst mixture was vaporized at the front impinged by the incident concentrated solar energy. In 2005, Luxembourg [25] demonstrated the production of SWCNTs in few gram of quantity by solar process using a 50 kW solar reactor.

Ball milling and subsequent annealing is another simple method for the production of CNTs. The method consists of placing graphite powder into a stainless steel container along with four hardened steel balls. The container is purged, and argon is introduced. The milling is carried out at room temperature for up to 150 hours. Following milling, the powder is annealed under an inert gas flow at temperatures of 1400°C for six hours. In 2001, Pierard et al. [26] produced short MWCNTs with open tips using mechanical ball milling. In 2003, Liu et al. [27] prepared short MWCNTs by ball milling and studied their hydrogen absorption behavior.

Among all the techniques reported above, arc discharge still remains the best method to synthesize high quality carbon nanotubes. Though the arc discharge method is discontinuous and cannot produce the large quantity of CNTs in general as compared to CVD, however, few scientists report [2-5] synthesizing CNTs in bulk using arc discharge. The yield of CNTs depends on the stability of the plasma formed between the electrodes, the current density, inert gas pressure and cooling of electrodes and chamber.

Apart from methods available to synthesize CNTs, researchers have used variety of precursors in synthesis of CNT. Various precursors used in synthesis of CNTs as reported in published literature are briefed in next section.

1.3 Precursors for CNTs Synthesis

In general till date, the synthesis of CNTs is carried out by sublimation of a carbon precursor using an external power source; in case of arc discharge, the high temperature of plasma is obtained by applying current ablates the carbon precursor to form carbon vapors, which further nucleates to form a nanotube. Most of the arc discharge synthesis of CNTs has been carried out using graphite as precursor. Some

researchers have used coal as a starting material to synthesize CNTs. Coal is a mixture of aromatic and aliphatic hydrocarbon molecules, which are highly reactive in nature. In 2007 Qiu et al. [28] discussed coal as an ideal starting material for large synthesis of Double walled Carbon nanotubes(DWCNTs). When high arc current passes through coal, the weak linkages between the polymeric aryl structures get broken down into alkyne and aromatic species that further form DWCNTs. Coal contains sulphur, which favors the growth of DWCNTs and affects the diameter distribution of the nanotubes produced.

Other carbon sources like poly-vinyl-alcohol is additional carbon source to synthesize carbon nanotubes using arc discharge method [29]. In 2005 tire powder was injected into an electric arc for growing multiwall carbon nanotubes [30]; further in 2005 DWCNTs were synthesized in a large scale by hydrogen arc discharge method using MWCNT/carbon nanofibers [31]. In 2005, mixture of ferrocene-nicklocene was used as catalyst and xylene as carbon source for growth of carbon nanotube. In 2007, toluene as hydrocarbon solvent was utilized for the formation of CNTs [32], in 2010 fullerene waste soot was used as raw material to fabricate DWCNTs by arc discharge in a mixture of Ar and H₂ [33] , in 2011 thermal decomposition of benzene using ac arc discharge plasma process [34] have been utilized to produce carbon nanostructures.

Some groups have used CB as a raw material to produce CNTs. In 2002, Doherty et al. [35] reported the synthesis of high crystalline quality MWCNTs from carbon black without catalyst. In 2006, Chen et al. [36] have utilized the CB as a dot carbon source in formation of DWCNTs and discussed that the structure of carbon black plays a significant role in influencing purity, bundle formation and purifications of DWCNTs. In 2006, Doherty et al. [37] suggested the growth of carbon nanotubes from carbon black in high temperature arc furnace with an externally applied magnetic field. In 2008, Donnet et al.[38] discussed the growth of MWCNTs on carbon black by combustion flame method. Nanotube formation takes place in three stages, in first stage transformation of carbon black to graphitic seeds; in second stage generation of tubes from graphitic seeds due to high condensation of ad atoms. Finally, the continuous growth of these tubes by adsorption of carbon atoms onto nanotubes. In 2009, Labeledz et al. [39] observed the influence of various carbon

powders on synthesis of SWCNTs in carbon arc plasma. In 2011, Nishizaka et al. [40] synthesized SWCNT-containing soot using arc discharge with a poorly graphitized carbon rod (PGC rod), and investigated the production of graphite contained in the soot. A PGC rod was produced using a mixture of coal tar and carbon black and was heat treated to 1000°C. In 2012, Doherty et al. [41] discussed the solid state transformation of carbon black to MWCNTs from high temperature arc furnace without a catalyst.

In published literature, the CB to CNT conversion still remains less investigated. Keeping this in view we have used carbon black as a precursor to synthesize Carbon nanotubes in our investigations in the thesis. CB is amorphous in nature, easily available material on earth and can be a potential precursor to synthesize CNT due to techno-economic reasons. Currently in industries, carbon black is used as the black pigment in printing ink, water colors, and carbon paper. CB is also used as filler in rubber products such as tires and in plastic compounds.

1.4 Motivation

Carbon nanotubes are long tubular chain of carbon molecule. CNTs are allotropes of Carbon with cylindrical nanostructures that possess properties which find advantageous usage in field such as electronics, mechanical, electrical, chemical and thermal applications. Over the last two decades researchers have mainly used graphite as carbon precursor in formation of carbon nanotubes using arc discharge method. The primary motivation behind this research was to investigate on an alternate precursor which is more potential candidate for conversion to CNTs because of techno-economic reasons and since CB is comparatively less perused, the investigation on transformation of CB to CNT additionally forms interesting premises of research and investigations. CB is a low cost and easily available material. Using CB as precursor in arc discharge method, various experiments were performed at low arc current level with different grades of carbon black using DC and Pulsed arc discharge method. In order to investigate and conclude on transformation of CB to CNT using arc discharge method, a comprehensive literature review to assess state of art and gaps thereof is pertinent as first step.

1.5 Summary

In this present chapter we introduces about carbon, its allotrope and methods to synthesize carbon nanotube. Various precursors used in synthesis of CNTs as reported in published scientific literature are briefed. The motivation of this research is also discussed at the end of the chapter.

The available literature on CB from CNTs is presented chronologically in next chapter.

References:

- [1] “Diamond Structure.” Available: <https://www.uwgb.edu/dutchs/Petrology/Diamond%20Structure>.
- [2] “Graphite Structure.” Available: http://www.bbc.co.uk/schools/gcsebitesize/science/add_ocr_gateway/chemical_economics/nanochemistryrev2.
- [3] “Fullerene Structure.” Available: <http://www.niharsworld.com/2010/09/04/what-is-buckyball-buckyball-wikipedia-buckyball-uses-buckyball-structure-buckyball-google-doodle-25th-anniversary-and-history-of-fullerene>.
- [4] “CNTs.” Available: <http://www.nanoscience.com/applications/education/overview/cnt-technology-overview/>
- [5] “Coke Carbon.” Available: <https://in.pinterest.com/explore/petroleum-coke/>
- [6] “Charcoal Carbon.” Available: <http://www.acarbons.com/>
- [7] “Carbon Black.” Available: <https://www.2b1stconsulting.com/samsung-tops-the-carbon-black-unit-in-ruwais-refinery/>
- [8] S. Iijima, “Helical microtubules of graphitic carbon,” *Nature.*, vol. 354, no. 6348, pp. 56–58, Nov. 1991.
- [9] T. W. Ebbesen and P. M. Ajayan, “Large-scale synthesis of carbon nanotubes,” *Nature.*, vol. 358, no. 6383, pp. 220–222, Jul. 1992.
- [10] X. K. Wang, X. W. Lin, V. P. Dravid, J. B. Ketterson, and R. P. H. Chang, “Carbon nanotubes synthesized in a hydrogen arc discharge,” *Appl. Phys. Lett.*, vol. 66, no. 18, pp. 2430–2432, Mar. 1995.
- [11] C. Journet, W. K. Maser, P. Bernier, a Loiseau, M. L. delaChapelle, S. Lefrant, P. Deniard, R. Lee, and J. E. Fischer, “Large-scale production of single-walled carbon nanotubes by the electric-arc technique,” *Nature.*, vol. 388, no. 6644, pp. 756–758, Aug. 1997.
- [12] Z. Shi, Y. Lian, X. Zhou, Z. Gu, Y. Zhang, S. Iijima, L. Zhou, K. T. Yue, and S. Zhang, “Mass-production of single-wall carbon nanotubes by arc discharge method,” *Carbon.*, vol. 37, no. 9, pp. 1449–1453, Jan. 1999.
- [13] N. M. Mubarak, E. C. Abdullah, N. S. Jayakumar, and J. N. Sahu, “An overview on

- methods for the production of carbon nanotubes,” *J. Ind. Eng. Chem.*, vol. 20, no. 4, pp. 1186–1197, Jul. 2014.
- [14] T. Guo, P. Nikolaev, A. G. Rinzler, D. Tomanek, D. T. Colbert, and R. E. Smalley, “Self-Assembly of Tubular Fullerenes,” *J. Phys. Chem.*, vol. 99, no. 27, pp. 10694–10697, Jul. 1995.
- [15] A. Thess, R. Lee, P. Nikolaev, H. Dai, P. Petit, J. Robert, C. Xu, Y. H. Lee, S. G. Kim, A. G. Rinzler, D. T. Colbert, G. E. Scuseria, D. Tomanek, J. E. Fischer, and R. E. Smalley, “Crystalline Ropes of Metallic Carbon Nanotubes,” *Science.*, vol. 273, no. 5274, pp. 483–487, Jul. 1996.
- [16] M. S. Rao, A.M.; Richter, E.; Bandow, S.; Chase, B.; Eklund, P.C.; Williams, K.A.; Fang, S.; Subbaswamy, K.R.; Menon, M.; Thess, A.; Smalley, R.E.; Dresselhaus, G.; Dresselhaus, “Diameter-selective Raman scattering from vibrational modes in carbon nanotubes,” *Science.*, vol. 275, no. 5297, pp. 187–191, Jan. 1997.
- [17] G. Cao, "Nanostructures and Nanomaterials - Synthesis, Properties and Applications," *World Scientific.*, Apr. 2004.
- [18] J. W. Seo, A. Magrez, M. Milas, K. Lee, V. Lukovac, and L. Forr, “Catalytically grown carbon nanotubes : from synthesis to toxicity,” *J. Phys. D: Appl. Phys.*, vol. 40, pp. 109-120, Mar. 2007.
- [19] M. José-Yacamán, M. Miki-Yoshida, L. Rendón, and J. G. Santiesteban, “Catalytic growth of carbon microtubules with fullerene structure,” *Appl. Phys. Lett.*, vol. 62, no. 6, pp. 657-659, Feb. 1993.
- [20] Y. Gogotsi and J. A. Libera, “Hydrothermal synthesis of multiwall carbon nanotubes,” *J. Mater. Research.*, vol. 15, no. 12, pp. 2591–2594, Dec. 2000.
- [21] S. Manafi, H. Nadali, and H. R. Irani, “Low temperature synthesis of multi-walled carbon nanotubes via a sonochemical/hydrothermal method,” *Mater. Lett.*, vol. 62, no. 26, pp. 4175–4176, Oct. 2008.
- [22] W. K. Hsu, J. P. Hare, M. Terrones, H. W. Kroto, D. R. M. Walton, and P. J. F. Harris, “Condensed-phase nanotubes,” *Nature.*, vol. 377, no. 6551, pp. 687–687, Oct. 1995.
- [23] J. B. Bai, “Synthesis of SWNTs and MWNTs by a molten salt (NaCl) method,”

- Chem. Phys. Lett.*, vol. 365, no. 1, pp. 184–188, Oct. 2002.
- [24] D. Laplaze, P. Bernier, W. K. Maser, G. Flamant, T. Guillard, and A. Loiseau, “C1. Laplaze, D. et al. Carbon nanotubes: The solar approach. Carbon N. Y. 36, 685–688 (1998).arbon nanotubes: The solar approach,” *Carbon.*, vol. 36, no. 5–6, pp. 685–688, Jan. 1998.
- [25] D. Luxembourg, G. Flamant, and D. Laplaze, “Solar synthesis of single-walled carbon nanotubes at medium scale,” *Carbon.*, vol. 43, no. 11, pp. 2302–2310, Sep. 2005.
- [26] N. Pierard, A. Fonseca, Z. Konya, I. Willems, and G. Van Tendeloo, “Production of short carbon nanotubes with open tips by ball milling,” *Chem. Phys. Lett.*, vol. 335, no. 1, pp. 1–8, Feb. 2001.
- [27] F. Liu, X. Zhang, J. Cheng, J. Tu, F. Kong, W. Huang, and C. Chen, “Preparation of short carbon nanotubes by mechanical ball milling and their hydrogen adsorption behavior,” *Carbon.*, vol. 41, no. 13, pp. 2527–2532, Jan. 2003.
- [28] J. Qiu, Z. Wang, Z. Zhao, and T. Wang, “Synthesis of double-walled carbon nanotubes from coal in hydrogen-free atmosphere,” *Fuel.*, vol. 86, no. 1–2, pp. 282–286, Jan. 2007.
- [29] Y.-H. Wang, S.-C. Chiu, K.-M. Lin, and Y.-Y. Li, “Formation of carbon nanotubes from polyvinyl alcohol using arc-discharge method,” *Carbon.*, vol. 42, no. 12–13, pp. 2535–2541, Jan. 2004.
- [30] L. E. Murr, D. K. Brown, E. V. Esquivel, T. D. Ponda, F. Martinez, and a. Virgen, “Carbon nanotubes and other fullerenes produced from tire powder injected into an electric arc,” *Mater. Charact.*, vol. 55, no. 4–5, pp. 371–377, Nov. 2005.
- [31] L. Li, F. Li, C. Liu, and H.-M. Cheng, “Synthesis and characterization of double-walled carbon nanotubes from multi-walled carbon nanotubes by hydrogen-arc discharge,” *Carbon.*, vol. 43, no. 3, pp. 623–629, Jan. 2005.
- [32] T. Okada, T. Kaneko, and R. Hatakeyama, “Conversion of toluene into carbon nanotubes using arc discharge plasmas in solution,” *Thin Solid Films.*, vol. 515, no. 9, pp. 4262–4265, Mar. 2007.
- [33] J. Qiu, G. Chen, Z. Li, and Z. Zhao, “Preparation of double-walled carbon nanotubes

- from fullerene waste soot by arc-discharge,” *Carbon.*, vol. 48, no. 4, pp. 1312–1315, Apr. 2010.
- [34] S. Zhao, R. Hong, Z. Luo, H. Lu, and B. Yan, “Carbon Nanostructures Production by AC Arc Discharge Plasma Process at Atmospheric Pressure,” *J. Nanomater.*, vol. 2011, pp. 1–6, Jan. 2011.
- [35] S. P. Doherty and R. P. H. Chang, “Synthesis of multiwalled carbon nanotubes from carbon black,” *Appl. Phys. Lett.*, vol. 81, no. 13, pp. 2466–2468, Sept. 2002.
- [36] Z.-G. Chen, F. Li, W.-C. Ren, H. Cong, C. Liu, G. Q. Lu, and H.-M. Cheng, “Double-walled carbon nanotubes synthesized using carbon black as the dot carbon source,” *Nanotechnology.*, vol. 17, no. 13, pp. 3100–3104, Jul. 2006.
- [37] S. P. Doherty, D. B. Buchholz, and R. P. H. Chang, “Semi-continuous production of multiwalled carbon nanotubes using magnetic field assisted arc furnace,” *Carbon.*, vol. 44, no. 8, pp. 1511–1517, Jul. 2006.
- [38] J. B. Donnet, H. Oulanti, and T. Le Huu, “Mechanism growth of multiwalled carbon nanotubes on carbon black,” *Diam. Relat. Mater.*, vol. 17, no. 7–10, pp. 1506–1512, Jul. 2008.
- [39] O. Łabędź, H. Lange, a. Huczko, J. Borysiuk, M. Szybowicz, and M. Bystrzejewski, “Influence of carbon structure of the anode on the synthesis of single-walled carbon nanotubes in a carbon arc plasma,” *Carbon.*, vol. 47, no. 12, pp. 2847–2854, Oct. 2009.
- [40] H. Nishizaka, M. Namura, K. Motomiya, Y. Ogawa, Y. Udagawa, K. Tohji, and Y. Sato, “Influence of carbon structure of the anode on the production of graphite in single-walled carbon nanotube soot synthesized by arc discharge using a Fe–Ni–S catalyst,” *Carbon.*, vol. 49, no. 11, pp. 3607–3614, Sep. 2011.
- [41] S. P. Doherty, D. B. Buchholz, B.-J. Li, and R. P. H. Chang, “Solid-state synthesis of multiwalled carbon nanotubes,” *J. Mater. Res.*, vol. 18, no. 4, pp. 941–949, Jan. 2012.

2.1 Introduction

In the previous chapter, we discussed the importance of carbon on earth and brief introduction about carbon nanotubes and its synthesis method. Carbon nanotubes (CNTs) possess excellent mechanical, electronic, thermal, optical and chemical properties which have revolutionized the research in application of the newer allotrope of carbon. CNTs have been broadly classified as SWCNTs, DWCNTs and MWCNTs. Researchers have devised different routes to synthesize CNTs which we have already discussed in the previous chapter in Section 1.2.

Among various methods of CNT synthesis over the last two decades, researchers have demonstrated a successful use of arc discharge technique in the production of high quality CNTs. A bar graph shown in Figure 2.1 depicts the number of papers (on x-axis) published year wise shows (on y-axis) for CNT synthesis using arc discharge. It is observable from graph that number of publication in 2005 was maximum. Some insights of nanotube growth process and the fundamental role of few arc discharge parameters have been understood and published in literature.

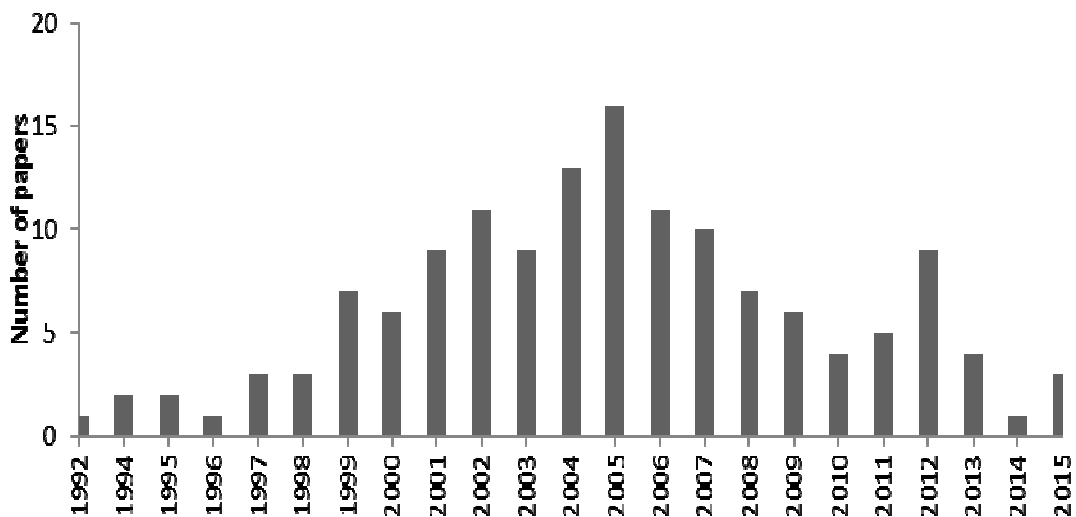


Figure 2.1: Bar graph showing papers published on arc discharge synthesis of CNT

However, the literature lacks comprehensive study on the mechanism of nanotube formation and needs investigation on correlation between growth conditions and synthesized nanotubes. The requirement to understand the role of growth conditions lays in selective growth of nanotubes using arc discharge, which remains largely unexplored.

For researchers taking up the nanotube synthesis using arc discharge, the availability of comprehensive review on the process is quintessential. Previously, Ando and Zhao [1] discussed the synthesis of SWCNTs and MWCNTs using arc discharge. In 2007, Harris [2] investigated the models of nanotube growth in arc discharge and laser ablation processes. In 2010, Ando [3] presented the chronological aspect of arc grown nanotubes in hydrogen atmosphere. In 2011, Tessonier and Su [4] briefly discussed the nucleation and growth process of nanotube in arc grown CNTs. In 2011, Prasek et al. [5] reviewed the different routes of nanotube synthesis. In 2012, Journet et al. [6] discussed low or medium temperature techniques to synthesize CNTs. In 2014, Hrivas et al. [7] reviewed the method for carbon nanotubes production and its mechanical properties. In 2014, Mubarak et al. [8] discussed survey of experimental work require for the synthesis of CNTs. In 2015, Yan et al. [9] presented the review article on understanding of manufacturing and functionalizing of carbon nanotubes through arc discharge, laser ablation and chemical vapor deposition method. In 2015, Sarangdevot et al. [10] reviewed the history, types, structure and different synthesis methods of CNTs.

In next sections, we update and detail experimental attempts to manufacture carbon nanotubes using arc discharge technique. The growth mechanism of nanotubes, as published in literature has been briefed. It is further discussed in the next section the role of synthesis parameters like setup modification, power supply, arc current, catalyst, pressure, grain size, electrode geometry and temperature on the nanotube production. From the review, we understand that few parameters like pressure and catalyst have been investigated quantitatively in literature but the exact role of the growth conditions still requires extensive investigation.

The review has been divided into four sections. Section 2.1 introduces literature published on arc discharge method. Section 2.2 discusses the nanotube growth in arc discharge. Section 2.3 outlines the arc discharge parameters and their corresponding physics is detailed in next subsections and finally concluded with carbon precursor in Section 2.4.

2.2 Nanotube Growth in Arc Discharge

2.2.1 Arc Discharge Setup

Arc discharge is the electrical breakdown of a gas to generate plasma. This technique of generating arc using electric current was first used by Iijima to produce CNTs [11] in 1991. A schematic of an arc discharge chamber is shown in Figure 2.2. Generally, the chamber consists of two electrodes which are mounted horizontally or vertically; one of which (anode) is filled with powdered carbon precursor along with the catalyst and the other electrode (cathode) is usually a pure graphite rod. The chamber is filled with a gas or submerged inside a liquid environment. The inlet and outlet for gas are shown in Figure 2.2 for representation only.

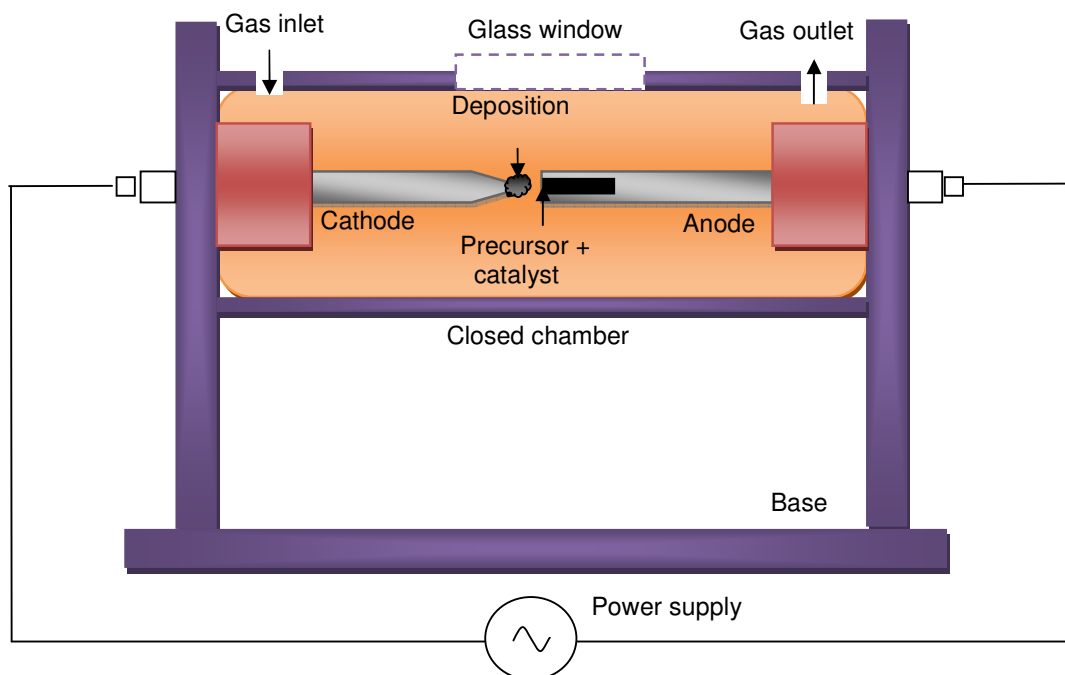


Figure 2.2: Schematic of an arc discharge setup

In actual, their placement may suit the design of the chamber. A power supply (AC/DC) as shown is required to initiate and maintain the arc. The electrodes are brought in contact to generate an arc and are kept at an intermittent gap of 1–2 mm to attain a steady discharge. A constant current is maintained through the electrodes to obtain a non-fluctuating arc for which normally closed loop automation is employed to adjust the gap automatically. The details of the power supply and control circuit is given in next chapter Section 3.2. A fluctuating arc results in unstable plasma and

affects adversely the quality of the synthesized CNTs. Therefore, a non-fluctuating arc is quintessential which is obtained maintaining constant current. The arc current generates plasma of very high temperature ~4000-6000 K, which sublimes the carbon precursor filled inside the anode. The carbon vapors aggregate in the gas phase and drift towards the cathode where it cools down due to the temperature gradient. After an arc application time of few minutes the discharge is stopped and cathodic deposit which contains CNTs along with the soot is collected from the walls of chamber. The deposit is purified and analyzed for morphology and other properties.

2.2.2 Growth Mechanism of Carbon Nanotubes in Arc Discharge

Researchers have investigated and suggested growth conditions for nanotube formation based on their experimental observations. Despite many studies, no clear understanding of the growth mechanism of CNTs in arc discharge has been established. Understanding the physics of the mechanism of growth will be seminally useful for the growth of nanotubes with desirable properties and yield. In this section, we present an outline of the synthesis mechanism in the growth of CNTs in arc discharge as reported in literature.

As mentioned earlier in Section 2.2.1, the two electrodes in Figure 2.2 are brought in contact and upon application of voltage; constant current is made to flow through them using control circuits. The electric current results in resistive heating and raises the temperature of the electrodes. The anode is moved back to maintain a gap (~1 mm) between the electrodes for continuous deposition of carbon vapours. Meanwhile, the high temperature ~4000-6000 K facilitates the breakdown of the surrounding gas filled inside the chamber. Physics involved in arc discharge process remains unexplained in published literature and books. In 2014, we discussed the physics of the growth mechanism of CNTs in arc discharge. The gas ionizes into electrons and ions and results in hot plasma formation between the electrodes. Stable plasma grows uniformly over the electrode surface corresponding to stable anode and cathode voltage. The collisions of ions and electrons in the plasma emit photons responsible for the glow in plasma. The electrons ejected from cathode hit the anode at high velocity and sputter the carbon precursor filled at the center of the anode. The high temperature resulting from resistive heating results in sublimation of carbon precursor and converts them into carbon vapours. The carbon vapors are decomposed

in carbon ions. The decomposition occurs due to high heat flux or thermal energy of the plasma. The carbon vapors aggregate to form viscous carbon clusters and drift towards the cathode, which is cooler as compared to anode. The carbon vapors undergo a phase change and get converted into liquid carbon. The temperature gradient at cathode and quenching effect of atmosphere solidifies and crystallizes the liquid carbon to form cylindrical deposits that grow steadily on cathode. The cathodic deposit is composed of a grey outer shell and a dark inner core. The grey deposit consists of the rolls of graphene sheets known as carbon nanotubes. The addition of hexagonal carbon atom clusters lead to the growth of nanotube. However, instability in plasma leads to capping of nanotubes. The diameter of the nanotubes is governed by the density of carbon vapors in the plasma. Variation in temperature gradients strongly affects the diameter distribution of CNTs produced and nanotubes are formed in bundles due to van der Waals interaction.

Further in published literature, various affiliated aspect in nanotube synthesis has been explained by few more researchers. Citing from literature, in 1993 Iijima [12] proposed a model for tubular growth and explained the capping of nanotubes in terms of pentagons and heptagons. In 1994, Ugarte [13] studied the heat treatment of carbon soot generated by electric arc between two graphite electrodes and run in a low inert gas helium pressure. In 1995 Ebbesen and Gamaly [14] developed a model based on physical properties of arc discharge for nanotube formation. In 1995, Amelinckx et al. [15] reported model to explain the microstructure of graphite multi shell nanotubes grown by arc discharge. In 1999, Liu et al. [16] discussed semi continuous hydrogen arc discharge method for synthesizing SWCNTs. In 2000, Kukovitsky et al. [17] performed catalytic synthesis of various carbon forms on nickel supported catalyst using carbon vapor as precursor. In 2001, Farhat et al. [18] reported method for controlling diameter of SWCNTs during electric arc discharge process. In 2001, Gavillet et al. [19] investigated the catalytic growth of SWCNTs. In 2002 Jong et al. [20] observed large scale synthesis of carbon nanotubes by plasma rotating arc discharge. In 2005, Heer et al. [21] discussed the formation of carbon nanotubes in a pure carbon arc in a helium atmosphere. In 2006, Kim et al. [22] investigated CNTs synthesis by DC arc discharge method using carbon cathode coated with metal catalyst. In 2006, Yusoff et al. [23] studied the effect of physical parameter of arc on substrate

surface temperature and on CNTs grown. In 2007, Keidar et al. [24] developed model of SWCNTs interactions with thermal plasma in arc discharge. In 2008, Joshi et al. [25] synthesized CNTs using arc discharge method with a rotating graphite disc as cathode. In 2008, Donnet et al. [26] studied the growth of MWCNTs using combustion oxygen/ acetylene flame method. In 2010, Scalese et al. [27] investigated the influence of electrode size and discharge current on structural quality of nanotubes. In 2011, Zhao et al. [28] produced carbon nanostructures by decomposition of benzene using arc discharge plasma at atmospheric pressure. In 2012, Liang et al. [29] synthesized MWCNTs and polyhedral graphite particles under atmospheric pressure. In 2012, Wu et al. [30] synthesized graphene/ SWCNTs hybrid materials and performance in super capacitors has been studied. In 2012, Kim et al. [31] reported synthesis of metallic impurity free MWCNTs using stabilized arc discharge under atmospheric conditions. But the exact growth mechanism is still remained debatable due to different theories of nanotube and possibilities of growth in vapor phase [14], liquid phase [21], solid phase [32] and crystal phase [33].

2.2.2.1 Vapor phase growth

In 1995 Gamaly and Ebbesen [14] detailed the vapor phase growth of MWCNTs and suggested that the carbon vapors condense and nucleate to form nanotubes. They proposed a model for the velocity distribution of carbon vapors and divided the carbon vapours in two groups depending upon their velocity distributions. One group of carbon vapors will have the isotropic (Maxwellian) velocity distribution. The other group of carbon particles has higher velocities than the first group which is due to the acceleration of carbon vapours between the electrodes. According to Gamaly and Ebbesen, the nanotube growth occurs in three steps - seed formation, tube growth and termination. The seeds are formed as a result of the two velocity distributions. In the beginning, the carbon vapours possess Maxwellian distributions which result in nanoparticle formation. Upon increasing the current, the other group of directed carbon vapours results in open structures or seeds. Once the current reaches a stable value, the carbon ions flow perpendicular to the cathode surface resulting in the nanotube growth. Finally the nanotube growth is terminated due to instabilities in the plasma. A similar theory has also been validated by other researchers too [34-37]. In 2002, Louchev et al. [34] show the effect of surface diffusion feeding nanotube

growth from behind the growth interface to stabilize open edge morphology. In 2002, Sato et al. [35] suggested the open edge stability of nanotube growth depend on kinetically competition between pentagon and hexagon formation. In 2003, Louchev et al. [36] discussed detailed analysis of nanotube nucleation from graphitic nanofragments by thermal vibration. In 2006, Liu et al. [37] investigated uncatalyzed edge growth of carbon nanotubes.

2.2.2.2 Liquid phase growth

The liquid phase growth model was suggested by Heer et al. [21] in 2005. He proposed that the liquid carbon solidifies to result in nanotubes. They found beads of amorphous carbon within the nanotubes which result during solidification of liquid drops. According to them, when the electric arc is applied to heat the carbon precursor, the electrons bombarding the surface result in localized heating, which causes the surface to liquefy. The liquid droplets are ejected from the anode and are drifted towards cathode. These globules of liquid carbon tend to cool at the cathode surface. The cooling propagates from outer layer towards the center, resulting in multilayered tubular structures.

2.2.2.3 Solid phase growth

Solid phase growth of nanotubes was proposed by Harris et al. [38] in 1994. They found that nanotubes are synthesized by high temperature heat treatment of fullerene soot. Based on their observations, they proposed that initially carbon vapors in the gas phase condense onto the cathode to form fullerene soot. Since the temperature of cathode is high due to continuous arc, the fullerene soot is converted to MWCNTs via the seed-growth-termination process. The requiem for this process is rapid heating of fullerene soot since slow heating of fullerene results in nanoparticle formation [32]. In order to improve upon the existing theories, experimental investigations are necessary to develop a strong correlation between the synthesized CNTs and input parameters. In literature, large number of experimental reports has been published establishing correlation between variation in arc parameters with quality and quantity of synthesized nanotubes of various reported experimental work and are discussed in the next section.

2.3 Arc Discharge Parameters

The arc discharge process is dependent on several parameters like type of power supply, environment, pressure, electrode geometry, catalyst and temperature that influence the quality and quantity of the synthesized product. Researchers have studied the variation of these parameters and have attempted to establish an optimal range of the parameters for improving quality and quantity of CNTs using arc discharge. The implication of these parameters and their corresponding physics is detailed in the next subsections.

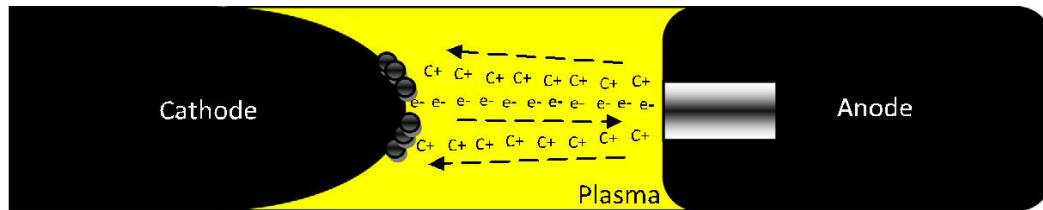
2.3.1 Effect of Power Supply

The power supply controls the arc current and voltage which govern the energy distribution of electron discharge. This affects the plasma temperature that plays decisive role in the product of arc discharge. In this section we have detailed the effect of type of power supply, voltage, arc current and frequency on quality and yield of synthesized nanotubes.

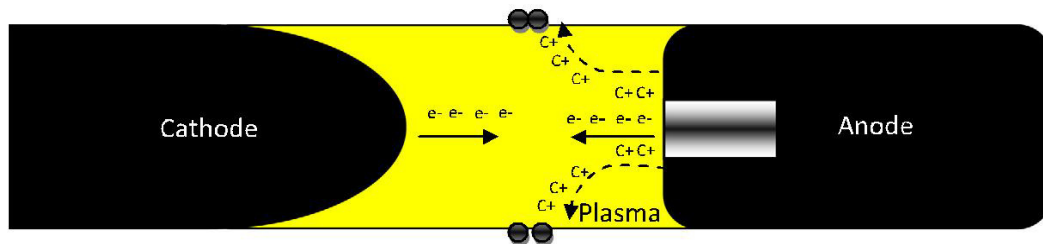
2.3.1.1 Type of power supply

The type of power supply plays a vital role in nanotube formation. In Figure 2.3(a), (b), (c) two electrodes are mounted horizontally and are shown schematically; the cathode and anode are of pure graphite rod of cylindrical shape with anode having a drilled hole at the center filled with carbon precursor. Figure 2.3(a) shows the DC arc discharge setup, when DC arc current is applied across the electrodes, electrons are emitted continuously from cathode as indicated by e^- travelling in straight arrow. Emitted electrons bombards the anode at high velocity and as a result carbon vapors i.e. C^+ ion ejected from anode move towards cathode as indicated by inclined arrow. The cathode diameter is usually larger than the anode diameter, which results in lower current density at cathode than anode. Thus, a high temperature gradient across the electrodes is obtained which sublimates the carbon precursor filled inside the anode and results in the formation of CNTs. In AC arc discharge schematically shown in Figure 2.3(b), the current alters periodically across the electrodes which results in emission of electrons (e^-) as indicated by straight arrow from both side and no deposition is observed at either side of the electrodes. The carbon vapors (C^+) fly out of the plasma to move towards the wall indicated in Figure 2.3(b) inclined arrow. This happens due to thermal effects i.e. the temperature of electrodes increases by

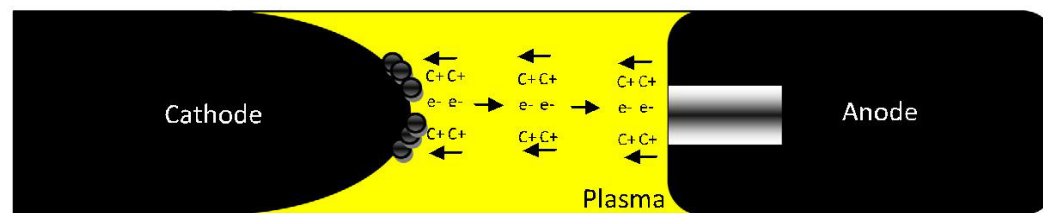
resistive heating in plasma with an applied arc current which results in CNT formation at the walls of the chamber. Figure 2.3(c) shows the setup of pulsed arc method. In pulsed arc, CNT formation takes place with short range and long range pulses, normally of the millisecond width. Electron emitted from cathode move towards anode as indicated by arrow and C^+ ions ejected from anode and move towards cathode as shown by arrow. Pulse striking the anode surface and vaporizes the carbon ion and deposited on to the cathode.



(a) **DC Arc Discharge:** Continuous movement of ions and electrons in the plasma between the electrodes. Continuous Deposition obtained at Cathode



(b) **AC Arc Discharge:** The polarity of the electrodes changes after every cycle. Thus electrons are discharged from both side and results in C^+ ions from anode flying away from the plasma. The deposition is obtained the reactor chamber walls. Lesser deposition obtained compared to DC and Pulsed Discharge.



(c) **Pulsed Arc Discharge:** Accelerated electrons are discharged from cathode in short pulses after a time interval ranging from micro to milliseconds. The deposition occurs at cathode.

Figure 2.3: Schematic showing the formation of CNTs using different power supplies

In case of DC arc discharge setup, the ionized gas drifts towards cathode and hinders the continuous deposition of carbon ions on cathode. In order to remove the gas ions, the cathode should not be negatively charged. This problem may be overcome by using an AC or pulsed power supply. The disadvantage of using AC supply is that the formation of nanotubes occurs only in positive cycle and thus the yield is reduced. Thus, pulsed arc

discharge is the most favorable for nanotube formation as the formation occur in some short and long range pulses.

In 2010, Ashraf et al. [39] compared the continuous and pulsed arc discharges and their effect on nanotube formation. They observed variation in type and quantity of atomic carbon species on using different power supply. According to them, the continuous arc discharge results in higher amount of C₂ (diatomic carbon) and it is the precursor for nanotube formation. The pulsed discharge contained additional amount of C₁ (one carbon atom) due to disintegration of C₂, which does not form closed carbon structures. However, pulsed arc is advantageous as it provides more control over the process.

The pulsed arc is found to be more energetic than a continuous arc. The energy of an electron is higher at the time of ejection and it takes microseconds for the electron to attain the Maxwellian energy distribution. Thus, continuous bombardment of anode with pulses of width shorter than this time results in higher electron energy which increases the yield [40]. On contrary to this, continuous power supply has lesser electron energy distribution. We have classified the existing literature on CNT synthesis based on the type of power supply and plotted a Pie chart showing the percentage of papers published in these categories as shown in Figure 2.4. It can be clearly seen from Figure 2.4 that the DC is most widely used type of power supply to synthesize CNT using arc discharge method.

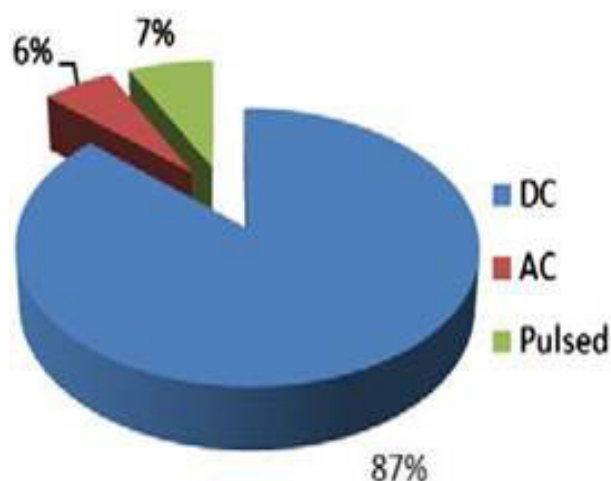


Figure 2.4: Pie chart showing percentage of papers published on arc discharge synthesis of CNT

The first attempts to synthesize MWCNTs [11] and SWCNTs [41], [42] using DC power supply were reported in 1991 and 1993 respectively. Some of the early insightful works include large scale synthesis of CNTs in helium atmosphere by Ebbesen and Ajayan [43] in 1992. In 1995, Wang et al. [44] produced MWCNTs in hydrogen atmosphere using arc discharge. In 1997, Journet et al. [45] demonstrated large scale synthesis of SWCNTs in helium atmosphere. Shi et al. [46] in 1999 demonstrated bulk synthesis of SWCNTs in high pressure helium atmosphere. High yields of 6.5 g/h CNTs have been demonstrated by Zhao[47]. In 2004, Itkis et al. [48] produced 5-15 g CNTs using DC arc discharge. Chronological attempts of synthesizing CNTs using DC power supply have been listed in Table 2.1. In column 1 of Table 2.1, year and lead author name are given. Column 2-column 6 gives corresponding important information of the work namely arc current, synthesis time, precursor used, catalyst if any, environment, pressure and type of CNTs and its diameter respectively. From Table 2.1 we observed that mainly CNTs synthesis were attempted using graphite as carbon precursor, few researchers used carbon black and coal.

Table 2.1: Arc discharge synthesis of CNT using DC power supply

Year - Author	Arc current, synthesis time	precursor	catalyst	Environment, pressure	Type of CNTs, diameter, yield
1991 - Iijima [11]		Graphite		Argon, 100torr	MWCNT, 5-20nm
1992 - Ebbesen and Ajayan[43]	100A	Graphite		Helium, 500torr	CNT, 2-20nm
1993 - Iijima et al. [41]	200A	Graphite		Argon, 40torr	CNT, 1nm
1993- Bethune et al.[27]	95-105A	Graphite	Co	Helium, 100-500torr	SWCNT, 20nm
1994 - Lin et al.[49]		Graphite			
1994 - Guerret-Plecoart et al.[50]	100-110A, 30-60 min	Graphite		Helium, 0.6bar	CNT
1995 - Wang et al.[44]	90A	Graphite		Hydrogen, 50-700torr	MWCNT
1995 - Zhou and Seraphin[51]	220A/cm ²				Branched CNT
1996 - Loiseau and Pascard[52]	100-110A, 30-45 min	Graphite		Helium, 0.6bar	CNT
1997 - Lange et al.[53]	60-70A, 4min	Graphite		Helium, 500torr	
1997 - Journet et al.[45]	100A, 2min	Graphite	Ni-Co-Y	Helium, 500torr	SWCNT, 5-20nm
1997 - Zhao et al.[54]	20-100A	Graphite		Hydrogen, 10-200torr	MWCNT, 1nm
1998 - Saito et al.[55]	70A & 100A, 1-3 min	Graphite	Ru/Pd/Rh/Pt	Helium, 1520torr	SWCNT, 1.28 nm
1998 - Chang et al.[56]	55-65A	Graphite		Helium, 500torr	CNTs, 10-40nm

Year - Author	Arc current, synthesis time	precursor	catalyst	Environment, pressure	Type of CNTs, diameter, yield
1998 - Zhao and Ando[57]	50A, 30-60s	Graphite		Hydrogen, 60torr	MWCNT, 1-20nm
1999 - Takizawa et al.[58]	100A, 10s	Graphite	Ni-Y ₂ O ₃	Helium, 500torr	SWCNT
1999 - Yudasaka et al.[59]	100A, 10s	Graphite		Helium, 500torr	SWCNT
1999 - Shi et al.[60]	40-100A	Graphite	Ni-Y	Helium, 100-700torr	SWCNT, 1.3nm, 1.5g
1999 - Zhao et al.[61]	50A, 30-60s			Hydrogen, 60torr	MWCNT
1999 - Shi et al.[46]	40A, ~120min	Graphite	Ni-Y	Helium, 1520torr	SWCNT, 5g
1999 - Kiselev et al.[62]	80A, 60s	Graphite		Helium, 100torr	MWCNT, 115 mg/min
1999 - Liu et al.[16]	150A, 3min	Graphite		Hydrogen, 200torr	SWCNT, 20nm, 100mg
2000 - Ishigami et al.[63]	60A	Graphite		Liquid Nitrogen	MWCNT, 44mg/min/cm ²
2000 - Tang et al.[64]	58A	Graphite		Helium, 400torr	CNT
2000 - Shi et al.[65]	40-60A, ~120min	Graphite	Ni-Y	Helium, 500-700torr	SWCNT, 5g
2000 - Ando et al.[66]	50-100A, ~3min	Graphite	Ni-Y	Helium, 400-700torr	SWCNT, 1.28-1.52nm, 1.24 g/min
2000 - Ando et al.[67]	50A,30-60s	Graphite		Hydrogen, 30-120torr	MWCNT
2000 - Cheng et al.[68]	150A, 3min	Graphite	Ni-Fe-Co-FeS	Hydrogen, 200torr	SWCNT, 100mg
2001 - Ando et al.[69]	50-100A, 3min	Graphite	Ni-Y	Helium, 400-700torr	SWCNT, 1.34-1.53nm
2001 - Srivastav et al.[70]	200A, 3 min	Graphite		Helium, 500torr	CNT
2001 - Farhat et al.[18]	100A	Graphite	Ni-Y	Helium & Argon, 495 torr	SWCNT
2001 - Hutchison et al.[71]	75-80A, 40min	Graphite		Hydrogen-Argon, 350torr	DWCNT, 2.7-4.7 nm
2001 - Kanai et al.[72]	20-40A, 30min	Graphite	Ni-Y	Helium, 600torr	SWCNT
2001 - Shimotani et al.[73]	100A, 2min	Graphite		Helium-Hydrocarbons, 150-500torr	MWCNT
2001 - Li et al.[74]	30A, 5min	Graphite		Helium, 15kPa	MWCNT/SWCNT, 0.34nm
2001 - Ando et al.[75]	50A, 30-60s	Graphite		Hydrogen, 8kPa	MWCNT
2001 - Lai et al.[76]	60-90A	Hydrocarbon (Xylene, Pyrene)		Helium, 300-600torr	CNT, 10-50µm
2002 - Osvath et al.[77]	100A, 2min			Helium, 660mbar	Branched CNT, 10 & 20 nm
2002 - Jain et al.[78]	900A, 15-20min	Graphite		Helium, 800torr	MWCNT

Year - Author	Arc current, synthesis time	precursor	catalyst	Environment, pressure	Type of CNTs, diameter, yield
2002 - Tang et al.[79]	75-85A	Graphite		Helium, 400torr	MWCNT
2002 - Li et al.[80]	50A, 1min	Graphite		Hydrogen-CO	MWCNT, 10-20nm
2002 - Jong Lee et al.[20]	80-120A	Graphite		Helium, 500torr	CNT
2002 - Park et al.[81]	60-80A, 5min	Graphite	Ni-Co-Fe-S	Helium, 100-500torr	SWCNT, 10-20 nm
2002 - Ando et al.[82]	60A, 10min			Hydrogen, 13kPa	MWCNT
2002 - Sheng et al.[83]	85-95A	Graphite		Helium, 375torr	CNT
2002 - Cadek et al.[84]	~57A	Graphite		Helium, 500torr	MWCNT
2002 - Zhen-Hua et al.[85]	50-80A,10min	Graphite	Ni-Y	Helium, 100-200torr	SWCNT, 10-20nm
2002 - Doherty and Chang[86]	100A, 1min	Carbon Black		Helium, 100torr	MWCNT
2003 - Antisari et al.[87]	30-70A, 1min	Graphite		Liquid Nitrogen, Deionized Water,	MWCNT
2003 - Doherty et al.[88]	100A, 1min	Carbon Black		Helium, 100torr	MWCNT
2003 - Saito et al.[89]	50A	Graphite	FeS-NiS-CoS	Hydrogen-Helium, 300torr	DWCNT, 2-5nm
2003 - Qiu et al.[90]	50-70A, 20min	Coal	Fe	Helium, 490torr	SWCNT, 10-20nm
2003 - Jung et al.[91]	80A	Graphite		Liquid Nitrogen	MWCNT, 20-50nm
2003 - Zhao et al.[92]	30-70A, 3min	Graphite	Fe	Hydrogen-Argon, 60-500torr	SWCNT
2003 - Lange et al.[93]	30-40A,10 min			Deionized water	Nanocarbon/ CNT
2003 - Cui et al.[94]	35-44A, 3min	Graphite		Nitrogen, 0.02-900torr	MWCNT
2003 - Osvath et al.[95]	100A, 2 min	Graphite	Ni-Y	Helium, 500torr	Branched CNT, 10nm
2003 - Tarasov et al.[96]	50-130A	Graphite	Ni-Co + YNi ₂	Helium, 400-800torr	SWCNT
2004 - Liu et al.[97]	100A,10 min	Graphite		Hydrogen, 50kPa	Amorphous CNT
2004 - Waldorff et al.[98]	78.5A, 180s	Graphite	Ni-Y	Helium, 500-700torr	SWCNT, 2nm
2004 - Nishio et al.[99]	60A, 2-8s	Graphite		Helium, 760torr	CNT
2004 - Wang et al.[100]	60-450A	Polyvinyl Alcohol	Fe	Helium, 260torr	MWCNT
2004 - Zhao et al.[47]	80A, 5min	Graphite	Ni-Co	Hydrogen, 500torr	Amorphous CNT, 7-20nm, 6.5g/hr
2004 - Bera et al.[101]	35A	Graphite		PdCl ₂	CNT
2004 - Cui et al.[102]	35-44A, 50-120s	Graphite		Nitrogen, 0-900torr	MWCNT/SWCNT
2004 - Zhao and Liu[103]	60A, 5min	Graphite		Helium, 400torr	SWCNT

Year - Author	Arc current, synthesis time	precursor	catalyst	Environment, pressure	Type of CNTs, diameter, yield
2004 - Jinno et al.[104]	50A, 30-60s	Graphite		Hydrogen-Nitrogen, 70torr	MWCNT, 1nm
2004 - Keidar and Waas[105]					CNT
2004 - Itkis et al. [48]	90A, 60-90min	Graphite	Ni-Y	Helium, 680torr	SWCNT, 5-15g
2004 - Qiu et al.[106]	50-70A	Coal		Helium, 250-570torr	MWCNT
2004 - Sano et al.[107]	60A, 45s	Graphite	Ni	Liquid Nitrogen	SWCNT
2005 - Murr et al.[108]	50-100A	Tire Powder		Helium, 250torr	MWCNT, 5-50nm
2005 - Hahn et al.[109]	60A	Graphite		Hydrogen, 13kPa	MWCNT
2005 - Shang et al.[110]	50A	Graphite		Helium, 30-120torr	MWCNT, 1.1nm
2005 - de Heer et al.[111]	100A	Graphite		Helium, 375torr	MWCNT, 3-20nm
2005 - Ando et al.[112]	40-70A,15min	Graphite	Fe	Hydrogen-Nitrogen, 200torr	SWCNT
2005 - Yang et al.[113]	100-120A	Graphite		Hydrogen-Argon, 70torr H ₂ , 50torr Argon	DWCNT
2005 - Guo et al.[114]	30-70A	Graphite	Fe	Hydrogen-Argon, 200torr	SWCNT
2005 - Li et al.[115]	120A, 3min	Graphite	Ni-Co-Fe-S	Hydrogen, 240torr	DWCNT, 4g/h
2005 - Wang et al.[116]	50A, 60 sec	Graphite		NaCl	SWCNT, 0.89nm MWCNT, 8.9nm
2005 - XinLv et al.[117]	90-120A, 30-150 min	Graphite		Helium, 530-550torr	SWCNT
2005 - Makita et al.[118]	50-60A	Graphite	Ni-Co	Helium, Argon, Nitrogen 50-1000torr	SWCNT
2005 - Yao et al.[119]	90A, 5-10min	Graphite	Ni-H ₂ O ₃	Helium, 600torr	SWCNT, 10-30 nm, 0.6-1g
2005 - Montoro et al.[120]	65A, 20 min			H ₃ VO ₄ aqueous solution	SWCNT/MWCNT, 20-30nm
2005 - Zhao et al.[121]	80A	Graphite		Hydrogen, 500torr	Amorphous CNT, 7-20 nm
2005 - Tang et al.[122]	85-95A	Graphite		Helium, 400torr	CNT
2005 - Wang et al.[123]	50A, 60s	Graphite	Fe	Deionized water, open air	CNT
2006 - Doherty et al. [124]	100A, 1min	Carbon Black		Helium, 100torr	CNT
2006 - Wang et al.[125]	70A	Graphite	Ni-Y	Helium, 120torr	SWCNT, 10g
2006 - Chen et al.[126]	120A	Carbon Black	Co-CoS	Hydrogen-Argon	DWCNT
2006 - Qiu et al.[127]	70A, 15min	Graphite	FeS-KCl	Hydrogen, 350torr	DWCNT

Year - Author	Arc current, synthesis time	precursor	catalyst	Environment, pressure	Type of CNTs, diameter, yield
2006 - Wang et al.[128]	70A,15min	Coal		Argon, 80-90kPa	CNT, 30-80nm
2006 - Lange et al.[129]	25A & 55A	Graphite/ Carbon Black	Fe	Hydrogen-Argon, 200torr	SWCNT
2006 - Zhao et al.[130]	50A, 3-20min	Graphite	Fe	Hydrogen-Inert Gases, 50-500torr	SWCNT
2006 - Suzuki et al.[131]	60A,10min	Graphite		Hydrogen-Helium, 100torr	MWCNT, 900mg
2006 - Yusoff et al.[23]	16A	Graphite		Nitrogen, 760torr	CNT
2006 - HH Kim and HJ Kim[132]	40-80A	Graphite		Air, 100-760torr	MWCNT
2006 - Wang et al.[133]	70-80A, 10min			Helium, 50-60kPa	Branched CNT
2006 - HH Kim and HJ Kim[22]	40-100A	Graphite	Ni-Co-Ti	Helium, 500torr	MWCNT/ SWCNT
2007 - Cazzanelli et al.[134]	60A, 100s	Graphite	Ni-Cr	Helium, 375torr	MWCNT
2007 - Okada et al.[135]	1-20A, 30s	Toluene	Ni-Mo-Fe	Toluene	CNT
2007 - Mathur et al.[136]	100-120A	Graphite + Coke powder		Helium, 600torr	MWCNT/ SWCNT
2007 - Song et al.[137]	100A, 5-8min	Graphite	Co-S-Pt	Hydrogen, 300torr	MWCNT
2007 - HH Kim and HJ Kim[138]	10-70A	Xylene	Ferrocene	Xylene Ferrocene, 30-500torr	MWCNT/ SWCNT
2007 - Guo et al.[139]	50A	Graphite		Deionized water	MWCNT, 5-20nm
2007 -Duncan et al.[140]	80A &100A, 5min			Helium-Argon, 500-700mbar	MWCNT
2007 - Qiu et al.[141]	50-60A,10min	Coal	Fe	Helium, 375-525torr	DWCNT, 1-5nm
2007 - Sun et al.[142]	70-100A, 10min	Graphite	Fe ₃ O ₄	Hydrogen-Argon, 200torr	SWCNT, 0.8g
2007 - Delong He et al.[143]	80-280A	Graphite	Ni-Co	Helium, 500torr	SWCNT
2007 - Xing et al.[144]	30-75A	Graphite		Deionized water	MWCNT, 10-20nm
2008 - Grebenyukov et al.[145]	65A	Graphite	Ni-Y ₂ O ₃	Nitrogen, 50-760torr	SWCNT
2008 - Li et al.[146]	90A	Graphite	NiO-Y ₂ O ₃	Helium, 300torr	SWCNT
2008 - Fetterman et al.[147]	40-70A, 12-480s	Graphite		Helium, 600torr	CNT
2008 - Joshi et al.[25]	150A/cm ²	Graphite		Open Air, Helium, 500torr	MWCNT
2008 - Keidar et al.[148]	70-80A	Graphite	Ni-Y	Helium, 500-700torr	SWCNT
2008 - Keidar et al.[149]	180s	Graphite	Ni-Y	Helium, 500-700torr	SWCNT

Year - Author	Arc current, synthesis time	precursor	catalyst	Environment, pressure	Type of CNTs, diameter, yield
2008 - Kim et al.[150]	10A, 2min	Graphite		Beer Foam	MWCNT
2009 - Kim et al.[151]	15A	Graphite		Beer Foam	MWCNT
2009 - Charinpanitkul et al.[152]	50-250A	Graphite		Liquid Nitrogen;	MWCNT, 8-25 nm
2009 - Ha et al.[153]	30-70A, 20min	Graphite	Fe	Hydrogen, 50-450torr	SWCNT
2009 - Labeledz et al.[154]	40-60A	Graphite/Carbon black		Hydrogen-Argon, 30kPa	SWCNT
2009 - Hoa et al.[155]	85A/cm ² , 1min	Graphite	Fe-Ni-Mo	Hydrogen, 400torr	SWCNT
2009 - Jahanshahi et al.[156]		Graphite	Ni-Mo	LiCl	MWCNT/SWCN, 7.7mg/min
2010 - Jahanshahi et al.[157]	100A, 60s	Graphite	Ni-Mo	NaCl	MWCNT
2010 - Scalese et al.[158]	80A, 60s	Graphite		Liquid Nitrogen	MWCNT
2010 - Scalese et al. [159]	80A, 30sec	Graphite		Liquid Nitrogen	CNT
2010 - J Qiu et al. [160]	85-110A	Fullerene Waste soot		Hydrogen-Argon, 300torr	DWCNT, 1.08-1.44nm
2011 - Nishizaka et al. [161]	10 min	Graphite +Coal +Carbon Black		Helium, 100torr	SWCNT
2011 - Ding et al. [162]	120A	Graphite		Hydrogen-Helium, 400torr	CNTs
2011 - Hou et al. [163]	150A, 3min	Graphite	Ni-Fe-Co	Hydrogen, 200torr	SWCNT, 1g
2011 - Zhang et al. [164]	120A	Graphite		Hydrogen, 240torr	MWCNT
2011 - Su et al. [165]	100A	Graphite	Ni-Y	Helium-CO, 225torr	SWCNT
2012 - Tripathi et al. [166]	105A, 5-8min	Graphite			CNT
2012 - Kim et al. [31]	100A	Graphite		Argon	MWCNT
2012 - Zhao et al. [167]	80A	Graphite		Air, 60torr	MWCNT
2012 - Wu et al. [30]	120A	Graphite	Ni-Y ₂ O ₃	Hydrogen-Helium, 530torr	SWCNT
2012 - Su et al. [168]	90A	Graphite	Ni-Y	Helium, 375torr	SWCNT
2012 - Liang et al. [29]	80A, 100A, 150A, 8min	Graphite		Helium, 760torr	MWCNT
2012 - Zhang [169]	50A	Graphite	Fe-Rh	Hydrogen-Argon, 200torr	Few-walled CNT, 1-10nm
2012 - Zhao et al.[170]	80A, 20min	Graphite		Air, 40-300torr	MWCNT
2012 - Cai et al.[171]	210A, 4 min	Graphite		Hydrogen, 50torr	CNT, 40-60nm
2012- Hosseini et al.	70A	Graphite		NaCl Solution	MWCNT, 25-30nm

Year - Author	Arc current, synthesis time	precursor	catalyst	Environment, pressure	Type of CNTs, diameter, yield
2013 - Zhao et al.[172]	80A, 20 min	Graphite		Air, 50torr	DWCNT
2013 - Mohammad et al.[173]	75-95A, 5min	Graphite	Ni-Y ₂ O ₃	Hydrogen-Argon,150torr	CNTs, 34-44mg
2013 - Fang et al.[174]	80A, 10 min	Graphite	Fe-W	Hydrogen-Argon, 200torr	SWCNT, 10-30nm, 100-200mg
2013 - Su et al. [175]	90A	Graphite	Fe-S	Air, 0.75-135torr	Few-walled CNT, 1.6-6 nm
2014- Chaudhary et al.[176]	90A	Graphite		Methane,100, 300 and 500torr	MWCNT,10-20nm
2014- Hassan et al. [177]	30-90A	Graphite	Ni	NaCl Solution	Carbon nanostructure
2014- Anshu Sharma et al. [178]	95-100A	Graphite		Deionized water	MWCNT, 20-40nm
2015- Reis et al. [179]	85A	Graphite		Argon/Acetone, 375 to 750torr	CNT/Al
2015- Meenakshi Goyal et al. [180]	100, 150A	Graphite		Deionized water	MWCNT
2015- Anupkumar Sharma et al. [181]	100-200A, <1min	Graphite		Deionized water	MWCNTs , 15-150nm
2015- Essa et al. [182]	50A	Graphite		Ar/N ₂ /O ₂ (10 ⁻³ ,10 ⁻⁴ ,10 ⁻⁵) mbar	CNT Powder

Researchers have also used AC power supply of constant frequency to generate arc between the electrodes. The advantage of using AC arc discharge is the formation of deposits on the wall of chamber. Very few experimental attempts have been made to synthesize CNTs using AC arc discharge. In 1992, Ebbesen and Ajayan [43] reported CNTs using AC arc discharge. In 1998, Zeng et al. [183] reported MWCNTs at 700 A arc current. In 1999, Ohkohchi [184] first reported SWCNTs using AC arc discharge. In 2007, Matsuura et al. [185] reported poor quality of CNT synthesized by AC arc discharge. CNT yield in AC is found to be smaller than that of DC as it is produced during one part of cycle [43]. Chronological attempts using AC power supply have been listed in Table 2.2. In column 1 of Table 2.2 year and lead author names are given and further in column 2-column 5 gives information of arc current , synthesis time, precursor used for CNTs synthesis, environment, pressure and type of CNTs respectively. From Table 2.2 we noticed graphite has been used as carbon precursor, no literature is available on carbon black for synthesis of CNTs using AC arc discharge.

Table 2.2: Arc discharge synthesis of CNT using AC power supply

Year - Author	Arc current, synthesis time	Precursor	Environment, pressure	Type of CNTs, diameter, yield
1992 - Ebbesen and Ajayan[43]	100A	Graphite	Helium, 500torr	CNT, 2-20nm
1997 - Zeng et al.[183]	700A	Graphite	Helium, 140torr	MWCNT
1999 - Ohkohchi M[184]	85A, 1-2min	Graphite	Helium, 400torr	SWCNT
2003 - Biro et al.[186]	45-85A	Graphite	Deionized water	MWCNT, 5-10mg/min
2006 - Horvath et al.[187]	40A, 1-2 hr	Graphite	Deionized water	MWCNT, 10-35nm
2007 - Matsuura et al.[185]	70-100A	Graphite	Helium, 600torr	MWCNT
2010 - Matsuura et al.[188]	110-120A	Graphite		CNT
2011 - Zhao et al.[28]	6-20A	Benzene	Argon, 760torr	MWCNT
2012 - Jia-Shiang Su[189]	2.5A, 1.4ms	Graphite	Air	CNT
2013 - Yousef et al.[190]	75A	Graphite	Deionized water	MWCNT, 0.6gm/hr
2013 - Kia and Bonabi[191]	50A, 5-10min	Hydrocarbon	Argon, 525torr	MWCNT, 50-100nm

Few researchers have synthesized carbon nanotubes using pulsed DC power supply. In 2004 Parkansky et al. [192] suggested that the pulsed arc is advantageous over other power supply as no pressure chamber is required and can be performed in open air. Yield is found to be increased in case of pulsed as compared to DC supply [47, 48]. In 2000 Sugai et al. [195] have found yield of SWCNT increases as pulse width increases. Cathode is also found to be consumed by pulsed arc method [196]. One observation from pulsed discharge is that the CNT formation is reported at low current levels. Chronological attempts using pulsed power supply have been listed in Table 2.3. In Table 2.3 column 1 refers to year and lead name of author, column 2-column 6 gives information of arc current, synthesis time, precursor, catalyst, environment and pressure to synthesize type of CNTs. From Table 2.3 we observed CNTs synthesis were attempted using graphite as carbon precursor.

Table 2.3: Arc discharge synthesis of CNT using pulsed DC power supply

Year - Author	Arc current, synthesis time	Precursor	Catalyst	Environment, pressure	Type of CNTs, diameter, yield
2000 - Sugai et al.[195]	22A, 3-30hr	Graphite	Ni-Co	Argon, 500torr	SWCNT, 2-10mg
2001 - Murooka et al.[197]	1-2A, 1-3s	Graphite		Argon, 250-500 torr	Nanoparticles
2003 - Sugai et al.[198]	40-60A	Graphite	Ni-Y	Argon	DWCNT
2004 - Parkansky et al.[199]	7-100A	Graphite		Open air	MWCNT
2004- Sugai et al. [200]	100A	Graphite	Ni-Y	Argon	DWCNT
2005- Muhl et al. [201]	1000A	Graphite		Open air, 45mtorr	Carbon metal particles
2006 - Imasaka et al.[193]	30A, 4hr	Graphite		De-ionized water	MWCNT
2007 - Roch et al.[194]	100A	Graphite	Ni-Co	Argon, 75torr	SWCNT
2008 - Tsai et al.[202]	2-2.5A, 800-1300 μ s	Graphite	Fe	Open Air	MWCNT
2008 - Yoshida et al.[196]	50A	Graphite	Metal Catalysts	Argon, 760torr	DWCNT
2009 - Tsai et al.[203]	2.5A, 1ms	Graphite		Open Air,760torr	MWCNT
2010 - Jia-Shiang Su[204]	3-5A,1.2ms	Graphite		Open Air	MWCNT
2012 - Kia and Bonabi[205]	10A, 15min	Acetone		Argon,525torr	MWCNT
2012 - Takekosh et al.[206]	20A, 60 min	Graphite	Metal Catalysts	De-ionized water	CNT, 5 nm

2.3.1.2 Effect of voltage

In arc discharge, voltage is applied across the electrodes to generate electrical breakdown of the dielectric gas. The voltage across the electrodes for CNT synthesis ranges between 15 and 30 V. This voltage must be kept constant for stable plasma. The sudden change in arc voltage results in the formation of bamboo like structures as observed by [82]. In 2010, Scalese et al. [159] suggested that the major effect of voltage variation was found to be the spatial distribution and sharpness of CNT pillars in the deposit. In 2009, Jahanshahi et al. [156] observed fullerenes at 10 V and observed CNTs upon increasing the voltage to 30 V. In 2003, Antisari et al. [207] observed deposits of amorphous carbon with few nanotubes for voltages less than 22 V and found no cathodic deposits for voltages higher than 27 V. They have also reported

an increase in quality of nanotubes when the voltage is increased from 15 V to 20 V. Synthesis at high voltages (~700V) has been also reported [23], [53], [185], [186], [191], [208]. In Besides voltage, the synthesis time has also been investigated in literature for CNT formation. Generally, the voltage across the electrodes is maintained for 30-120s. However CNTs have been synthesized at time ranging from milliseconds [129], [204], [209] to high synthesis time of 15 min [62,63], 20 min [64–66], 40 min [71], 30-150 min [117], 60 min [206], 60-90 min [48], 1-2 h [210], and 3-30 h arc run time [195]. This is an interesting parameter and raises a question of impact of arc application time in the formation of carbon nanotubes.

2.3.1.3 Effect of arc current

One of the significant parameters in arc discharge method is the arc current. It affects the quality, yield and size of synthesized nanotubes. In an arc discharge apparatus, arc current results in emission of electrons from cathode which travel at high velocity towards anode. These electrons hit the anode surface which results in sputtering of carbon precursors. Upon increasing the arc current, the number of electrons striking the anode surface increases, thereby sputtering more carbon precursor from the anode. The applied current produces resistive heating which results in high temperature. Due to high temperature, the carbon precursor filled in anode sublimates to form carbon vapours and nucleates at cathode resulting in nanotube formation. There also exists a minimum discharge current called as chopping current at which the plasma production is insufficient and leads to arc extinction.

During the synthesis, non-fluctuating current of an order of 50-100A is maintained to ablate the anode. In 1995 Ebbesen and Gamaly [14] suggested that the current density for synthesis of CNTs should be around 165-195 A/cm². In 2002, Cadek et al. [84] studied the dependence of arc current on the yield of nanotubes and concluded that the yield increases as current density is varied from 165 A/cm² to 195 A/cm². In 2009, Matsuura et al. [188] observed better yields of SWCNT at a current density of ~450 A/cm². In 2011 Nishizaka et al. [161] found the optimal current density for SWCNT formation as 250-270 A/cm². In literature, vast variations have been reported in arc current, from 2.5 A/cm² to 900 A/cm², which creates an ambiguity of the optimum arc current rating. A Bar graph in Figure 2.5 shows the comparative view of the current ratings on x-axis and number of papers on y-axis used in published literature on synthesis of CNT using

arc discharge. It can be observed from the graph that majority of the experiments have been conducted between the range of 50 and 100 A.

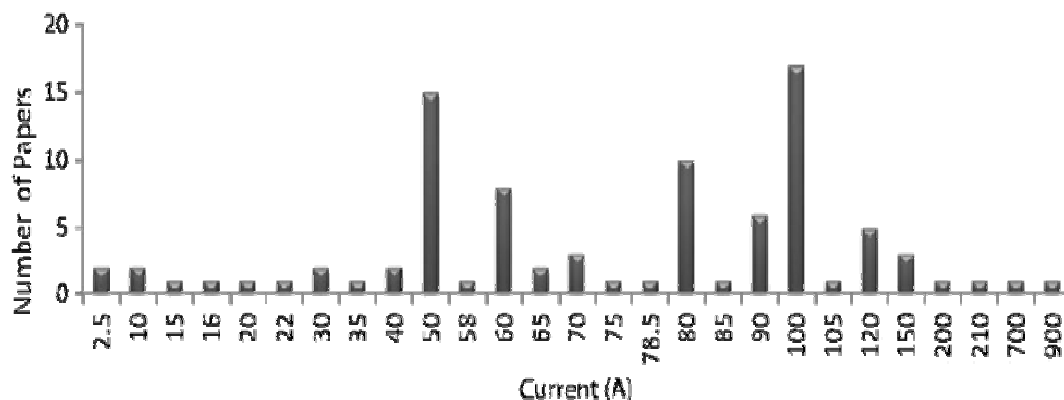


Figure 2.5: Variation in current values used in literature to synthesize CNTs using arc discharge

Attempts to understand the effect of variation of current has been done by many researchers in literature. In 2002, Cadek et al. [84] studied the effect of varying current density and pressure during arc generation on yield and purity of MWCNTs. In 2011, Nishizaka et al.[161] observed the production of graphite in the soot and found it to be dependent on current density of arc discharge. In 2009, Matsuura et al. [188] developed techniques for obtaining new type plasma reactor with twelve phase AC discharge with varying current. It has been observed that at currents below 30 A, the arc is unstable and lower yields are obtained. The anomalies in the current levels corresponding to CNT formation are noteworthy. In 2007, Okada et al. [135] have reported a low current synthesis of 1-20 A whereas in 2007 Delong. He et al. [143] suggested that the nanotube formation takes place at current levels beyond 100 A. In 1999 Takizawa et al. [58] found the highest nanotube yield at 100 A. Researchers have produced CNTs at low arc current of 2-10 A [205], [211][189], [202], [212] and at high arc currents of 700 A [183] and 900A [78].

It has been observed that as current increases, the yield increases [186][77, 87] however increasing the arc current does not improve the structure of CNT [159]. In 2007, He et al. [143] observed that the increase in arc current reduces the amount of SWCNTs and favors the formation of amorphous carbon particles. In 2012, Zhao et al. [170] studied the variation of pressure along with the variation in arc current. In 2002, Tang et al. [79] investigated reduction in the arc current by changing the shape of cathode. In 2006, Lange et al. [129] observed that a carbon precursor with smaller

grain size requires lesser arc current for nanotube formation. However, it raises an interesting debate on the optimum current requirements for nanotube formation. There obviously as the range of current requirement is very wide ranges from 1A to 900A is a critical need to develop a strong correlation between optimum current levels and formation of nanotubes.

2.3.1.4 Frequency

The frequency of the power supply has been found to affect the quality of the deposits produced in arc discharge. First reported by Ohkohchi et al. [184] in 1999, AC arc discharge has been found to produce high quality SWCNTs. In literature, the effect of variation in frequency has not been explored that emphatically as other parameter. In 2012, Kia and Bonabi [205] found that at low frequencies of 50 Hz, better growth of CNTs is observed at anode, however at high frequencies of 400 Hz, the rate of soot production on cathode increases. This can be an interesting area for investigation and may lead to value addition to studies available on growth mechanism of CNTs.

2.3.1.5 Effect of grain size

One of the less explored aspects of arc discharge is the effect of grain size of electrode material i.e. of graphite, soot and carbon black on current requirement and nanotube production. It seems logical that a smaller size of grain size particle available for conversion to CNTs requires lesser energy to vaporize. Solid state properties namely cohesive energy of cathode and anode play vital role in the quality of the nanotubes formed. The cohesive energy [213] is found to depend upon the particle size [214]. In 2006, Lange et al. [129] used carbon precursors with different grain sizes and found that the current requirement reduces drastically by changing the grain size. In 2009, Labedz et al. [154] investigated the effect of particle size and the carbon density of the electrode. They found that the anode with smallest particle size and more electrode density yields lesser CNTs and more carbonaceous particles. Also, the particle size may affect the diameter of the synthesized nanotubes. It was observed that larger grain size results in smaller diameter of synthesized CNTs [154]. Investigation on grain size of electrode material may be a potential area and validations are required to develop a link with formation of nanotubes.

2.3.1.6 Role of catalyst

The catalyst used in arc discharge synthesis of CNTs is usually a metal, which is powdered and filled in either side of the electrode along with a carbon precursor. The metal should have low boiling temperature and high evaporation rate acts as a good catalyst in nanotube formation [22]. Figure 2.6(a), (b), (c) consist of two electrodes mounted horizontally; cathode with hemispherical shape at corner from center and similarly anode of pure graphite rod but having a hole at the center filled with carbon precursor and metal particle.

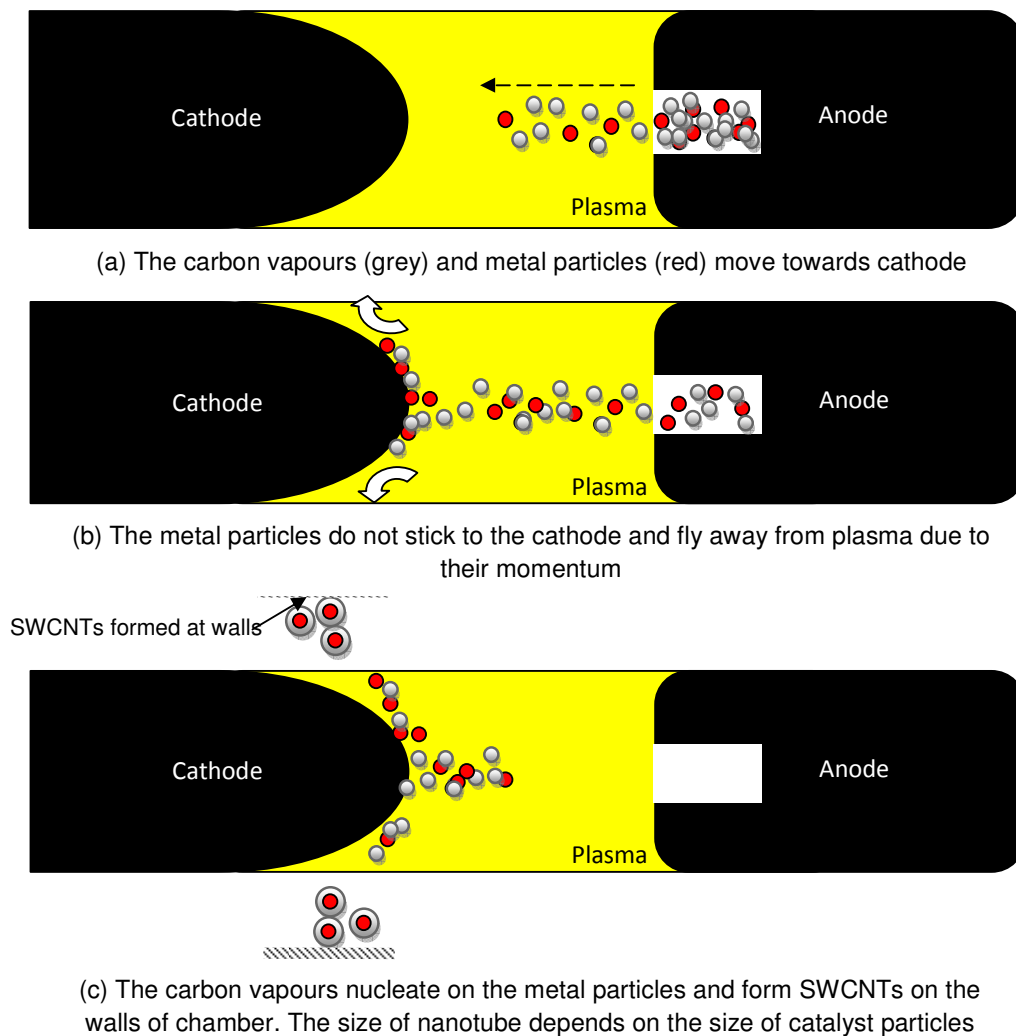


Figure 2.6: Role of catalyst in growth of CNTs

In Figure 2.6(a) when arc current is applied, the metal atoms as indicated in figure by red circle vaporize along with the carbon precursor i.e. grey circle and move straight as directed by arrow towards cathode. The metal particles agglomerate with carbon

vapours and nucleate at arc reactor walls as shown in Figure 2.6(b). Since metal particles i.e. red circle do not stick to the surface of the cathode, they fly away due to their momentum and moves in circular motion towards the wall and form SWCNTs. There is no established reason for deposition of SWCNTs on walls of chamber as shown in Figure 2.6(c) instead of cathode and is an open area for investigation. A probable reason for this behavior may be that the carbon vapours along with the liquid metal move towards cathode in the plasma. The size of nanotube formed depends on the size of catalyst particles.

The catalyst favors the growth of SWCNTs than MWCNTs. In 1994, Lin et al. [49] experimentally confirmed that the presence of metal catalyst in gas phase which on the surface of the cathode alters the temperature distribution and prevents the growth of MWCNTs on cathode. The most commonly used catalysts are Nickel (Ni), Iron (Fe), and Cobalt (Co) along with Yttrium(Y), Sulphur(S), and Chromium (Cr) added as a promoter. Mostly, SWCNTs are observed in the presence of catalyst, whereas MWCNTs are produced in its absence. However some reports on MWCNT formation in the presence of catalyst have been reported in literature [132], [156], [209] [93,94,95,96,97]. The interesting observation among these reports is that MWCNT synthesis occurs with binary catalyst means by using two catalysts. Zhao et al. [121] reported that no CNT formation occurs without the use of catalyst.

Few researchers have investigated the role of various catalysts on the quality of the CNTs formed. Among the metals, Ni and Fe have been most widely used catalyst for the growth of high quality CNTs. Both Ni and Fe increase the yield and quality of CNTs. Nickel is found to produce more crystalline nanotubes as reported in literature. Ni is mixed with elements like Y, (Molybdenum) Mo, Fe, Co, and Cr to improve the synthesized product. Fe is generally added with sulphur or W to facilitate growth of SWCNTs. The drawback of using Fe as catalyst is the formation of its oxides (Fe_2O_3) which doesn't act as catalyst and retards the growth of SWCNTs. In 2001, Li et al. [217] suggested that the Fe promotes the length of the nanotubes. In 2013, Zhao et al. [172] suggested that the addition of sulphur to Fe catalyst results in the development of a core/shell at the cathode due to different melting points. This core/shell promotes the growth of DWCNTs. In 2005, Zhao et al. [121] observed a more uniform distribution of (Amorphous Carbon nanotubes) ACNT diameter upon using FeS catalyst as

compared to Ni/Co alloy. In 2006, Wang et al. [133] suggested that sulphur plays a major role in the formation of branched CNTs. It forms an active site on the surface of the catalyst where nucleation of carbon vapours takes place. In 2001, Ando et al. [75] observed that sulphur promotes the growth of CNTs by removal of the terminating species at the nanotube ends. The catalyst may also control the wall number of synthesized CNTs. In 2005, Yang et al. [113] observed addition of KCl to Ni-Co mixture changes wall number from single to double walled nanotubes. In 2005, Montoro et al. [120] observed that VO (Vanadium(II) oxide) group also promote nucleation of carbon vapors in the synthesis of CNTs. In 2006, Qiu et al. [127] observed that KCl also promotes the formation of DWCNTs.

The size of nanotubes can be readily controlled by using appropriate size of metal catalyst particles. The carbon vapors move along with the metal particles and nucleate on these to form nanotubes. Thus, the size of metal particles plays a vital role in nanotube diameter distribution. The concentration of metal particles is found to affect the yield of nanotubes produced. The composition of catalyst also plays a major role in the existence of CNTs. In 2004, Wang et al. [100] reported that the maximum concentration of iron particles in the anode composition must not exceed 10% for CNT formation. One reason for this may be that larger concentration of catalyst particles restricts the motion of carbon vapors towards cathode. In 2007, Keidar [24] suggested that SWCNT synthesis is governed by catalyst - carbon phase diagram. The effect of various catalysts on CNT formations as reported in literature is tabulated in Table 2.4. In column 1 of Table 2.4 base catalyst are given and Column 2 represents the mixture of catalyst used for formation of CNTs. Column 3 gives the information about the effect of catalyst to synthesize nanotubes.

Table 2.4: Effect of catalyst on CNT formation

Base catalyst	Mixture used	Comments
Ni	Ni	Promotes the growth of SWCNT [22]
	Ni -Y	Y alone cannot synthesize CNT formation [48] Addition of Y to Ni reduces the yield [59] Y promotes the growth of SWCNT [45]
	Ni -Mo	Mo does not affect CNT formation [135]

Base catalyst	Mixture used	Comments
	Ni -Mo-Fe	Mo-Fe favours CNT formation [135]
	Ni -Co	Results in SWCNT formation [113]
	Ni -Co + KCl	Results in DWCNT formation [113]
	Ni -Cr	Results in MWCNT formation [134]
	Ni -Ho	Increases yield and purity [184]
	Ni-Co-Fe-S	Diameter of SWCNT increases with sulphur[81][89]
Fe	Fe	Affects yield and diameter of MWCNT [100]
	Fe-FeS	Addition of sulphur promotes growth of DWCNT and increases the yield [172]
	Fe-Fe ₂ O ₃	Retards the growth of CNT [116]
	Fe-Fe ₃ O ₄	Increases the yield of SWCNT [142]
	Fe-W	Tungsten reduces the diameter and increases yield of SWCNT [174]
	Fe-Fe(C ₅ H ₅) ₂	Improves yield of SWCNT [138]
Ca	Ca	Produces smaller diameter CNT than Ni [65][46]
Rh-Pt	Rh-Pt	Increases the yield [55]
Co	Co	Superior catalyst for DWCNT production [115] Increases the mean diameter of DWCNT [196]
	Co-CoS	Addition of Sulphur promotes CNT production [126]

2.3.1.7 Role of atmosphere

The atmosphere plays an important role in thermo-ionic effects, plasma formation, and provides the thermal growth of CNT and the necessary annealing effects. When the arc current flows through the electrodes, the gas gets ionized due to high temperatures and plasma is formed. The ionized gas acts as a highly conducting medium which provides transfer of mass on either side. The ions in the plasma are thermally agitated and provide the necessary energy for movement of carbon vapors. The atmosphere also plays a significant role in the thermal growth of CNTs. The thermal conductivity of the atmosphere provides annealing effects at the cathode which is essential for nanotube formation. The atmosphere also regulates the temperature of plasma depending on its ionization potential.

The gas with higher ionization potential will require large arc current for breakdown. Thus, the choice of atmosphere depends on its ionization potential and thermal and electrical conductivity.

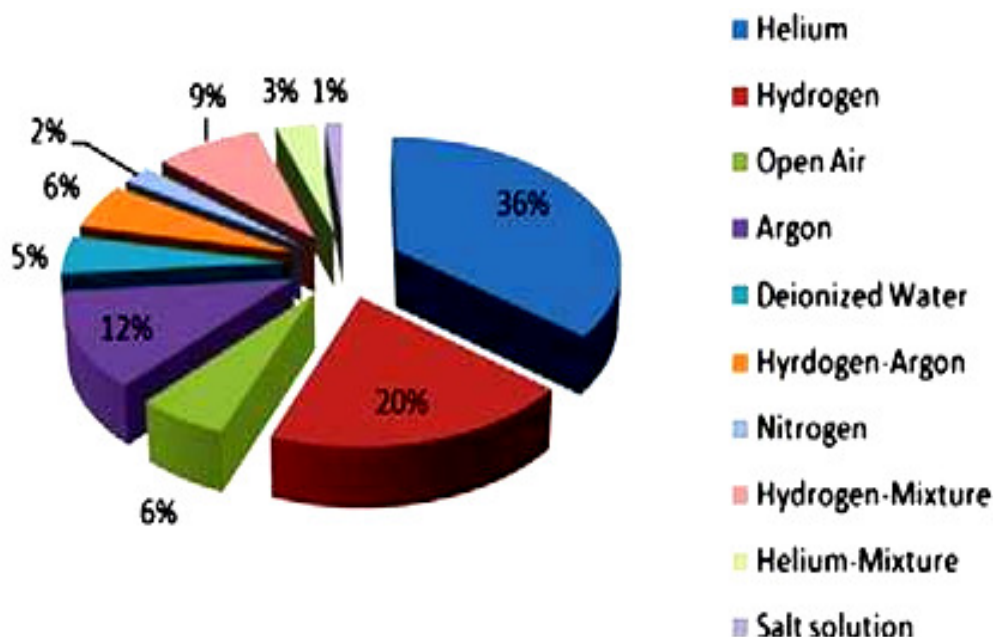


Figure 2.7: Pie chart showing percentage of papers on synthesis of CNT using arc discharge method under different atmosphere

Figure 2.7 shows the pie chart of percentage of papers published under different atmosphere. It can be observed from pie chart Helium is most used atmosphere and salt solution is least used. The arc chamber is pressurized with a gas like nitrogen, hydrogen, helium or argon or immersed in a liquid environment. Hydrogen has the highest thermal conductivity and is regarded as the most efficient quencher in nanotube growth. In 1998 Zhao and Ando [57] suggested that hydrogen promotes the growth of CNTs and reduces the carbonaceous materials by forming hydrocarbons with them. In 2000, Tang et al. [64] observed that rapid introduction of hydrogen prevents the ends of nanotube from closing. Due to this problem, hydrogen is generally mixed with a noble gas like argon or helium to stabilize the plasma. In 2000, Shi et al. [65] observed that helium atmosphere strongly affects the yield of SWCNTs. In 2001, Farhat et al. [18] controlled the diameter of nanotubes by changing the composition of argon-helium gas ratio. In 2003, Li et al. [91] found that hydrogen results in a cleaner CNT surface as it selectively etches the amorphous carbon impurities. However, In 2003 Zhao [92] suggested that pure hydrogen is unfavorable for mass production of SWCNT

due to the instability of arc discharge plasma. In 2004, Liu et al. [97] found that changing of gas from hydrogen to helium promotes the growth of SWCNT. In 2005, Ando et al. [112] observed the increase in yield upon addition of nitrogen to hydrogen when compared to H₂-Ar mixture. The H₂-N₂ has more enthalpy than H₂-Ar which promotes the evaporation of C-Fe mixture. In 2011, Su et al. [165] investigated the effect of CO concentration on the amount of impurities present in SWCNTs. They suggested that lower concentration of CO should be preferred for better SWCNT yield.

Apart from the gaseous atmosphere, liquid environments have also been used to produce CNTs. In case of liquid environments the CNTs are found to be floating on the surface of the liquid. The most popular choice of the liquid environment in the literature is deionized water. Few works [101, 114] have synthesized CNTs in NaCl solution owing to its good electrical conductivity, better cooling ability than deionized water and lower cost than liquid nitrogen and helium. NaCl dissociates into Na⁺ and Cl⁻ ions which provide better ionic conductivity to the plasma. The concentration of Na⁺ ions is a critical parameter for better yields. The excess of Na⁺ ions hinders the locomotion of carbon vapors from anode and reduces the yield of the SWCNTs [116]. Other solutions like LiCl [156], H₃PO₄ aqueous solution [120], and beer froth [150] have been used as atmosphere in synthesizing CNTs using arc discharge. In 2008 Kim et al. [150] suggested that the agglomerating effect of both beer froth and carbon nanotubes helps in obtaining a cleaner product. The CNTs stick to beer froth and the other carbonaceous materials get separated out. The effects of different atmosphere in arc discharge chamber on yield, quality and size of nanotubes are listed in Table 2.5. In Table 2.5 column 1 refers to type of atmosphere and column 2-column 3 represents effect of atmosphere on yield, quality and size of nanotubes.

Table 2.5: Effect of different environment on CNT formation

Type of Atmosphere	Effect on yield and quality of nanotubes	Effect on size of nanotubes	Comments
Hydrogen	Formation of MWCNT is highly graphitized and have crystalline perfection[75]	H ₂ discharge is better compared to He as it produces twice aspect ratio nanotubes [75]	Hydrogen is more effective for MWCNT formation [132]
Hydrogen - Helium		H ₂ -He produces in growth of CNT with small diameter [169]as compared to H ₂ -Ar.	
Hydrogen - Argon	H ₂ added to Argon increases the yield [114][71]		

Type of Atmosphere	Effect on yield and quality of nanotubes	Effect on size of nanotubes	Comments
Helium	Yield of SWCNT increases in He [55]	Diameter of synthesized CNT in air atmosphere is smaller than in He [132]	He results in uniform cathode deposit[82]
Argon		Argon produces smaller diameter CNT compared to He [4][218]	
Nitrogen	N ₂ at low pressure yield more SWCNT [118] and MWCNTs [207]	Diameter of MWCNTs decreases with the increase of the N ₂ [145]	Nitrogen atom incorporated for closure of CNT[219]
Hydrogen-Nitrogen		Diameter distribution can be controlled by varying the mixture ratio of H ₂ and N ₂ gas.[112]	
Open Air	Better yield in open air than He[25]		
CO		CO plays requisite role for selective diameter growth of SWCNT [165]	
Krypton	Yield of SWCNT is more in Kr compared to Ar [195]		
NaCl Solution		Observed short CNTs in NaCl solution [116]	

2.3.1.8 Effect of pressure

In arc discharge method, the role of pressure is to provide energy to the gas molecules and to act as a wall for a steady flow of ions between the electrodes. In literature the effects of pressure on yield and quality of synthesized nanotubes have been vastly explored. In 2003, Cui et al. [219] found that the nanotube yield decreases for low and high pressures of nitrogen. In 2006, Kim and Kim [132] observed MWCNTs in air and helium at 300 Torr and 500 Torr respectively. In 2008, Grebenyukov et al. [145] found that the efficient pressure for nitrogen is 350 Torr. In case of air, 45-90 Torr has been found to be the optimum pressure [175]. The yield of synthesizing CNTs is reduced upon increasing the air pressure from 40 to 300 Torr [170]. The pressure versus yield trend for helium has been studied by few groups [13,104,123,124] and pressure ranging from 500 to 700 Torr has been found to be optimum. However reversal in trend has been shown by Park et al. in 2002 [81] who observed a decrease in yield on increasing the pressure from 100 to 500 Torr. Also, Shi et al. [46] in 1999 reported high yield of 2.5 g/h for helium pressure of 1520 Torr. Optimum hydrogen pressure is found to be 500 Torr [47]. The yield increases from 100 to 700 Torr but decreases beyond 700 Torr [127]. In 2001 Farhat et al. [18] have reported that the optimum argon pressure is

100 Torr. It may be concluded from the reports in literature that the optimum pressure condition for high yield of CNTs has been found to be ~500 Torr. Figure 2.8 the bar graph showing the range of pressure on x-axis and number of paper on y-axis for CNT synthesis, the optimum range of pressure has been found ranging from 300 to 700 Torr. At pressure below 300 Torr, the yield is found to be very low as the density of ions is low resulting in unstable plasma. Whereas at high pressure, more number of ions participate in the plasma thereby restricting the motion of carbon vapors from anode to cathode and decreases the yield. That is why high pressure is unfavorable for the synthesis of CNTs and very less number of researchers has used pressure beyond 700 Torr as shown in Figure 2.8. However, some anomalies that have been reported need to be investigated for better understanding of the growth mechanism.

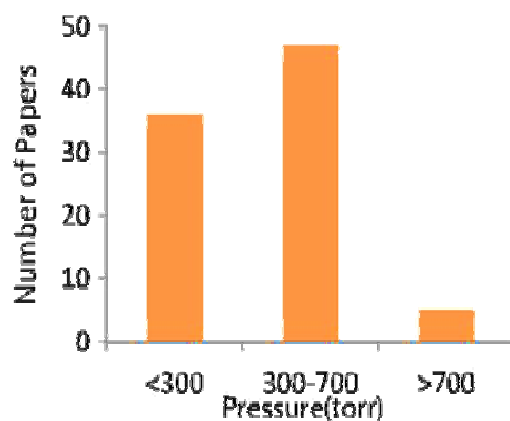


Figure 2.8: Bar graph showing number of papers published at different range of pressure

2.3.1.9 Role of temperature

The temperature ionizes the gas and forms the plasma. It simultaneously sublimates the carbon precursor and provides thermal flux for decomposition of carbon vapors into ions. It is responsible for thermo-ionic emission of carbon ions and finally helps in nucleation of carbon vapors at cathode to form CNTs. Temperature variation in plasma significantly affects the quality and size of the CNTs. Temperature required for growth and nucleation in arc discharge synthesis is achieved by the electric arc. The temperature increases as the current density is increased, thereby sublimating the anode at a faster rate. Higher temperature results in more crystalline CNTs. The temperature of the plasma is regulated by the thermal properties of atmosphere. Hydrogen plasma generates higher temperature of 3600-3800 K, whereas Argon plasma restricts the plasma temperature to 2200-

2400 K. The temperature gradient across the two electrodes is dependent on the diameter of the electrodes. A smaller diameter anode has higher current density and has high temperature which is favorable for sublimation of carbon precursor, whereas cathode with larger diameter has less current density and is cooler than anode and facilitates nucleation of CNTs. This is why cathode diameter is selected to be greater than anode diameter. In literature, the effect of temperature on nanotube formation has not been vastly explored and is a potential area of investigation for better understanding of the growth of CNTs. Among few published reports, In 2000 Sugai et al. [195] suggested that SWCNT formation takes place in strong annealing condition. In 2002 Doherty and Chang [220] observed a decrease in yield of MWCNT on an increase in temperature. In 2003, Lange et al. [221] have found an average plasma temperature ranging from 4000 to 6500°C in water for synthesizing well crystallized nano-onions and nanotubes. In 2004, Nishio et al. [99] observed high yield at high plasma temperature ~3500K. In 2004, Liu et al. [97] found that an increase in temperature increases the yield of CNT. However Zhao and Liu [103] in 2004 suggested that SWCNT diameter reduces with an increase in temperature but yield increases. In 2005, Zhao et al. [121] suggested that optimum temperature for CNT formation is 600°C beyond which diameter decreases. In 2007, Matsuura et al. [185] have suggested optimum range for CNT formation of 1000-1250°C. In 2007, Keidar [24] observed nanotube formation in region of plasma temperature of 1300-1800 K, where carbon reacts to form large molecules or clusters. In 2008, Joshi et al. [25] have found that temperature requirement for MWCNT is the least followed by DWCNT and SWCNT for nucleation and growth. Kim et al. [31] in 2012 have discussed that nanotube growth occurs below 2000°C even though inter-electrode temperature approaches more than 4000°C.

2.3.1.10 Effect of setup modification

The basic arc discharge apparatus described and shown in Figure 1 has been modified by the researchers over the years to improve the quality, size and yield of CNTs. In 2004 Zhao and Liu [103] reported an increase in yield of SWCNTs by using six anodes as shown in Figure 3.1(a). Researchers [16], [25], [31], [222] have used a rotating carbon cathode for a homogeneous micro-discharge resulting in good quality nanotubes. In 2008 Joshi et al. [25] found a 50-55% increase in yield at lower electrode disk rotation speed compared to higher disk speeds. In 2001, Kanai et al. [72] have proposed a gravity free discharge for high yields. In 2001, Ando et al. [69] inclined the

cathode and anode at an angle of 30° to improve the yield of the process as shown in Figure 3.1(d). In 2002, Lee et al. [222] suggested that rotating electrodes result in continuous growth of nanotubes as the carbon vapors move out due to centrifugal force resulting in uniformly distributed plasma. In 2006, Horvath et al. [210] also investigated the effect of angle between two electrodes immersed in water and found that highest yield is obtained at 90° inclination. Upon inclination of the electrodes, a majority of the product does not get deposited on the cathode and the deposition mostly flies away to the walls, thereby increasing the yield of SWCNTs.

2.3.1.11 Effect of cathode shape

The geometry of the electrodes is also a potential area of research and greatly affects the quality of the product. Usually the anode is chosen to be of smaller diameter than cathode which results in increased current density at anode, thereby subliming the precursor at lower current levels. Cathode being larger in diameter will be at lower temperature due to less current density and allows the liquid carbon to nucleate. Thus, flow of carbon ions is achieved from anode to cathode. The relative size of electrodes affects the plasma temperature distribution which directly affects the synthesized product. However, upon using similar electrodes the deposition is not found on cathode but on the chamber walls [183].

The effect of change in electrode shape and size has been studied in literature by few groups. Researchers [101], [171] have observed deposition on anode for cathode diameter less than anode diameter. In 2002, Tang et al. [79] have found a reduction in current requirement by using a cupped cathode and in their design, outer diameter of synthesized MWCNT increases. In 2004, Nishio et al. [99] and in 1999 Shi et al. [46] found that the yield decreases upon using a sharp cathode. In 2006, Wang et al. [125] suggested a reduction in cathode area in order to increase SWCNT production which is formed at the walls of chamber. In 2008, Joshi et al. [25] suggested that the cathode surface topography may play a decisive role in nanotube formation. In 2008, Fetterman et al. [147] have found an increase in yield for smaller diameter anode. In 2012, Raniszewski et al. [223] have suggested that anode tip diameter should be lower than 10 mm. In 2012, Kia and Bonabi [205] concluded that the shape of electrodes affects the yield of CNTs.

2.3.1.12 Size and yield of CNT in arc discharge

The major concern of arc discharge CNT synthesis is to improve the yield of the product. However, arc discharge technique has not been successful in producing pure CNTs at large scale due to difficulty in controlling the experimental parameters. The yields of nanotubes depend on the arc current, catalyst composition and its particle size, atmospheric effects and electrode shape and composition. In 2004, Nishio et al. [99] suggested that the yield of nanotube depends on the cooling rate too. However, cooling rate is dependent on arc current, cathode size, and thermal conductivity of gas and temperature gradient. Typical yields are of the order of few milligrams for a synthesis that runs several minutes and thus makes this technique less preferred over CVD. However researchers have improved the yield through this technique by controlling the synthesis parameters. Few studies related to modified setups have been already been discussed above which have improved yield of synthesizing CNTs substantially. Some reports on variations in current and pressure values, electrode diameters, catalyst composition and atmosphere have been suggested to optimize the arc discharge. The typical yield of nanotubes obtained in arc discharge is ~20-50 mg/min per synthesis. However few attempts to produce CNT through semi-continuous and continuous arc discharge have been made and yields of 2 g/h [68] and 6.5 g/h [47] have been achieved. The control of size and diameter in nanotubes is still unanswerable. The size of SWCNTs may be controlled by using the desired size of catalyst particles. SWCNT diameter increases by 0.2 Å upon increasing the argon helium ratio by 10% [18]. A summary of the effect of various parameters on size and yield of nanotubes has been tabulated in Table 2.6. In Table 2.6 Column 1 represent parameter and Column 2-column 3 gives the detail effect of different parameter on size and yield of CNTs.

Table 2.6: Effect of different growth parameters on size and yield of CNT

Parameter	Effect on size of nanotube	Effect on yield
Catalyst	<ul style="list-style-type: none"> • Diameter of SWCNT increases with sulphur [224][89] • Diameter increases by using Co[196] • Tungsten reduces the diameter of SWCNT [174] • Observed smaller diameter SWCNT when Ca- Ni catalyst [46] 	<ul style="list-style-type: none"> • Yield of 4g/h obtained by optimizing the composition of catalyst [115] • Increase in yield with catalyst [142]
Temperature	<ul style="list-style-type: none"> • Increase in temperature reduces the diameter [103][121]. • Diameter of MWCNT increases with increase in temperature [137] 	

Parameter	Effect on size of nanotube	Effect on yield
Electrodes	<ul style="list-style-type: none"> • electrode have significant effect on diameter and purity of SWCNT[223] • Increasing the cathode diameter from 0.8 to 2 cm, length of SWCNT increases from 1.2 to 1.8μm [168] 	<ul style="list-style-type: none"> • Smaller anode diameters increase the yield [147] • Adjusted the angle between two electrodes and found that 90^o angle produces the best yield. [69][187]
Atmosphere	<ul style="list-style-type: none"> • Observed short CNT in NaCl solution [116] • When atmosphere changes from H₂-Ar to H₂-He, it results in smaller diameter CNT[169], • Ar affects the diameter of SWCNT in He-Ar mixture [18][24] • Diameter distribution of SWCNT changes by varying the kind of inert gas[130] • Diameter of synthesized CNT in air atmosphere is smaller than in He .[132] 	<ul style="list-style-type: none"> • Krypton increases the yield [195]
Grain size	<ul style="list-style-type: none"> • Smaller diameter CNTs were formed with larger grain size[154] 	
Current	<ul style="list-style-type: none"> • Increasing the current increases the diameter[152] 	<ul style="list-style-type: none"> • Increase in current increases the yield [186] • Maximum yield at 8A [28]
Setup modification	<ul style="list-style-type: none"> • Diameter under 0G condition is 3.7 times larger than 1G[72] 	<ul style="list-style-type: none"> • Increase in yield by rotating electrodes [25][170]
Pressure	<ul style="list-style-type: none"> • Growth of SWCNT with small diameter can be suppressed when pressure of CO greater than 4kPa [165] • SWCNT diameter was independent of pressure in pure He environment [133] 	<ul style="list-style-type: none"> • Yield increases as pressure increases from 250 to 400 torr[173] • Low yield for pressure below 100 torr[85]

Apart from various arc parameters playing a vital role in synthesis of CNTs as well as their properties, the precursor used to synthesize CNTs are equally important. Published literature contains wide variety of precursors and which separately are curiosity of researchers. In next section, various precursors used in synthesis of CNTs using arc discharge are presented and reviewed.

2.4 Carbon Precursors in Arc Discharge

The synthesis of CNTs is carried out by sublimation of a carbon precursor using an external power source; in case of arc discharge, the applied current ablates the carbon precursor to form carbon vapors, which nucleates to form a nanotube. A pie chart in Figure 2.9 shows the percentage of papers published on CNT synthesis using various carbon precursors. It can be observed from the figure that most of the arc discharge synthesis of CNTs has been carried out using graphite as precursor. It is an excellent conductor of heat and electricity and is commercially available in high purity. When

graphite is subjected to high current, the lattice structure breaks and releases C1 or C2 carbon species that vaporize due to high temperature. Some researchers have used coal as a starting material to synthesize CNTs. Coal is a mixture of aromatic and aliphatic hydrocarbon molecules, which are highly reactive in nature. In 2007, Qiu et al. [225] have discussed coal as an ideal starting material for large synthesis of DWCNTs.

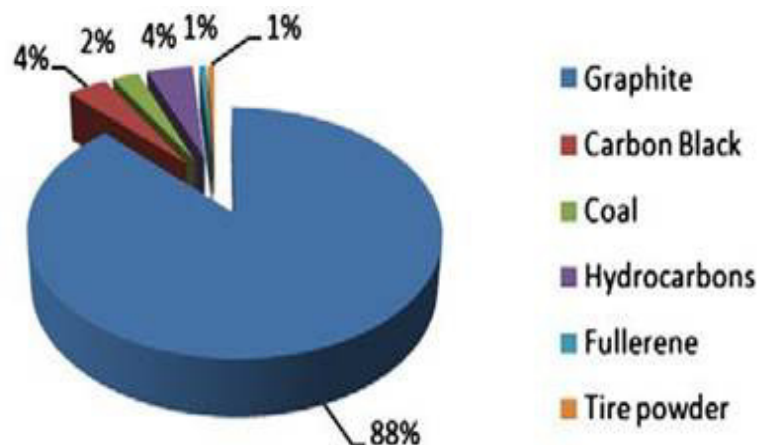


Figure 2.9: Pie chart showing percentage of papers using various carbon precursors for nanotube formation

When high arc current passes through coal, the weak linkages between the polymeric aryl structures get broken down into alkyne and aromatic species that further form DWCNTs. Coal contains sulphur, which favors the growth of DWCNTs and affects the diameter distribution of the nanotubes produced. Other carbon sources like fullerene waste soot [160], toluene [135], tire powder [108], poly-vinyl-alcohol [100], MWCNT/carbon nanofibers [115] and other hydrocarbons [28], [210] have been also used to produce CNTs by arc discharge method. Whereas graphite is the mostly investigated precursor, the other precursor materials are less explored and need further investigations.

Carbon black as carbon precursor for formation of carbon nanotube finds an important place in the pursuit of CNT synthesis. Synthesis of CNTs is obtained by subliming carbon precursor by applying the arc current. The applied current ablates the carbon black filled inside the anode to form carbon vapors then it gets deposited to cathode surface. Deposition was collected and observed using Field electron scanning electron micrographs (FESEM) and Transmission electron micrograph (TEM) analysis. Carbon black is

interesting as precursor due to its “waste to product” utility value, low cost and till date most challenging to get converted to CNTs.

Over the last two decades there are very few reports available on carbon black as a raw material in formation of carbon nanotubes. In 2000, Setlur et al. [226] proposed method for production of MWCNTs through heat treatment of various nongraphitizable carbon precursors. In 2002, Doherty et al. [86] reported the synthesis of high crystalline quality MWCNTs from carbon black without catalyst. In 2006, Doherty et al. [124] suggested the growth of CNTs from carbon black in high temperature arc furnace with an external applied magnetic field. In 2006, Lange et al. [129] used carbon black as a raw material for synthesis of SWCNTs. In 2006, Chen et al. [126] have utilized the carbon black as a dot carbon source in formation of DWCNTs and discussed that the structure of carbon black is significant for influencing purity, bundle formation and purifications of DWCNTs. Carbon black vaporizes into carbon clusters (C_2 and C_3) therefore it increases the supply of nanotube precursors to form DWCNTs. In 2008, Donnet et al. [26] discussed the growth of MWCNTs on carbon black by combustion flame method. Nanotube formation takes place in three stages, in first stage transformation of carbon black to graphitic seeds then in second stage generation of tubes from graphitic seeds due to high condensation of ad atoms. Finally, the continuous growth of these tubes happens by adsorption of carbon atoms onto nanotubes. In 2009, Labeledz et al. [154] observed the influence of various carbon powders on synthesis of SWCNTs in carbon arc plasma. In 2011, Nishizaka et al. [161] investigated the production of graphite in the soot of SWCNTs using poorly graphitized carbon (PGC) rod in comparison to graphite rod. PGC rod was produced by using mixture of coal tar and carbon black. In 2011, Dasgupta et al. [227] synthesized carbon nanotubes in large quantity in a fluidized bed reactor by catalytic cracking of acetylene and methane over carbon black. He has used low cost precursor in order to produce CNTs economically.

In 2012, Doherty et al. [228] discussed the solid state transformation of carbon black to MWCNTs from high temperature arc furnace without a catalyst. Researchers show that the presence of catalyst is not enough for SWCNTs growth but also carbon material structure also plays the role in formation. In 2012, Dasgupta et al. [229] observed the synthesis of bamboo-shaped MWCNT in a fluidized bed on a Nano-agglomerate material such as carbon black from acetylene. In 2015, Li et al. [230] discussed the synthesis and

characterization of carbon nanostructures by evaporating the pure graphite and carbon black by detonation gas arc discharge.

From Section 2.1 to 2.4, we comprehensively reported research on CNT synthesis through arc discharge route. In the reporting, various verticals like arc parameters, the arc chamber, atmosphere, power supply, carbonaceous precursors for synthesis and electrode shapes makes interesting contribution towards improvisation of yield and properties of synthesized CNTs. Understanding on most of these verticals are still half way through to clarity and all of them presents as beckoning problem to investigation. Keeping in view the time for completion of thesis and vitality in context to contribution, we defined the objectives for the thesis which are given in next.

Objective of the present work are the following:

1. To develop and design the arc discharge setup for synthesis of CNTs.
2. We choose different grades of Carbon black as carbon precursor to synthesize Carbon nanotube using arc discharge method since it has not been reported in literature.
3. Investigations on different grades of Carbon Black using DC arc discharge method.
4. Role of parameters such as arc current and temperature in synthesis of CNTs using DC arc discharge setup. Also the role of applying pulsation arc in comparison to application of DC arc discharge.

The objectives listed above are elaborated and explained below:

No standard design of arc discharge is available in literature; neither the setup is available off the shelf therefore a customized design of experimental set up including arc discharge chamber; controllable power supply and pulsating power supply have been done as first step towards working on further investigations. The design is presented in Chapter 3.

Most of the Literature is available on graphite as a precursor to form carbon nanotubes. Carbon black has been also used as precursor but in limited manner. We choose carbon black as precursor because of appealing “waste to product” associated with carbon black. CB is available in different grade but it has not been investigated and reported in literature that among many grades of available carbon black does every type of grade of

carbon black is amenable to conversion into CNTs? If not, what can be the reason and this becomes the first problem to be investigated and the results of investigation are presented in Chapter 4.

From literature review, constant current and non-fluctuating arc stands out as clear candidate influencing formation of good quality CNTs. But does a constant current lead to non-fluctuating arc? Is non-fluctuating arc characterized by constant temperature in the “zone of formation of CNTs”? In examinations reported in literature, significance of temperature in “zone of formation” has not been investigated. Hypothesizing a constant current, non-fluctuating arc and stable “zone of formation” indicates constant temperature, it is pertinent therefore to investigate the state of temperature in “zone of information” and conclude from there its importance using DC arc discharge setup. It further needs to be answered if time of arc application vis-a-vis magnitude of current has any correlation in formation of CNTs. Moreover, the effect of applying pulsed arc discharge in comparison to application of DC arc needs another investigation. These investigations have been reported in Chapter 5.

2.5 Summary

1. We have presented literature available for synthesis of CNTs using arc discharge method and we observe that there exist a big gap in correlating growth conditions and synthesized product. The literature review was divided into four sections. Section 2.1 introduces literature published on arc discharge method.
2. In Section 2.2 we have discussed growth mechanism of carbon nanotubes in arc discharge. From available literature we reported that the physics involved in arc discharge process remains unexplained and we have included the literature describing physics of nanotube growth.
3. In Section 2.3 effects of several arc parameters such as power supply, environment, pressure, electrode geometry, catalyst and temperature and their corresponding physics has been detailed.
4. In Section 2.4 we have reviewed and presented various carbon precursors used in synthesis of CNTs using arc discharge. Based on the review, we defined the objectives in the thesis and framed problem statement to work upon in the thesis. The first problem was to customize the design of the experimental setup.

In the next chapter we present the conceptual design of arc chamber. We discuss various designs available in literature; assess; customize and choose the design for the set objectives in the scope of the thesis. We have presented mechanical and electrical circuit design of the custom built arc chamber.

References:

- [1] Y. Ando and X. Zhao, "Synthesis of Carbon Nanotubes by Arc-Discharge Method," *New Diam. Front. Carbon Technol.*, vol. 16, no. 3, pp. 123–137, Jan. 2006.
- [2] P. J. F. Harris, "Solid state growth mechanisms for carbon nanotubes," *Carbon.*, vol. 45, no. 2, pp. 229–239, Feb. 2007.
- [3] Y. Ando, "Carbon Nanotube : Story in Ando Laboratory Discovery of CNTs," *J. nanoscience & nanotechnology.*, vol. 3, no. 1, pp. 3–22, Jun. 2010.
- [4] J.-P. Tessonier and D. S. Su, "Recent progress on the growth mechanism of carbon nanotubes: a review.," *ChemSusChem.*, vol. 4, no. 7, pp. 824–47, Jul. 2011.
- [5] J. Prasek, J. Drbohlavova, J. Chomoucka, J. Hubalek, O. Jasek, V. Adam, and R. Kizek, "Methods for carbon nanotubes synthesis—review," *J. Mater. Chem.*, vol. 21, no. 40, pp. 15872, Aug. 2011.
- [6] C. Journet, M. Picher, and V. Jourdain, "Carbon nanotube synthesis: from large-scale production to atom-by-atom growth.," *Nanotechnology.*, vol. 23, no. 14, p. 142001, Apr. 2012.
- [7] Y. A. S. Hrivas, "A Review on Carbon Nano -Tubes Production and Its Mechanical Properties," *Journal of Scientific Engineering and Technology Research.*, vol. 3, no. 41, pp. 8385–8389, Nov. 2014.
- [8] N. M. Mubarak, E. C. Abdullah, N. S. Jayakumar, and J. N. Sahu, "An overview on methods for the production of carbon nanotubes," *J. Ind. Eng. Chem.*, vol. 20, no. 4, pp. 1186–1197, Jul. 2014.
- [9] Y. Yan, J. Miao, Z. Yang, F.-X. Xiao, H. Bin Yang, B. Liu, and Y. Yang, "Carbon nanotube catalysts: recent advances in synthesis, characterization and applications.," *Chem. Soc. Rev.*, vol. 44, no. 10, pp. 3295–346, Apr. 2015.
- [10] K. Sarangdevot and B. S. Sonigara, "The wondrous world of carbon nanotubes : Structure , synthesis , properties and applications," *J. Chem. Pharm. Res.*, vol. 7, no. 6, pp. 916–933, 2015.
- [11] S. Iijima, "Helical microtubules of graphitic carbon," *Nature.*, vol. 354, no. 6348, pp. 56–58, Nov. 1991.
- [12] S. Iijima, "Growth of carbon nanotubes," *Mater. Sci. Eng. B.*, vol. 19, no. 1–2, pp. 172–180, Apr. 1993.
- [13] D. Ugarte, "High-temperature behaviour of 'fullerene black,'" *Carbon.*, vol. 32, no. 7, pp. 1245–1248, Jan. 1994.
- [14] E. Gamaly and T. Ebbesen, "Mechanism of carbon nanotube formation in the arc discharge," *Phys. Rev. B.*, vol. 52, no. 3, pp. 2083–2089, Jul. 1995.
- [15] S. Amelinckx, D. Bernaerts, X. B. Zhang, G. Van Tendeloo, and J. Van Landuyt,

- “A structure model and growth mechanism for multishell carbon nanotubes.,” *Science*, vol. 267, no. 5202, pp. 1334–8, Mar. 1995.
- [16] C. Liu, H. . Cong, F. Li, P. . Tan, H. . Cheng, K. Lu, and B. . Zhou, “Semi-continuous synthesis of single-walled carbon nanotubes by a hydrogen arc discharge method,” *Carbon.*, vol. 37, no. 11, pp. 1865–1868, Jan. 1999.
- [17] E. F. Kukovitsky, S. G. L’vov, and N. A. Sainov, “VLS-growth of carbon nanotubes from the vapor,” *Chem. Phys. Lett.*, vol. 317, no. 1–2, pp. 65–70, Jan. 2000.
- [18] S. Farhat, M. Lamy de La Chapelle, A. Loiseau, C. D. Scott, S. Lefrant, C. Journet, and P. Bernier, “Diameter control of single-walled carbon nanotubes using argon–helium mixture gases,” *J. Chem. Phys.*, vol. 115, no. 14, pp. 6752, Oct. 2001.
- [19] J. Gavillet, A. Loiseau, C. Journet, F. Willaime, F. Ducastelle, and J.-C. Charlier, “Root-Growth Mechanism for Single-Wall Carbon Nanotubes,” *Phys. Rev. Lett.*, vol. 87, no. 27, pp. 275504, Dec. 2001.
- [20] S. Jong Lee, H. Koo Baik, J. Yoo, and J. Hoon Han, “Large scale synthesis of carbon nanotubes by plasma rotating arc discharge technique,” *Diam. Relat. Mater.*, vol. 11, no. 3–6, pp. 914–917, Mar. 2002.
- [21] W. a Heer, P. Poncharal, C. Berger, J. Gezo, Z. Song, J. Bettini, and D. Ugarte, “Liquid carbon, carbon-glass beads, and the crystallization of carbon nanotubes.,” *Science*, vol. 307, no. 5711, pp. 907–10, Feb. 2005.
- [22] H. H. Kim and H. J. Kim, “The preparation of carbon nanotubes by dc arc discharge using a carbon cathode coated with catalyst,” *Mater. Sci. Eng. B.*, vol. 130, no. 1–3, pp. 73–80, Jun. 2006.
- [23] H. M. Yusoff, R. Shastry, T. Querrioux, and J. Abrahamson, “Nanotube deposition in a continuous arc reactor for varying arc gap and substrate temperature,” *Curr. Appl. Phys.*, vol. 6, no. 3, pp. 422–426, Jun. 2006.
- [24] M. Keidar, “Factors affecting synthesis of single wall carbon nanotubes in arc discharge,” *J. Phys. D. Appl. Phys.*, vol. 40, no. 8, pp. 2388–2393, Apr. 2007.
- [25] R. Joshi, J. Engstler, P. K. Nair, P. Haridoss, and J. J. Schneider, “High yield formation of carbon nanotubes using a rotating cathode in open air,” *Diam. Relat. Mater.*, vol. 17, no. 6, pp. 913–919, Jun. 2008.
- [26] J. B. Donnet, H. Oulanti, and T. Le Huu, “Mechanism growth of multiwalled carbon nanotubes on carbon black,” *Diam. Relat. Mater.*, vol. 17, no. 7–10, pp. 1506–1512, Jul. 2008.
- [27] S. Scalese, V. Scuderi, S. Bagiante, F. Simone, P. Russo, L. D’Urso, G. Compagnini, and V. Privitera, “Controlled synthesis of carbon nanotubes and linear C chains by arc discharge in liquid nitrogen,” *J. Appl. Phys.*, vol. 107, no. 1, pp. 14304, Jan. 2010.

- [28] S. Zhao, R. Hong, Z. Luo, H. Lu, and B. Yan, "Carbon Nanostructures Production by AC Arc Discharge Plasma Process at Atmospheric Pressure," *J. Nanomater.*, vol. 2011, pp. 1–6, Jan. 2011.
- [29] F. Liang, T. Shimizu, M. Tanaka, S. Choi, and T. Watanabe, "Selective preparation of polyhedral graphite particles and multi-wall carbon nanotubes by a transferred arc under atmospheric pressure," *Diam. Relat. Mater.*, vol. 30, pp. 70–76, Nov. 2012.
- [30] Y. Wu, T. Zhang, F. Zhang, Y. Wang, Y. Ma, Y. Huang, Y. Liu, and Y. Chen, "In situ synthesis of graphene / single-walled carbon nanotube hybrid material by arc-discharge and its application in supercapacitors," *Nano Energy.*, vol. 1, no. 6, pp. 820–827, Nov. 2012.
- [31] Y. A. Kim, H. Muramatsu, T. Hayashi, and M. Endo, "Catalytic metal-free formation of multi-walled carbon nanotubes in atmospheric arc discharge," *Carbon.*, vol. 50, no. 12, pp. 4588–4595, Oct. 2012.
- [32] D. Ugarte, "High-temperature behaviour of 'fullerene black,'" *Carbon.*, vol. 32, no. 7, pp. 1245–1248, Jan. 1994.
- [33] D. Zhou and L. Chow, "Complex structure of carbon nanotubes and their implications for formation mechanism," *J. Appl. Phys.*, vol. 93, no. 12, pp. 9972, Jun. 2003.
- [34] O. Louchev, Y. Sato, and H. Kanda, "Morphological stabilization, destabilization, and open-end closure during carbon nanotube growth mediated by surface diffusion," *Phys. Rev. E.*, vol. 66, no. 1, pp. 11601, Jul. 2002.
- [35] O. A. Louchev, Y. Sato, and H. Kanda, "Mechanism of thermokinetic selection between carbon nanotube and fullerene-like nanoparticle formation," *J. Appl. Phys.*, vol. 91, no. 12, pp. 10074, Jun. 2002.
- [36] O. A. Louchev and J. R. Hester, "Kinetic pathways of carbon nanotube nucleation from graphitic nanofragments," *J. Appl. Phys.*, vol. 94, no. 3, pp. 2002, Aug. 2003.
- [37] Y. W. Liu, L. Wang, and H. Zhang, "A possible mechanism of uncatalyzed growth of carbon nanotubes," *Chem. Phys. Lett.*, vol. 427, no. 1–3, pp. 142–146, Aug. 2006.
- [38] P. J. F. Harris, S. C. Tsang, J. B. Claridge, and M. L. H. Green, "High-resolution electron microscopy studies of a microporous carbon produced by arc-evaporation," *J. Chem. Soc. Faraday Trans.*, vol. 90, no. 18, pp. 2799, 1994.
- [39] A. Ashraf, K. Yaqub, S. Javeed, and S. Zeeshan, "Sublimation of graphite in continuous and pulsed arc discharges," *Turkish Journal of Physics.*, vol. 34, pp. 33–42, Nov. 2010.
- [40] R. A. Scholl, "Power supplies for pulsed plasma technologies: State-Of-The-Art And Outlook," 2001.

- [41] S. Iijima and T. Ichihashi, "Single-shell carbon nanotubes of 1-nm diameter," *Nature.*, vol. 363, no. 6430, pp. 603–605, Jun. 1993.
- [42] D. S. Bethune, C. H. Klang, M. S. de Vries, G. Gorman, R. Savoy, J. Vazquez, and R. Beyers, "Cobalt-catalysed growth of carbon nanotubes with single-atomic-layer walls," *Nature.*, vol. 363, no. 6430, pp. 605–607, Jun. 1993.
- [43] T. W. Ebbesen and P. M. Ajayan, "Large-scale synthesis of carbon nanotubes," *Nature.*, vol. 358, no. 6383, pp. 220–222, Jul. 1992.
- [44] X. K. Wang, X. W. Lin, V. P. Dravid, J. B. Ketterson, and R. P. H. Chang, "Carbon nanotubes synthesized in a hydrogen arc discharge," *Appl. Phys. Lett.*, vol. 66, no. 18, pp. 2430, May. 1995.
- [45] C. Journet, W. K. Maser, P. Bernier, a Loiseau, M. L. delaChapelle, S. Lefrant, P. Deniard, R. Lee, and J. E. Fischer, "Large-scale production of single-walled carbon nanotubes by the electric-arc technique," *Nature.*, vol. 388, no. 6644, pp. 756–758, Aug. 1997.
- [46] Z. Shi, Y. Lian, X. Zhou, Z. Gu, Y. Zhang, S. Iijima, H. Li, K. T. Yue, and S.-L. Zhang, "Production of Single-Wall Carbon Nanotubes at High Pressure," *J. Phys. Chem. B.*, vol. 103, no. 41, pp. 8698–8701, Oct. 1999.
- [47] T. Zhao, "Gas and pressure effects on the synthesis of amorphous carbon nanotubes," *Chinese Sci. Bull.*, vol. 49, no. 24, pp. 2569, Dec. 2004.
- [48] M. E. Itkis, D. E. Perea, S. Niyogi, J. Love, J. Tang, a. Yu, C. Kang, R. Jung, and R. C. Haddon, "Optimization of the Ni–Y Catalyst Composition in Bulk Electric Arc Synthesis of Single-Walled Carbon Nanotubes by Use of Near-Infrared Spectroscopy," *J. Phys. Chem. B.*, vol. 108, no. 34, pp. 12770–12775, Aug. 2004.
- [49] X. Lin, X. K. Wang, V. P. Dravid, R. P. H. Chang, and J. B. Ketterson, "Large scale synthesis of single-shell carbon nanotubes," *Appl. Phys. Lett.*, vol. 64, no. 2, pp. 181, Jan. 1994.
- [50] C. Guerret-Piécourt, Y. Bouar, A. Loiseau, and H. Pascard, "Relation between metal electronic structure and morphology of metal compounds inside carbon nanotubes," *Nature.*, vol. 372, no. 6508, pp. 761–765, Dec. 1994.
- [51] D. Zhou and S. Seraphin, "Complex branching phenomena in the growth of carbon nanotubes," *Chem. Phys. Lett.*, vol. 238, no. 4–6, pp. 286–289, Jun. 1995.
- [52] A. Loiseau and H. Pascard, "Synthesis of long carbon nanotubes filled with Se, S, Sb and Ge by the arc method," *Chem. Phys. Lett.*, vol. 256, no. 3, pp. 246–252, Jun. 1996.
- [53] H. Lange, P. Baranowski, A. Huczko, and P. Byszewski, "An optoelectronic control of arc gap during formation of fullerenes and carbon nanotubes," *Rev. Sci. Instrum.*, vol. 68, no. 10, pp. 3723, Oct. 1997.
- [54] X. Zhao, M. Ohkohchi, M. Wang, S. Iijima, T. Ichihashi, and Y. Ando, "Preparation of high-grade carbon nanotubes by hydrogen arc discharge,"

- Carbon.*, vol. 35, no. 6, pp. 775–781, Jan. 1997.
- [55] Y. Saito, Y. Tani, N. Miyagawa, K. Mitsushima, A. Kasuya, and Y. Nishina, “High yield of single-wall carbon nanotubes by arc discharge using Rh–Pt mixed catalysts,” *Chem. Phys. Lett.*, vol. 294, no. 6, pp. 593–598, Sep. 1998.
- [56] Chang, B.H., S. S. Xie, W. Y. Zhou, L. X. Qian, Z. W. Pan, J. M. Mao, and W. Z. Li, “Loosely-entangled carbon nanotubes prepared in modified arc-discharge,” *J. Mater. Sci. Lett.*, vol. 17, no. 12, pp. 1015–1017, Jun. 1998.
- [57] X. Zhao and Y. Ando, “Raman Spectra and X-Ray Diffraction Patterns of Carbon Nanotubes Prepared by Hydrogen Arc Discharge,” *Jpn. J. Appl. Phys.*, vol. 17, no. Part 1, No. 9A, pp. 4846–4849, Sep. 1998.
- [58] M. Takizawa, S. Bandow, T. Torii, and S. Iijima, “Effect of environment temperature for synthesizing single-wall carbon nanotubes by arc vaporization method,” *Chem. Phys. Lett.*, vol. 302, no. 1–2, pp. 146–150, Mar. 1999.
- [59] M. Yudasaka, N. Sensui, M. Takizawa, S. Bandow, T. Ichihashi, and S. Iijima, “Formation of single-wall carbon nanotubes catalyzed by Ni separating from Y in laser ablation or in arc discharge using a C target containing a NiY catalyst,” *Chem. Phys. Lett.*, vol. 312, no. 2–4, pp. 155–160, Oct. 1999.
- [60] Z. Shi, Y. Lian, X. Zhou, Z. Gu, Y. Zhang, S. Iijima, L. Zhou, K. T. Yue, and S. Zhang, “Mass-production of single-wall carbon nanotubes by arc discharge method,” *Carbon.*, vol. 37, no. 9, pp. 1449–1453, Jan. 1999.
- [61] X. Zhao, M. Ohkohchi, H. Shimoyama, and Y. Ando, “Morphology of carbon allotropes prepared by hydrogen arc discharge,” *J. Cryst. Growth.*, vol. 198–199, pp. 934–938, Mar. 1999.
- [62] N. a. Kiselev, a. P. Moravsky, a. B. Ormont, and D. N. Zakharov, “SEM and HREM study of the internal structure of nanotube rich carbon arc cathodic deposits,” *Carbon.*, vol. 37, no. 7, pp. 1093–1103, Jan. 1999.
- [63] M. Ishigami, J. Cumings, A. Zettl, and S. Chen, “A simple method for the continuous production of carbon nanotubes,” *Chem. Phys. Lett.*, vol. 319, no. 5–6, pp. 457–459, Mar. 2000.
- [64] D. . Tang, S. . Xie, W. Liu, B. . Chang, L. . Sun, Z. . Liu, G. Wan, and W. . Zhou, “Evidence for an open-ended nanotube growth model in arc discharge,” *Carbon.*, vol. 38, no. 3, pp. 480–483, Jan. 2000.
- [65] Z. Shi, Y. Lian, F. H. Liao, X. Zhou, Z. Gu, Y. Zhang, S. Iijima, H. Li, K. T. Yue, and S. Zhang, “Large scale synthesis of single-wall carbon nanotubes by arc-discharge method,” *J. Phys. Chem. Solids.*, vol. 61, no. 7, pp. 1031–1036, Jul. 2000.
- [66] Y. Ando, X. Zhao, K. Hirahara, K. Suenaga, S. Bandow, and S. Iijima, “Mass production of single-wall carbon nanotubes by the arc plasma jet method,” *Chem. Phys. Lett.*, vol. 323, no. 5–6, pp. 580–585, Jun. 2000.

- [67] Y. Ando, X. Zhao, H. Kataura, Y. Achiba, K. Kaneto, M. Tsuruta, S. Uemura, and S. Iijima, "Multiwalled carbon nanotubes prepared by hydrogen arc," *Diam. Relat. Mater.*, vol. 9, no. 3–6, pp. 847–851, Apr. 2000.
- [68] Cheng.H.M, Liu.C, Fan.Y.Y, Li.F, Su.G, He.L.L, and Liu.M, "Synthesis and hydrogen storage of carbon nanofibers and single wall Carbon nanotubes," *Z Met.*, vol. 91, no. 4, pp. 306–410, Sept. 2000.
- [69] Y. Ando, X. Zhao, K. Hirahara, K. Suenaga, S. Bandow, and S. Iijima, "Arc plasma jet method producing single-wall carbon nanotubes," *Diam. Relat. Mater.*, vol. 10, no. 3–7, pp. 1185–1189, Mar. 2001.
- [70] A. Srivastava, a. K. Srivastava, and O. N. Srivastava, "Curious aligned growth of carbon nanotubes under applied electric field," *Carbon.*, vol. 39, no. 2, pp. 201–206, Feb. 2001.
- [71] J. L. Hutchison, N. A. Kiselev, E. P. Krinichnaya, A. V. Krestinin, R. O. Loutfy, A. P. Morawsky, V. E. Muradyan, E. D. Obraztsova, J. Sloan, S. V. Terekhov, and D. N. Zakharov, "Double-walled carbon nanotubes fabricated by a hydrogen arc discharge method," *Carbon.*, vol. 39, no. 5, pp. 761–770, Apr. 2001.
- [72] M. Kanai, a. Koshio, H. Shinohara, T. Mieno, a. Kasuya, Y. Ando, and X. Zhao, "High-yield synthesis of single-walled carbon nanotubes by gravity-free arc discharge," *Appl. Phys. Lett.*, vol. 79, no. 18, pp. 2967, Oct. 2001.
- [73] K. Shimotani, K. Anazawa, H. Watanabe, and M. Shimizu, "New synthesis of multi-walled carbon nanotubes using an arc discharge technique under organic molecular atmospheres," *Appl. Phys. A.*, vol. 73, no. 4, pp. 451–454, Feb. 2014.
- [74] Y. Li, S. Xie, W. Zhou, D. Tang, Z. Liu, X. Zou, and G. Wang, "Small diameter carbon nanotubes synthesized in an arc-discharge," *Carbon.*, vol. 39, no. 9, pp. 1429–1431, Aug. 2001.
- [75] Y. Ando, X. Zhao, and H. Shimoyama, "Structure analysis of purified multiwalled carbon nanotubes," *Carbon.*, vol. 39, no. 4, pp. 569–574, Apr. 2001.
- [76] H. . Lai, M. C. . Lin, M. . Yang, and a. . Li, "Synthesis of carbon nanotubes using polycyclic aromatic hydrocarbons as carbon sources in an arc discharge," *Mater. Sci. Eng. C.*, vol. 16, no. 1–2, pp. 23–26, Oct. 2001.
- [77] Z. Osváth, A. . Koós, Z. . Horváth, J. Gyulai, A. . Benito, M. . Martínez, W. . Maser, and L. . Biró, "Arc-grown Y-branched carbon nanotubes observed by scanning tunneling microscopy (STM)," *Chem. Phys. Lett.*, vol. 365, no. 3–4, pp. 338–342, Oct. 2002.
- [78] P. K. Jain, Y. R. Mahajan, G. Sundararajan, A. V Okotrub, N. F. Yudanov, and A. I. Romanenko, "Development of Carbon Nanotubes and Polymer Composites Therefrom," *Carbon Sci.*, vol. 3, no. 3, pp. 142–145, 2002.
- [79] D. Tang, S. Xie, W. Zhou, Z. Liu, L. Ci, X. Yan, H. Yuan, Z. Zhou, Y. Liang, D. Liu, and W. Liu, "Effect of cupped cathode on microstructures of carbon

- nanotubes in arc discharge,” *Carbon.*, vol. 40, no. 9, pp. 1609–1613, Aug. 2002.
- [80] X. Li, H. Zhu, B. Jiang, J. Ding, C. Xu, and D. Wu, “High-yield synthesis of multi-walled carbon nanotubes by water-protected arc discharge method,” *Carbon.*, vol. 41, no. 8, pp. 1664–1666, Jan. 2003.
- [81] Y. S. Park, K. S. Kim, H. J. Jeong, W. S. Kim, J. M. Moon, K. H. An, D. J. Bae, Y. S. Lee, G.-S. Park, and Y. H. Lee, “Low pressure synthesis of single-walled carbon nanotubes by arc discharge,” *Synth. Met.*, vol. 126, no. 2–3, pp. 245–251, Feb. 2002.
- [82] Y. Ando, X. Zhao, S. Inoue, and S. Iijima, “Mass production of multiwalled carbon nanotubes by hydrogen arc discharge,” *J. Cryst. Growth.*, vol. 237–239, pp. 1926–1930, Apr. 2002.
- [83] T. Dong-Sheng, Z. Wei-Ya, Y. Xiao-Qin, Ci Li-Jie, Y. Hua-Jun, L. Ying-Xin, Zhou Zhen-Ping, L. Dong-Fang, and L. Wei, “Morphologies and microstructures of carbon nanotubes prepared by self-sustained arc discharging,” *Chinese Phys.*, vol. 11, no. 5, pp. 496–501, May 2002.
- [84] M. Cadek, R. Murphy, B. McCarthy, A. Drury, B. Lahr, R. . Barklie, M. in het Panhuis, J. . Coleman, and W. . Blau, “Optimisation of the arc-discharge production of multi-walled carbon nanotubes,” *Carbon.*, vol. 40, no. 6, pp. 923–928, May 2002.
- [85] L. Zhen-Hua, W. Miao, W. Xin-Qing, Z. Hai-Bin, L. Huan-Ming, and Y. Ando, “Synthesis of Large Quantity Single-Walled Carbon Nanotubes by Arc Discharge,” *Chinese Phys. Lett.*, vol. 19, no. 1, pp. 91–93, Jan. 2002.
- [86] S. P. Doherty and R. P. H. Chang, “Synthesis of multiwalled carbon nanotubes from carbon black,” *Appl. Phys. Lett.*, vol. 81, no. 13, pp. 2466, Sept. 2002.
- [87] M. Vittori Antisari, R. Marazzi, and R. Krsmanovic, “Synthesis of multiwall carbon nanotubes by electric arc discharge in liquid environments,” *Carbon.*, vol. 41, no. 12, pp. 2393–2401, Jan. 2003.
- [88] S. P. Doherty, D. B. Buchholz, B.-J. Li, and R. P. H. Chang, “Solid-state synthesis of multiwalled carbon nanotubes,” *J. Mater. Res.*, vol. 18, no. 4, pp. 941–949, Jan. 2002.
- [89] Y. Saito, T. Nakahira, and S. Uemura, “Growth Conditions of Double-Walled Carbon Nanotubes in Arc Discharge,” *J. Phys. Chem. B.*, vol. 107, no. 4, pp. 931–934, Jan. 2003.
- [90] J. Qiu, Y. Li, Y. Wang, T. Wang, Z. Zhao, Y. Zhou, F. Li, and H. Cheng, “High-purity single-wall carbon nanotubes synthesized from coal by arc discharge,” *Carbon.*, vol. 41, no. 11, pp. 2170–2173, Jan. 2003.
- [91] S.-H. Jung, M.-R. Kim, S.-H. Jeong, S.-U. Kim, O.-J. Lee, K.-H. Lee, J.-H. Suh, and C.-K. Park, “High-yield synthesis of multi-walled carbon nanotubes by arc discharge in liquid nitrogen,” *Appl. Phys. A Mater. Sci. Process.*, vol. 76, no. 2,

- pp. 285–286, Feb. 2003.
- [92] X. Zhao, “Macroscopic oriented web of single-wall carbon nanotubes,” *Chem. Phys. Lett.*, vol. 373, no. 3–4, pp. 266–271, May 2003.
- [93] H. Lange, M. Sioda, A. Huczko, Y. Q. Zhu, H. W. Kroto, and D. R. M. Walton, “Nanocarbon production by arc discharge in water,” *Carbon.*, vol. 41, no. 8, pp. 1617–1623, Jan. 2003.
- [94] S. Cui, P. Scharff, C. Siegmund, L. Spiess, H. Romanus, J. Schawohl, K. Risch, D. Schneider, and S. Klötzer, “Preparation of multiwalled carbon nanotubes by DC arc discharge under a nitrogen atmosphere,” *Carbon.*, vol. 41, no. 8, pp. 1648–1651, Jan. 2003.
- [95] Z. Osváth, a. a. Koós, Z. E. Horváth, J. Gyulai, a. M. Benito, M. T. Martínez, W. Maser, and L. P. Biró, “STM observation of asymmetrical Y-branched carbon nanotubes and nano-knees produced by the arc discharge method,” *Mater. Sci. Eng. C.*, vol. 23, no. 4, pp. 561–564, Jun. 2003.
- [96] B. P. Tarasov, V. E. Muradyan, Y. M. Shul’ga, E. P. Krinichnaya, N. S. Kuyunko, O. N. Efimov, E. D. Obratsova, D. V. Schur, J. P. Maehlen, V. A. Yartys, and H. Lai, “Synthesis of carbon nanostructures by arc evaporation of graphite rods with Co–Ni and YNi₂ catalysts,” *Carbon.*, vol. 41, no. 7, pp. 1357–1364, Jan. 2003.
- [97] Y. Liu, S. Xiaolong, Z. Tingkai, Z. Jiewu, M. Hirscher, and F. Philipp, “Amorphous carbon nanotubes produced by a temperature controlled DC arc discharge,” *Carbon.*, vol. 42, no. 8–9, pp. 1852–1855, Jan. 2004.
- [98] E. I. Waldorff, A. M. Waas, P. P. Friedmann, and M. Keidar, “Characterization of carbon nanotubes produced by arc discharge: Effect of the background pressure,” *J. Appl. Phys.*, vol. 95, no. 5, pp. 2749, Mar. 2004.
- [99] M. Nishio, S. Akita, and Y. Nakayama, “Cooling effect on the growth of carbon nanotubes and optical emission spectroscopy in short-period arc-discharge,” *Thin Solid Films.*, vol. 464–465, pp. 304–307, Oct. 2004.
- [100] Y.-H. Wang, S.-C. Chiu, K.-M. Lin, and Y.-Y. Li, “Formation of carbon nanotubes from polyvinyl alcohol using arc-discharge method,” *Carbon.*, vol. 42, no. 12–13, pp. 2535–2541, Jan. 2004.
- [101] D. Bera, S. C. Kuiry, M. McCutchen, A. Kruize, H. Heinrich, M. Meyyappan, and S. Seal, “In-situ synthesis of palladium nanoparticles-filled carbon nanotubes using arc-discharge in solution,” *Chem. Phys. Lett.*, vol. 386, no. 4–6, pp. 364–368, Mar. 2004.
- [102] S. Cui, P. Scharff, C. Siegmund, D. Schneider, K. Risch, S. Klötzer, L. Spiess, H. Romanus, and J. Schawohl, “Investigation on preparation of multiwalled carbon nanotubes by DC arc discharge under N₂ atmosphere,” *Carbon.*, vol. 42, no. 5–6, pp. 931–939, Jan. 2004.
- [103] T. Zhao and Y. Liu, “Large scale and high purity synthesis of single-walled

- carbon nanotubes by arc discharge at controlled temperatures,” *Carbon.*, vol. 42, no. 12–13, pp. 2765–2768, Jan. 2004.
- [104] M. Jinno, S. Bandow, and Y. Ando, “Multiwalled carbon nanotubes produced by direct current arc discharge in hydrogen gas,” *Chem. Phys. Lett.*, vol. 398, no. 1–3, pp. 256–259, Nov. 2004.
- [105] M. Keidar and M. Waas, “On the conditions of carbon nanotube growth in the arc discharge,” *Nanotechnology.*, vol. 15, no. 11, pp. 1571–1575, Nov. 2004.
- [106] J. Qiu, Y. Li, Y. Wang, and W. Li, “Production of carbon nanotubes from coal,” *Fuel Process. Technol.*, vol. 85, no. 15, pp. 1663–1670, Oct. 2004.
- [107] N. Sano, J. Nakano, and T. Kanki, “Synthesis of single-walled carbon nanotubes with nanohorns by arc in liquid nitrogen,” *Carbon.*, vol. 42, no. 3, pp. 686–688, Jan. 2004.
- [108] L. E. Murr, D. K. Brown, E. V. Esquivel, T. D. Ponda, F. Martinez, and a. Virgen, “Carbon nanotubes and other fullerenes produced from tire powder injected into an electric arc,” *Mater. Charact.*, vol. 55, no. 4–5, pp. 371–377, Nov. 2005.
- [109] J. Hahn, J.-E. Yoo, J. Han, H. B. Kwon, and J. S. Suh, “Field emission from the film of the finely dispersed arc discharge black core material,” *Carbon.*, vol. 43, no. 5, pp. 937–943, Jan. 2005.
- [110] H. Shang, H. Xie, H. Zhu, F. Dai, D. Wu, W. Wang, and Y. Fang, “Investigation of strain in individual multi-walled carbon nanotube by a novel moiré method,” *J. Mater. Process. Technol.*, vol. 170, no. 1–2, pp. 108–111, Dec. 2005.
- [111] W. a de Heer, P. Poncharal, C. Berger, J. Gezo, Z. Song, J. Bettini, and D. Ugarte, “Liquid carbon, carbon-glass beads, and the crystallization of carbon nanotubes,” *Science.*, vol. 307, no. 5711, pp. 907–10, Feb. 2005.
- [112] Y. Ando, X. Zhao, S. Inoue, T. Suzuki, and T. Kadoya, “Mass production of high-quality single-wall carbon nanotubes by H₂-N₂ arc discharge,” *Diam. Relat. Mater.*, vol. 14, no. 3–7, pp. 729–732, Mar. 2005.
- [113] Q.-H. Yang, Y. Tong, C. Liu, F. Li, and H.-M. Cheng, “Some indications of the formation mechanism for double-walled carbon nanotubes by hydrogen-arc discharge,” *Carbon.*, vol. 43, no. 9, pp. 2027–2030, Aug. 2005.
- [114] Y. Guo, T. Okazaki, T. Kadoya, T. Suzuki, and Y. Ando, “Spectroscopic study during single-wall carbon nanotubes production by Ar, H₂, and H₂-Ar DC arc discharge,” *Diam. Relat. Mater.*, vol. 14, no. 3–7, pp. 887–890, Mar. 2005.
- [115] L. Li, F. Li, C. Liu, and H.-M. Cheng, “Synthesis and characterization of double-walled carbon nanotubes from multi-walled carbon nanotubes by hydrogen-arc discharge,” *Carbon.*, vol. 43, no. 3, pp. 623–629, Jan. 2005.
- [116] S.-D. Wang, M.-H. Chang, K. M.-D. Lan, C.-C. Wu, J.-J. Cheng, and H.-K. Chang, “Synthesis of carbon nanotubes by arc discharge in sodium chloride solution,” *Carbon.*, vol. 43, no. 8, pp. 1792–1795, Jul. 2005.

- [117] X. Lv, F. Du, Y. Ma, Q. Wu, and Y. Chen, "Synthesis of high quality single-walled carbon nanotubes at large scale by electric arc using metal compounds," *Carbon.*, vol. 43, no. 9, pp. 2020–2022, Aug. 2005.
- [118] Y. Makita, S. Suzuki, H. Kataura, and Y. Achiba, "Synthesis of single wall carbon nanotubes by using arc discharge technique in nitrogen atmosphere," *Eur. Phys. J. D.*, vol. 34, no. 1–3, pp. 287–289, Jul. 2005.
- [119] M. Yao, B. Liu, Y. Zou, L. Wang, D. Li, T. Cui, G. Zou, and B. Sundqvist, "Synthesis of single-wall carbon nanotubes and long nanotube ribbons with Ho/Ni as catalyst by arc discharge," *Carbon.*, vol. 43, no. 14, pp. 2894–2901, Nov. 2005.
- [120] L. A. Montoro, R. C. Z. Lofrano, and J. M. Rosolen, "Synthesis of single-walled and multi-walled carbon nanotubes by arc-water method," *Carbon.*, vol. 43, no. 1, pp. 200–203, Jan. 2005.
- [121] T. Zhao, Y. Liu, and J. Zhu, "Temperature and catalyst effects on the production of amorphous carbon nanotubes by a modified arc discharge," *Carbon.*, vol. 43, no. 14, pp. 2907–2912, Nov. 2005.
- [122] D. Tang, L. Sun, J. Zhou, W. Zhou, and S. Xie, "Two possible emission mechanisms involved in the arc discharge method of carbon nanotube preparation," *Carbon.*, vol. 43, no. 13, pp. 2812–2816, Nov. 2005.
- [123] S. Wang, M.-H. Chang, J.-J. Cheng, H.-K. Chang, and K. M.-D. Lan, "Unusual morphologies of carbon nanoparticles obtained by arc discharge in deionized water," *Carbon.*, vol. 43, no. 6, pp. 1322–1325, May 2005.
- [124] S. P. Doherty, D. B. Buchholz, and R. P. H. Chang, "Semi-continuous production of multiwalled carbon nanotubes using magnetic field assisted arc furnace," *Carbon.*, vol. 44, no. 8, pp. 1511–1517, Jul. 2006.
- [125] M. Wang, X. Wang, Z. Li, Z. Liu, and P. He, "An efficient method to produce single-walled carbon nanotubes by round-trip arc discharge," *Mater. Chem. Phys.*, vol. 97, no. 2–3, pp. 243–246, Jun. 2006.
- [126] Z.-G. Chen, F. Li, W.-C. Ren, H. Cong, C. Liu, G. Q. Lu, and H.-M. Cheng, "Double-walled carbon nanotubes synthesized using carbon black as the dot carbon source," *Nanotechnology.*, vol. 17, no. 13, pp. 3100–3104, Jul. 2006.
- [127] H. Qiu, Z. Shi, L. Guan, L. You, M. Gao, S. Zhang, J. Qiu, and Z. Gu, "High-efficient synthesis of double-walled carbon nanotubes by arc discharge method using chloride as a promoter," *Carbon.*, vol. 44, no. 3, pp. 516–521, Mar. 2006.
- [128] Z. Wang, Z. Zhao, and J. Qiu, "In situ synthesis of super-long Cu nanowires inside carbon nanotubes with coal as carbon source," *Carbon.*, vol. 44, no. 9, pp. 1845–1847, Aug. 2006.
- [129] H. Lange, M. Bystrzejewski, and A. Huczko, "Influence of carbon structure on carbon nanotube formation and carbon arc plasma," *Diam. Relat. Mater.*, vol. 15, no. 4–8, pp. 1113–1116, Apr. 2006.

- [130] X. Zhao, M. Ohkohchi, S. Inoue, T. Suzuki, T. Kadoya, and Y. Ando, "Large-scale purification of single-wall carbon nanotubes prepared by electric arc discharge," *Diam. Relat. Mater.*, vol. 15, no. 4–8, pp. 1098–1102, Apr. 2006.
- [131] T. Suzuki, Y. Guo, S. Inoue, X. Zhao, M. Ohkohchi, and Y. Ando, "Multiwalled carbon nanotubes mass-produced by dc arc discharge in He–H₂ gas mixture," *J. Nanoparticle Res.*, vol. 8, no. 2, pp. 279–285, Apr. 2006.
- [132] H. H. Kim and H. J. Kim, "Preparation of carbon nanotubes by DC arc discharge process under reduced pressure in an air atmosphere," *Mater. Sci. Eng. B.*, vol. 133, no. 1–3, pp. 241–244, Aug. 2006.
- [133] Z. Wang, Z. Zhao, and J. Qiu, "Synthesis of branched carbon nanotubes from coal," *Carbon.*, vol. 44, no. 7, pp. 1321–1324, Jun. 2006.
- [134] E. Cazzanelli, L. Caputi, M. Castriota, a. Cupolillo, C. Giallombardo, and L. Papagno, "Carbon linear chains inside multiwalled nanotubes," *Surf. Sci.*, vol. 601, no. 18, pp. 3926–3932, Sep. 2007.
- [135] T. Okada, T. Kaneko, and R. Hatakeyama, "Conversion of toluene into carbon nanotubes using arc discharge plasmas in solution," *Thin Solid Films.*, vol. 515, no. 9, pp. 4262–4265, Mar. 2007.
- [136] R. B. Mathur, S. Seth, C. Lal, R. Rao, B. P. Singh, T. L. Dhimi, and a. M. Rao, "Co-synthesis, purification and characterization of single- and multi-walled carbon nanotubes using the electric arc method," *Carbon.*, vol. 45, no. 1, pp. 132–140, Jan. 2007.
- [137] X. Song, Y. Liu, and J. Zhu, "Multi-walled carbon nanotubes produced by hydrogen DC arc discharge at elevated environment temperature," *Mater. Lett.*, vol. 61, no. 2, pp. 389–391, Jan. 2007.
- [138] H. H. Kim and H. J. Kim, "New DC Arc Discharge Synthesis Method for Carbon Nanotubes Using Xylene Ferrocene as Floating Catalyst," *Jpn. J. Appl. Phys.*, vol. 46, no. 4A, pp. 1818–1820, Apr. 2007.
- [139] J. Guo, X. Wang, Y. Yao, X. Yang, X. Liu, and B. Xu, "Structure of nanocarbons prepared by arc discharge in water," *Mater. Chem. Phys.*, vol. 105, no. 2–3, pp. 175–178, Oct. 2007.
- [140] R. Duncan, V. Stolojan, and C. Lekakou, "Manufacture of Carbon Multi-Walled Nanotubes by the Arc Discharge Technique," in *World Congress on Engineering.*, vol.7, 2007.
- [141] J. Qiu, Z. Wang, Z. Zhao, and T. Wang, "Synthesis of double-walled carbon nanotubes from coal in hydrogen-free atmosphere," *Fuel.*, vol. 86, no. 1–2, pp. 282–286, Jan. 2007.
- [142] X. Sun, W. Bao, Y. Lv, J. Deng, and X. Wang, "Synthesis of high quality single-walled carbon nanotubes by arc discharge method in large scale," *Mater. Lett.*, vol. 61, no. 18, pp. 3956–3958, Jul. 2007.

- [143] D. He, T. Zhao, Y. Liu, J. Zhu, G. Yu, and L. Ge, "The effect of electric current on the synthesis of single-walled carbon nanotubes by temperature controlled arc discharge," *Diam. Relat. Mater.*, vol. 16, no. 9, pp. 1722–1726, Sep. 2007.
- [144] G. Xing, S. Jia, and Z. Shi, "The production of carbon nano-materials by arc discharge under water or liquid nitrogen," *New Carbon Mater.*, vol. 22, no. 4, pp. 337–341, Dec. 2007.
- [145] V. V. Grebenyukov, E. D. Obraztsova, a. S. Pozharov, N. R. Arutyunyan, a. a. Romeikov, and I. a. Kozyrev, "Arc-synthesis of Single-walled Carbon Nanotubes in Nitrogen Atmosphere," *Fullerenes, Nanotub. Carbon Nanostructures.*, vol. 16, no. 5–6, pp. 330–334, Sep. 2008.
- [146] Z. Li, L. Wei, and Y. Zhang, "Effect of heat-pretreatment of the graphite rod on the quality of SWCNTs by arc discharge," *Appl. Surf. Sci.*, vol. 254, no. 16, pp. 5247–5251, Jun. 2008.
- [147] A. J. Fetterman, Y. Raitses, and M. Keidar, "Enhanced ablation of small anodes in a carbon nanotube arc plasma," *Carbon.*, vol. 46, no. 10, pp. 1322–1326, Aug. 2008.
- [148] M. Keidar, I. Levchenko, T. Arbel, M. Alexander, A. M. Waas, and K. (Ken) Ostrikov, "Increasing the length of single-wall carbon nanotubes in a magnetically enhanced arc discharge," *Appl. Phys. Lett.*, vol. 92, no. 4, pp. 43129, Jan. 2008.
- [149] M. Keidar, I. Levchenko, T. Arbel, M. Alexander, A. M. Waas, and K. K. Ostrikov, "Magnetic-field-enhanced synthesis of single-wall carbon nanotubes in arc discharge," *J. Appl. Phys.*, vol. 103, no. 9, pp. 94318, May. 2008.
- [150] Y. Kim, E. Nishikawa, and T. Kioka, "Multiwalled Carbon Nanotubes Produced by Direct-Current Arc Discharge in Foam," *e-Journal Surf. Sci. Nanotechnol.*, vol. 6, no. June, pp. 167–170, Jun. 2008.
- [151] Y.-I. Kim, E. Nishikawa, and T. Kioka, "Carbon Nano Materials Produced by Using Arc Discharge in Foam," *J. Korean Phys. Soc.*, vol. 54, no. 3, pp. 1032, Mar. 2009.
- [152] T. Charinpanitkul, W. Tanthapanichakoon, and N. Sano, "Carbon nanostructures synthesized by arc discharge between carbon and iron electrodes in liquid nitrogen," *Curr. Appl. Phys.*, vol. 9, no. 3, pp. 629–632, May 2009.
- [153] B. Ha, T. H. Yeom, and S. H. Lee, "Ferromagnetic properties of single-walled carbon nanotubes synthesized by Fe catalyst arc discharge," *Phys. B Condens. Matter.*, vol. 404, no. 8–11, pp. 1617–1620, May 2009.
- [154] O. Łabędź, H. Lange, a. Huczko, J. Borysiuk, M. Szybowicz, and M. Bystrzejewski, "Influence of carbon structure of the anode on the synthesis of single-walled carbon nanotubes in a carbon arc plasma," *Carbon.*, vol. 47, no. 12, pp. 2847–2854, Oct. 2009.
- [155] N. D. Hoa, N. Van Quy, Y. Cho, D. Kim, and N. Van Quy, "Porous single-wall

- carbon nanotube films formed by in Situ arc-discharge deposition for gas sensors application,” *Sensors Actuators B Chem.*, vol. 135, no. 2, pp. 656–663, Jan. 2009.
- [156] M. Jahanshahi, J. Raouf, and R. Jabari Seresht, “Voltage effects on the production of nanocarbons by a unique arc-discharge set-up in solution,” *J. Exp. Nanosci.*, vol. 4, no. 4, pp. 331–339, Dec. 2009.
- [157] M. Jahanshahi, M. Shariaty-niassar, A. A. Rostami, and H. Molavi, “Arc-discharge Carbon Nanotube Fabrication in Solution: Electrochemistry and Voltametric Tests,” *Aust. J. Basic Appl. Sci.*, vol. 4, no. 12, pp. 5915–5922, 2010.
- [158] S. Scalese, V. Scuderi, S. Bagiante, F. Simone, P. Russo, L. D’Urso, G. Compagnini, and V. Privitera, “Controlled synthesis of carbon nanotubes and linear C chains by arc discharge in liquid nitrogen,” *J. Appl. Phys.*, vol. 107, no. 1, pp. 14304, Jan. 2010.
- [159] S. Scalese, V. Scuderi, S. Bagiante, S. Gibilisco, G. Faraci, and V. Privitera, “Order and disorder of carbon deposit produced by arc discharge in liquid nitrogen,” *J. Appl. Phys.*, vol. 108, no. 6, pp. 64305, Sept. 2010.
- [160] J. Qiu, G. Chen, Z. Li, and Z. Zhao, “Preparation of double-walled carbon nanotubes from fullerene waste soot by arc-discharge,” *Carbon.*, vol. 48, no. 4, pp. 1312–1315, Apr. 2010.
- [161] H. Nishizaka, M. Namura, K. Motomiya, Y. Ogawa, Y. Udagawa, K. Tohji, and Y. Sato, “Influence of carbon structure of the anode on the production of graphite in single-walled carbon nanotube soot synthesized by arc discharge using a Fe–Ni–S catalyst,” *Carbon.*, vol. 49, no. 11, pp. 3607–3614, Sep. 2011.
- [162] J. Ding, X. Yan, B. K. Tay, and Q. Xue, “One-step synthesis of pure Cu nanowire/carbon nanotube coaxial nanocables with different structures by arc discharge,” *J. Phys. Chem. Solids.*, vol. 72, no. 12, pp. 1519–1523, Dec. 2011.
- [163] P. Hou, C. Liu, Y. Tong, S. Xu, M. Liu, and H. Cheng, “Purification of single-walled carbon nanotubes synthesized by the hydrogen arc-discharge method,” *J. Mater. Res.*, vol. 16, no. 9, pp. 2526–2529, Jan. 2011.
- [164] Y. Zhang, L. Zhang, P. Hou, H. Jiang, C. Liu, and H. Cheng, “Synthesis and field emission property of carbon nanotubes with sharp tips,” *New Carbon Mater.*, vol. 26, no. 1, pp. 52–56, Jan. 2011.
- [165] Y. Su, Z. Yang, H. Wei, E. S.-W. Kong, and Y. Zhang, “Synthesis of single-walled carbon nanotubes with selective diameter distributions using DC arc discharge under CO mixed atmosphere,” *Appl. Surf. Sci.*, vol. 257, no. 7, pp. 3123–3127, Jan. 2011.
- [166] G. Tripathi, B. Tripathi, M. K. Sharma, Y. K. Vijay, A. Chandra, and I. P. Jain, “A comparative study of arc discharge and chemical vapor deposition synthesized carbon nanotubes,” *Int. J. Hydrogen Energy.*, vol. 37, no. 4, pp. 3833–3838, Feb. 2011.

- [167] J. Zhao, L. Wei, Z. Yang, and Y. Zhang, "Continuous and low-cost synthesis of high-quality multi-walled carbon nanotubes by arc discharge in air," *Phys. E Low-dimensional Syst. Nanostructures.*, vol. 44, no. 7–8, pp. 1639–1643, Apr. 2012.
- [168] Y. Su, Y. Zhang, H. Wei, B. Qian, Z. Yang, and Y. Zhang, "Length-controlled synthesis of single-walled carbon nanotubes by arc discharge with variable cathode diameters," *Phys. E Low-dimensional Syst. Nanostructures.*, vol. 44, no. 7–8, pp. 1548–1551, Apr. 2012.
- [169] Y. Zhang, "Synthesis of few-walled carbon nanotube–Rh nanoparticles by arc discharge: Effect of selective oxidation," *Mater. Charact.*, vol. 68, pp. 102–109, Jun. 2012.
- [170] J. Zhao, J. Zhang, Y. Su, Z. Yang, L. Wei, and Y. Zhang, "Synthesis of straight multi-walled carbon nanotubes by arc discharge in air and their field emission properties," *J. Mater. Sci.*, vol. 47, no. 18, pp. 6535–6541, May 2012.
- [171] X. Cai, H. Cong, and C. Liu, "Synthesis of vertically-aligned carbon nanotubes without a catalyst by hydrogen arc discharge," *Carbon.*, vol. 50, no. 8, pp. 2726–2730, Jul. 2012.
- [172] J. Zhao, Y. Su, Z. Yang, L. Wei, Y. Wang, and Y. Zhang, "Arc synthesis of double-walled carbon nanotubes in low pressure air and their superior field emission properties," *Carbon.*, vol. 58, pp. 92–98, Jul. 2013.
- [173] M. I. Mohammad, A. a. Moosa, J. H. Potgieter, and M. K. Ismael, "Carbon Nanotubes Synthesis via Arc Discharge with a Yttria Catalyst," *ISRN Nanomater.*, vol. 2013, pp. 1–7, Aug. 2013.
- [174] L. Fang, L. Sheng, K. An, L. Yu, W. Ren, Y. Ando, and X. Zhao, "Effect of adding W to Fe catalyst on the synthesis of SWCNTs by arc discharge," *Phys. E Low-dimensional Syst. Nanostructures.*, vol. 50, pp. 116–121, May. 2013.
- [175] Y. Su, P. Zhou, J. Zhao, Z. Yang, and Y. Zhang, "Large-scale synthesis of few-walled carbon nanotubes by DC arc discharge in low-pressure flowing air," *Mater. Res. Bull.*, vol. 48, no. 9, pp. 3232–3235, Sep. 2013.
- [176] K. T. Chaudhary, J. Ali, and P. P. Yupapin, "Growth of small diameter multi-walled carbon nanotubes by arc discharge process," *Chinese Phys. B.*, vol. 23, no. 3, pp. 35203, Mar. 2014.
- [177] B. Email, K. Centers, A. Physics, B. Hassan, and B. Accepted, "Discharge Characteristics on the Synthesis of Carbon Nanostructures through Arc-Plasma in Water," *Eng. & Tech. Journal.*, vol. 32, no. 6, pp. 1121–1127, May. 2014.
- [178] A. Sharma, S. K. Singh, and Y. K. Vijay, "Low Cost Production of Carbon Nanotubes Using DC Arc Discharge Under Deionized Water," *Adv. Sci. Focus.*, vol. 2, no. 2, pp. 125–129, 2014.
- [179] Marcos Allan Leite dos Reis, Elizabeth M. S. Rodrigues, Jordan Del Nero, Sônia Simões, Filomena Viana, Manuel F. G. Vieira, and Maria T. F. Vieira, "One-Step

- Synthesis and Characterization of a Nanocomposite Based on Carbon Nanotubes/Aluminum and Its Reinforcement Effect on the Metal Matrix,” *J. Mater. Sci. Eng. B.*, vol. 5, no. 8, pp. 311–319, 2015.
- [180] M. Goyal, S. K. Kansal, N. Goyal, A. Khurana, G. Singh, and V. Dhar, “Preparation and Characterization of Multi-Walled Carbon Nano Tubes By Liquid Arc-Discharge Method,” *Int. J. Adv. Sci. Eng. & Tech.*, vol. 3, no. 3, pp. 62–64, Jul. 2015.
- [181] R. Sharma, A. K. Sharma, V. Sharma, and E. Harkin-Jones, “Synthesis of carbon nanotubes by arc-discharge and chemical vapor deposition method with analysis of its morphology, dispersion and functionalization characteristics,” *Cogent Eng.*, vol. 2, no. 1, pp. 1094017, Sept. 2015.
- [182] I. M. Al-essa, G. Y. Hermiz, and G. H. Mohammed, “Structure of Carbon Nanotubes Grown by Arc-Discharge Technique under Argon , N₂ and O₂ Atmosphere at Different Conditions,” *Int. J. Curr. Eng. & Tech.*, vol. 5, no. 2, pp. 834–839, Apr. 2015.
- [183] H. Zeng, L. Zhu, G. Hao, and R. Sheng, “Synthesis of various forms of carbon nanotubes by AC arc discharge,” *Carbon.*, vol. 36, no. 3, pp. 259–261, Jan. 1998.
- [184] M. Ohkohchi, “Synthesis of Single-Walled Carbon Nanotubes by AC Arc Discharge,” *Jpn. J. Appl. Phys.*, vol. 38, no. Part 1, No. 7A, pp. 4158–4159, Jul. 1999.
- [185] T. Matsuura, K. Taniguchi, and T. Watanabe, “A new type of arc plasma reactor with 12-phase alternating current discharge for synthesis of carbon nanotubes,” *Thin Solid Films.*, vol. 515, no. 9, pp. 4240–4246, Mar. 2007.
- [186] L. P. Biró, Z. E. Horváth, L. Szalmás, K. Kertész, F. Wéber, G. Juhász, G. Radnóczy, and J. Gyulai, “Continuous carbon nanotube production in underwater AC electric arc,” *Chem. Phys. Lett.*, vol. 372, no. 3–4, pp. 399–402, Apr. 2003.
- [187] Z. E. Horváth, K. Kertész, L. Pethő, a. a. Koós, L. Tapasztó, Z. Vértesy, Z. Osváth, A. Darabont, P. Nemes-Incze, Z. Sárközi, and L. P. Biró, “Inexpensive, upscalable nanotube growth methods,” *Curr. Appl. Phys.*, vol. 6, no. 2, pp. 135–140, Feb. 2006.
- [188] T. Matsuura, Y. Kondo, and N. Maki, “Selective mass production of carbon nanotubes by using multi-layered and multi-electrodes AC arc plasma reactor,” *International Plasma Chemistry Society.*, pp. 1-4, 2009.
- [189] J.-S. Su, “Investigation on carbon nanotube growth using one-pulse discharge with shield,” *Proc. Inst. Mech. Eng. Part N J. Nanoeng. Nanosyst.*, vol. 226, no. 4, pp. 175–180, Aug. 2012.
- [190] S. Yousef, a. Khattab, T. a. Osman, and M. Zaki, “Effects of Increasing Electrodes on CNTs Yield Synthesized by Using Arc-Discharge Technique,” *J. Nanomater.*, vol. 2013, pp. 1–9, Jan. 2013.

- [191] K. Kazemi Kia and F. Bonabi, "Using hydrocarbon as a carbon source for synthesis of carbon nanotube by electric field induced needle-pulsed plasma," *Thin Solid Films.*, vol. 534, pp. 162–167, May 2013.
- [192] N. Parkansky, R. L. Boxman, B. Alterkop, I. Zontag, Y. Lereah, and Z. Barkay, "Single-pulse arc production of carbon nanotubes in ambient air," *J. Phys. D. Appl. Phys.*, vol. 37, no. 19, pp. 2715–2719, Oct. 2004.
- [193] K. Imasaka, Y. Kanatake, Y. Ohshiro, J. Suehiro, and M. Hara, "Production of carbon nanoions and nanotubes using an intermittent arc discharge in water," *Thin Solid Films.*, vol. 506–507, pp. 250–254, May 2006.
- [194] A. Roch, O. Jost, B. Schultrich, and E. Beyer, "High-yield synthesis of single-walled carbon nanotubes with a pulsed arc-discharge technique," *Phys. Status Solid.*, vol. 244, no. 11, pp. 3907–3910, Nov. 2007.
- [195] T. Sugai, H. Omote, S. Bandow, N. Tanaka, and H. Shinohara, "Production of fullerenes and single-wall carbon nanotubes by high-temperature pulsed arc discharge," *J. Chem. Phys.*, vol. 112, no. 13, p. 6000, Apr. 2000.
- [196] H. Yoshida, T. Sugai, and H. Shinohara, "Fabrication, Purification, and Characterization of Double-Wall Carbon Nanotubes via Pulsed Arc Discharge," *J. Phys. Chem. C.*, vol. 112, no. 50, pp. 19908–19915, Dec. 2008.
- [197] Y. Murooka, Y. Maede, M. Ozaki, and M. Hibino, "Self-assembling of hot carbon nanoparticles observed by short pulse-arc-discharge," *Chem. Phys. Lett.*, vol. 341, no. 5–6, pp. 455–460, Jun. 2001.
- [198] T. Sugai, H. Yoshida, T. Shimada, T. Okazaki, H. Shinohara, and S. Bandow, "New Synthesis of High-Quality Double-Walled Carbon Nanotubes by High-Temperature Pulsed Arc Discharge," *Nano Lett.*, vol. 3, no. 6, pp. 769–773, Jun. 2003.
- [199] N. Parkansky, R. L. Boxman, B. Alterkop, I. Zontag, Y. Lereah, and Z. Barkay, "Single-pulse arc production of carbon nanotubes in ambient air," *J. Phys. D. Appl. Phys.*, vol. 37, no. 19, pp. 2715–2719, Oct. 2004.
- [200] T. Sugai, T. Okazaki, H. Yoshida, and H. Shinohara, "Syntheses of single- and double-wall carbon nanotubes by the HTPAD and HFCVD methods," *New J. Phys.*, vol. 6, no. 1, pp.21, Feb. 2004.
- [201] S. Muhl, F. Maya, and S. Rodil, "High-current pulsed arc preparation of carbon and metal-carbon nanoparticles," *J. Optoelectronics & adv. mater.*, vol. 7, no. 1, pp. 231–236, Feb. 2005.
- [202] Y. Y. Tsai, J. S. Su, and C. Y. Su, "A novel method to produce carbon nanotubes using EDM process," *Int. J. Mach. Tools Manuf.*, vol. 48, no. 15, pp. 1653–1657, Dec. 2008.
- [203] Y. Y. Tsai, J. S. Su, C. Y. Su, and W. H. He, "Production of carbon nanotubes by single-pulse discharge in air," *J. Mater. Process. Technol.*, vol. 209, no. 9, pp.

- 4413–4416, May 2009.
- [204] J.-S. Su, “Direct Route to Grow CNTs by Micro-Electrodischarge Machining without Catalyst in Open Air,” *Mater. Manuf. Process.*, vol. 25, no. 12, pp. 1432–1436, Dec. 2010.
- [205] K. K. Kia and F. Bonabi, “Electric field induced needle-pulsed arc discharge carbon nanotube production apparatus: circuitry and mechanical design.,” *Rev. Sci. Instrum.*, vol. 83, no. 12, pp. 123907, Dec. 2012.
- [206] K. Takekoshi, T. Kizu, S. Aikawa, and E. Nishikawa, “One-Step Synthesis of Metal-Encapsulated Carbon Nanotubes by Pulsed Arc Discharge in Water,” *e-Journal Surf. Sci. Nanotechnol.*, vol. 10, pp. 414–416, Aug. 2012.
- [207] M. V. Antisari, R. Marazzi, and R. Krsmanovic, “Synthesis of multiwall carbon nanotubes by electric arc discharge in liquid environments,” *Carbon.*, vol. 41, pp. 2393–2401, Dec. 2003.
- [208] E. I. Waldorff, “Characterization of carbon nanotubes produced by arc discharge: Effect of the background pressure,” *J. Appl. Phys.*, vol. 95, no. 5, pp. 2749, Mar. 2004.
- [209] Y. Y. Tsai, J. S. Su, C. Y. Su, and W. H. He, “Production of carbon nanotubes by single-pulse discharge in air,” *J. Mater. Process. Technol.*, vol. 209, no. 9, pp. 4413–4416, May 2009.
- [210] Z. E. Horváth, K. Kertész, L. Pethő, a. a. Koós, L. Tapasztó, Z. Vértesy, Z. Osváth, A. Darabont, P. Nemes-Incze, Z. Sárközi, and L. P. Biró, “Inexpensive, upscalable nanotube growth methods,” *Curr. Appl. Phys.*, vol. 6, no. 2, pp. 135–140, Feb. 2006.
- [211] J.-S. Su, “Direct Route to Grow CNTs by Micro-Electrodischarge Machining without Catalyst in Open Air,” *Mater. Manuf. Process.*, vol. 25, no. 12, pp. 1432–1436, Dec. 2010.
- [212] Y. Murooka, Y. Maede, M. Ozaki, and M. Hibino, “Self-assembling of hot carbon nanoparticles observed by short pulse-arc-discharge,” *Chem. Phys. Letters.*, vol. 341, no. 5, pp. 455–460, Jun. 2001.
- [213] A. Anders, B. Yotsombat, and R. Binder, “Correlation between cathode properties, burning voltage, and plasma parameters of vacuum arcs,” *J. Appl. Phys.*, vol. 89, no. 12, pp. 7764, Jun. 2001.
- [214] W. H. Qi and M. P. Wang, “Size effect on the cohesive energy of nanoparticle,” *J. of Mat. Science Letters.*, vol. 21, no. 22, pp. 1743–1745, Nov. 2002.
- [215] H. H. Kim and H. J. Kim, “New DC Arc Discharge Synthesis Method for Carbon Nanotubes Using Xylene Ferrocene as Floating Catalyst,” *Jpn. J. Appl. Phys.*, vol. 46, no. 4A, pp. 1818–1820, Apr. 2007.
- [216] M. Jahanshahi, M. Shariaty-niassar, A. A. Rostami, and H. Molavi, “Arc-discharge Carbon Nanotube Fabrication in Solution: Electrochemistry and

- Voltametric Tests." *Australian J. Basic and Applied Sci.*, vol. 4, no. 12, pp. 5915–5922, 2010.
- [217] Y. Li, S. Xie, W. Zhou, D. Tang, Z. Liu, X. Zou, and G. Wang, "Small diameter carbon nanotubes synthesized in an," *Chinese Academy of Sciences.*, vol. 39, pp. 1429–1431, Feb. 2001.
- [218] J. M. Chem, J. Prasek, J. Drbohlavova, J. Chomoucka, J. Hubalek, O. Jasek, and R. Kizek, "Methods for carbon nanotubes synthesis — review," *J. Materials Chem.*, vol. 21, no. 40, pp. 15872–15884, Jul. 2011.
- [219] S. Cui, P. Scharff, C. Siegmund, L. Spiess, H. Romanus, J. Schawohl, K. Risch, D. Schneider, and S. Klotzer, "Preparation of multiwalled carbon nanotubes by DC arc discharge under a nitrogen atmosphere," *Carbon.*, vol. 41, no. 8, pp. 1648–1651, 2003.
- [220] S. P. Doherty and R. P. H. Chang, "Synthesis of multiwalled carbon nanotubes from carbon black," *Appl. Phys. Lett.*, vol. 81, no. 13, pp. 2466, Sept. 2002.
- [221] H. Lange, M. Sioda, A. Huczko, Y. Q. Zhu, H. W. Kroto, and D. R. M. Walton, "Nanocarbon production by arc discharge in water," *Carbon.*, vol. 41, pp. 1617–1623, Dec. 2003.
- [222] S. Jong Lee, H. Koo Baik, J. Yoo, and J. Hoon Han, "Large scale synthesis of carbon nanotubes by plasma rotating arc discharge technique," *Diam. Relat. Mater.*, vol. 11, no. 3–6, pp. 914–917, Mar. 2002.
- [223] G. RANISZEWSKI, L. SZYMANSKI, and Z. KOLACINSKI, "Carbon Nanotubes Synthesis by Electric Arc Plasma with External Magnetic Field," in *4th International Conference Nanocon.*, pp. 131–137, 2012.
- [224] Y. S. Park, K. S. Kim, H. J. Jeong, W. S. Kim, J. M. Moon, K. H. An, D. J. Bae, Y. S. Lee, G. Park, and Y. H. Lee, "Low pressure synthesis of single-walled carbon nanotubes by arc discharge," *Synth. Met.*, vol. 126, no. 2–3, pp. 245–251, Feb. 2002.
- [225] J. Qiu, Z. Wang, Z. Zhao, and T. Wang, "Synthesis of double-walled carbon nanotubes from coal in hydrogen-free atmosphere," *Fuel.*, vol. 86, pp. 282–286, Jan. 2007.
- [226] A. A. Setlur, S. P. Doherty, J. Y. Dai, and R. P. H. Chang, "A promising pathway to make multiwalled carbon nanotubes," *Appl. Phys. Lett.*, vol. 76, no. 21, pp. 3008–3010, May. 2000.
- [227] K. Dasgupta, J. B. Joshi, and S. Banerjee, "Fluidized bed synthesis of carbon nanotubes – A review," *Chem. Eng. J.*, vol. 171, no. 3, pp. 841–869, Jul. 2011.
- [228] S. P. Doherty, D. B. Buchholz, B.-J. Li, and R. P. H. Chang, "Solid-state synthesis of multiwalled carbon nanotubes," *J. Mater. Res.*, vol. 18, no. 4, pp. 941–949, Jan. 2012.
- [229] K. Dasgupta, D. Sen, T. Mazumdar, R. K. Lenka, R. Tewari, S. Mazumder, J. B.

- Joshi, and S. Banerjee, "Formation of bamboo-shaped carbon nanotubes on carbon black in a fluidized bed," *J. Nanoparticle Res.*, vol. 14, no. 3, pp. 728, Mar. 2012.
- [230] B. Li, Y. Nan, P. Zhang, Z. Wang, Q. Lu, and X. Song, "Synthesis and characterization of carbon nanostructures by evaporating pure graphite and carbon black in detonation-gas arc discharge," *Diam. Relat. Mater.*, vol. 55, pp. 87–94, May. 2015.

Design of Experimental Set Up

3.1 Introduction

In the previous chapter, comprehensive literature review including carbon nanotubes, its synthesis method, effect of various parameters such as power supply, current, voltage, frequency, catalyst, atmosphere, pressure, various carbon precursor required in formation of carbon nanotubes have been presented chronologically. We identified gaps in research and correspondingly defined scope and problem statement within the scope. As a first problem at hand, in an attempt to synthesize carbon nanotubes from carbon black arc discharge set up needs to be designed. The objective of the design is to obtain a stable arc and a constant arc current across the electrode.

Constant current across electrodes is required to improve the reliability of the process and synthesized product [1]. With the perspective to understand the science involved in making of carbon nanotubes we hypothesized that not only constant arc current but a stable arc also plays a vital role in synthesis of CNTs. Arc discharge chamber was conceptually designed and custom fabricated by the vacuum chamber manufacturer (Excel Instruments, Mumbai, India). In next section, we discuss various designs available in literature, assess and customize the design choice for the set objectives within scope of the thesis. We have considered mechanical and electrical circuit design of the custom built arc chamber in rest of two sections respectively in this chapter.

3.2 Arc Discharge Setup Design

The schematic diagram of arc discharge set up modification of electrodes are shown in Figure 3.1 was first reported by [2] and have been mentioned repeatedly in [3]–[9]. The setup has been modified by the researchers over the passage of time to improve the quality, size and yield of CNTs. Zhao and Liu [2] used a modified conventional arc discharge apparatus to increase the yield of CNTs. In the setup of [2] six electrodes are mounted on a wheel at an equal distance from each other as shown in Figure 3.1(a).

The electrodes are rotated in order to change the active anode. Zhao et al. [2] observed high quality SWCNTs at inner wall of the chamber.

Among various published literature researchers [3]–[6] have used a rotating carbon electrode for a homogeneous micro-discharge resulting in good quality nanotubes. Joshi et al. [3] reported that rotating the carbon cathode in an arc discharge setup has a significant impact on the quality and yield of CNTs as shown in Figure 3(b). It was observed that rotating the cathode drags plasma away from high temperature region formed between two electrodes. This produce sudden quenching of reactive plasma which leads to proper mixing of carbon vapor results in significant high yield. It was observed yield was increased 50-50% at lower electrode disk rotation speed compared to higher disk speeds.

Lee et al. [4] reported that large scale synthesis of carbon nanotubes is achieved by rotating plasma in arc discharge setup shown in Figure 3.1(c). In plasma rotating electrode process, whole area of anode is evaporated uniformly and nanotubes are collected in collector near the electrodes. This results in continuous growth of nanotubes as the carbon vapors move out due to centrifugal force resulting in uniformly distributed plasma.

Liu et al. [5] reported a hydrogen arc discharge method by which high quality SWCNTs synthesized by rotating the anode in arc discharge chamber so that hole filled with raw material on cathode side can be shifted to suitable position for continuous synthesis. Kim et al. [6] produced crystalline and short MWCNTs by using hollow graphite anode and a rotating high resistive cathode.

Kanai et al. [7] have proposed a gravity free arc discharge for high yields. Under gravity free condition, the arc plasma has been stabilized when strong heat convection is suppressed. This makes the anode surface to be efficiently heated to increase the sublimation rate which results in production of nanotubes with high density. The formation of SWCNTs is closely proportional to the evaporation rate of the composite rod (anode).

Ando et al. [8] inclined the cathode and anode at an angle of 30° as shown in Figure 3.1(d) to improve the yield of the process. Ando reported in conventional method the production of SWCNTs occur when two electrodes are kept opposite at gap

distance of 1-2 mm then carbon atom evaporated from anode and directly deposited on cathode. Whereas in case of arc plasma jet method, cathode was set at an angle of 30° with anode at a gap distance of approximately 5 mm. Due to larger gap distance, little part of 20% evaporated material reaches the cathode and 80% becomes cotton like soot forms SWCNTs.

Horvath et al. [9] also investigated the effect of angle between two electrodes immersed in water and found that highest yield is obtained at 90° inclination. Upon inclination of the electrodes, a majority of the product does not get deposited on the cathode and the deposition mostly flies away to the walls, thereby increasing the yield of SWCNTs.

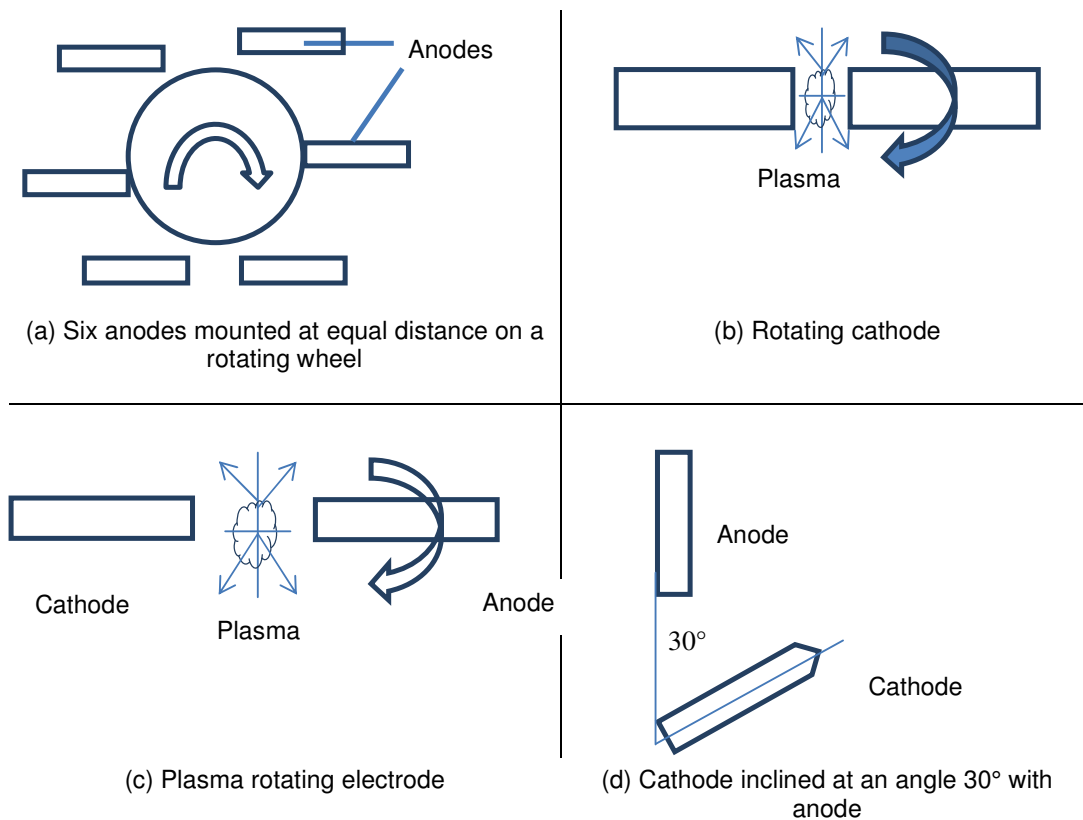


Figure 3.1: Schematic diagram of set up modification of electrodes (a) Six electrodes are mounted on a wheel at an equal distance; (b) Rotating cathode; (c) Plasma rotating electrode; (d) Cathode inclined at an angle 30° with anode

Among various design and disposition of electrodes available, we conceived a simple arrangement of two electrodes mounted horizontally. The disposition of two horizontal electrodes allowed ease of handling and design of arc chamber simpler too. With the

simple design, we focused on conversion of chosen precursor (CB) to synthesize CNT as that is the scope of investigation in the thesis. As a first step, set up was designed in creo view software by considering the dimensions of electrodes and built up design of a vacuum chamber which is detailed in next section.

3.2.1 Mechanical Design

Arc chamber was modeled by drawing each part using creo view software. This software creates interactive assembly and has various elements that creates customized product. Firstly, we have two graphite electrodes taken out from standard D-cell battery as it is easily available. Figure 3.2 shows the two electrodes of diameter 6 mm mounted horizontally inside the chamber on the left hand side we have cathode in black color and on right side we have anode of red color.



Figure 3.2: Two electrodes mounted horizontally

Cathode and anode are given proper fixtures by holding screw of dimension 20 mm to avoid falling of electrode into the chamber. Holding screw provide the proper grip to the electrodes as shown in Figure 3.3.

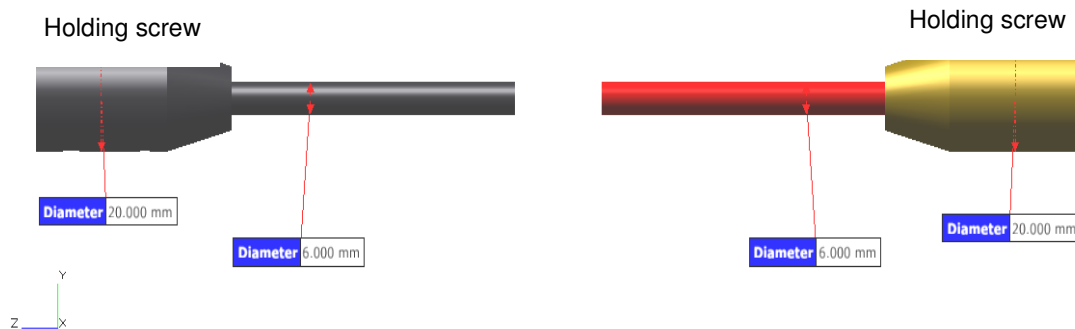


Figure 3.3: Shows holding screw giving proper gripping to the electrodes

Figure 3.4 shows copper pipe of 12 mm attached to the electrode with holding screw for easy movement of electrodes in chamber.

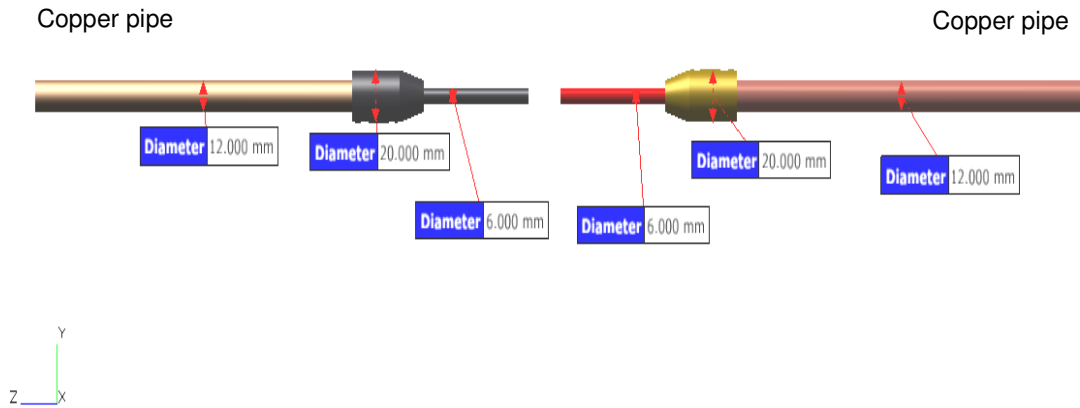


Figure 3.4: Copper pipe attached to the electrodes

Bellow flange assembly was connected over the copper pipe on anode side as shown in Figure 3.5. Bellow flange assembly consist of bellow end part 1 and part 2 of diameter 18 mm and part in between bellow end part1 and 2 of diameter 23.45 mm. Bellow Flange was used to prevent stresses on pipe. Stresses may occur due to various reasons such as internal or external pressure at working temperature, weight of the pipe, parts supported on it and attributed to thermal expansion.

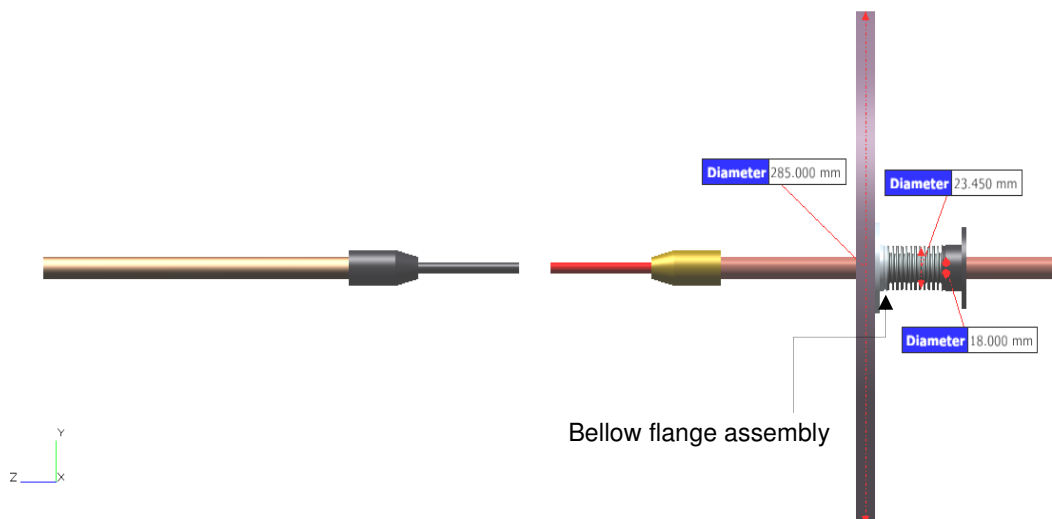


Figure 3.5: Bellow flange assembly

Figure 3.6 shows Teflon guide and Teflon push fit part of 40 mm and 14 mm. Teflon guide was connected below bellow end part 1 and Teflon push fit part after bellow part. Teflon guide and push fit were used to hold the bellow part in place without having to permanently glue it.

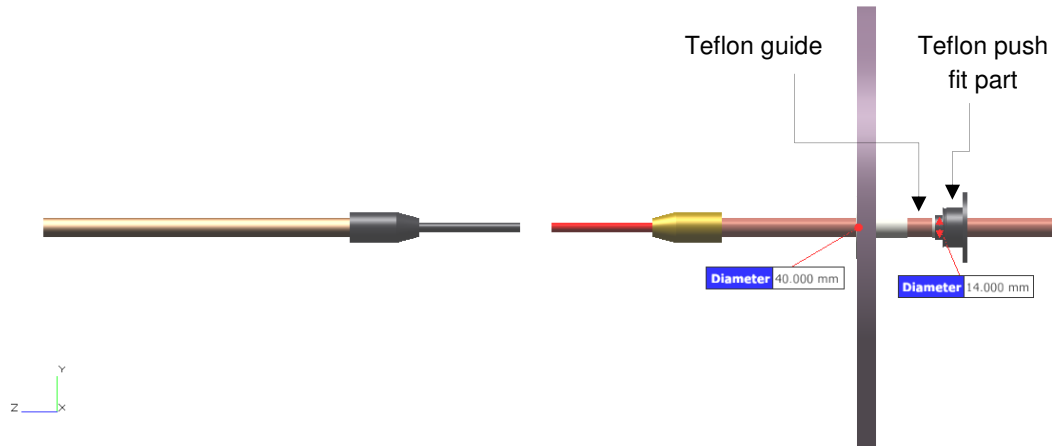


Figure 3.6: Teflon guide and Teflon push fit part

Nut, washer and Support Patti part were connected towards anode as shown in Figure 3.7. Washer was connected to distribute the pressure of the nut over the surface, so that surface is not damaged and also to ensure that nut is pressed against a surface, reducing the chances of looseness. Support Patti was connected in between the nut and washer to provide electrical connection from power supply to anode side.

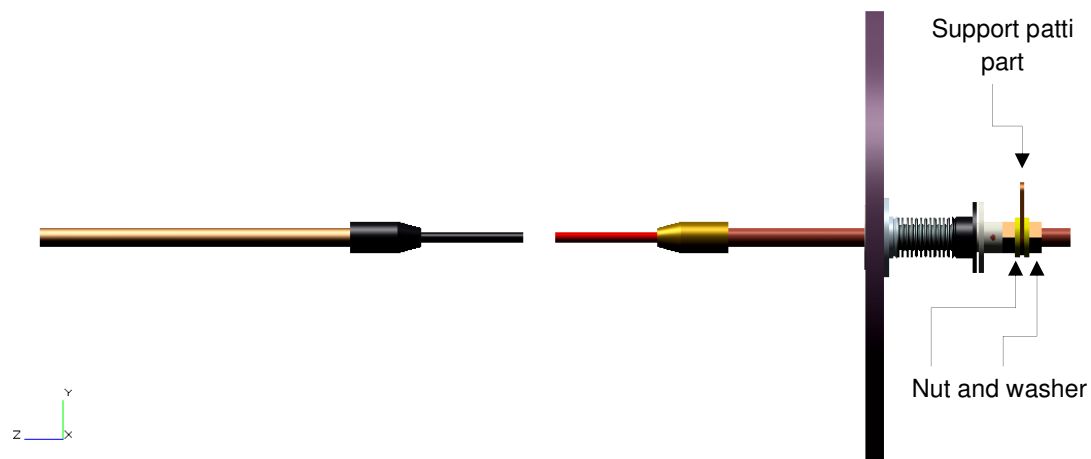


Figure 3.7: Nut, washer and support Patti part

Three studs, a metal rod having threads on both side of electrodes of diameter 8 mm one side was connected to flange and other side of electrode was connected to motor mounting through bearing plate as shown in Figure 3.8. Half inch BSW (British Standard Whitworth) tap pipe part of 26 mm diameter was connected over the copper pipe to bearing plate part. Nema 23 stepper motor is a hybrid stepping motor and has a 1.8° step angle (200 steps/ revolution) was connected after the motor plate part. A screw-gauge micrometer on stepper motor with automatic arc controller interface provide the automatic gap adjustment between the electrode which is attached to the positive electrode i.e. anode. The micrometer which moves is connected as a lever arrangement, was calibrated using law of similar triangles as, for one division of rotation in pitch scale, it moves the electrode by 0.04156 inches.

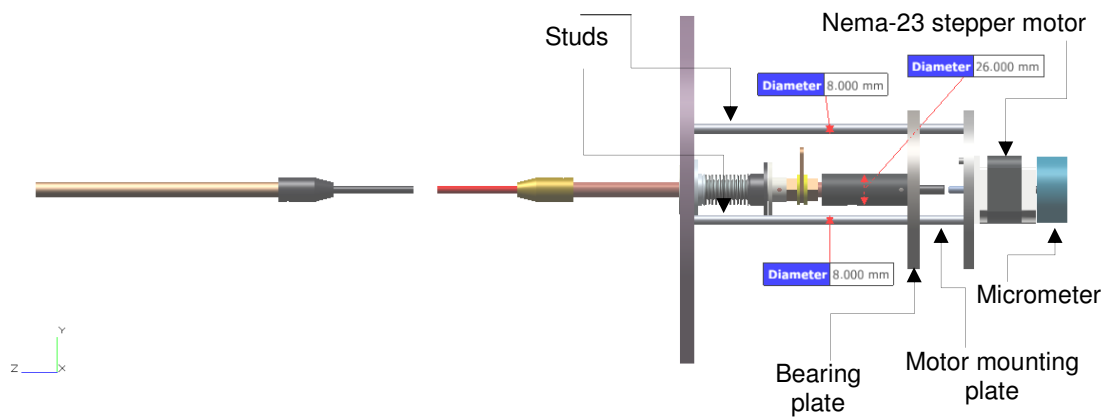


Figure 3.8: Three studs, motor mounting plate, bearing plate and Nema 23 stepper motor

Figure 3.9 shows coupler part connected in between bearing and motor mounting plate and three linear bearing part were used for connecting stud part to bearing plate with the help of washer so that stud should not misplace from its position.

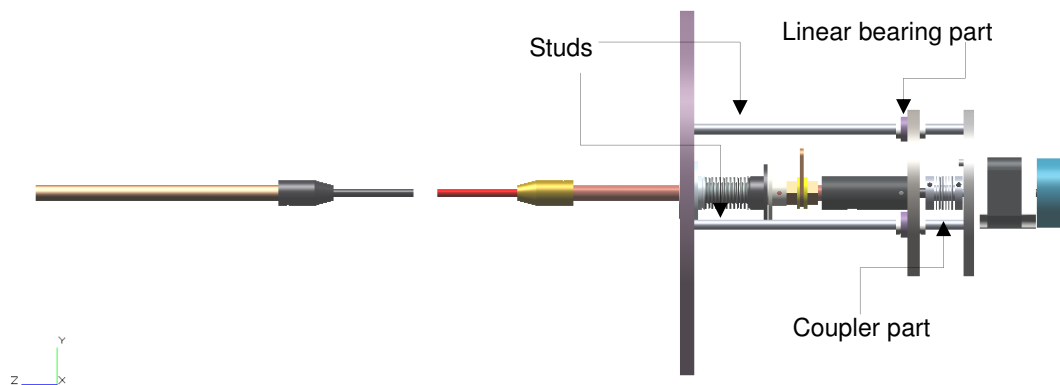


Figure 3.9: Coupler and linear bearing part

Push fit 1-8 inch part was connected for water supply as shown in Figure 3.10. Water supply was used to provide cooling outside the chamber to avoid the sagging of chamber due to high temperature of plasma inside the chamber while performing the experiments.

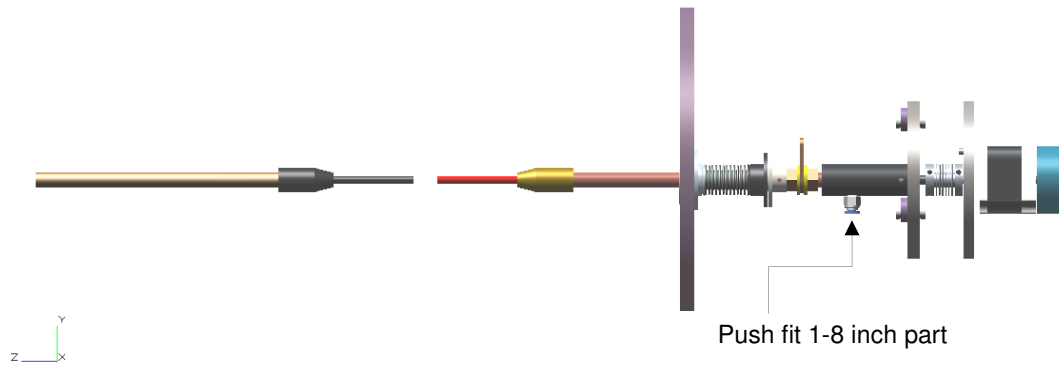


Figure 3.10: Push fit 1-8 inch part

Now CF 35 part (ConFlat) flanges of diameter 285 mm is attached to anode and cathode in arc discharge setup as shown in Figure 3.11. ConFlat Flange use a copper gasket and knife-edge flange to achieve an ultrahigh vacuum seal.

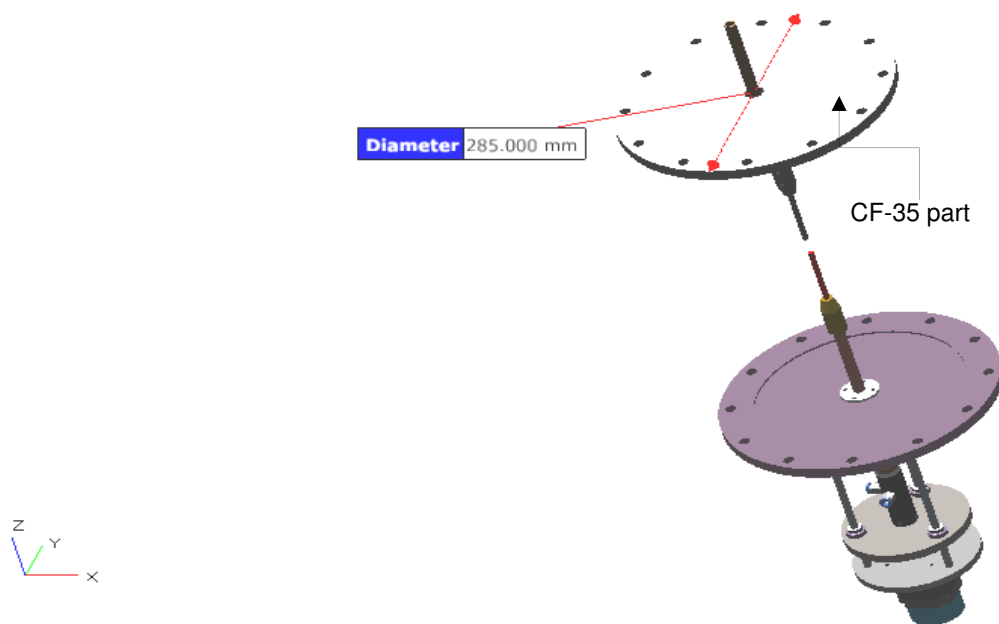


Figure 3.11: CF-35 part

To provide a rotary mechanical feed through for transmitting rotational mechanical motion through the walls of a vacuum system. The feed through part of 20 mm diameter as shown in Figure 3.12 and connected through feed through nut of 24 mm diameter in cathode side.

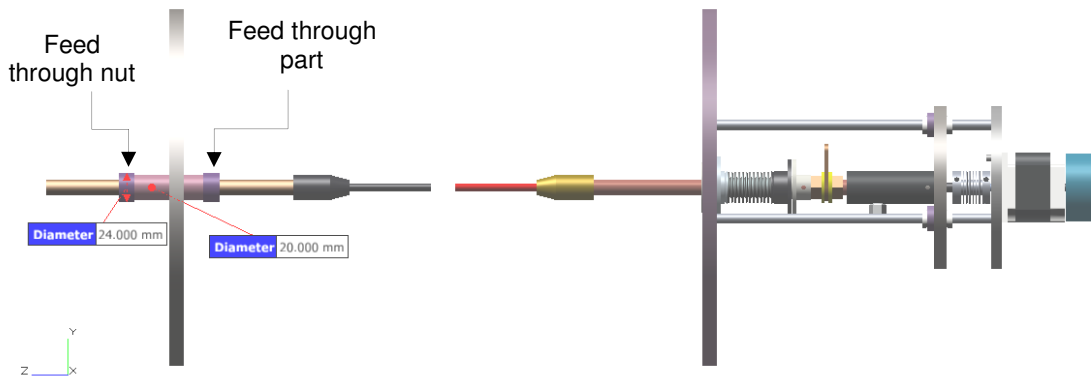


Figure 3.12: Feed through and feed through nut part

Support Patti was connected through washer and nut to provide electrical power supply to cathode as shown in Figure 3.13.

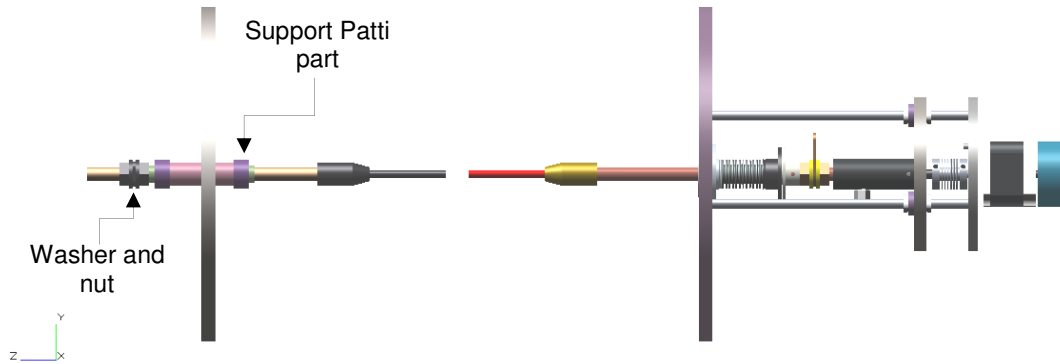


Figure 3.13: Support Patti, washer and nut part to cathode side

Delrin part and two push fit 1-8 inch parts were connected for inlet connection in the chamber for gaseous environment. Second push fit 1-8 inch part was used for water outlet as shown in Figure 3.14.

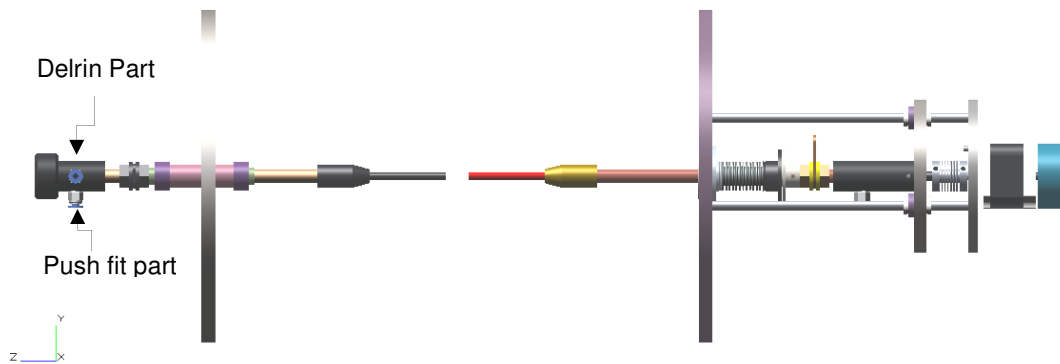


Figure 3.14: Delrin and push fit part

The whole apparatus is designed above enclosed in a cylindrical chamber pipe with left and right window of 208 mm diameter with four window door open of diameter 101 mm as shown in Figure 3.15.

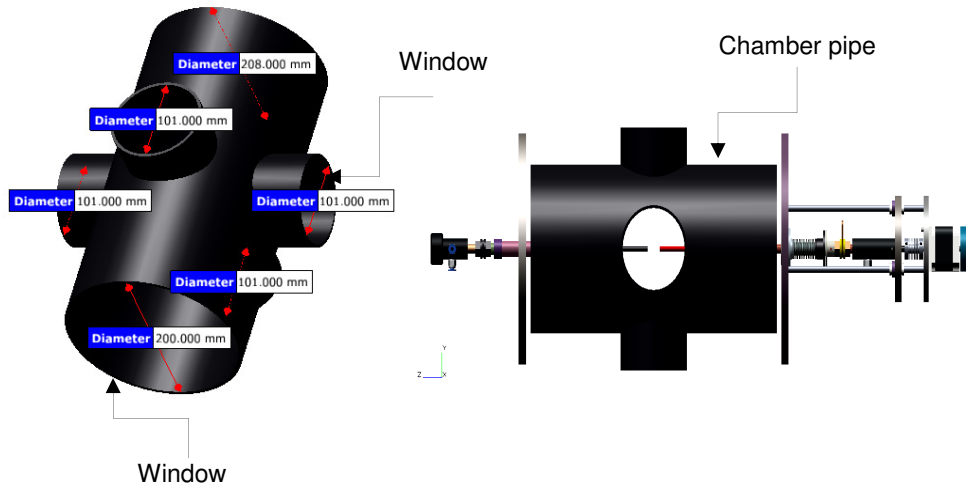


Figure 3.15: Chamber pipe

The chamber has four windows of diameter 101 mm each for monitoring and watching the process as shown in Figure 3.16. Two windows (a) and (c) are closed with plain glass, third window (b) which is closed with shaded glass to prevent the eye affecting by the direct arc and in fourth window (d) thermal imaging camera was connected to measure the temperature of arc as shown in Figure 3.17.

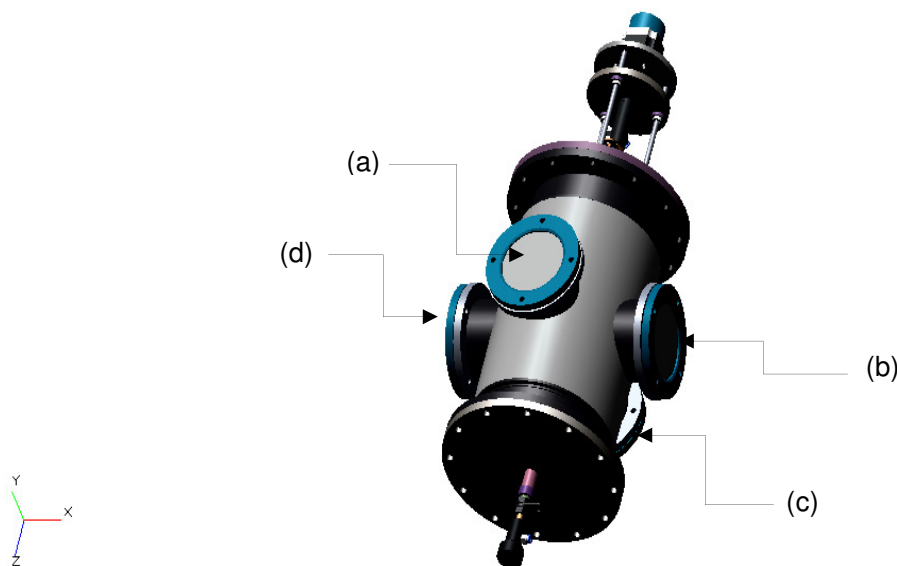


Figure 3.16: Window cover with door glass

Thermal imaging cameras are devices that translate thermal energy (heat) into visible light in order to analyze a particular object. It uses ultra violet rays to record the temperature at the focused point. It has to be focused manually on to the point where the temperature has to be read and the digital read and plot could be observed and recorded for future reference.

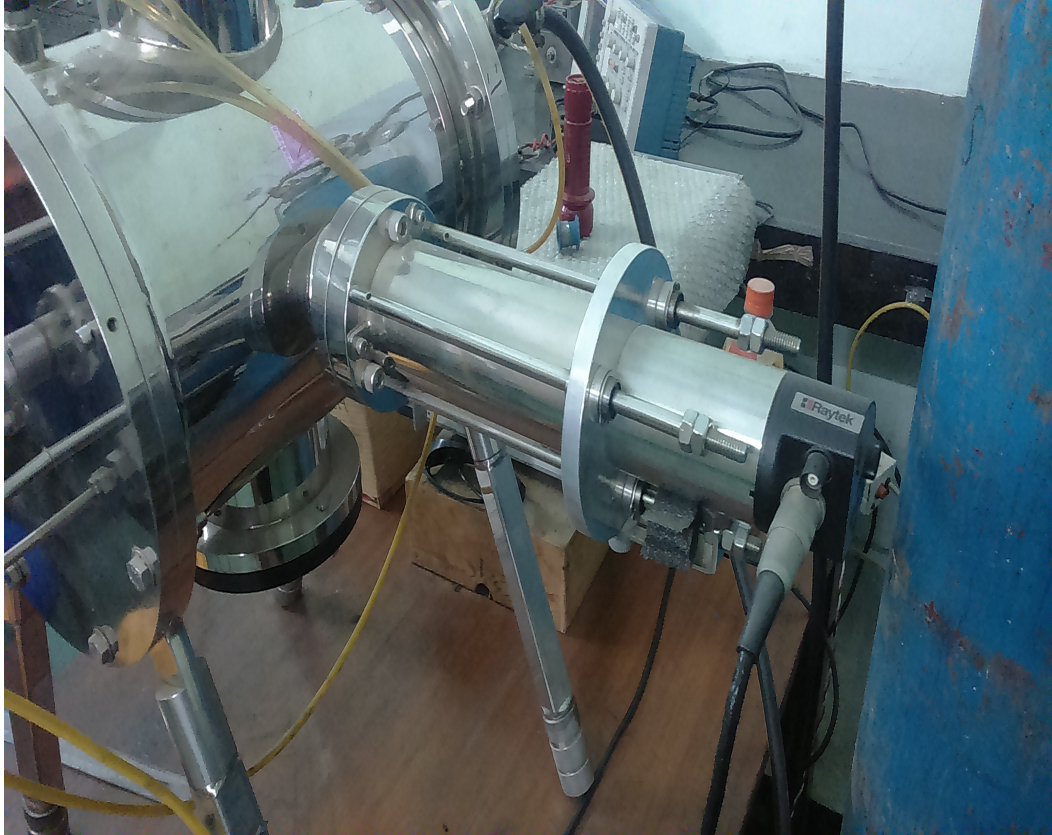


Figure 3.17: Thermal imaging camera i.e. fitted to arc discharge set up

Since the experiment has to be conducted in inert atmosphere; the chamber is properly sealed with gasket of 152 mm provided in all windows. To protect the sagging of the chamber water cooled jacket of diameter 226 mm was connected within the chamber as shown in Figure 3.18. In order to create an inert atmosphere inside the chamber, an Argon gas cylinder is attached to the chamber through a rubber pipe and the flow is adjusted using a regulator and valves.

ISO flange are connected to both side of the electrodes and two 1-4 base coupling part are attached as shown in Figure 3.19. ISO flange is a centering ring for alignment and support of the sealing ring. Flanges are used to create a complete vacuum system.

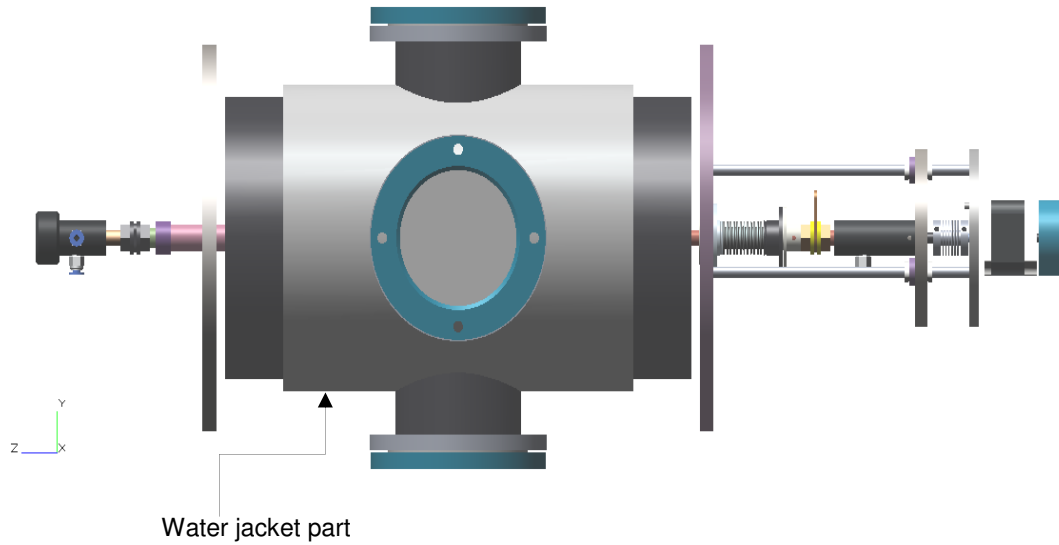


Figure 3.18: Water cooled jacket

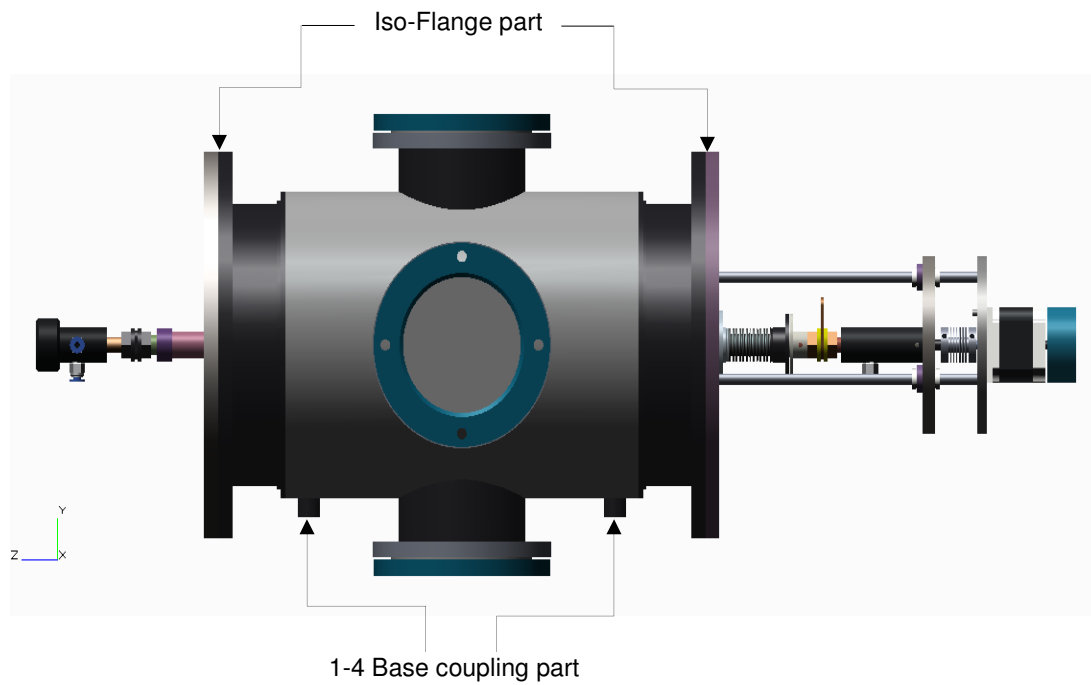


Figure 3.19: ISO-Flange and two 1-4 base coupling part

The complete structure is supported for stand stability by providing four legs. Figure 3.20 shows the leg assembly of arc chamber. Leg assembly supports the whole arc discharge chamber.

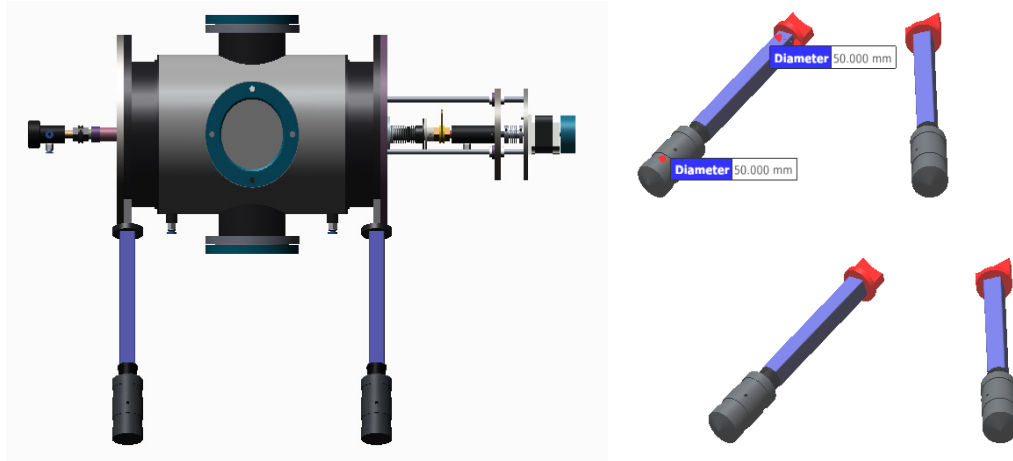


Figure 3.20: Leg assembly

The customized design of arc discharge setup has several advantages such as water cooled jacket to prevent heating up, stand-alone programmable arc current controller interface, compact design, built in motor power supply.

In the next subsection we detail design of electrical circuit to generate constant arc current across the electrodes.

3.2.2 Design of Electrical Circuit

Electrical circuit is designed with an objective of generating a constant current across the electrodes in the range of 20 A to 40 A with a step of 5 A. The input supply to obtain the objective is normal commercial electrical supply of 230 V; 50 Hz. The input is transformed into two ways namely DC and pulsed power supply for the investigation. Arc current, effects the emission of electrons from cathode which travels at high velocity towards anode. The electrons hit the anode surface which results in sputtering of carbon precursors. Upon increasing the arc current, the number of electrons striking the anode surface increases, thereby sputtering more carbon precursor from the anode. We have varied arc current to see the transformation of carbon black to carbon nanotube. It has been observed from published literature, majority of the experiments were conducted at high value of current density. Ebbesen and Gamaly [10] suggested that the current density for synthesis of CNTs should be around 165-195 A/cm². Cadek et al. [11] studied the dependence of arc current on the yield of nanotubes and concluded that the yield increases as current density is varied from 165 A/cm² to 195 A/cm². Nishizaka et al. [12] found the optimal current density for SWCNT formation as 250-270 A/cm². Matsuura et

al. [13] observed better yields of SWCNT at a current density of $\sim 450 \text{ A/cm}^2$. Our aim was to reduce current level to investigate on synthesis of CNTs. In order to do so, we have performed experiments at low amperage level using Carbon Black as carbon precursor and using DC power supply and pulsed power supply. The details of circuit used to obtain DC and pulsed power supply are given below in next subsections.

3.2.2.1 DC power supply

In DC power circuit, the main power supply of 230 V is connected to autotransformer or a variable autotransformer (Dimmerstat type providing output 0-270 V and maximum load of 15 A) schematically shown as first element in Figure 3.2. The images of components namely variac, transformer are shown in Figure 3.22. Next element autotransformer is a single coil transformer which means two portion of the same coil are used as the primary and secondary. Autotransformer varies the voltage from 0 to 260 V and is joined to two other transformers linked in parallel to provide current up to 60 A (each transformer providing current of 30 A). As an example to get an output current, consider obtaining 40 A, we vary the autotransformer to 150 V and set the value of current as 16.7 A in the arc controller interface. The motor then adjust the gap automatically through automatic arc controller interface in order to generate an arc of 40 A across the electrodes. Further, rectifier is internally connected in the transformer on output side to convert alternating current into direct current as shown in Figure 3.23. The output from the transformer is connected to electrodes inside the arc discharge chamber.

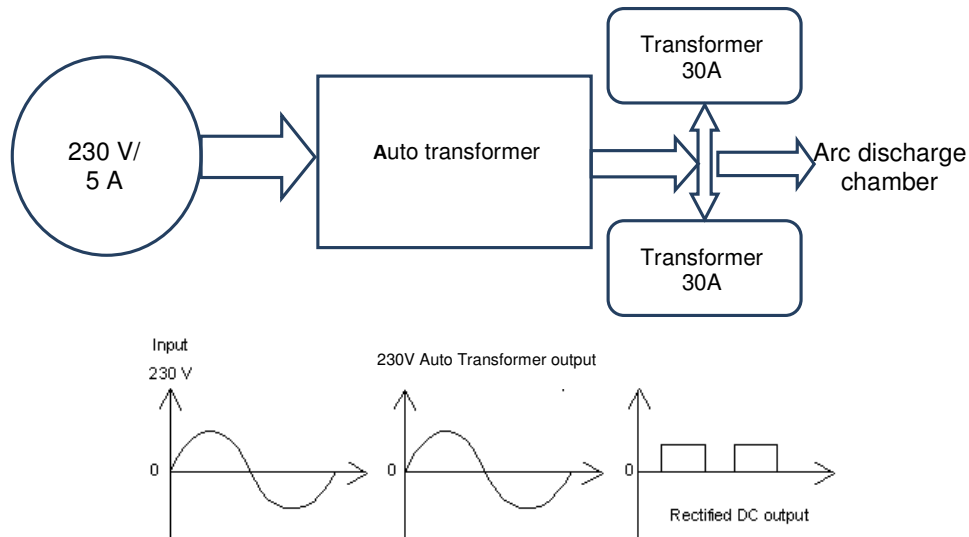


Figure 3.21: Flow chart diagram of DC power supply

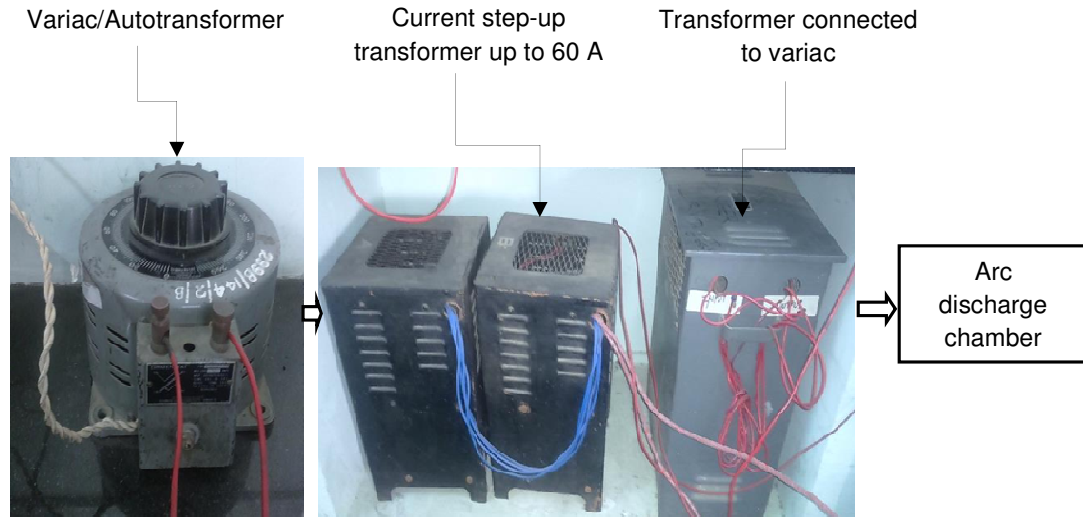


Figure 3.22: DC arc discharge setup

The circuit of pulsed power supply is explained in next subsection.

3.2.2.2 Pulsed power supply

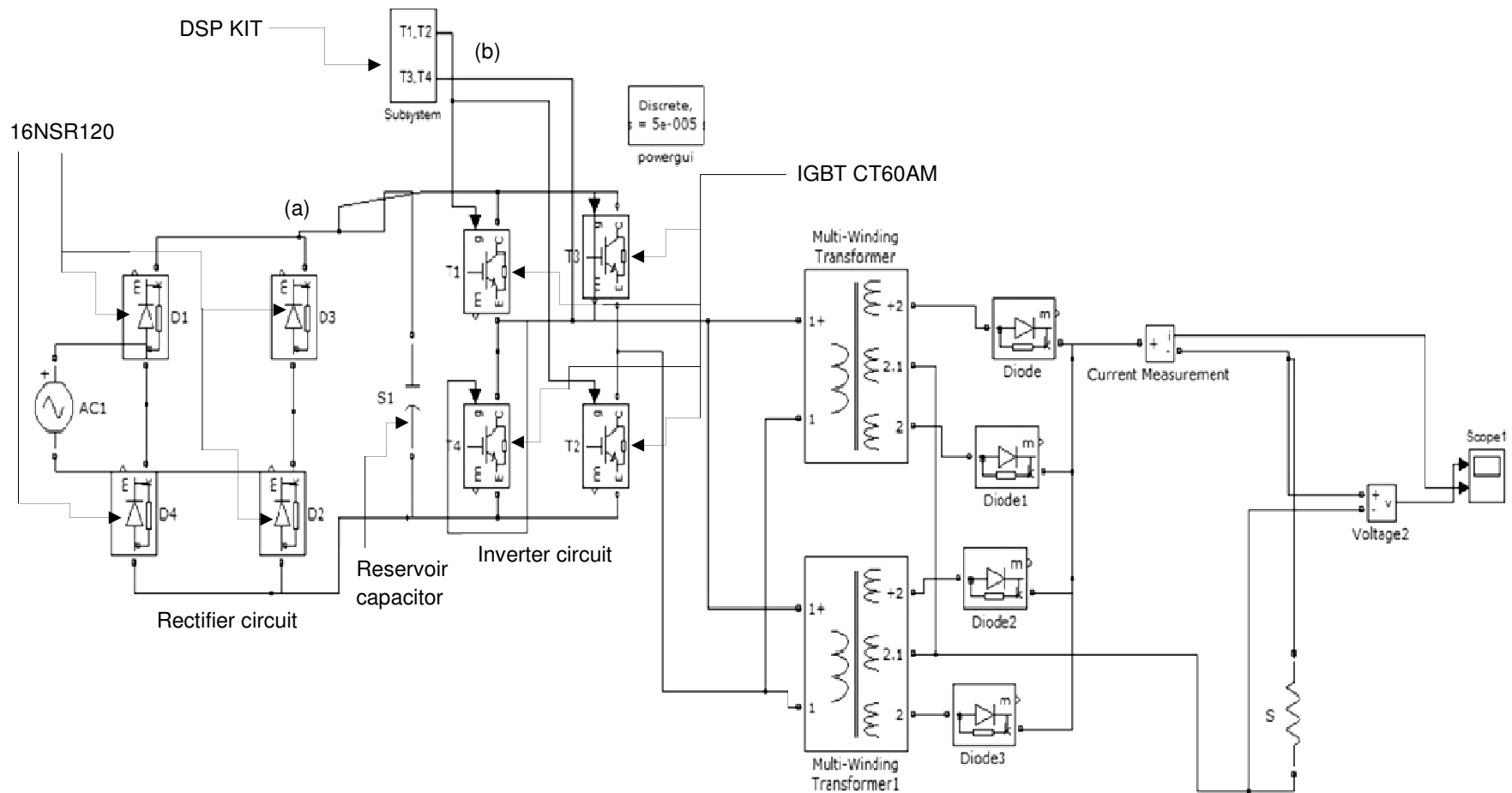
Few researchers have synthesized carbon nanotubes using pulsed power supply. Sugai et al. [14] used pulsed arc discharge method to synthesize SWCNT at pulse width of 1 ms at 22 A. Sugai et al. [15] produced high quality DWCNTs at 1500 V, 100 A for pulse width range of 300 μ s - 100 ms. Sugai et al. [16] synthesized DWNTs at high temperature pulse arc discharge with Y/Ni alloy catalysts at 1250°C. Parkansky et al. [17] produced MWCNTs using pulsed arc of 7-100 A and pulse width of 0.2-26 μ s. Tsai et al. [18] produced carbon nanotubes at 80 V, 2.5 A at pulse width of 1 ms. Kia and Bonabi [19] studied the formation of CNT using pulsed arc discharge at 500 V, 10 A at a frequency of 40-400 Hz and pulse width of 0.3 μ s. In these studies [14-19], CNTs have been synthesized from graphite. There is no research available on pulsed power circuit using carbon black as precursor for CNT synthesis.

Our aim was to design the circuit for pulsed power supply to synthesize CNT using carbon black as precursor. We want pulsed output of varying arc current and of varying duty cycle for that we were in need of a frequency varying power supply. Due to high cost involved in customizing frequency varying power supply, we conducted experiment on single frequency pulsed power supply. The duty cycle decides the average output voltage across the output leads and the current. Since the current was

pulsating it is expected to obtain results different from a direct current supply. The reason for expected variation is that as the intensity of the energy delivered is more in a pulsating wave than in one that is continuous supply i.e. DC power supply. With the expectation of finding a variation in synthesized CNTs, we designed a circuit to obtain pulsed power supply.

The schematic diagram of designed circuit to obtain the pulsed power supply is as shown in Figure 3.23. Main power supply of 230 V/15 A is connected to variac/ autotransformer. On which we vary the voltage according to the current at the output. Output of autotransformer was connected to full wave bridge rectifier circuit as shown in Figure 3.23. In full wave bridge rectifier four diodes 16NSR120 (specification are given in Appendix A.1.) are connected and convert AC input to DC. The output of the midpoint full wave bridge rectifier as shown by point (a) is DC. Considering the output of the rectifier is not maintained ripple free then it might affect the proper operation of the switch used. Reservoir capacitor (470 μ F) is connected across the output terminals of the rectifier to filter out the input ripple. Output from rectifier circuit was fed to inverter input then get pulsating current at inverter output. In inverter circuit four IGBT CT60AM switches as shown in Figure 3.23 are connected in order to give pulse waveform. CT60AM IGBT IC was used as inverter switch which has the current rating up to 60 A as required by the circuit and specification are given in Appendix A.2.

Pulse DC signal is applied at the gate of IGBT switch by DSP kit as shown in Figure 3.23 by point (b) which generates the pulse by interfacing through four opto coupler 6N137 as shown in Figure 3.24. Two 6N137 IC generate low side pulse and is connected to pin no. 12 (L1, L2) of IR2113 and another two 6N137 generate high side pulse and is connected to pin no. 10 (H1, H2) of IR2113. Output Pulse (L1, H1 and L2, H2) from IR2113 is applied to gate of IGBT switch as IR2113 is a gate driver IC specification is given in Appendix A.3. 6N137 (specification given in Appendix A.4.) is designed for use in high speed digital interfacing applications that require high voltage isolation between DSP kit and IR 2110 gate driver IC so that any voltage in circuit would not affect DSP kit directly. In Gate driver IC (IR2110/2113) there are two switches i.e. high side switch (H1, H2) and low side switch (L1, L2) as shown in Figure 3.24.



Current step up transformer providing current up to 60A

Figure 3.23: Schematic diagram of the pulsed power supply

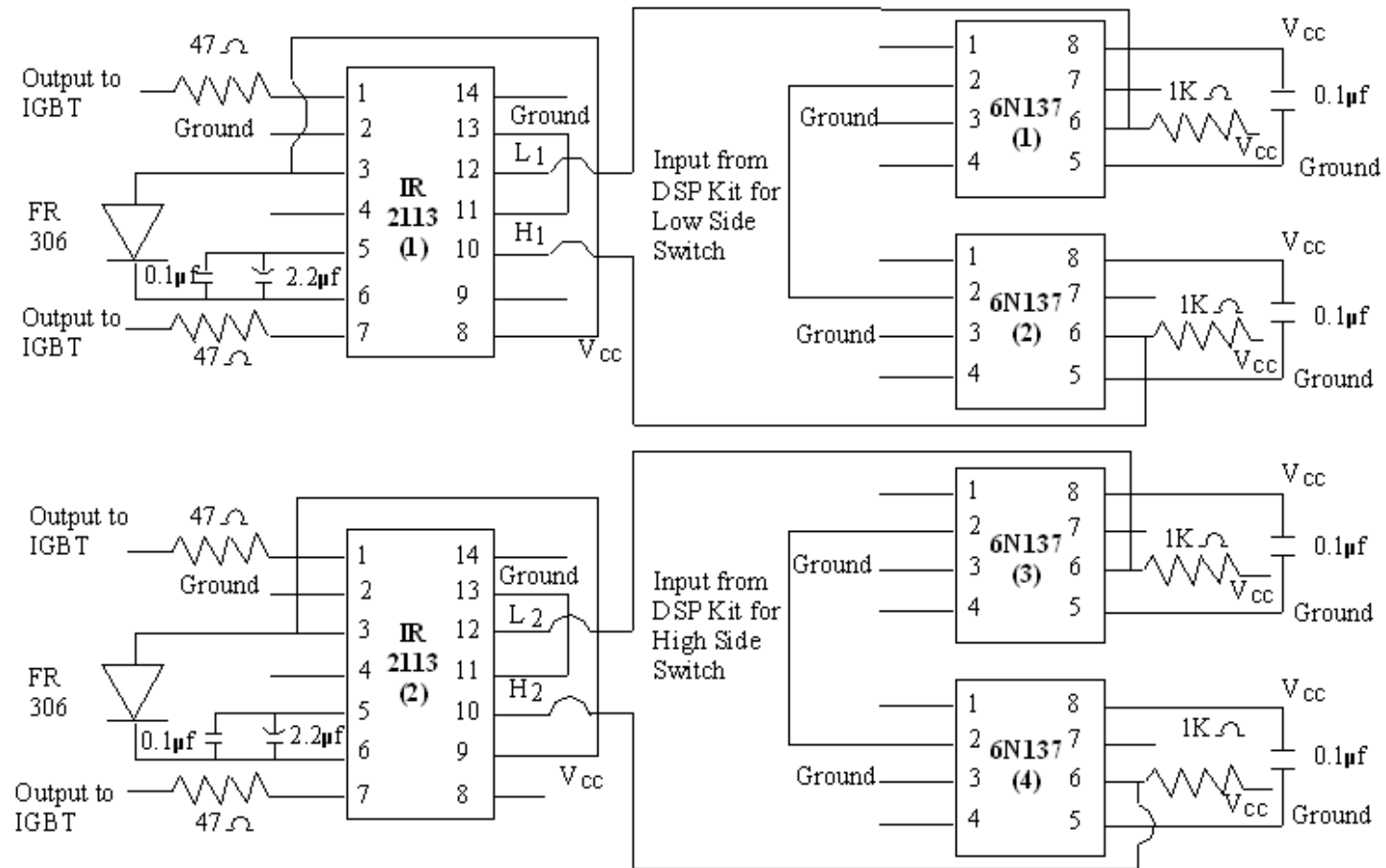


Figure 3.24: Shows gate driver IR2113 and optocoupler 6N137

Pulsating DC output from inverter connected to the transformer connected in output side as shown in Figure 3.23 providing current up to 60 A. After switching on the main power supply, voltage was set in the variac according to the arc current required at the output.

3.3 Conclusion

We have discussed the various design of arc chamber available in literature. We have designed the arc discharge chamber by considering mechanical design and electrical circuit design of DC and pulsed arc discharge setup for the custom built arc chamber.

In next chapter first we brief introduce carbon black, its chemistry and morphology and next we investigate the amenability of conversion of different grades of CB to nanotube using DC arc discharge set up designed in this chapter.

References:

- [1] N. Arora and N. N. Sharma, "Sustained arc temperature: better marker for phase transformation of carbon black to multiwalled carbon nanotubes in arc discharge method," *Mater. Res. Express.*, vol. 3, no. 10, pp. 105030, Oct. 2016.
- [2] T. Zhao and Y. Liu, "Large scale and high purity synthesis of single-walled carbon nanotubes by arc discharge at controlled temperatures," *Carbon.*, vol. 42, no. 12–13, pp. 2765–2768, Jan. 2004.
- [3] R. Joshi, J. Engstler, P. K. Nair, P. Haridoss, and J. J. Schneider, "High yield formation of carbon nanotubes using a rotating cathode in open air," *Diam. Relat. Mater.*, vol. 17, no. 6, pp. 913–919, Jun. 2008.
- [4] S. Jong Lee, H. Koo Baik, J. Yoo, and J. Hoon Han, "Large scale synthesis of carbon nanotubes by plasma rotating arc discharge technique," *Diam. Relat. Mater.*, vol. 11, no. 3–6, pp. 914–917, Mar. 2002.
- [5] C. Liu, H. . Cong, F. Li, P. . Tan, H. . Cheng, K. Lu, and B. . Zhou, "Semi-continuous synthesis of single-walled carbon nanotubes by a hydrogen arc discharge method," *Carbon.*, vol. 37, no. 11, pp. 1865–1868, Jan. 1999.
- [6] Y. A. Kim, H. Muramatsu, T. Hayashi, and M. Endo, "Catalytic metal-free formation of multi-walled carbon nanotubes in atmospheric arc discharge," *Carbon.*, vol. 50, no. 12, pp. 4588–4595, Oct. 2012.
- [7] M. Kanai, a. Koshio, H. Shinohara, T. Mieno, a. Kasuya, Y. Ando, and X. Zhao, "High-yield synthesis of single-walled carbon nanotubes by gravity-free arc discharge," *Appl. Phys. Lett.*, vol. 79, no. 18, pp. 2967, Oct. 2001.
- [8] Y. Ando, X. Zhao, K. Hirahara, K. Suenaga, S. Bandow, and S. Iijima, "Arc plasma jet method producing single-wall carbon nanotubes," *Diam. Relat. Mater.*, vol. 10, no. 3–7, pp. 1185–1189, Mar. 2001.
- [9] Z. E. Horváth, K. Kertész, L. Pethő, a. a. Koós, L. Tapasztó, Z. Vértesy, Z. Osváth,

- A. Darabont, P. Nemes-Incze, Z. Sárközi, and L. P. Biró, “Inexpensive, upscalable nanotube growth methods,” *Curr. Appl. Phys.*, vol. 6, no. 2, pp. 135–140, Feb. 2006.
- [10] E. Gamaly and T. Ebbesen, “Mechanism of carbon nanotube formation in the arc discharge,” *Phys. Rev. B.*, vol. 52, no. 3, pp. 2083–2089, Jul. 1995.
- [11] M. Cadek, R. Murphy, B. McCarthy, A. Drury, B. Lahr, R. . Barklie, M. in het Panhuis, J. . Coleman, and W. . Blau, “Optimisation of the arc-discharge production of multi-walled carbon nanotubes,” *Carbon.*, vol. 40, no. 6, pp. 923–928, May. 2002.
- [12] H. Nishizaka, M. Namura, K. Motomiya, Y. Ogawa, Y. Udagawa, K. Tohji, and Y. Sato, “Influence of carbon structure of the anode on the production of graphite in single-walled carbon nanotube soot synthesized by arc discharge using a Fe–Ni–S catalyst,” *Carbon.*, vol. 49, no. 11, pp. 3607–3614, Sep. 2011.
- [13] T. Matsuura, Y. Kondo, and N. Maki, “Selective mass production of carbon nanotubes by using multi-layered and multi-electrodes AC arc plasma reactor,” in *International Plasma Chemistry Society.*, 2009.
- [14] T. Sugai, H. Omote, S. Bandow, N. Tanaka, and H. Shinohara, “Production of fullerenes and single-wall carbon nanotubes by high-temperature pulsed arc discharge,” *J. Chem. Phys.*, vol. 112, no. 13, pp. 6000, Apr. 2000.
- [15] T. Sugai, H. Yoshida, T. Shimada, T. Okazaki, H. Shinohara, and S. Bandow, “New Synthesis of High-Quality Double-Walled Carbon Nanotubes by High-Temperature Pulsed Arc Discharge,” *Nano Lett.*, vol. 3, no. 6, pp. 769–773, Jun. 2003.
- [16] T. Sugai, “Production and Purification of Nanocarbon Materials by High-Temperature Pulsed Arc Discharge,” *New Dia. & Frontier Tech.*, vol. 16, no. 3, pp. 151–162, Jan. 2006.
- [17] N. Parkansky, R. L. Boxman, B. Alterkop, I. Zontag, Y. Lereah, and Z. Barkay, “Single-pulse arc production of carbon nanotubes in ambient air,” *J. Phys. D. Appl. Phys.*, vol. 37, no. 19, pp. 2715–2719, Oct. 2004.
- [18] Y. Y. Tsai, J. S. Su, and C. Y. Su, “A novel method to produce carbon nanotubes

using EDM process,” *Int. J. Mach. Tools Manuf.*, vol. 48, no. 15, pp. 1653–1657, Dec. 2008.

- [19] K. K. Kia and F. Bonabi, “Electric field induced needle-pulsed arc discharge carbon nanotube production apparatus: circuitry and mechanical design.,” *Rev. Sci. Instrum.*, vol. 83, no. 12, pp. 123907, Dec. 2012.

Experiments with Different Grades of Carbon Black

4.1 Introduction

In the previous chapter arc discharge set up was designed by considering mechanical and electrical design with the objective of obtaining a stable arc and a constant arc current across the electrode. In the present chapter, we first discuss about the carbon black, its basic chemistry, morphology, surface activity. Next, from various types of carbon black we choose five commercially and easily available grades of furnace black. Using these five grades of carbon black as precursor for CNT synthesis we did experiment in the designed arc chamber as shown in Figure 3.22 and analyzed to conclude on amenability of transformation of different CB grades to CNTs.

Carbon black is an elemental carbon in the form of extremely fine particles having amorphous molecular structure. Within the amorphous structure microcrystalline array of condensed rings is covered. The arrays appear to be similar to layered condensed ring exhibited by graphite, which is another form of carbon [1]. The physical appearance of CB is of a black, finely divided pellet or powder. In 2000, Berezkin et al. [2] proposed a model of the formation of carbon black particles. The particles of CB grow through the deposition of carbon layers on the surface of fullerene. Berezkin also discussed that the carbon black is most stable allotropic form of carbon. In 2008, Donnet et al. [3] discussed that Carbon black consist of sp^2 carbon with some graphitic order in turbostratic stacking(random stacking of carbon material).

Structure of carbon black constitutes of primary particles that are interconnected with each other forming aggregates. High structure carbon black is described by aggregates composed of many primary particles that are held in branching and chaining whereas low structure carbon black is characterized by lower extent of aggregation. In 2002, Izhik et al. [4] measured the surface properties of carbon black and comparatively analyzed electrical properties(electrical resistance and capacitance) of carbon black.

Carbon black is in the top 50 industrial chemicals manufactured worldwide, based on annual tonnage. Current worldwide production is about 18 billion pounds per year [8.1 million metric tons]. In 2001, Richard et al. [5] surveyed and found that approximately 90% of carbon black is used in rubber applications, 9% as a pigment, and the remaining 1% as an essential ingredient in hundreds of diverse applications.

Mostly carbon black is produced by the oil furnace processes from liquid, aromatic hydrocarbons. Carbon black is used as a reinforcing agent in rubber, a pigment in plastics, inks and coatings, an electrically conductive material and in a variety of applications. In 2002, Kohls et al. [6] reviewed the morphology and structure of fillers requires for interaction with rubber. It has been observed that filler like carbon black and silica have different surface area so they reinforce differently from each other. In selecting a carbon black for specific application, modified grade of carbon black should be considered. There are various subtypes of carbon black available in literature explained below. Each type of carbon black has specific method of production.

1. Acetylene Black- acetylene black formed by an exothermic decomposition of acetylene. It provides carbon black with higher structures and higher crystallinity, and is mainly used for electric conductive agents.
2. Channel Black- channel black is fine carbon black obtained as soot by impingement of small gas flames on metal surface.
3. Furnace Black- Furnace black is a type of carbon black that is produced industrially in a furnace by incomplete combustion of hydrocarbons. This method is suitable for mass production due to its high yield, and allows wide control over its properties such as particle size or structure. This is currently the most common method used for manufacturing carbon black for various applications from rubber reinforcement to coloring.
4. Lamp Black- This method obtains carbon black by collecting soot from fumes generated by burning oils or pine wood. It is used as raw material for ink sticks as provides carbon black with specific color.
5. Thermal Black- Thermal black is made by thermal decomposition of hydrocarbons (natural gas and acetylene) in preheated furnace.

4.2 Morphology of Carbon Black

Important parameters of morphology of carbon black include its particle size, structure and surface activity. Different types of carbon black have wide range of particle size that varies in degree of aggregation. Carbon black is composed of spheroidal primary particles strongly fused together to form discrete units called aggregates. The aggregate consist of few or hundreds of chain of carbon particles that are fused together in a random way to form the branching structure. The aggregates are loosely held together by weak forces forming larger units called agglomerates. The agglomerates will break down into aggregates if adequate amount of force is applied, so the aggregates are the smallest ultimate dispersible unit of carbon black. A carbon black has high structure if degree of aggregation is high. It means structure is determined by size and shape of primary particle that form aggregation. The difference between primary particle, aggregate and agglomerate is presented in Figure 4.1.

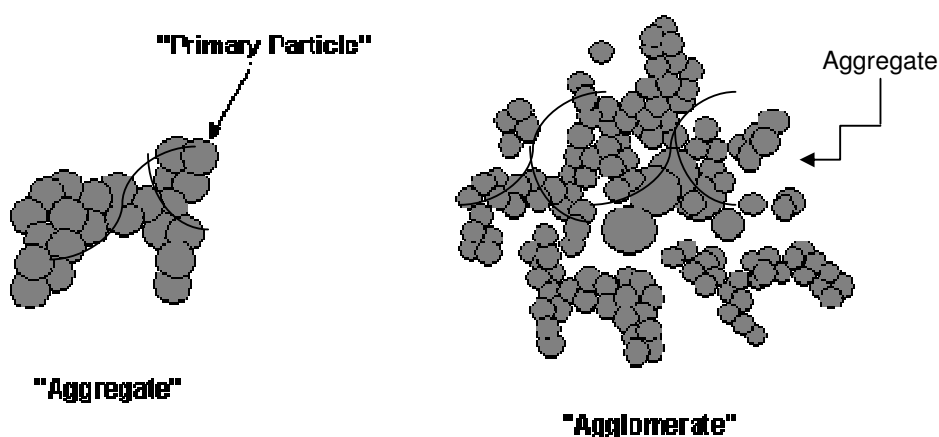


Figure 4.1: Shows primary particle, aggregate and agglomerate

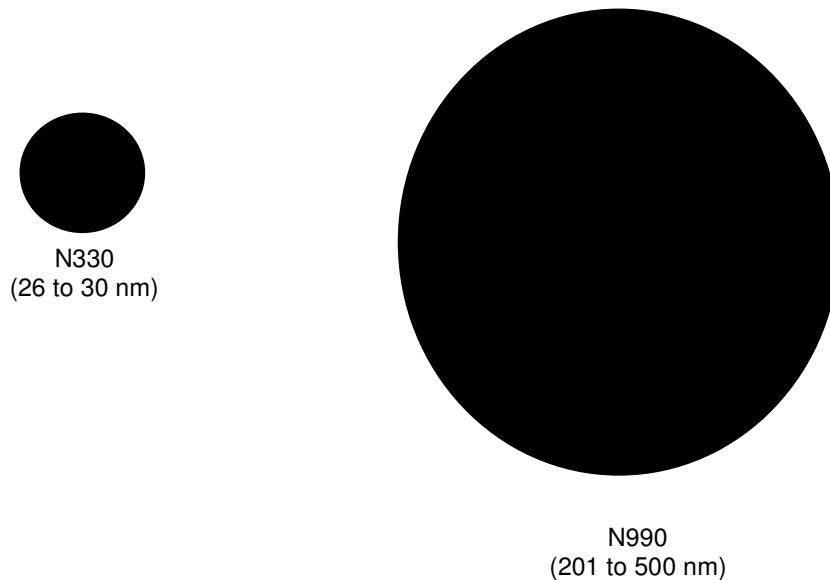
Particle size can be measured through surface area determination of carbon black. Surface area can be measured by two methods i.e. Iodine absorption (expressed in mg/g of carbon) it measures the amount of iodine that can be absorbed on the given mass of carbon black. The second method involves nitrogen surface area measurement which includes the amount of nitrogen which can be absorbed on given mass of carbon black.

The ASTM (American Society for Testing and Materials) introduced a system which uses a letter followed by three numbers. The letter N is for normal cure rate and S is for slow cure rate. The first of the three numbers after the letter N or S indicates the particle size and typical average size corresponding to various numbers of carbon black are given in Table 4.1 [1].

Table 4.1: First digit assignment by ASTM in carbon black nomenclature system

First digit	Typical average particle size (nm)
0	1 to 10
1	11 to 19
2	20 to 25
3	26 to 30
4	31 to 39
5	40 to 48
6	49 to 60
7	61 to 100
8	101 to 200
9	201 to 500

Thermal carbon black is classified as N900 series carbon black and furnace black is classified as N100 to N700 series [7]. Thermal black have large particle size and low surface area whereas furnace black have small particle size and large surface area. Lamp black have high degree of aggregation of mid- size particles and small surface area. Acetylene black have high degree of aggregation and is most crystalline or graphitic carbon black. Channel black has small particle size and high level of surface area. The comparison between the particle size of furnace and thermal black is shown in Figure 4.2.

**Figure 4.2: Furnace and thermal black particle size comparison [7]**

The measurement of the structure of carbon black is a challenging task. In Literature researchers have used dibutyl phthalate absorption number (DBP) to measure the relative structure of carbon black by determining the amount of DBP absorbed for a given mass of carbon black. Higher structures of carbon black are easier to disperse than low structure carbon black of same area because their larger and bulkier aggregates cannot pack tightly together. At equal surface area, high structure carbon black has high electrical conductivity than low structure black.

Having understood the basic structure, morphology and properties of different CB, we choose five commercially grades of carbon black Tread *A (non-ASTM), N134, N121, N660 and N330 and were procured from industry (Aditya Birla Science and Technology Limited, India). These grades come under the category of furnace carbon black. Furnace black is the most common available method and is important due to its high yield and better control over its properties such as particle size and structure. The chosen five currently furnace black carbon grades are used for rubber reinforcement to coloring. The five grades samples were taken for experimentation and have been named as sample A, sample B, sample C, sample D and sample E respectively for Tread *A (non-ASTM), N134, N121, N660 and N330 . It is observable from Table 4.2 that the properties of the five types are tabulated in Table 4.2 depicting their iodine adsorption number, nitrogen surface area and DBP carbon black have declining trend in Iodine Adsorption number as we go from sample A to sample E. Surface area indicates particle size of carbon black which can be calculated by iodine surface area and Nitrogen surface area. Kohls et al. [6] observed that the surface area plays an important role in fillers reinforcement property. DBP Adsorption number measures the relative structure of carbon black by determining amount of DBP a given mass of carbon black absorbs. From Table 4.2 we also observe that sample D have the lowest DBP number indicating low structure carbon black i.e. very little particle aggregation or structure with large size of spherical structure whereas sample C have high DBP number i.e. high structure carbon black which means it does not consist of individual sphere of carbon but exist as large number of particle aggregation forming chain or branches.

Table 4.2: Details of various grades of carbon black

Sample	Grade	Iodine adsorption number (iodine surface area) (mg/gm)	Nitrogen surface area (m ² /gm)	DBP adsorption number (structure) (ml/100gm)
Sample A	Tread *A (non-ASTM)	164.1	158.7	127.7
Sample B	N134	142	143	127
Sample C	N121	121	122	132
Sample D	N660	36	35	90
Sample E	N330	82	78	102

Brief summary about characteristics of five different grades of carbon black is mentioned below:

1. N134:

It is a high reinforcing, high structure pelleted carbon black. It has high surface area per unit mass. The product is characterized by easy dispersion in any elastomeric compounds. N134 can be used as a component of tread compounds for high performance passenger car tires. It provides maximum tread wear resistance.

2. N121:

N121 is high-amplifying (highly reinforced) and high-structured carbon black. It is easily dispersed in the mixtures on the basis of any elastomer for the manufactures of tire treads and provides maximum durability of the tread.

3. N660:

N660 is medium-dispersing and medium-amplifying carbon black with low structure. Provides higher swelling extruded flow, high elasticity at relatively high rates of hardness. Used in rubber products, single ply roofing systems and Insulation and cable products.

4. N330:

It is high-dispersing and amplifying carbon black. It provides high tensile strength, good abrasion resistance. Used in massive tire carcass hoses, conveyor belts, rubber products.

In 2002, Kohls et al. [6] compared the carbon black grade (N330) with silica. Kohls observed that fillers that are highly branched and they have higher specific surface area; they will have more locations to contact with rubber matrix. In 1994, Okel et al. [8] reported how the specific area of carbon black and silica affects the mechanical properties (stress/strain, tear strength). Okel observed that when the surface area of silica increases it will require more energy for mixing in rubber and also the tear and tensile strength of the rubber also increases. In 1998, Wang et al. [9] suggested that the surface of carbon black is also covered with various functional groups like carboxyl, phenol, lactones and quinonic groups.

In 2002, Schroder et al. [10] discussed about four adsorption sites of carbon black surface as shown in Figure 4.3 where I represent the graphitic planes with sp^2 hybridization of the carbon atoms. Site II related to amorphous carbon in a sp^3 hybridization. Sites III and IV corresponds to micro crystallites edges and slit shaped pores.

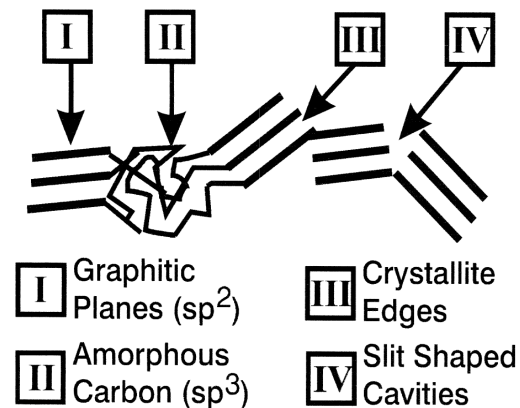


Figure 4.3: Schematic of carbon black surface adsorption sites [10]

For furnace black the concentration of active sites (II-IV) varies between 5% and 20% on the surface and contribution to absorption from other sites is 95-80% i.e. from graphitic planes. The carbon black grade N330 has 10% of II, III and IV sites and the remaining 90% of the carbon black surface comprise of graphitic planes. Ooiji et al. [11] discussed that sites are important in rubber filler and filler-filler interaction. N330 grade (sample E) have 90% surface consist of graphitic planes and is much higher in comparison to that existing in other four chosen grades. Higher graphitic planes indicate higher surface area and a larger availability of surface favors larger absorption

of energy. The amount of energy or power availability to break C-C bond in graphitic planes during transformation of CB to CNT will be less as compared to other four grades. This leads to hypothesize that N330 is more amendable for conversion to CNT. In order to validate on hypothesis and investigation our second problem of interest (refer to chapter 2 page no. 50). We did various set of experiment using sample A to sample E, which are detailed in next section.

4.3 Experiment with Different Carbon Black Grades

In this section we performed experiments in designed arc discharge chamber to convert five grades of CB to CNT (Tread *A (non-ASTM), N134, N121, N660 and N330). The experiments were conducted at 40 A current for 60 sec with the power supply of 40 A.

4.3.1 Experimental Setup

The schematic diagram of the arc discharge apparatus for nanotube formation was shown in Figure 2.2 and is represented again in Figure 4.4(a). Figure 4.4(b) shows the picture of actual arc discharge set up that consists of two graphite electrodes mounted horizontally with an arc controller to maintain constant arc current. The anode (8 mm) is drilled with a hole of diameter 4 mm and is filled with powdered carbon black grades. The cathode is a pure graphite rod (8 mm) which is sharpened at the tip.

The chamber is first purged with argon at 20 psi to clean the chamber and make surrounding environment inert. The voltage is applied across the electrodes and electrodes are brought in contact. The anode is adjusted using arc controller interface to maintain the gap of ~1 mm between the electrodes. By maintaining the gap constant, we obtain constant current which is the first objective in the design.

The earlier published literature lacked a clear compilation of an explanation of possible mechanism of transformation of precursor to CNT. We published [12] a possible mechanism which is now widely accepted and highly cited. To start the conversion of precursor to CNT, the gas ionizes into electrons and ions and results in hot plasma formation between the electrodes. Stable plasma grows uniformly over the electrode surface corresponding to stable anode and cathode voltage. The collisions of ions and electrons in the plasma emit photons responsible for the glow in plasma. The electrons are ejected from cathode hit the anode at high velocity and sputter the carbon precursor

in the present case CB filled at the center of the anode. The high temperature resulting from resistive heating of results in sublimation of carbon precursor and converts them into carbon vapours. The carbon vapours are decomposed in carbon ions. The decomposition occurs due to high heat flux or thermal energy of the plasma. The carbon vapours aggregate to form viscous carbon clusters and drift towards the cathode, which is cooler as compared to anode. The carbon vapours undergo a phase change and get converted into liquid carbon. The temperature gradient at cathode and quenching effect of atmosphere solidifies and crystallizes the liquid carbon to form cylindrical deposits that grow steadily on cathode. The cathodic deposit is composed of a grey outer shell and a dark inner core. The grey deposit consists of the rolls of graphene sheets known as carbon nanotubes. The addition of hexagonal carbon atom clusters lead to the growth of nanotube. However, instability in plasma leads to capping of nanotubes. The diameter of the nanotubes is governed by the density of carbon vapours in the plasma. Variation in temperature gradients strongly affects the diameter distribution of CNTs produced and nanotubes are formed in bundles due to van der Waals interaction.

During experimentation, temperature of arc was recorded for each experiment pertaining to all samples and recording of arc temperature was done using thermal imaging camera which was mounted at back side of experimental setup [Refer in Figure 4.4(c)].

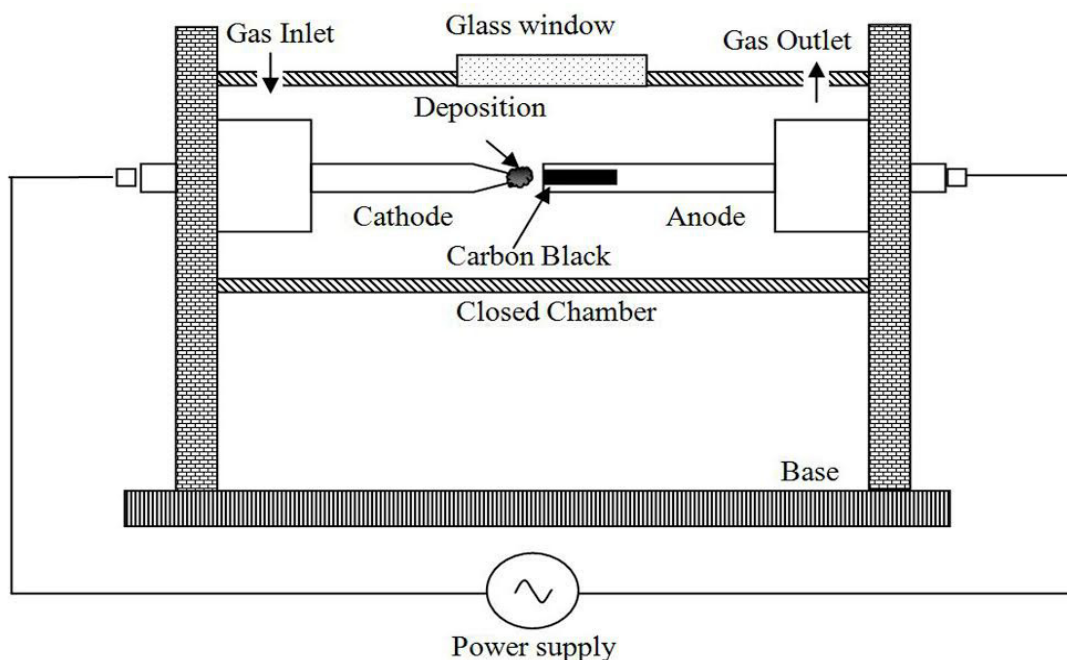


Figure 4.4(a): Schematic of an arc discharge setup

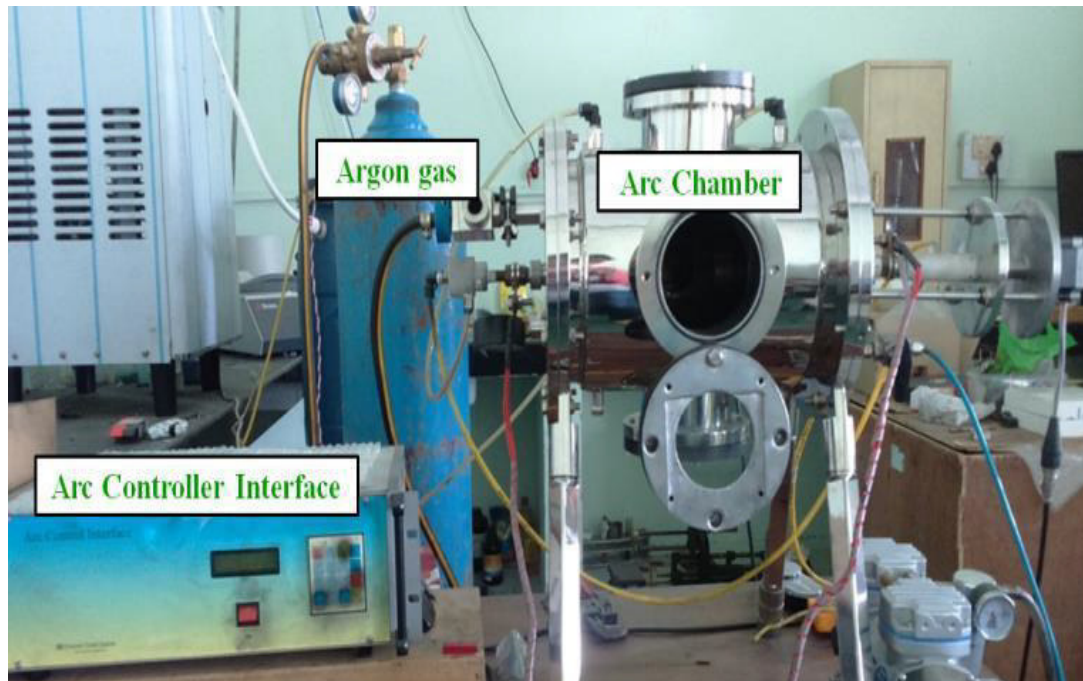


Figure 4.4(b): Front view of setup consist of arc discharge chamber with automatic controller

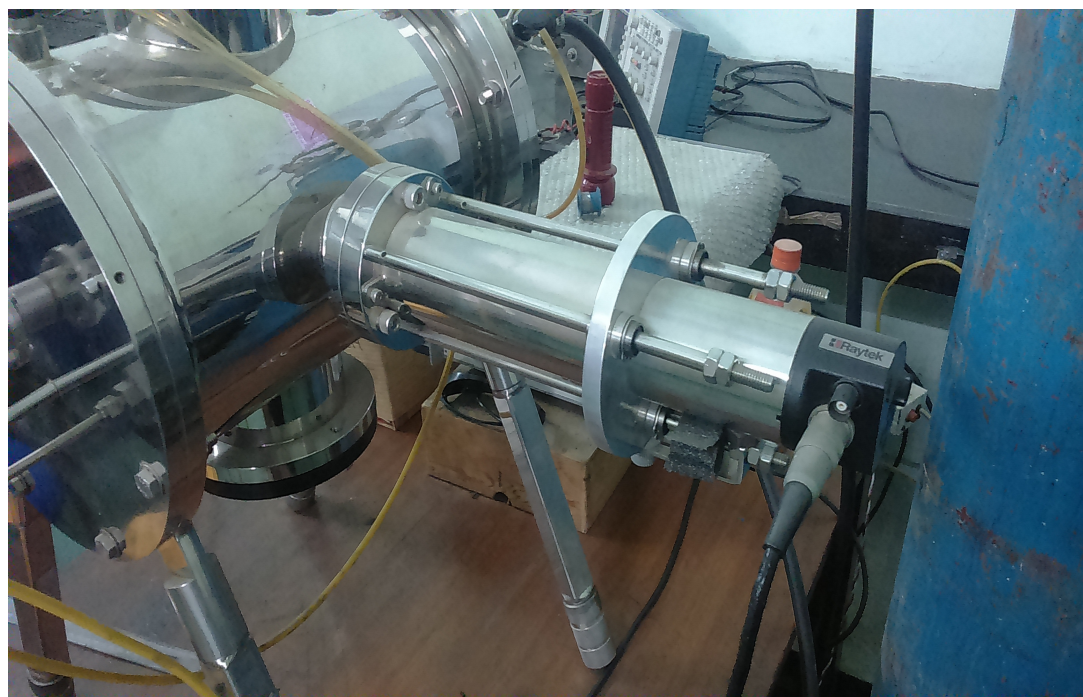


Figure 4.4(c): Back view has thermal imaging camera i.e. fitted to arc discharge set up

We performed around 30 experiments for each sample i.e. Sample A to Sample E. The flow chart showing each step for experimentation is shown in Fig 4.5. Firstly, we take graphite electrode from D-cell battery and drill a hole of diameter 4mm at the center of graphite rod and making an anode. The center hole is drilled to the depth of 4 mm and is filled with carbon black. We measure the amount of filled carbon black with the help of weighing machine. After switching on the power supply, the electrodes are brought in contact to generate an arc and are kept at an intermittent gap of 1-2mm. A constant current is maintained through the electrodes to obtain non fluctuating arc. We have repeated this experiment on 5 samples and in each sample we did around 30 experiments. After end of 60sec we allowed the chamber to cool for 5 minutes. After cooling of chamber the front window open and removed cathode, sample was collected and we observed the synthesized sample with FESEM and TEM. The observations are given in next section.

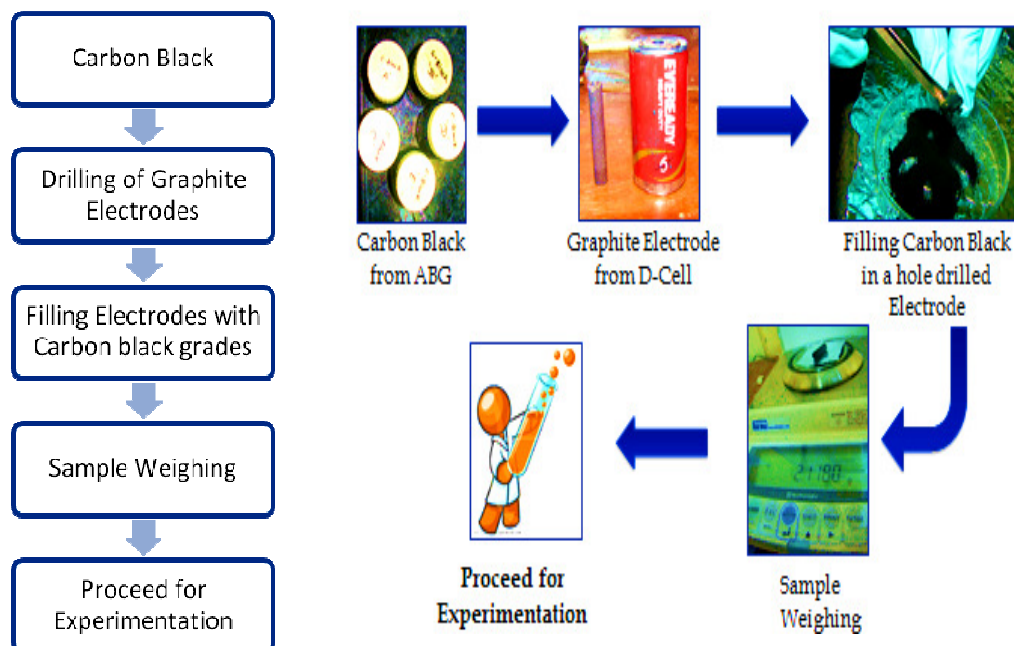


Figure 4.5: Sample preparation

After performing 30 set of experiments for each carbon black grade, the carbonaceous deposit resulting from different carbon black grades, was collected from cathode .We have chosen three random samples for each grade and then characterized the sample using FESEM and TEM. Field emission Scanning electron micrographs is done show the surface morphology of formed product. To observe inner morphology of various

structure we did TEM (JEOL 2100F) of the chosen samples. Figure 4.6 shows the granular structure of untreated Carbon black Sample N330 grade of different particle size with FESEM and TEM image. Figure 4.7(a) to 4.7(c) shows the FESEM images of three randomly collected sample from Tread *A (non-ASTM) grade which shows the conversion of granular carbon black particle to fly ash particle.

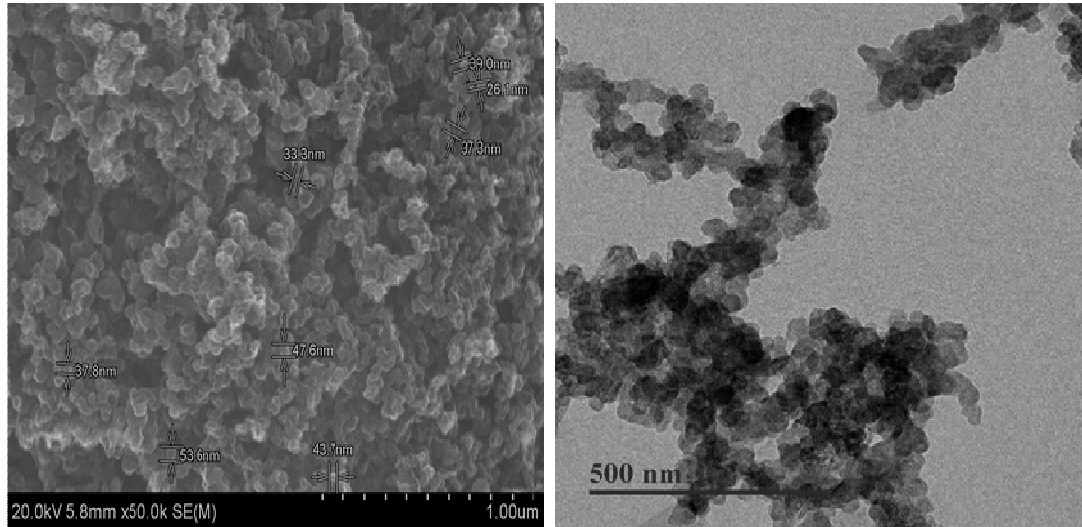


Figure 4.6: Shows granular structure of carbon black FESEM and TEM image

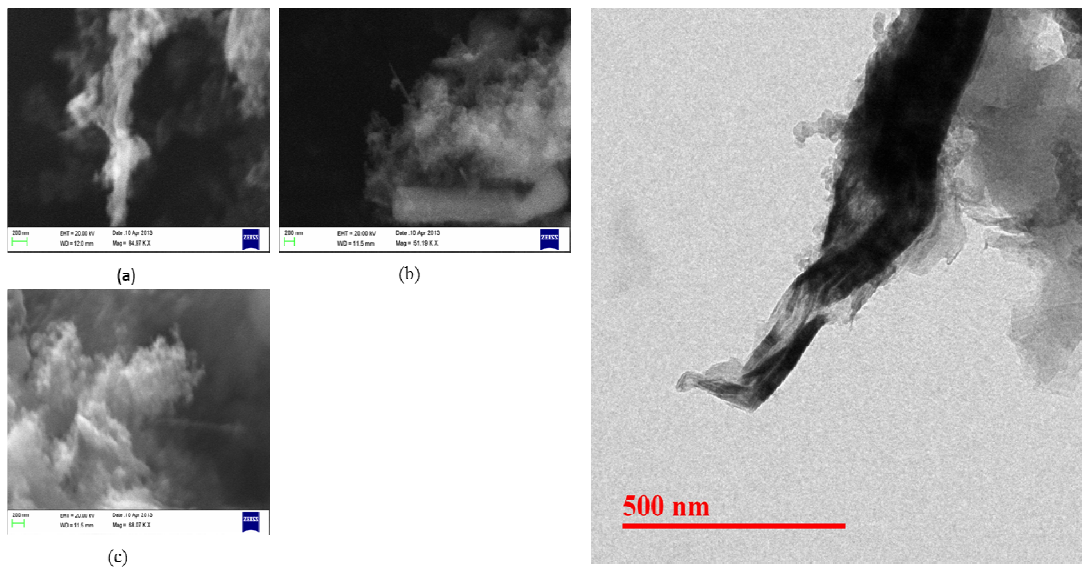


Figure 4.7: Shows the FESEM images on the left side of sample A [Tread *A (non-ASTM)] at 40 A for 60 sec and TEM image on the right side

Dense Nano fibers are formed over the graphene sheet from N134 carbon black grade when an arc current of 40 A for 60 sec was applied across the electrodes and on right side we have the TEM image as shown in Figure 4.8(a) to 4.8(c)

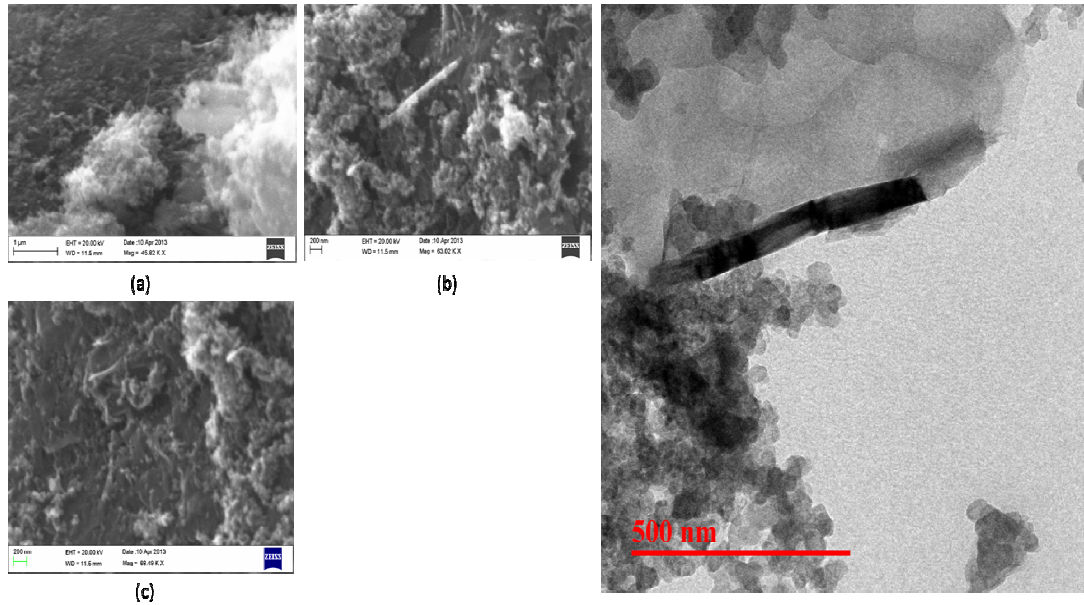


Figure 4.8: Shows the FESEM images on the left side of sample B (N134) at 40 A for 60 sec and TEM image on the right side

Sample C (N121) carbon black grade was converted to Nano rods attached to the carbon nanoparticle as shown in Figure 4.9(a) to 4.9(c) and right hand side shows the TEM structure.

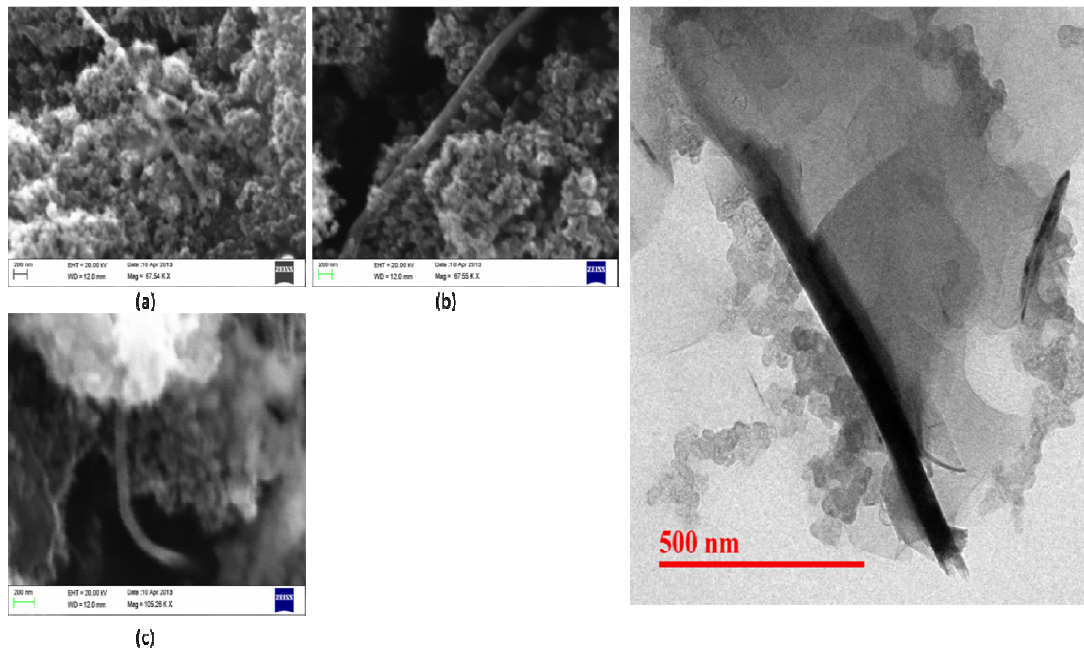


Figure 4.9: Shows the SEM images on the left side of sample C (N121) at 40 A for 60 sec and TEM image on the right side

Tubes start growing from the edges when arc current 40 A applied to N660 grade for 60sec as shown in Figure 4.10 and TEM image on the right side shows the presence of tube.

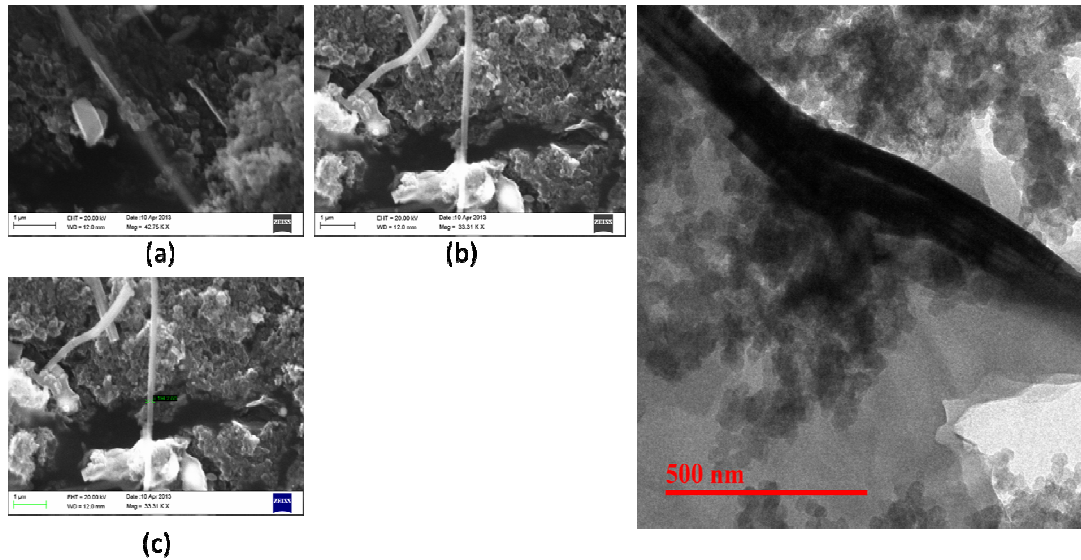


Figure 4.10: Shows the FESEM images on the left side of sample D (N660) at 40 A for 60 sec and TEM image on the right side

It was observed from Figure 4.11(a) to 4.11(c) that Carbon Black grade N330 suggests the formation of MWCNTs varying diameter around ~12 nm for an arc current of 40A for 60sec as compared to other grades.

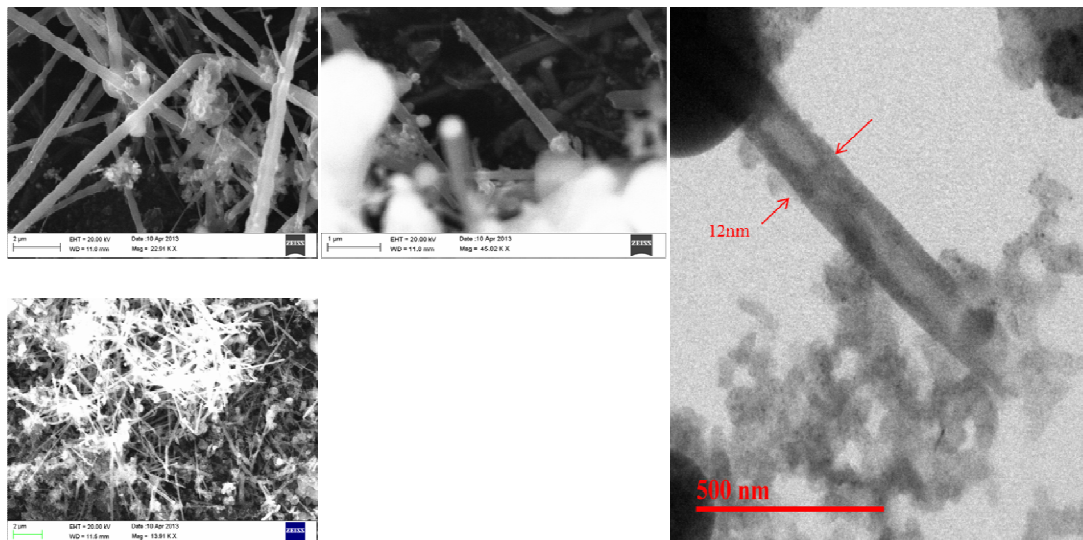


Figure 4.11: Shows the FESEM images on the left side of sample E (N330) at 40 A for 60 sec and TEM image on the right side

From FESEM and TEM, we observe that N330 CB grade transformed into CNTs as compared to other four chosen CB grades.

4.4 Conclusion

1. We have briefly discussed about carbon black, its chemistry, morphology and surface activity in Section 4.1. In Section 4.2 we have specified about various types of carbon black used in literature. From various grades of carbon black we have chosen five type of carbon black grade that comes under class of furnace carbon black type.
2. The five types of CB as carbon precursor we did 30 experiments for each carbon black grade. The experiments were done with an objective to transform CB to CNT and were conducted using DC arc discharge for an arc current of 40 A for a duration of 60 sec in argon atmosphere. The details of experiments were presented in Section 4.3.
3. After completing each experiment, the deposited material from surface of cathode was collected. Out of 30 collected samples for each grade we did FESEM for three randomly selected samples for each grade of CB to observe the surface morphology.
4. To conform the presence of MWCNTs, we did TEM analysis. It was observed from the FESEM and TEM, N330 carbon black grade gets converted to Carbon nanotubes. The possible attribution for this conversion is that N330 carbon black grade have the presence of four adsorption sites 90% of which has been graphitic planes. As hypothesized it is easy to break C-C bonds on graphitic sites and transformation did occur for N330 grade to CNTs.
5. The finding that on application of constant current of 40A, CB of particular grade transforms to CNT led us to further question as to why it did not happen with every particulate of CB? Our next problem statement was framed around the query as to what other parameter can affect the transformation? The answer to this query will in fact reveal more on conversion mechanism and parameter effecting the conversion.

In the next chapter we therefore, investigate the role of arc current and temperature of arc on synthesis of carbon nanotubes. The experiments were continued on N330 carbon black grade. The temperature of arc was taken as an index for stability of available

energy. Also, we investigate the effect of arc current and time duration on N330 Carbon Black grade for synthesis of carbon nanotube using pulsed arc discharge method.

References:

- [1] J. Melorose, R. Perroy, and S. Careas, “No Title No Title,” *Statew. Agric. L. Use Baseline 2015*, vol. 1, 2015.
- [2] V. I. Berezkin, “Fullerenes as nuclei of carbon black particles,” *Phys. Solid State.*, vol. 42, no. 3, pp. 580–585, Mar. 2000.
- [3] J. B. Donnet, H. Oulanti, and T. Le Huu, “Mechanism growth of multiwalled carbon nanotubes on carbon black,” *Diam. Relat. Mater.*, vol. 17, no. 7–10, pp. 1506–1512, Jul. 2008.
- [4] A. P. Izhik and N. B. Uriev, “Surface properties and specific features of structurization of disperse carbon black with different degrees of oxidation,” *Colloid J.*, vol. 64, no. 5, pp. 562–566, Sept. 2002.
- [5] R. A. Scholl, “Power supplies for pulsed plasma technologies: State-Of-The-Art And Outlook,” 2001.
- [6] D. J. Kohls and G. Beaucage, “Rational design of reinforced rubber,” *Curr. Opin. Solid State Mater. Sci.*, vol. 6, no. 3, pp. 183–194, Jun. 2002.
- [7] S. Residue and S. Area, “Physical & Chemical Properties Properties.”
- [8] T. A. Okel and W. H. Waddell, “Silica Properties/Rubber Performance Correlation. Carbon Black-Filled Rubber Compounds,” *Rubber Chem. Technol.*, vol. 67, no. 2, pp. 217–236, May. 1994.
- [9] M.-J. Wang, “Effect of Polymer-Filler and Filler-Filler Interactions on Dynamic Properties of Filled Vulcanizates,” *Rubber Chem. Technol.*, vol. 71, no. 3, pp. 520–589, Jul. 1998.
- [10] A. Schröder, M. Klüppel, R. H. Schuster, and J. Heidberg, “Surface energy distribution of carbon black measured by static gas adsorption,” *Carbon.*, vol. 40, pp. 207–210, Feb. 2002.
- [11] W. J. Van Ooij, “Mechanistic Investigations of Surface Modification of Carbon

Black and Silica by Plasma Polymerisation,” *Plasma Chem. & Plasma Process.*, vol. 28, no. 2, pp. 273–287, Apr. 2008.

- [12] N. Arora and N. N. Sharma, “Arc discharge synthesis of carbon nanotubes: Comprehensive review,” *Diam. Relat. Mater.*, vol. 50, pp. 135–150, Nov. 2014.

Role of Parameters in Synthesis of CNTs from Carbon Black

5.1 Introduction

In the previous chapter, we discussed about the morphology of carbon black that include surface area, particle size, structure and different grades of carbon black. We did various experiments using DC discharge set up at 40A arc current in order to find which grade gives phase transformation of carbon black to CNTs. It was observed that N330 is more amenable for transformation to CNTs.

In the present chapter, we investigate the role of temperature and role of current in the formation of MWCNTs from N330 carbon black grade using DC arc discharge. Also, we investigate the role of arc current and time duration on N330 Carbon Black grade for synthesis of carbon nanotube using pulsed arc discharge method which has not been reported in literature.

Arc discharge production of nanotubes is dependent on several parameters like arc current, applied voltage, chamber pressure, arc temperature, presence of catalyst, type of carbon precursors, electrode shape etc. [1]. Over last two decades, researchers have published several reports pertaining to arc grown CNTs. In 2012, Su et al. reported synthesis of CNTs using magnetic assisted arc discharge with controlled diameter [2] and High quality CNTs with low cost can be synthesized using low pressure air arc discharge. In 2012, Zhao et al. [3] found straight MWCNTs using direct current arc discharge with a rotating graphite anode in low pressure air. In 2014, Su et al. [4] suggested low cost approach to synthesize SWCNTs using direct current arc discharge. In 2015, Berkman et al. [5] reported the synthesis of SWCNT and single walled carbon nanohorn hybrid in single step by electric arc discharge in open air at lower current densities. Several parameters (arc current, applied voltage, chamber pressure, arc temperature, presence of catalyst, type of carbon precursors, electrode shape etc. have been well investigated and reported literature [6][7]. Parameters like catalyst and

pressure has been studied in detail and reported in literature for their roles in formation of Carbon nanotubes. Arc current is regarded as the key parameter to effect nanotube formation. The role of arc current on CNTs synthesis as explained in published literature is explained in next section.

5.2 Role of Arc Current

Arc current effects the emission of electrons from cathode which travels at high velocity towards anode. These electrons hit the anode surface which results in sputtering of carbon precursors. Upon increasing the arc current, the number of electrons striking the anode surface increases, thereby sputtering more carbon precursor from the anode. The applied current produces resistive heating which results in high temperature. Due to high temperature, the carbon precursor filled in anode sublimates to form carbon vapours and nucleates at cathode resulting in nanotube formation. There also exists a minimum discharge current called as chopping current at which the plasma production is insufficient and leads to arc extinction. In published literature, there exist large variations of applied arc current (2.5 to 700 A) to initiate CNT formation which creates ambiguity in clear understanding of role of current in CNT formation.

For the carbon black as precursor, even the studies at various arc currents are not available in published literature. We, therefore conducted synthesis experiment with N330 (for experimental detail refer Chapter 4 Section 4.3) and collected samples of synthesized product one each at arc currents 25 A, 30 A, 35 A and 40A.

From Table 5.1 we observe the quantitative analysis of deposited sample from Carbon black which includes weight of anode, weight of cathode and amount of carbon black filled inside the anode before conducting experiment and also after experimentation keeping arc duration 60 sec. The deposition at cathode was collected and observed using FESEM for visualizing the formation of CNTs.

Table 5.1: Quantitative analysis of deposited sample from carbon black

Before Experiment					After Experiment		
SNo	Current (Ampere)	Weight of Anode(gram)	Weight of Cathode (gram)	Carbon Black (gram)	Weight of Anode (gram)	Weight of Cathode (gram)	Deposition (gram)
1	25	1.9291	3.0557	0.0788	1.9289	3.0555	0.0543
2	30	2.071	2.9162	0.0914	2.070	2.9160	0.0650
3	35	1.8551	3.1953	0.0913	1.8547	3.1952	0.0641
4	40	1.942	2.7617	0.0818	1.940	2.7614	0.0602

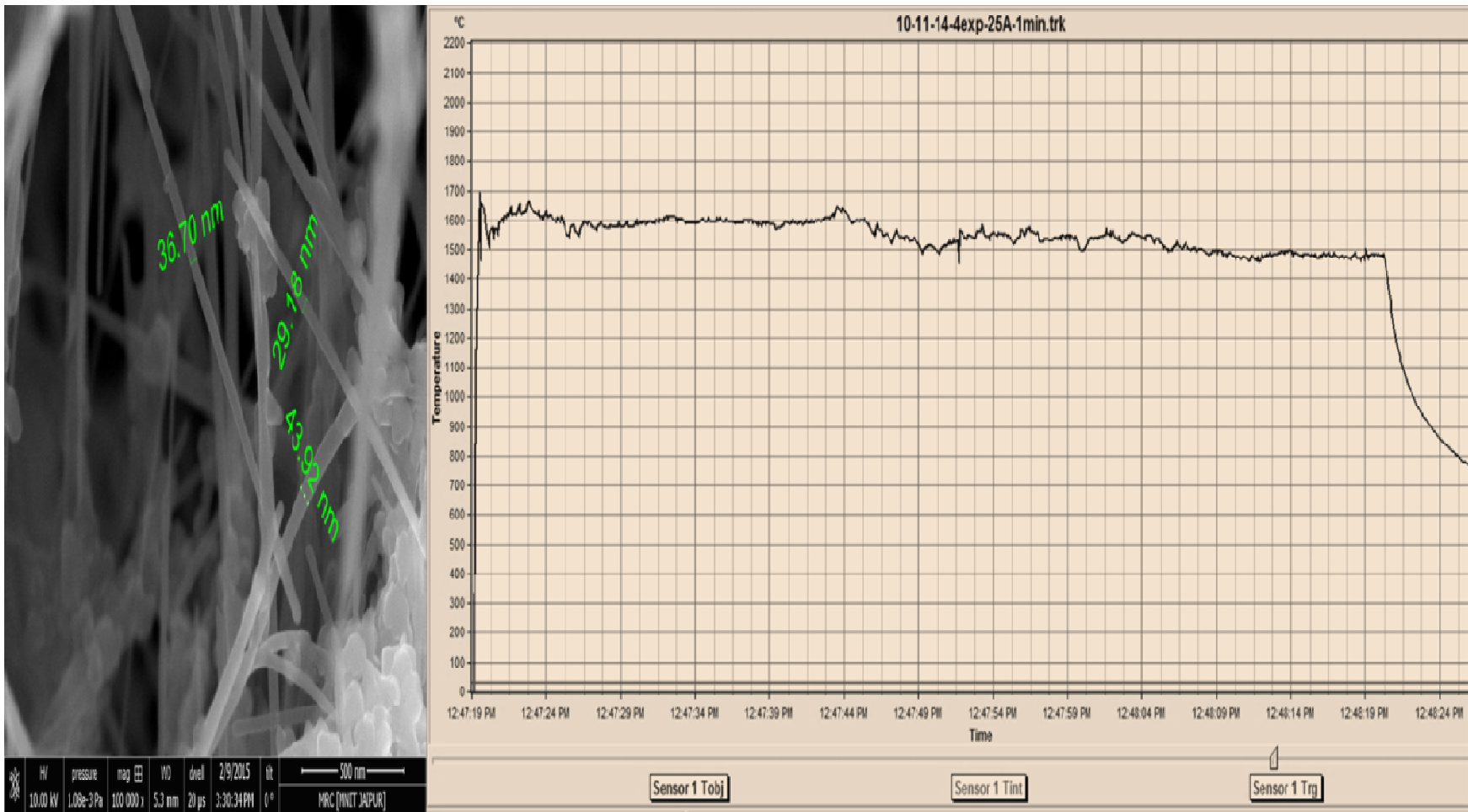
Each collected sample was observed in four different sample zones and FESEM image recorded. Figure 5.1 illustrates the micrographs of the deposited material at cathode at one randomly chosen site for each of the four current values namely the arc current of 25 A, 30 A, 35 A and 40 A. During the arc treatment we also recorded the arc temperature using the Raytek thermal imaging camera. For each recorded arc temperature readings we have in Figure 5.1 shown FESEM micrographs.

5.2.1 Characterization

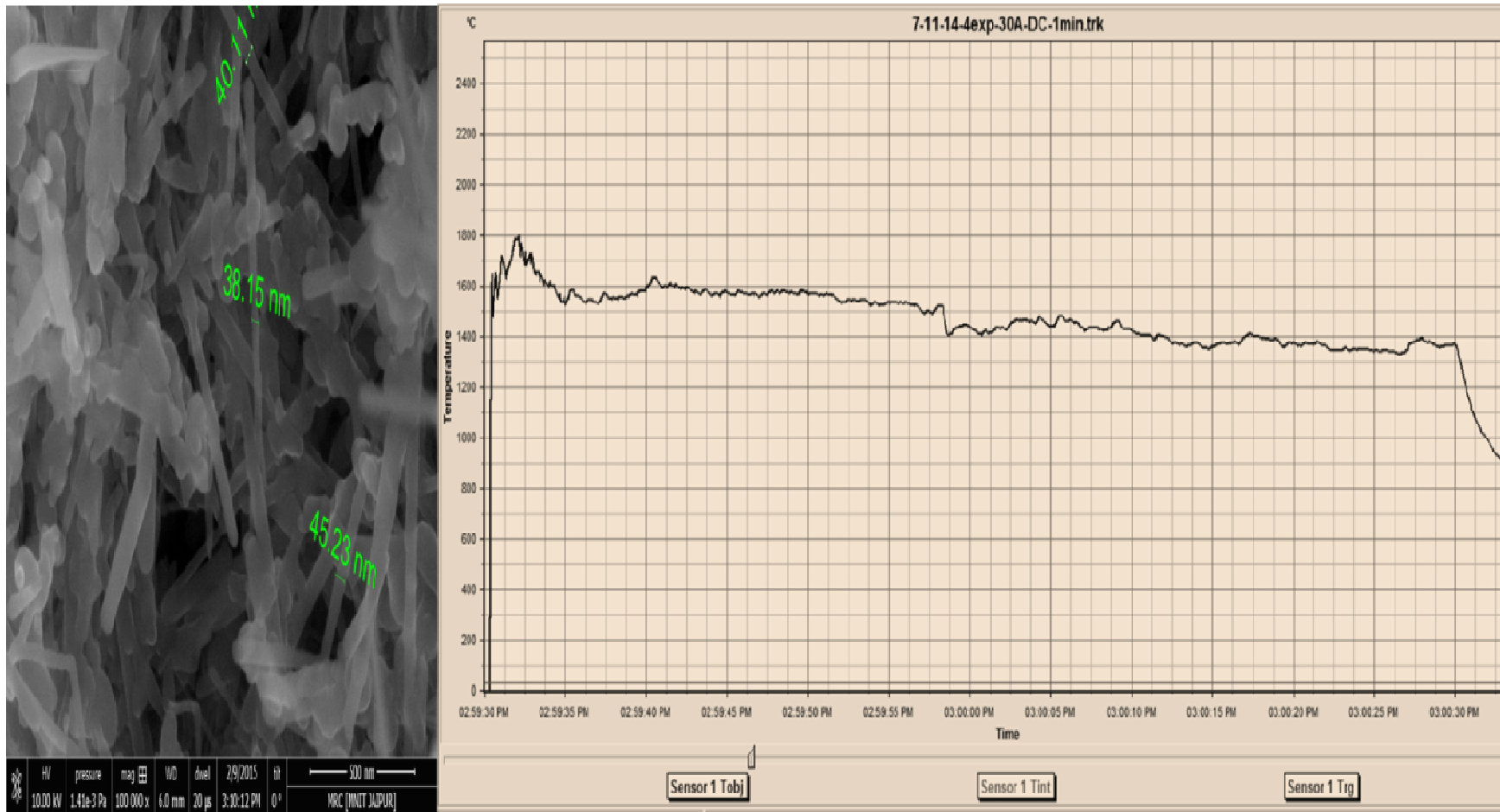
In order to study the surface morphology of the collected sample, we did FESEM and the corresponding temperature profile and analyzed for any correlation in between the two namely formation of CNTs and temperature of arc. We observe from Figure 5.1 that when we increase arc current from 25 A to 40 A with the step of 5 A for 60 sec at 1400-1600°C. The amount of MWCNTs increases as shown in FESEM images and diameter of the nanotubes decreases. High quantity of CNTs was observed at uniform arc temperature of around 40 sec as it indicates in Table 5.1.

In experiments where temperature fluctuated beyond 1400-1600°C range; we did not observe CNT formation. As was written earlier we did experiments on N330 at four values of current across electrodes. Among collected deposits from each of the experiments, we observed that almost collected sample had no CNT formation. The corresponding temperature profiles had shown large amount of arc temperature fluctuation with respect to time and range.

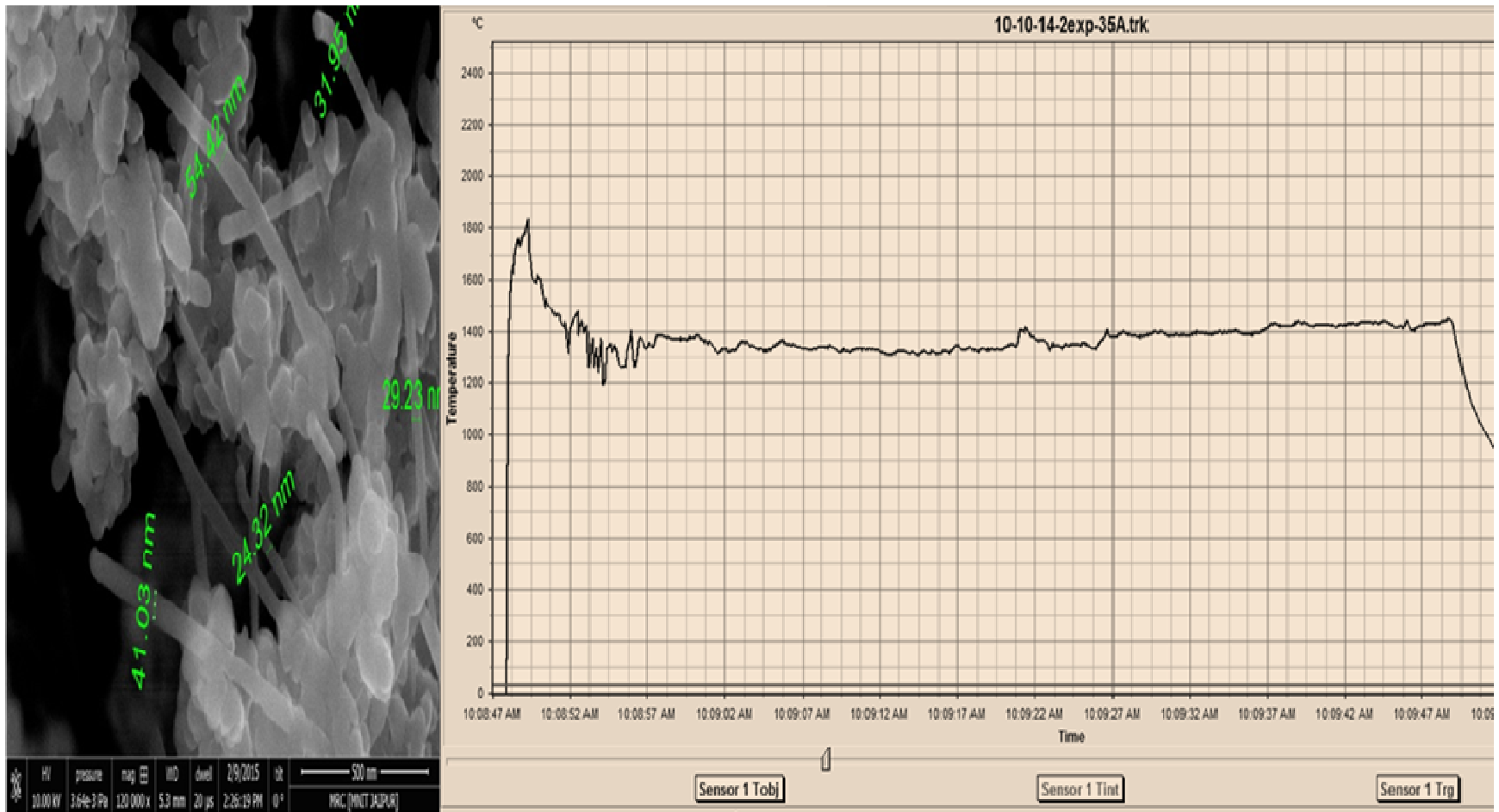
a) FESEM Analysis



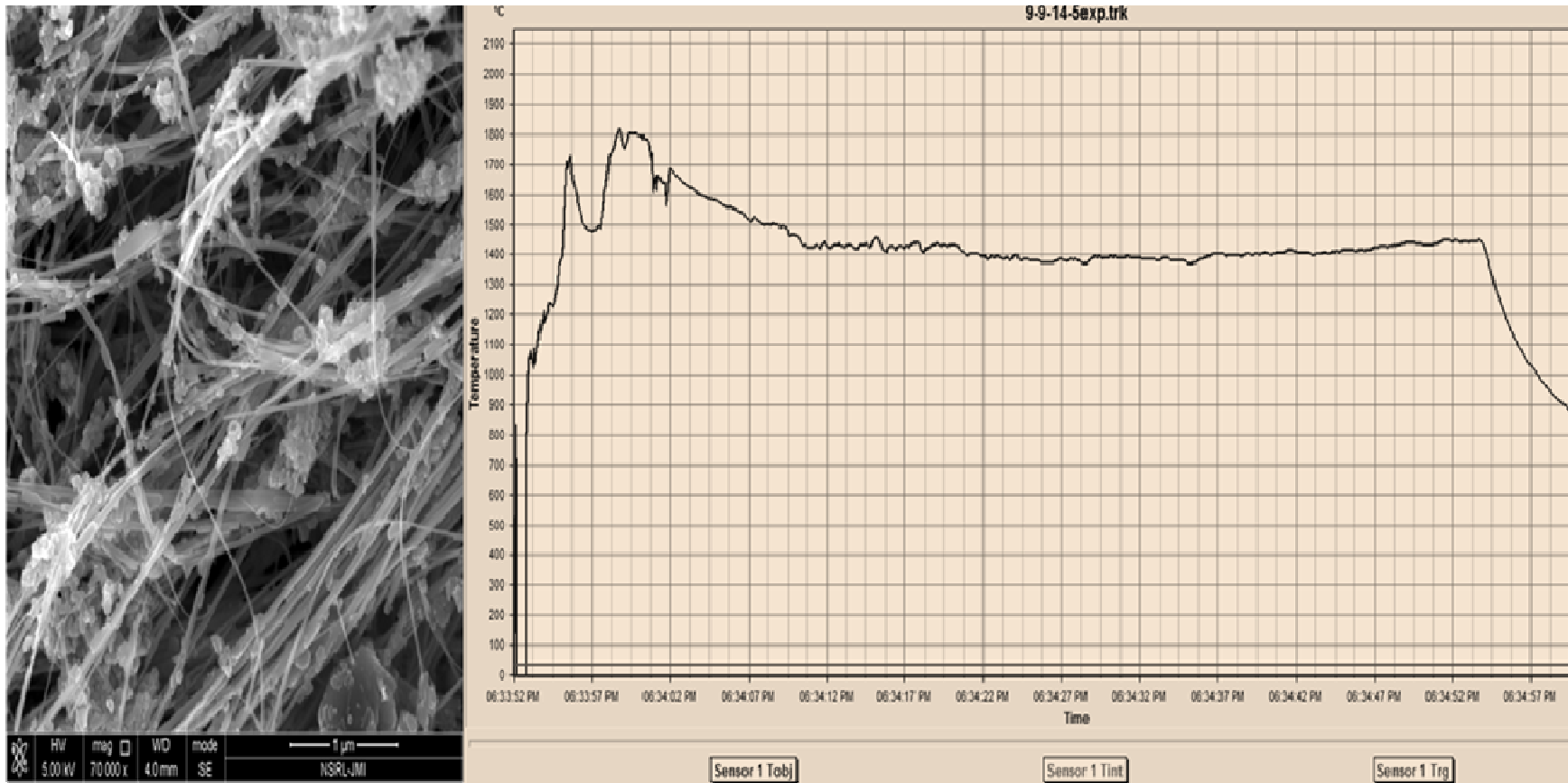
(a) 25 A, 1400-1600°C: High quantity CNTs observed at uniform arc temperature



(b) 30 A, 1400°C: High quantity CNTs observed at uniform arc temperature



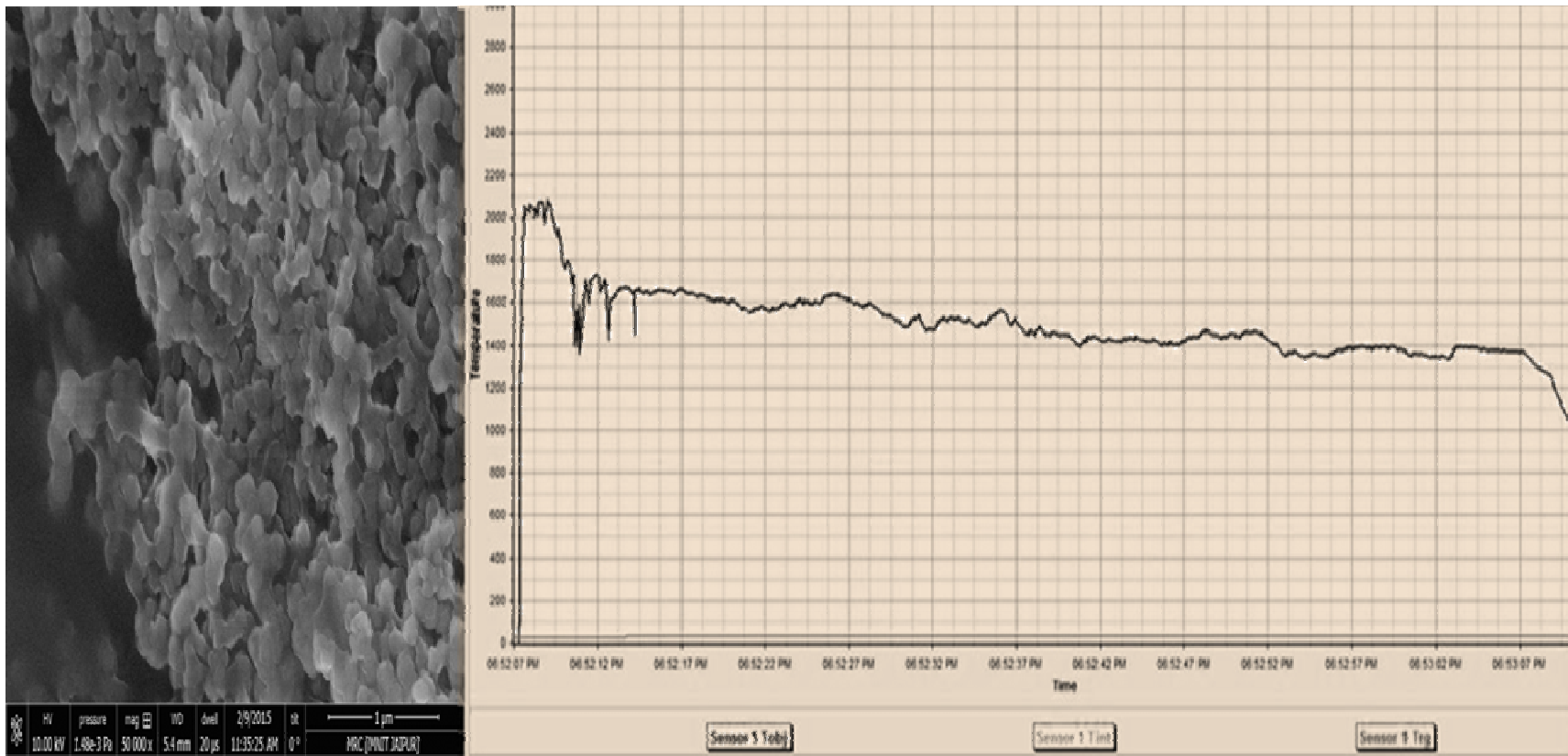
(c) 35 A, 1400°C: High quantity CNTs observed at uniform arc temperature



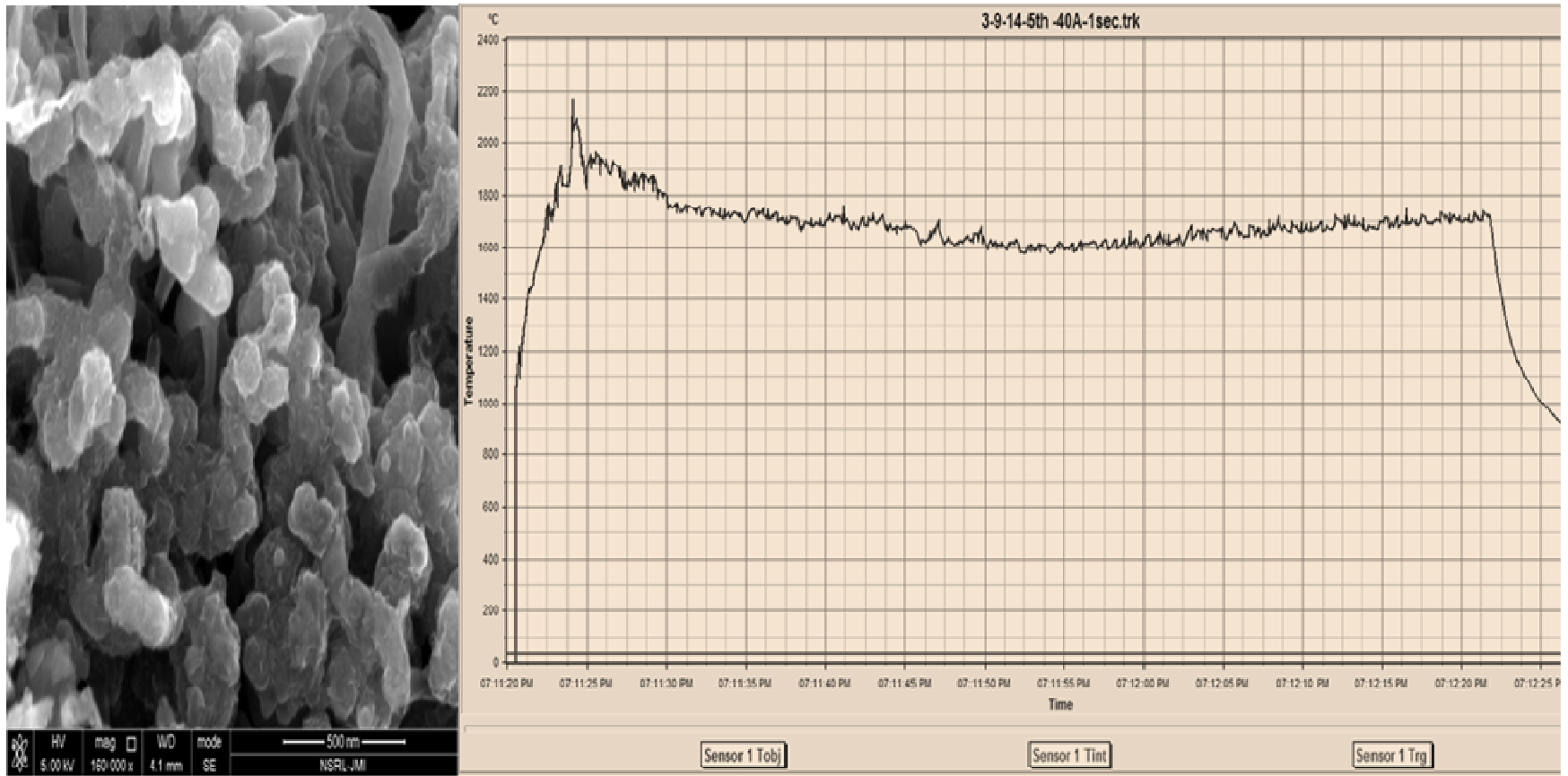
(d) 40 A, 1400°C: High quantity CNTs observed at uniform arc temperature

Figure 5.1: FESEM Micrographs showing MWCNTs formed at different arc current levels and their corresponding temperature profiles that a uniform arc temperature of 1400-1600°C is critical for synthesis of high quality MWCNTs, It can be observed that as the arc current increases the amount of MWCNTs increases and the diameters of nanotubes decreases

For illustration two such FESEM micrographs are shown with corresponding temperature profile in Figure 5.2(a) and Figure 5.2(b). Figure 5.2(a) shows no CNT formation at 35 A and Figure 5.2(b) shows carbon Nano rods formation at 40 A as arc temperature was not sustained at constant value for long duration. In both the illustrated results, the arc temperature fluctuated beyond 1400-1600°C range of temperature.



(a) 35 A: No CNTs formation as arc temperature was not sustained



(b) 40 A: Carbon Nano rods formation as arc temperature was not sustained

Figure 5.2: Shows the FESEM Micrographs and their arc temperature (a) at 35 A which results in poor formation of CNTs due to Unstable arc temperature (b) Shows formation of Carbon Nano rods at 40 A

b) TGA Analysis

From FESEM and temperature profiles of arc in time, it is imperative that the formation of CNTs attributes to a stable arc with prolonged constant temperature. For further analysis of formed CNTs we did TGA (Thermo gravimetric analysis) of the corresponding four samples (at, 25 A, 30 A, 35 A and 40 A) in which the CNTs were formed. TGA measures the decrease in sample weight as a function of annealed temperature. From TGA graph we can measure the initiation temperature, oxidation temperature and the residual mass [8]. Initiation temperature denotes temperature at which amount of material start to decompose. Oxidation temperature represents the thermal stability of the material and residual mass provides an estimate of the metal fraction, primarily consist of catalyst material. Figure 5.3 shows the TGA graph for as synthesized MWCNTs for the four samples. The TGA graph shows the weight percent loss starting from 568 to 940°C which is almost same for four samples as compared to typical MWCNTs from 400 to 600°C [8]. Typical MWCNTs relates to the CNTs as already being synthesized in literature.

From the collected sample in which the CNTs were visible from FESEM conducted a TGA. The results of TGA are plotted in Figure 5.3, on the x-axis of the plot we record temperature during TGA and on y-axis, we have weight % of the sample. In all TGA 10 mg of sample was used to observe the reduction of weight of sample versus temperature increase.

For the sample obtained at 25A, it is recorded (as can be seen from Figure 5.3(a)) that weight % reduction initiates at 450°C. The reduction continues till the temperature of 950°C after which there is no residual mass. In comparison to typical MWCNTs TGA analysis, the initiation happen at 400°C, the reduction happens 400°C to 650°C [8]. Comparing the values of initiation for as synthesized MWCNTs at 25A with typical values of MWCNTs, we find that initiation in the current experiments happened at almost same value of temperature but the oxidation temperature range is more in case of as synthesized MWCNTs 450-950°C which indicates as synthesized sample is more thermally stable as compared to typical MWCNTs. The range is recorded and is visible from plot in Figure 5.3(a). In comparable to range of temperature reported in literature [8], the current range is higher which indicates thermal stability in sample. The enhanced range is seen as a sharp curve in Figure 5.3(a) distinct from two flat plateaus (a) and (b).

For the sample obtained at 30A, it is recorded (as can be seen from Figure 5.3(b)) that weight % reduction initiates at 550°C. The reduction continues till the temperature of 950°C after which there is no residual mass. In comparison to typical MWCNTs TGA analysis, the initiation happens at 400°C, the reduction happens 400°C to 650°C [8]. Comparing the values of initiation for as synthesized MWCNTs at 30A with typical values of MWCNTs, we find that initiation in the current experiments happened at 550°C but the oxidation temperature range is more in case of as synthesized MWCNTs 550-950°C which indicates as synthesized sample is more thermally stable as compared to typical MWCNTs.

The range is recorded and is visible from plot in Figure 5.3(b). In comparison to range of temperature reported in literature [8], the current range is higher which indicates thermal stability in sample. The enhanced range is seen as a sharp curve in Figure 5.3(b) distinct from two flat plateaus (a) and (b).

For the sample obtained at 35A, it is recorded (as can be seen from Figure 5.3(c)) that weight % reduction initiates at 550°C. The reduction continues till the temperature of 950°C after which there is no residual mass. In comparison to typical MWCNTs TGA analysis, the initiation happens at 400°C, the reduction happens 400°C to 650°C [8]. Comparing the values of initiation for as synthesized MWCNTs at 35A with typical values of MWCNTs, we find that initiation in the current experiments happened at 550°C but the oxidation temperature range is more in case of as synthesized MWCNTs 550-950°C which indicates as synthesized sample is more thermally stable as compared to typical MWCNTs. The range is recorded and is visible from plot in Figure 5.3(c). In comparison to range of temperature reported in literature [8], the current range is higher which indicates thermal stability in sample. The enhanced range is seen as a sharp curve in Figure 5.3(c) distinct from two flat plateaus (a) and (b).

For the sample obtained at 40A, it is recorded (as can be seen from Figure 5.3(d)) that weight % reduction initiates at 500°C. The reduction continues till the temperature of 950°C after which there is no residual mass. In comparison to typical MWCNTs TGA analysis, the initiation happens at 400°C, the reduction happens 400°C to 650°C [8]. Comparing the values of initiation for as synthesized MWCNTs at 40A with typical values of MWCNTs, we find that initiation in the current experiments happened at

500°C but the oxidation temperature range is more in case of as synthesized MWCNTs 500-950°C which indicates as synthesized sample is more thermally stable as compared to typical MWCNTs.

The range is recorded and is visible from plot in Figure 5.3(d). In comparable to range of temperature reported in literature [8], the current range is higher which indicates thermal stability in sample. The enhanced range is seen as a sharp curve in Figure 5.3(d) distinct from two flat plateaus (a) and (b).

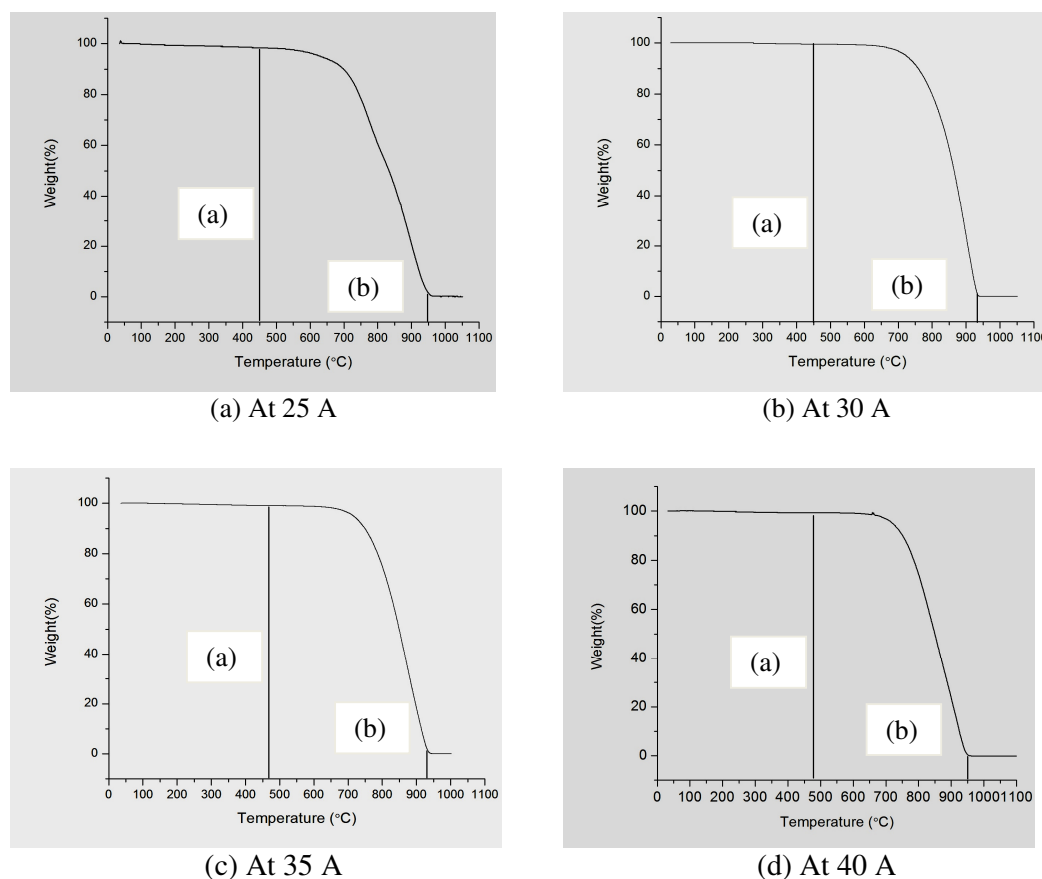


Figure 5.3: Thermo gravimetric analysis of as synthesized MWCNTs

From temperature profiling of arc temperature and corresponding formation of CNTs, it becomes obvious that temperature of arc plays a vital role in formation of CNTs. In order to study the role of temperature, we performed repeated experiments at 40 A and recorded arc temperatures for an arc application time of 60 s. The obtained results are presented and discussed in next section.

5.3 Role of Temperature

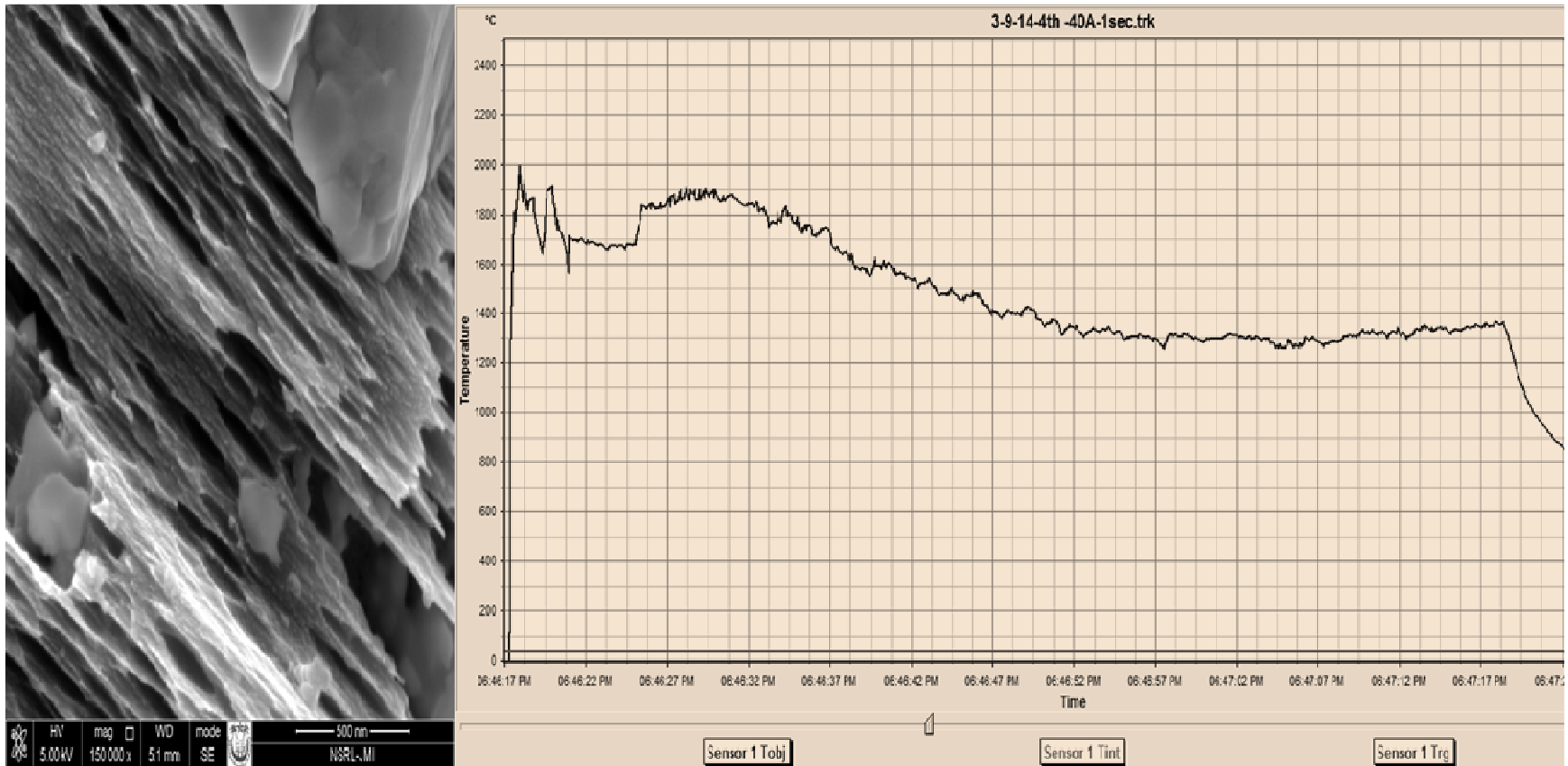
In this section, we study the role of temperature in formation of carbon nanotube from carbon black. Earlier also, there are published reports and studies available on effect of temperature for CNT formation using arc discharge method but a precursor other than CB. In 2000, Sugai et al. [9] suggested that SWCNTs formation takes place in strong annealing condition using pulsed arc discharge method. In 2003, Lange et al. [10] have found that plasma temperature ranging from 4000 to 6500 K is required for formation of carbon nanostructure in water. In 2004, Nishio et al. [11] observed that a high yield is achieved at high plasma temperature. In 2004, Liu et al. [12] concluded that CNTs diameter increases with increase in arc temperature. In 2004, Liu et al. [13] suggested that increase in arc temperature increases yield but SWCNT diameter reduces. In 2005, Zhao et al. [14] observed that optimum temperature of arc for formation of amorphous nanotube is 600°C; beyond which yield decreases. In 2007, Keidar et al. [15] observed that CNTs formation takes place in the region of low temperature plasma of 1300-1800K where carbon reacts to form large molecules and clusters. In 2007, Matsuura et al. [16] have suggested that the optimum temperature for nanotube formation is around in the range of 1000-1250°C. In 2008, Joshi et al. [17] suggested that temperature requirement for DWCNTs formation is in between the high temperature required for SWCNT and low temperature for MWCNT formation. In 2012, Kim et al. [18] have concluded that nanotube growth occur below 2000°C even though inter electrode temperature reaches 4000°C. In all these reports, graphite has been used as a precursor for nanotube formation. In our work, we have conducted experiments using CB as precursor at 40 A and 60 sec. FESEM results and their corresponding temperature profiles are presented in next section.

5.3.1 Characterization

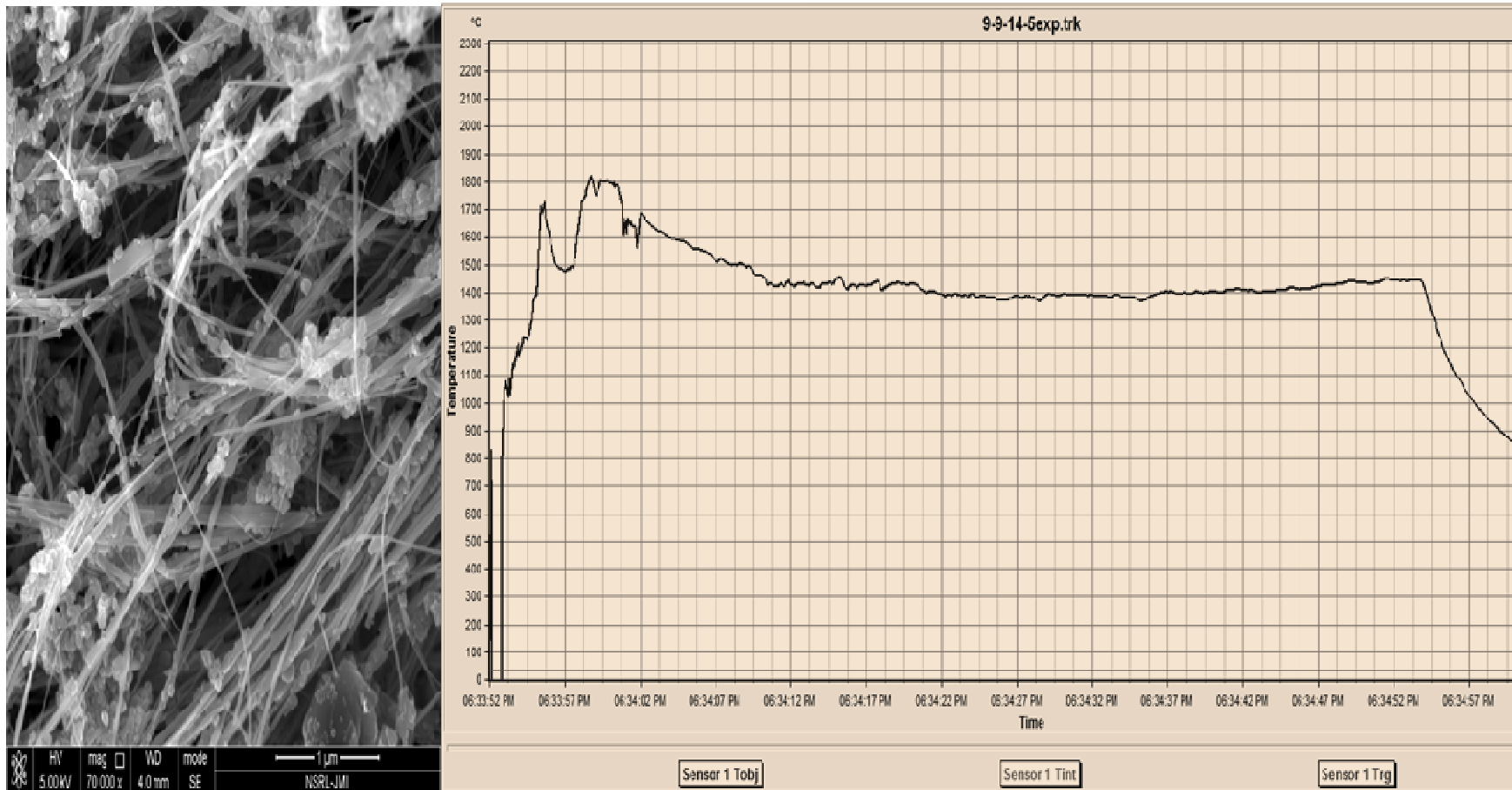
a) FESEM Analysis

Different samples prepared at 40A were observed under FESEM and results are shown in Figure 5.4. The corresponding temperatures profiles conducted for 60sec had shown for each FESEM result. We observed that temperature range between 1400-1600°C is critical for nanotube formation as shown in Figure 5.4(a) through Figure 5.4(d) while in Figure 5.4(a) some graphitic structure were observed at temperature below 1400°C there were high quantity MWCNTs formed when temperature was ranging between 1400-1600°C as visible from graph temperature was uniform for 40 sec shown in Figure 5.4(b).

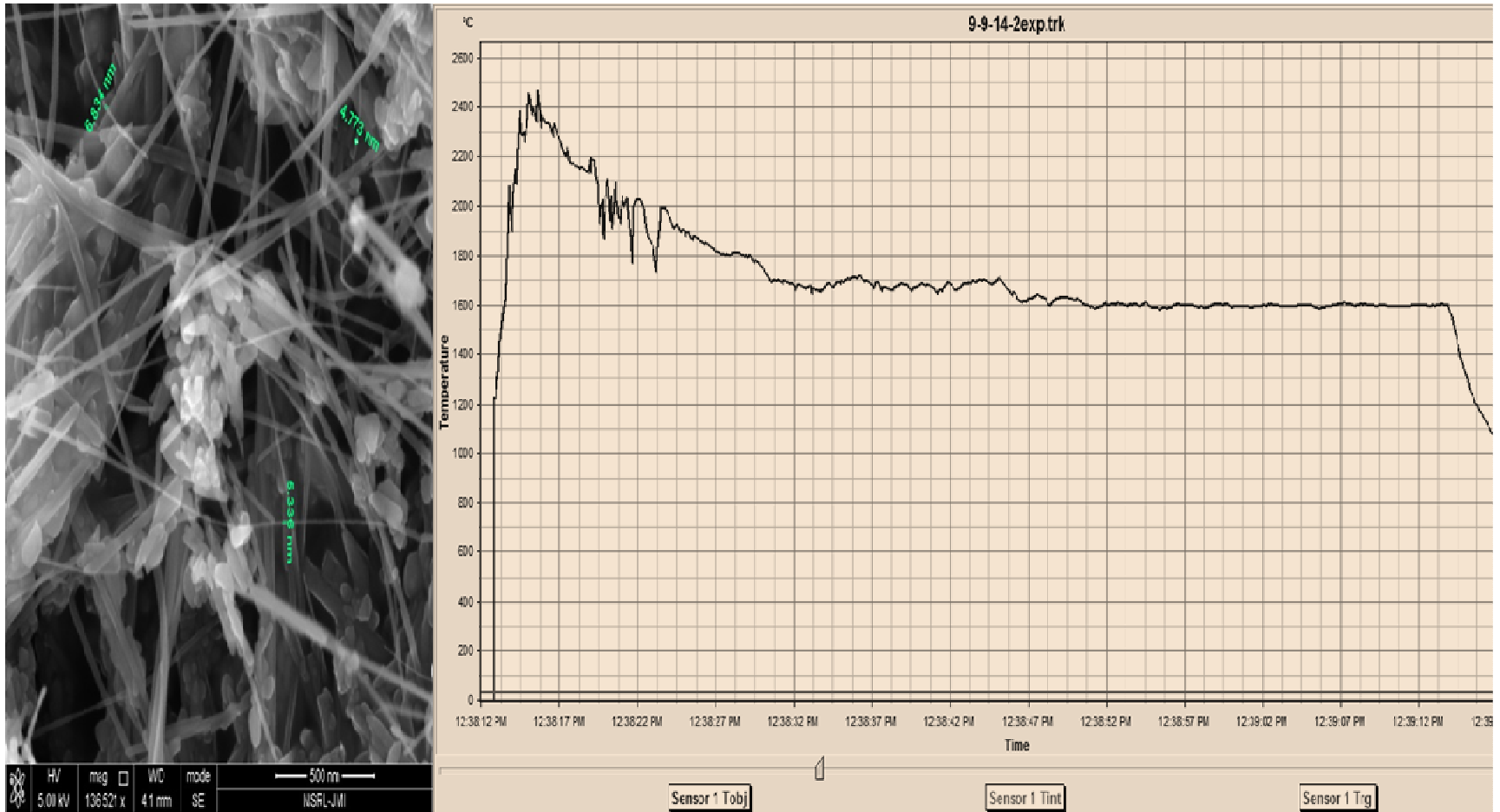
For temperatures ranging 1600-1800°C, very few nanotubes are observed as shown in Figure 5.4(d) and few or no CNTs are formed above 1800°C as arc temperature was fluctuated refer Figure 5.4(e) and Figure 5.4(f).



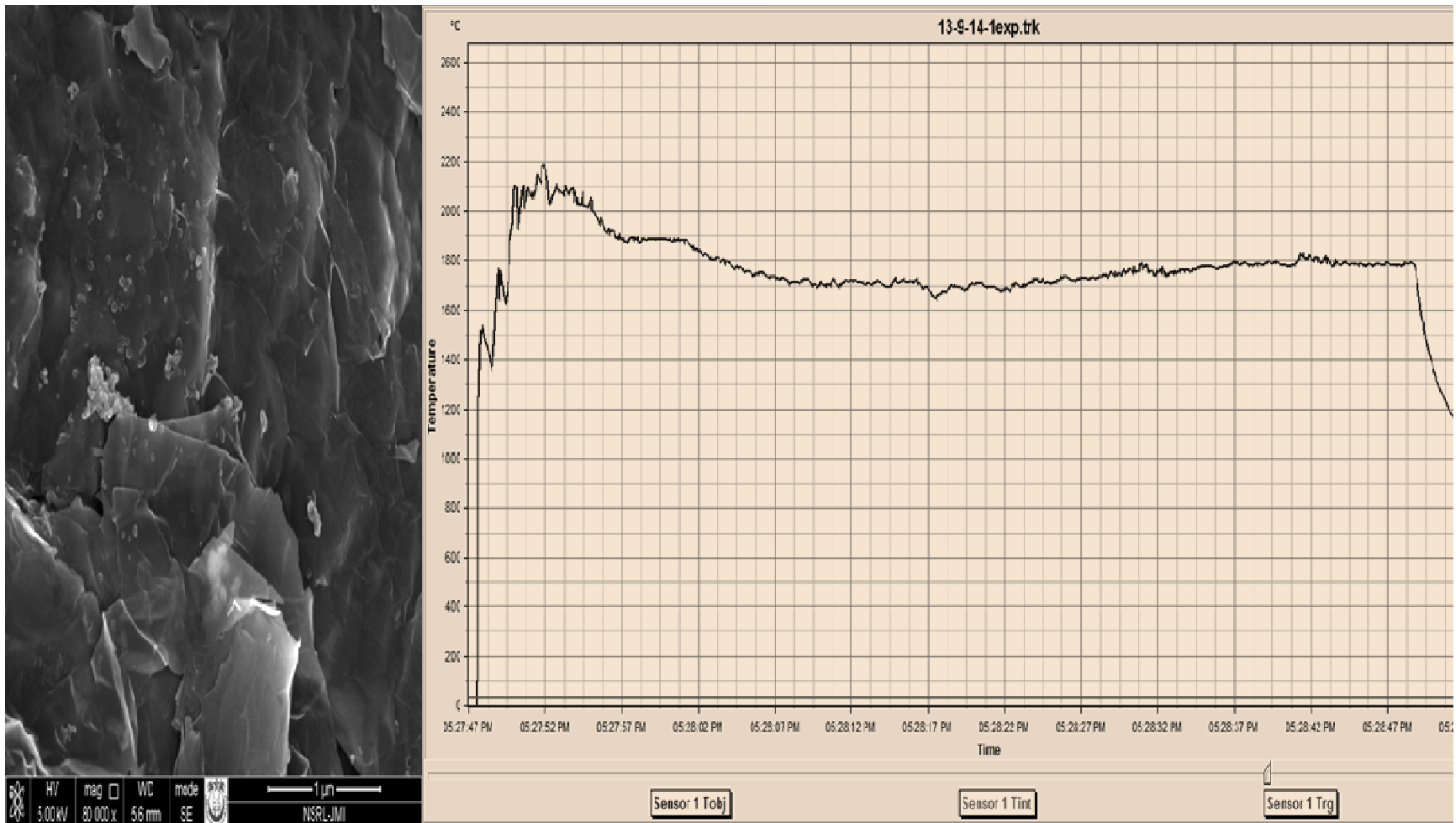
(a) 1300-1400°C: No CNTs observed



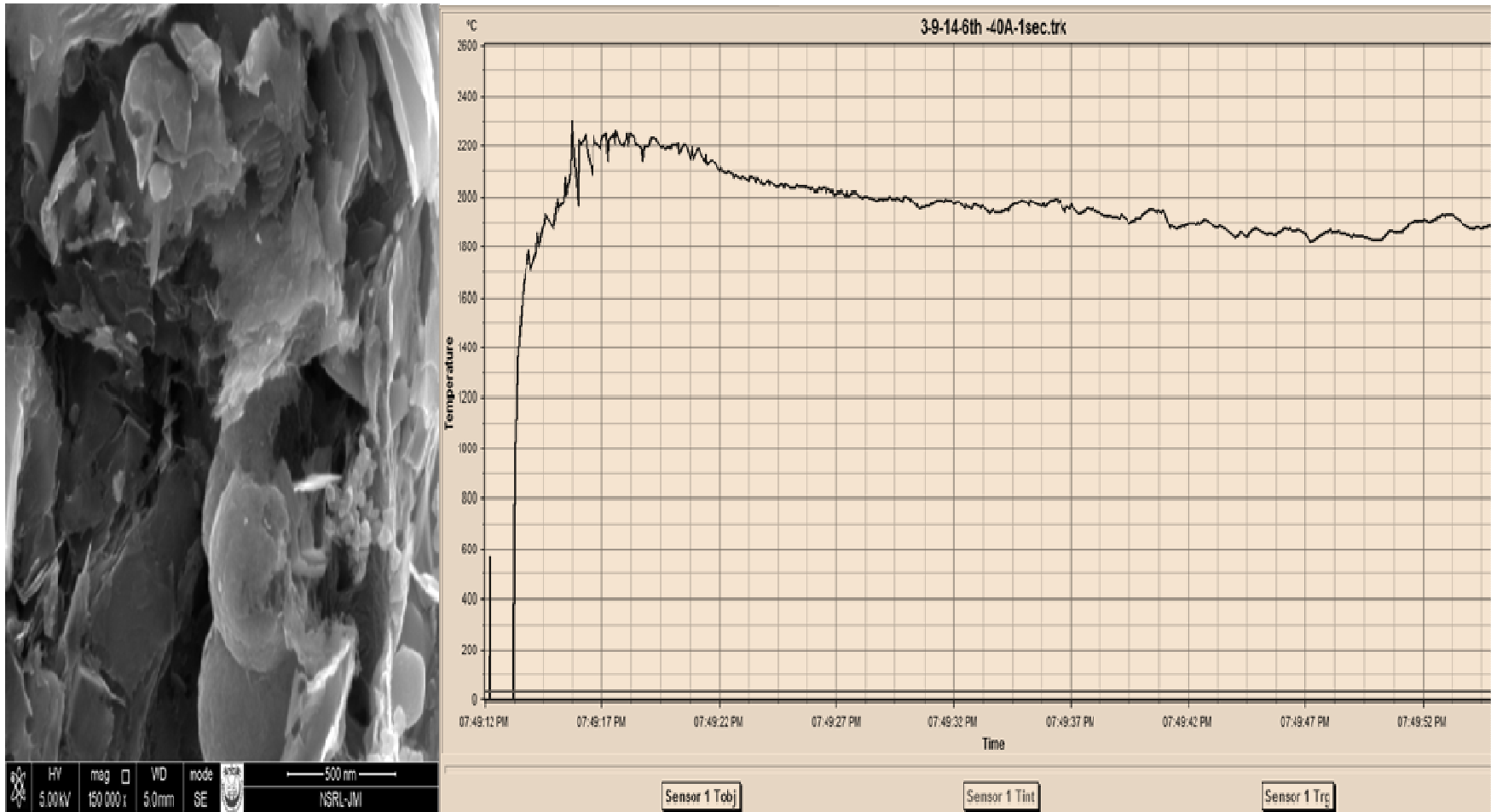
(b) 1400°C: High quantity CNTs observed at uniform arc temperature



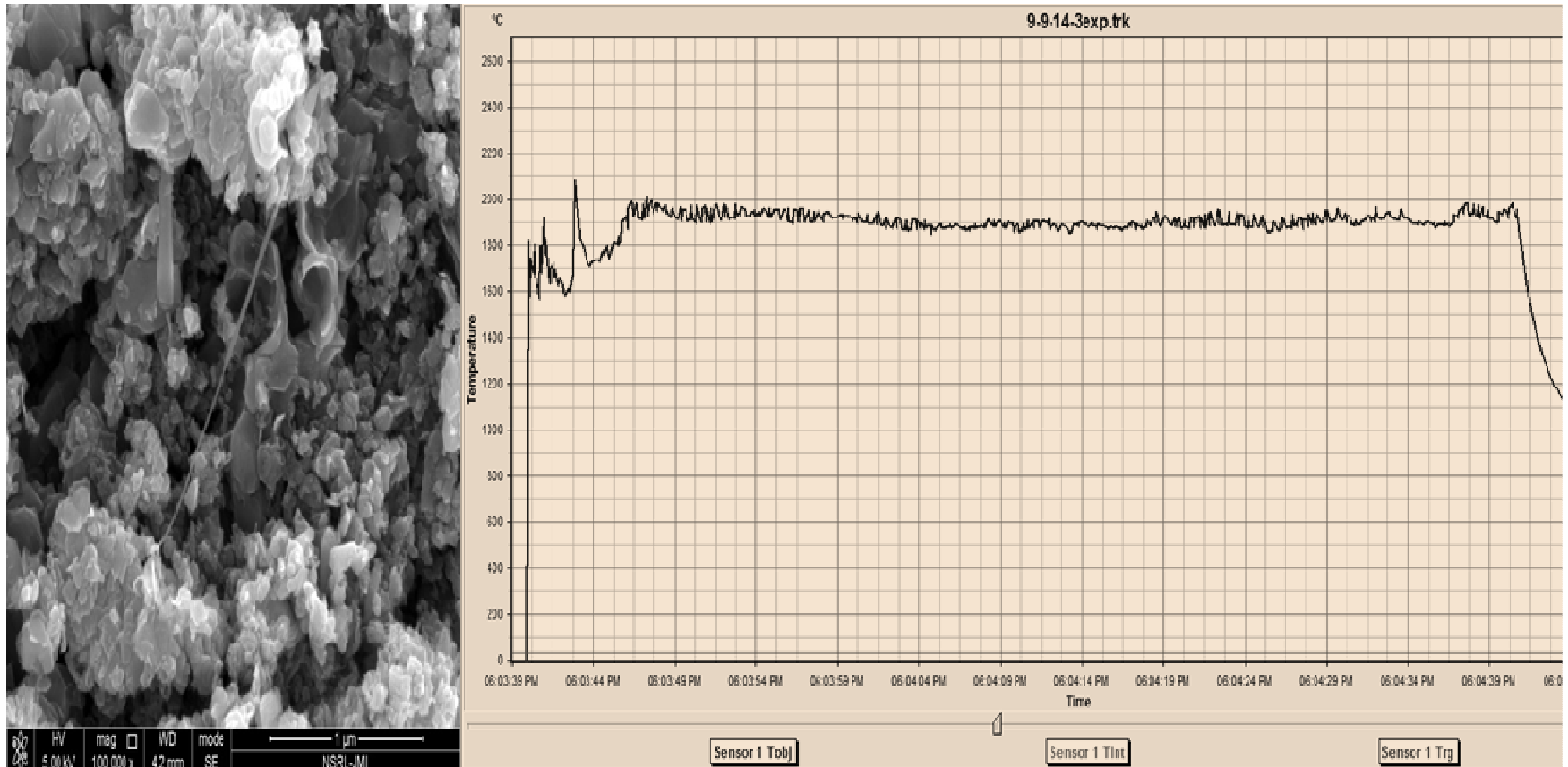
(c) 1600°C: High quantity CNTs observed at uniform arc temperature



(d) 1700-1800°C: No CNTs observed



(e) 1800-2000°C: No CNTs observed at high temperature



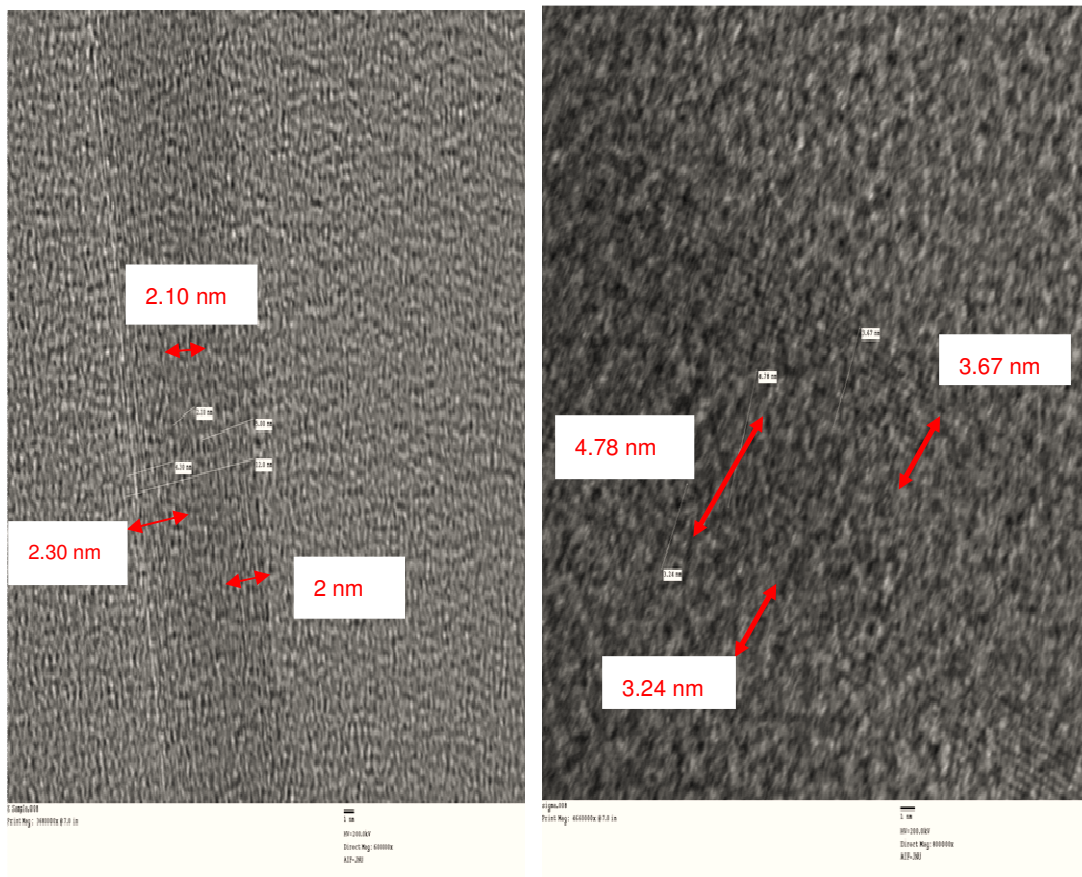
(f) 1900-2000°C: No CNTs observed at high fluctuating temperature

Figure 5.4: Effect of arc temperature on arc discharge products for a constant arc current of 40 A. It is evident from the micrographs and their corresponding temperature profiles that a uniform arc temperature of 1400-1600°C is critical for synthesis of high quantity MWCNTs

From FESEM result and their corresponding arc temperature profile, it become obvious that arc temperature range 1400-1600°C is critical for nanotube formation. In order to study the inner morphology of structure, we did TEM analysis.

b) TEM Analysis

In order to analyze the inner morphology of MWCNT structure we did TEM (Transmission Electron Microscopy) analysis of collected sample at 40 A. Figure 5.5 shows as synthesized MWCNTs with temperature of 1800°C and typical MWCNTs at 40 A with temperature of 1400-1600°C.



**Figure 5.5: TEM Micrographs of (a) As synthesized MWCNTs at 1800°C
(b) Typical MWCNTs formed at 40 A with Temperature of 1400-1600°C**

Typical MWCNTs structure reveals lesser number of walls which result in high purity and less structural defects and also longer and straight tube. The CNTs morphology establishes the better conducting network and electrical properties. Using number of walls, inner diameter and outer diameter, we can calculate the density of MWCNTs [19].

Considering the MWCNTs with inner diameter d_{int} , n number of walls and d_{ss} inter-shell distance, the weight of MWCNTs is given by [19]

$$W = \frac{1}{1315} \pi L \left[n d_{\text{int}} + 2 d_{\text{ss}} \sum_{t=0}^{n-1} t \right]$$

The volume of CNTs depend on outer diameter

$$V = \frac{(\pi L d_{\text{out}}^2)}{4}$$

Thus, the density of MWCNTs is given by

$$D = 1000 W/V = 4000/1315 \left[n/d_{\text{out}} - (2d_{\text{ss}} \sum_{i=0}^{n-1} i / d_{\text{out}}^2) \right]$$

Above calculations are based on published in literature: d_{ss} (inter-shell distance = 0.34 nm), L (length of CNTs = 10 μm). Figure 5.5(b) shows the TEM graph of typical MWCNTs and we observe d_{out} (outer diameter of MWCNT) is 7 nm and d_{int} (inner diameter of MWCNT) is 4.78 nm. The calculated density for MWCNTs is 2.43g/cm³. The dense and well aligned MWCNTs will be more useful for electrical and mechanical applications.

From FESEM and TEM and further analysis we noticed that at same arc current the arc temperature may fluctuate, this may occur due to varying distance between the electrodes which makes the arc unstable for DC arc discharge setup. The fluctuation may also happen due to local dynamic movement of carbon black and other transforming particle and transients within the arc. The transient phases cause improper vaporization of the carbon precursor. Depending upon the instantaneous shape of electrode, the electric field generated during arc can significantly vary. As CNTs growth is also influenced by the applied electric field between the electrodes, the shape of the electrode and within arc transient environment is very crucial in CNT formation. After each cycle of arcing, a general trend to get the electrode blunt may happen which require relative higher temperature to initiate the same growth process. Therefore, re stabilized arc or effectively stabilized temperature of arc is more critical than applying a constant current.

We achieved the stabilization of arc temperature dynamically adjusting the gap of electrode using proportional integral derivative (PID) feedback controller for electrode gap. It is but established from the present investigations and results that a temperature

control will be better practice to get high quantity CNTs rather than controlling and for maintaining constant current.

It further needs to be answered if time of arc application vis-a-vis magnitude of current has any correlation in formation of CNTs. Moreover, the effect of applying pulsed arc discharge in comparison to application of DC arc needs another investigation. To observe the effect of pulse of varying arc current and time we did experiment using pulse arc supply and presented in next section.

5.4 Role of Pulse Arc Discharge

In this section, we study the role of pulse arc in formation of carbon nanotube from carbon black. We investigate the effect of arc current on N330 Carbon Black grade for synthesis of carbon nanotube using pulsed arc discharge method keeping time duration constant at 60 sec which has not been reported in literature.

We did experiment using pulsed power supply details of which is presented in Chapter 3 in Section 3.2.2. We performed experiments on N330 carbon black grade using pulsed power supply for arc current varied from 22 to 40 A with the step of 4 A. The procedure for sample preparation discussed in Chapter 4 in Section 4.3.1. After performing set of experiments for arc current from N330 carbon black grade, the deposit from cathode was collected. We have chosen random sample for each arc current and then characterize the sample using FESEM. Figure 5.6(a) shows the FESEM image of carbon nanoparticle at an arc current of 22 A at 60 sec. As we kept increasing the current keeping time duration constant at 26 A these nanoparticles merged into multilayer sheets with scattered flower type structures randomly distributed on top of layer, these flowers contain some tubular items as shown in Figure 5.6(b). For arc current of 28 A circular disc like discrete layer was observed in Figure 5.6(c). When the arc current increased to 30 A tubes were begin to grow from layer edges as shown in Figure 5.6(d). For an arc current of 32 A more tubes start growing at the edges as shown in Figure 5.6(e). With 35A arc current tube at the edges become linear in pattern as shown in Figure 5.6(f). As current reaches 37 A fly ash particles i.e. spherical particles of different size appears in between the image with tube like structure shown in Figure 5.6(g). Finally at 40A arc current carbon nanotubes of different diameter get formed as shown in Figure 5.6(h).

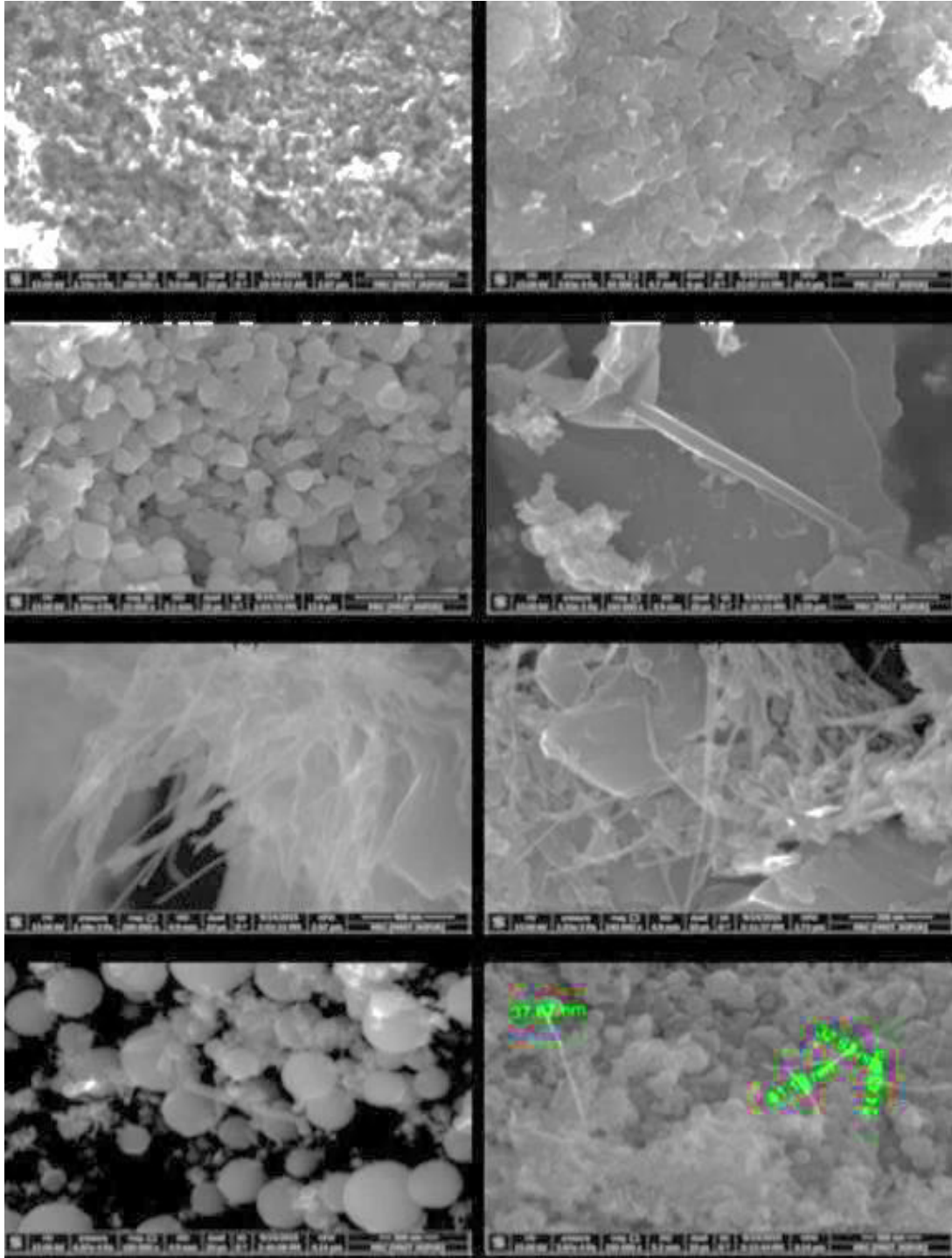


Figure 5.6: FESEM image of (a) Carbon nanoparticle at an arc current of 22 A for 60 sec (b) Nanoparticle merged into multilayer sheet of with scattered flower structure on top layer at 26 A (c) At 28A arc current circular disc like discrete layer was observed (d) tubes were begin to grow from layer edges at 30 A (e) At 32 A more tubes at layer edges (f) tubes at the edges become linear at 35 A arc current (g) At 37 A arc current fly ash like particle of different spherical diameter was observed (h) Formation of tubular structure (CNTs) at 40 A arc current for 60 sec

From above study we observe through FESEM the conversion of amorphous structure of N330 grade converted to tubular structure at 40 A for 60 sec. For further investigation we have examined the effect of varying amperage and time of the arc on N330 carbon black grade. Figure 5.7(a) shows the spherical particles of Carbon black at different diameter. The experiment was conducted at constant current 40 A for varying time duration. It was observed from the FESEM image of the sample in Figure 5.7(b) at 30 sec that the granular clusters of carbon black particles mutually fused and flattened to form graphene like sheets. When we increased the time duration to 60 sec keeping arc current constant, Figure 5.7(c) shows the FESEM image of formation of more tubular structures rather than graphene like sheets.

In an attempt to also observe the effect of current on the morphology of N330 grade of carbon black, two experiments were conducted at 30 A and 40 A for 30 sec. The FESEM images of the experiment conducted at 30 A for 30 sec partly granular with small island like structures were observed as shown in Figure 5.7(d), indicating the beginning of the transformation. When the current was increased to 40 A keeping the duration of the experiment constant it is seen that the sample is no longer granular and becomes planar and graphene sheet like structure as shown in Figure 5.7(e).

In next attempt, the experiments duration was kept constant at 60 sec. Then the FESEM image of the samples collected at 20 A reveals small transformation of granular carbon black into small planar areas as shown in Figure 5.7(f). Figure 5.7(g) shows the tubular structure with granules of CB at 30 A and at 40 A MWCNTs of varying diameter were observed in the sample as shown in Figure 5.7(h).

From the results obtained it is inferred that as the time progresses the granular CB undergoes the transformation from small islands like structures to planar graphite like sheets and then finally into tubular form as desired. It is also seen that as the current increases the time required for the synthesis for the carbon nanotubes decreases. The MWCNTs formed have diameter in the range of 36 nm to 85 nm as shown in Figure 5.7(i).

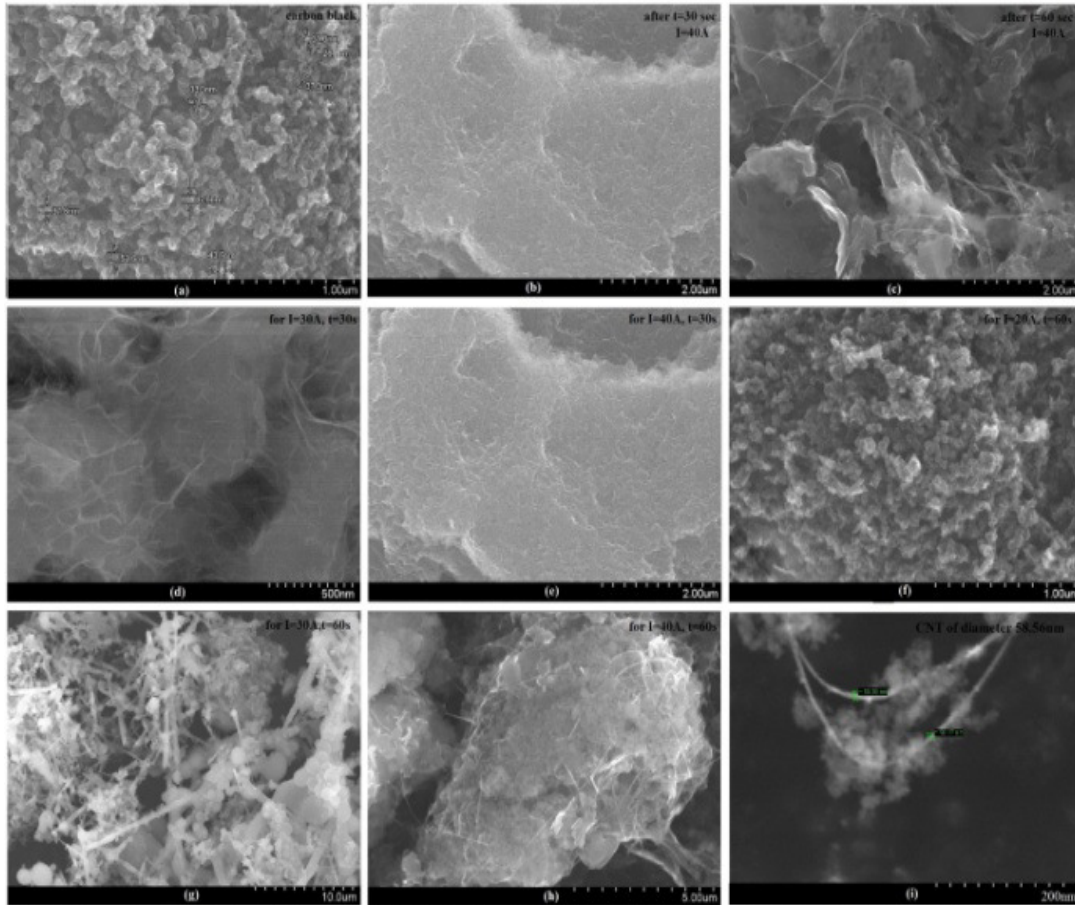


Figure 5.7: FESEM Images of various samples of experiment conducted under different conditions (1) For fixed arc current (40 A) & variable time durations (30s,60s) (a) Carbon black (b) Sample after 30s (c) Sample after 60s (2) For different arc current & fixed time durations (30s): (d) Sample when arc current is 30 A (e) Sample when arc current is 40 A. (3) For different arc current & fixed time duration (60s): Sample when arc current is 20 A (g) Sample when arc current is 30 A (h) Sample when arc current is 40 A. (i) CNT of diameter 58.56 nm

We observe through FESEM analysis the conversion of amorphous structure of N330 grade converted to tubular structure at 40 A for 60 sec.

5.5 Conclusion

1. We have successfully synthesized MWCNTs using CB as precursor at an arc current ranging from 25 to 40 A using DC arc discharge setup. Contrary to reported literature, where arc current is the critical parameter to govern the onset of nanotube formation, we report the importance of sustained constant arc temperature in the synthesis of carbon nanotubes. The production rate of the CNTs increases and diameter reduces when arc discharge current increases.

2. At higher arc current, the graphitic carbon gets converted to MWCNTs thereby improving the yield. Below 20 A, the arc was unstable and the cathode deposits were not formed. In previous reports [14, 16, 19, 20] the nanotubes were formed at a high arc current of 100 A, whereas we observed MWCNTs at low current levels of 25 A.
3. The critical observation in the formation of CNTs at lower current is attributed to sustaining constant arc temperature for prolonged time. We found that 1400-1600°C arc temperature range is critical for nanotube formation. If the temperature is outside this range, then very few or no CNTs are observed.
4. We have also investigated the role of arc current variation from 22 A to 40 A with the step of 4 A with respect to time using pulse arc discharge method. It was observed that the granular structure of CB transformed to graphene sheet with scattered flower type structure distributed on top layer and converted into tubular structure of different diameter at 40 A for 60 sec.
5. It is also established that endeavors towards understanding to maintain constant temperature rather than constant current will yield to pathway for further advancement in the methodology of phase transformation of CB to MWCNTs using arc discharge.

In the next chapter we present the overall conclusion and future scope of the thesis.

References:

- [1] N. Arora and N. N. Sharma, "Arc discharge synthesis of carbon nanotubes: Comprehensive review," *Diam. Relat. Mater.*, vol. 50, pp. 135–150, Nov. 2014.
- [2] Y. Su, Y. Zhang, H. Wei, L. Zhang, J. Zhao, Z. Yang, and Y. Zhang, "Magnetic-field-induced diameter-selective synthesis of single-walled carbon nanotubes," *Nanoscale.*, vol. 4, no. 5, pp. 1717–1721, Dec. 2011.
- [3] J. Qiu, Z. Wang, Z. Zhao, and T. Wang, "Synthesis of double-walled carbon nanotubes from coal in hydrogen-free atmosphere," *Fuel.*, vol. 86, no. 1–2, pp. 282–286, Jan. 2007.
- [4] Y. Su, H. Wei, T. Li, H. Geng, and Y. Zhang, "Low-cost synthesis of single-walled carbon nanotubes by low-pressure air arc discharge," *Mater. Res. Bull.*, vol. 50, pp. 23–25, Feb. 2014.
- [5] J. B. A. M. Jagannatham, R. R. D., and P. Haridoss, "Synthesis of thin bundled single walled carbon nanotubes and nanohorn hybrids by arc discharge technique in open air atmosphere," *Diam. Relat. Mater.*, vol. 55, pp. 12–15, May. 2015.
- [6] X. Cai, H. Cong, and C. Liu, "Synthesis of vertically-aligned carbon nanotubes without a catalyst by hydrogen arc discharge," *Carbon.*, vol. 50, no. 8, pp. 2726–2730, Jul. 2012.
- [7] L. Fang, L. Sheng, K. An, L. Yu, W. Ren, Y. Ando, and X. Zhao, "Effect of adding W to Fe catalyst on the synthesis of SWCNTs by arc discharge," *Phys. E Low-dimensional Syst. Nanostructures.*, vol. 50, pp. 116–121, May. 2013.
- [8] J. H. Lehman, M. Terrones, V. Meunier, E. Mansfield, and K. E. Hurst, "Evaluating the characteristics of multiwall carbon," *Carbon.*, vol. 49, no. 8, pp. 2581–2602, Jul. 2011.
- [9] T. Sugai, H. Omote, S. Bandow, N. Tanaka, and H. Shinohara, "Production of fullerenes and single-wall carbon nanotubes by high-temperature pulsed arc discharge," *J. Chem. Phys.*, vol. 112, no. 13, pp. 6000, Apr. 2000.
- [10] H. Lange, M. Sioda, A. Huczko, Y. Q. Zhu, H. W. Kroto, and D. R. M. Walton, "Nanocarbon production by arc discharge in water," *Carbon.*, vol. 41, pp. 1617–1623, Dec. 2003.
- [11] M. Nishio, S. Akita, and Y. Nakayama, "Cooling effect on the growth of carbon

- nanotubes and optical emission spectroscopy in short-period arc-discharge,” *Thin Solid Films.*, vol. 464–465, pp. 304–307, Oct. 2004.
- [12] Y. Liu, S. Xiaolong, Z. Tingkai, Z. Jiewu, M. Hirscher, and F. Philipp, “Amorphous carbon nanotubes produced by a temperature controlled DC arc discharge,” *Carbon.*, vol. 42, no. 8–9, pp. 1852–1855, Jan. 2004.
- [13] T. Zhao and Y. Liu, “Large scale and high purity synthesis of single-walled carbon nanotubes by arc discharge at controlled temperatures,” *Carbon.*, vol. 42, no. 12–13, pp. 2765–2768, Jan. 2004.
- [14] T. Zhao, Y. Liu, and J. Zhu, “Temperature and catalyst effects on the production of amorphous carbon nanotubes by a modified arc discharge,” *Carbon.*, vol. 43, no. 14, pp. 2907–2912, Nov. 2005.
- [15] M. Keidar, “Factors affecting synthesis of single wall carbon nanotubes in arc discharge,” *J. Phys. D. Appl. Phys.*, vol. 40, no. 8, pp. 2388–2393, Apr. 2007.
- [16] T. Matsuura, K. Taniguchi, and T. Watanabe, “A new type of arc plasma reactor with 12-phase alternating current discharge for synthesis of carbon nanotubes,” *Thin Solid Films.*, vol. 515, no. 9, pp. 4240–4246, Mar. 2007.
- [17] R. Joshi, J. Engstler, P. K. Nair, P. Haridoss, and J. J. Schneider, “High yield formation of carbon nanotubes using a rotating cathode in open air,” *Diam. Relat. Mater.*, vol. 17, no. 6, pp. 913–919, Jun. 2008.
- [18] Y. A. Kim, H. Muramatsu, T. Hayashi, and M. Endo, “Catalytic metal-free formation of multi-walled carbon nanotubes in atmospheric arc discharge,” *Carbon.*, vol. 50, no. 12, pp. 4588–4595, Oct. 2012.
- [19] C. Laurent, “Open Archive Toulouse Archive Ouverte (OATAO) The weight and density of carbon nanotubes versus the number of walls and diameter,” *Carbon.*, vol. 48, no. 10, pp. 2994–2996, 2010.

Overall Conclusion and Future Scope

6.1 Overall Conclusion

In this chapter, an insight of the research work done along with major contributions as explained in this thesis and the future scope of this research work are provided. For this purpose, a complete detail of the thesis chapter wise conclusion is explained below.

1. From literature review we studied graphite is the mostly investigated precursor in synthesis of carbon nanotubes, the other precursor such as coal, hydrocarbons, fullerene and tire powder need further understanding and investigations. Since Carbon black is less perused in literature, the investigation on transformation of CB to CNT forms interesting premises of research and investigations.
2. Comprehensive literature review including carbon nanotubes, its synthesis method, effect of various parameters such as power supply, current, voltage, frequency, catalyst, atmosphere, pressure, various carbon precursors required in formation of carbon nanotubes have been presented chronologically. Understanding on most of these verticals are still half way through to clarity and all of them presents as beckoning problem to investigation. Keeping in view the time for completion of thesis and vitality in context to contribution, we identified gaps in research and correspondingly defined scope and problem statement within the scope. As a first problem at hand, in an attempt to synthesize carbon nanotubes from carbon black arc discharge set up needs to be designed.
3. We have designed the arc discharge chamber by considering mechanical design and electrical circuit design of DC and pulsed arc discharge setup for the custom built arc chamber in chapter 3. The objective of the design is to obtain a stable arc and a constant arc current across the electrode. With this scope we investigate the amenability of conversion of different grades of CB to nanotube using DC arc discharge set up designed.

4. From various grades of carbon black we have chosen five type of carbon black grade that comes under class of furnace carbon black type. The five types of CB as carbon precursor we did 30 experiments for each carbon black grade. The experiments were done with an objective to transform CB to CNT and were conducted using DC arc discharge for an arc current of 40 A for a duration of 60 sec in argon atmosphere. After completing each experiment, the deposited material from surface of cathode was collected. Out of 30 collected samples for each grade we did analysis for three randomly selected samples for each grade of CB.
5. FESEM and TEM analysis conform the presence of MWCNTs. It was observed N330 carbon black grade gets converted to Carbon nanotubes. The possible attribution for this conversion was the presence of four adsorption sites 90% of which has been graphitic planes.
6. We report the importance of sustained constant arc temperature in the synthesis of carbon nanotubes. We found that 1400-1600°C arc temperature range is critical for nanotube formation. If the temperature is outside this range, then very few or no CNTs are observed.

We have also investigated the role of arc current variation from 22 A to 40 A with the step of 4 A with respect to time using pulse arc discharge method. It was observed that the nanoparticle merged into multilayer sheet with scattered flower type structure distributed on top layer and converted into tube like structure of different diameter at 40 A for 60 sec.

6.2 Future Scope of the Work

No research concludes with an absolute end. Several areas of synthesis of MWCNT from different grades of carbon black need better understanding so it can be improved further. Synthesis of carbon nanotube using grade of carbon black as precursor is not reported in literature. We have developed a method for conversion of carbon black grade into CNTs by DC and pulsed arc discharge method.

From the perspective of present work, the following aspects can be studied and investigated further.

1. From various grades of carbon black we have chosen five type of furnace carbon black grade for conversion of CB to CNTs from industrial aspect. The effect of other types of carbon black can be further investigated.
2. We have designed the circuit for pulsed power supply to synthesize CNT using carbon black as precursor. We were in need of a frequency varying power supply. Due to high cost involved in customizing frequency varying power supply, we conducted experiment on single frequency pulsed power supply. The effect of variation of duty cycle is a scope for improvisation by modifying the arc discharge parameters for better yield.
3. Since a large number of experimental reports have been published in the last two decades to synthesize CNTs, this field still needs further experiments and theoretical investigations to establish a correlation between various synthesis parameters and nucleation of carbon nanotubes and help us better understand the growth mechanism of carbon nanotubes.
4. It is an effort towards understanding of maintaining constant temperature rather than constant current in arc discharge will yield to pathway for further advancement in the methodology of phase transformation of CB to MWCNTs. There is wide scope of application of CNT from CB in day-to-day life due to light weight and high strength material. This provides an opportunity in innovative applications for materials such as reinforcing filler in tyres. However, in order to realize these scopes, more research is required to find the solutions to the challenges.

16NSR120 Diode

Features

- Diffused Series
- Industrial grade
- Available in Normal and Reverse polarity
- Metric and UNF thread type

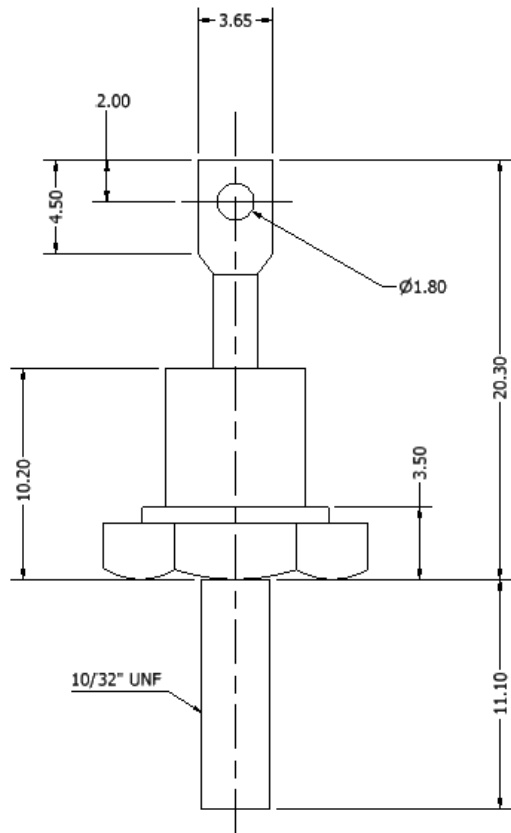
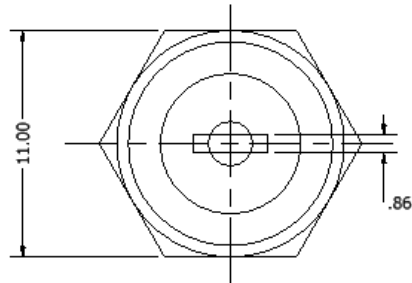
Electrical Specifications ($T_E = 25^\circ\text{C}$, unless otherwise noted)			
Symbol	Parameters	Values	Units
$I_F(AV)$	Maximum avg. forward current @ $T_E = 150^\circ\text{C}$	16	A
V _{FM}	Maximum peak forward voltage drop	1.3	V
I_{FSM}	Maximum peak one cycle (non-rep) surge current @ 10 msec	300	A
I_{FRM}	Maximum peak repetitive surge current	80	A
I^2t	Maximum I^2t rating (non-rep) for 5 to 10 msec	450	A^2sec



DO-203AA (DO-4)

Electrical Ratings ($T_E = 25^\circ\text{C}$, unless otherwise noted)						
Type number	Voltage Code	VRRM, Maximum repetitive peak reverse voltage (V)	VR(RMS), Maximum RMS reverse voltage (V)	VR, Maximum DC blocking voltage (V)	Recommended RMS working voltage (V)	IR(AV), Maximum avg. reverse leakage current (μA)
16NS(R)	10	100	70	100	40	100
	20	200	140	200	80	
	40	400	280	400	160	
	60	600	420	600	240	
	80	800	560	800	320	
	100	1000	700	1000	400	
	120	1200	840	1200	480	
	140	1400	980	1400	560	
	160	1600	1120	1600	640	

Thermal & Mechanical Specifications (TE = 25°C, unless otherwise noted)			
Symbol	Parameters	Values	Units
R _{th(JC)}	Maximum thermal resistance, junction to case	1.5	°C /W
T _J	Operating junction temperature range	-65 to 150	°C
T _{stg}	Storage temperature	-65 to 150	°C
	Mounting torque (non-lubricated threads)	0.14 (min)-0.17 (max)	
W	Approximate allowable weight	7	g

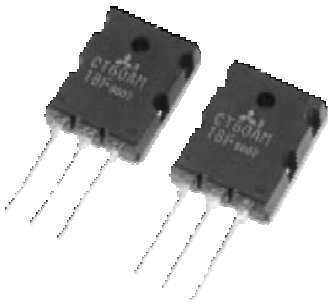


(all dimensions in mm)

CT60AM IGBT

INSULATED GATE BIPOLAR TRANSISTOR

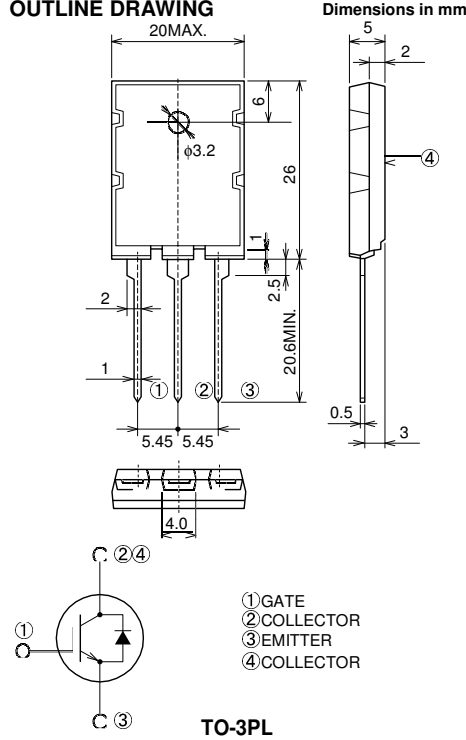
CT60AM-18F



- VCES 900V
- IC 60A
- Simple drive
- Integrated Fast-recovery diode
- Small tail loss
- Low VCE Saturation Voltage

OUTLINE DRAWING

Dimensions in mm



① GATE
② COLLECTOR
③ EMITTER
④ COLLECTOR

TO-3PL

APPLICATION

Microwave oven, Electromagnetic cooking devices, Rice-cookers

MAXIMUM RATINGS (Tc= 25°C)

Symbol	Parameter	Conditions	Ratings	Unit
VCES	Collector-Emitter Voltage	VGE = 0V	900	V
VGES	Gate-Emitter Voltage		±25	V
VGEM	Peak Gate-Emitter Voltage		±30	V
IC	Collector Current		60	A
ICM	Collector Current (Pulse)		120	A
IE	Emitter Current		40	A
PC	Maximum Power Dissipation		180	W
Tj	Junction Temperature		-40 ~ +150	°C
Tstg	Storage Temperature		-40 ~ +150	°C

ELECTRICAL CHARACTERISTICS (Tch = 25°C)

Symbol	Parameter	Test conditions	Limits			Unit
			Min.	Typ.	Max.	
ICES	Collector cutoff current	VCE = 900V, VGE = 0V	—	—	1.0	mA
IGES	Gate leakage current	VGE = ±20V, VCE = 0V	—	—	0.5	μA
VGE(th)	Gate-emitter threshold voltage	VCE = 10V, IC = 6mA	2.0	4.0	6.0	V
VCE(sat)	Collector-emitter saturation voltage	IC = 60A, VCE = 15V	—	2.1	2.7	V
Cies	Input capacitance	VCE = 25V, VGE = 0V, f = 1MHz	—	4400	—	pF
Coes	Output capacitance		—	115	—	pF
Cres	Reverse transfer capacitance		—	75	—	pF
td(on)	Turn-on delay time	VCC = 300V, IC = 60A, VGE = 15V, RG = 10Ω	—	0.05	—	μs
tr	Turn-on rise time		—	0.1	—	μs
td(off)	Turn-off delay time		—	0.2	—	μs
tf	Turn-off fall time		—	0.2	—	μs
Etail	Tail loss	ICP = 60A, Tj = 125°C, dv/dt = 200V/μs		0.6	1.0	mJ/pls
Itail	Tail current			8	12	A
VEC	Emitter-collector voltage	IE = 60A, VGE = 0V	—	2.2	3.0	V
trr	Diode reverse recovery time	IE = 60A, dis/dt = -20A/μs	—	0.5	2.0	μs
Rth(j-c)	Thermal resistance (IGBT)	Junction to case	—	—	0.69	°C/W
Rth(j-c)	Thermal resistance (Diode)	Junction to case	—	—	4.0	°C/w

IR2110/IR2113

HIGH AND LOW SIDE DRIVER

Features

- Floating channel designed for bootstrap operation
Fully operational to +500V or +600V
Tolerant to negative transient voltage
dV/dt immune
- Gate drive supply range from 10 to 20V
- Undervoltage lockout for both channels
- 3.3V logic compatible
Separate logic supply range from 3.3V to 20V
Logic and power ground $\pm 5V$ offset
- CMOS Schmitt-triggered inputs with pull-down
- Cycle by cycle edge-triggered shutdown logic
- Matched propagation delay for both channels
- Outputs in phase with inputs

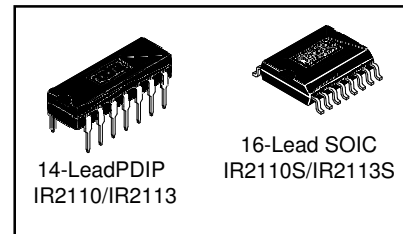
Product Summary

V_{OFFSET} (IR2110)	500V max.
(IR2113)	600V
max. I _O +/-	2A / 2A
V_{OUT}	10 - 20V
t _{on/off} (typ.)	120 & 94
nsDelayMatching(IR2110)	10 ns max.
(IR2113)	20 ns max.

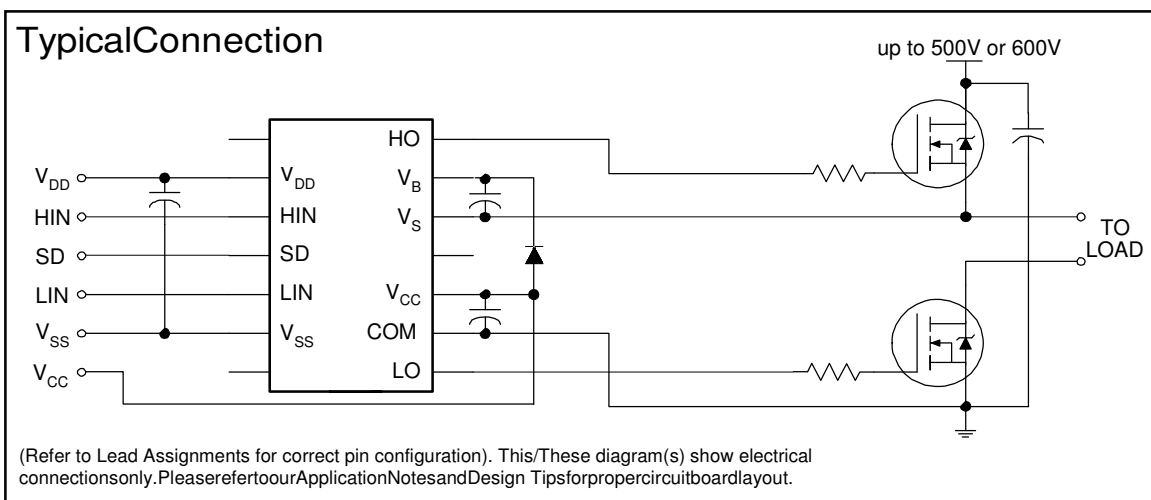
Description

The IR2110/IR2113 are high voltage, high speed power MOSFET and IGBT drivers with independent high and low side referenced output channels. Proprietary HVIC and latch immune CMOS technologies enable ruggedized monolithic construction. Logic inputs are compatible with standard CMOS or LSTTL output, down to 3.3V logic. The output drivers feature a high pulse current buffer stage designed for minimum driver cross-conduction. Propagation delays are matched to simplify use in high frequency applications. The floating channel can be used to drive an N-channel power MOSFET or IGBT in the high side configuration which operates up to 500 or 600 volts.

Packages



Typical Connection



Absolute Maximum Ratings

Absolute maximum ratings indicate sustained limits beyond which damage to the device may occur. All voltage parameters are absolute voltages referenced to COM. The thermal resistance and power dissipation ratings are measured under board mounted and still air conditions. Additional information is shown in Figures 28 through 35.

Symbol	Definition	Min.	Max.	Unit	
V _B	High side floating supply voltage (IR2110)	-0.3	525	V	
	(IR2113)	-0.3	625		
V _S	High side floating supply offset voltage	V _B - 25	V _B + 0.3		
V _{HO}	High side floating output voltage	V _S - 0.3	V _B + 0.3		
V _{CC}	Low side fixed supply voltage	-0.3	25		
V _{LO}	Low side output voltage	-0.3	V _{CC} + 0.3		
V _{DD}	Logic supply voltage	-0.3	V _{SS} + 25		
V _{SS}	Logic supply offset voltage	V _{CC} - 25	V _{CC} + 0.3		
V _{IN}	Logic input voltage (HIN, LIN & SD)	V _{SS} - 0.3	V _{DD} + 0.3		
dV _S /	Allowable offset supply voltage transient (figure 2)	—	50		V/ns
P _D	Package power dissipation @ T _A ≤ +25°C	(14 lead DIP)	—	1.6	W
		(16 lead SOIC)	—	1.25	
R _{THJA}	Thermal resistance, junction to ambient	(14 lead DIP)	—	75	°C/W
		(16 lead SOIC)	—	100	
T _J	Junction temperature	—	150	°C	
T _S	Storage temperature	-55	150		
T _L	Lead temperature (soldering, 10 seconds)	—	300		

Recommended Operating Conditions

The input/output logic timing diagram is shown in figure 1. For proper operation the device should be used within the recommended conditions. The V_S and V_{SS} offset ratings are tested with all supplies biased at 15V differential. Typical ratings at other bias conditions are shown in figures 36 and 37.

Symb	Definition	Min.	Max.	Unit	
V _B	High side floating supply absolute voltage	V _S + 10	V _S + 20	V	
V _S	High side floating supply offset voltage	(IR2110)	Note 1		500
		(IR2113)	Note 1		600
V _{HO}	High side floating output voltage	V _S	V _B		
V _{CC}	Low side fixed supply voltage	10	20		
V _{LO}	Low side output voltage	0	V _{CC}		
V _{DD}	Logic supply voltage	V _{SS} + 3	V _{SS} + 20		
V _{SS}	Logic supply offset voltage	-5 (Note 2)	5		
V _{IN}	Logic input voltage (HIN, LIN & SD)	V _{SS}	V _{DD}		
T _A	Ambient temperature	-40	125		°C

Note 1: Logic operational for V_S of -4 to +500V. Logic state held for V_S of -4V to -V_Bs. (Please refer to the Design Tip DT97-3 for more details).

Note 2: When V_{DD} < 5V, the minimum V_{SS} offset is limited to -V_{DD}.

Dynamic Electrical Characteristics

V_{BIAS} (V_{CC}, V_{BS}, V_{DD}) = 15V, C_L = 1000 pF, T_A = 25°C and V_{SS} = COM unless otherwise specified. The dynamic electrical characteristics are measured using the test circuit shown in Figure 3.

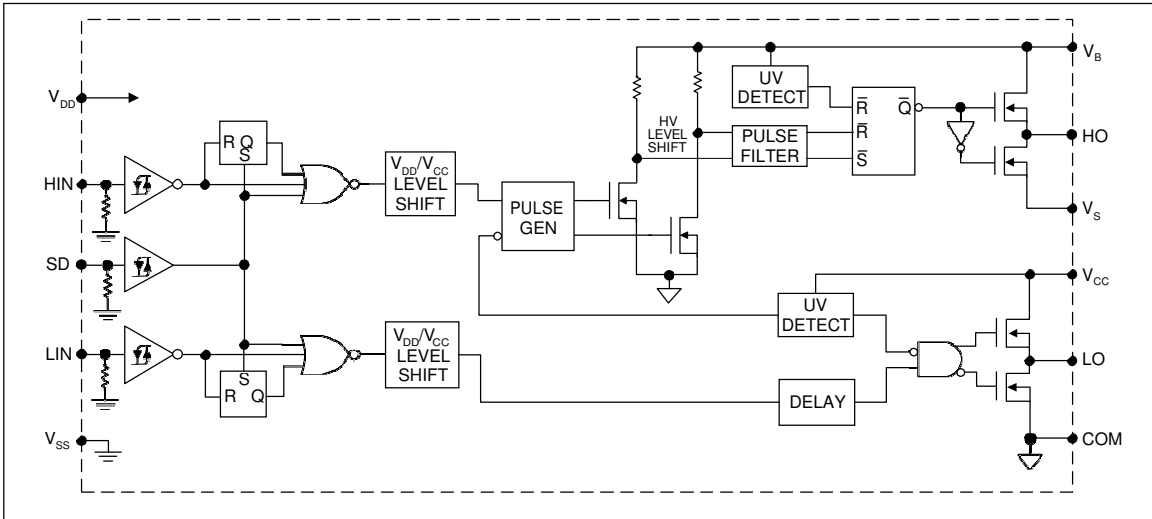
Symbol	Definition	Figure	Min.	Typ.	Max.	Units	Test Conditions
t _{on}	Turn-on propagation delay	7	—	120	150	ns	V _S = 0V
t _{off}	Turn-off propagation delay	8	—	94	125		V _S = 500V/600V
t _{sd}	Shutdown propagation delay	9	—	110	140		V _S = 500V/600V
t _r	Turn-on rise time	10	—	25	35		
t _f	Turn-off fall time	11	—	17	25		
MT	Delay matching, HS & LS turn-on/off	(IR2110) (IR2113)	—	—	—		10 20

Static Electrical Characteristics

V_{BIAS} (V_{CC}, V_{BS}, V_{DD}) = 15V, T_A = 25°C and V_{SS} = COM unless otherwise specified. The V_{IN}, V_{TH} and I_{IN} parameters are referenced to V_{SS} and are applicable to all three logic input leads: HIN, LIN and SD. The V_O and I_O parameters are referenced to COM and are applicable to the respective output leads: HO or LO.

Symbol	Definition	Figure	Min.	Typ.	Max.	Units	Test Conditions
V _{IH}	Logic "1" input voltage	12	9.5	—	—	V	
V _{IL}	Logic "0" input voltage	13	—	—	6.0		
V _{OH}	High level output voltage, V _{BIAS} - V _O	14	—	—	1.2		I _O = 0A
V _{OL}	Low level output voltage, V _O	15	—	—	0.1		I _O = 0A
I _{LK}	Offset supply leakage current	16	—	—	50	μA	V _B =V _S = 500V/600V
I _{QBS}	Quiescent V _{BS} supply current	17	—	125	230		V _{IN} = 0V or V _{DD}
I _{QCC}	Quiescent V _{CC} supply current	18	—	180	340		V _{IN} = 0V or V _{DD}
I _{QDD}	Quiescent V _{DD} supply current	19	—	15	30		V _{IN} = 0V or V _{DD}
I _{IN+}	Logic "1" input bias current	20	—	20	40		V _{IN} = V _{DD}
I _{IN-}	Logic "0" input bias current	21	—	—	1.0	V _{IN} = 0V	
V _{BSUV+}	V _{BS} supply undervoltage positive going threshold	22	7.5	8.6	9.7	V	
V _{BSUV-}	V _{BS} supply undervoltage negative going threshold	23	7.0	8.2	9.4		
V _{CCUV+}	V _{CC} supply undervoltage positive going threshold	24	7.4	8.5	9.6		
V _{CCUV-}	V _{CC} supply undervoltage negative going threshold	25	7.0	8.2	9.4		
I _{O+}	Output high short circuit pulsed current	26	2.0	2.5	—	A	V _O = 0V, V _{IN} = V _{DD} PW ≤ 10 μs
I _{O-}	Output low short circuit pulsed current	27	2.0	2.5	—		V _O = 15V, V _{IN} = 0V PW ≤ 10 μs

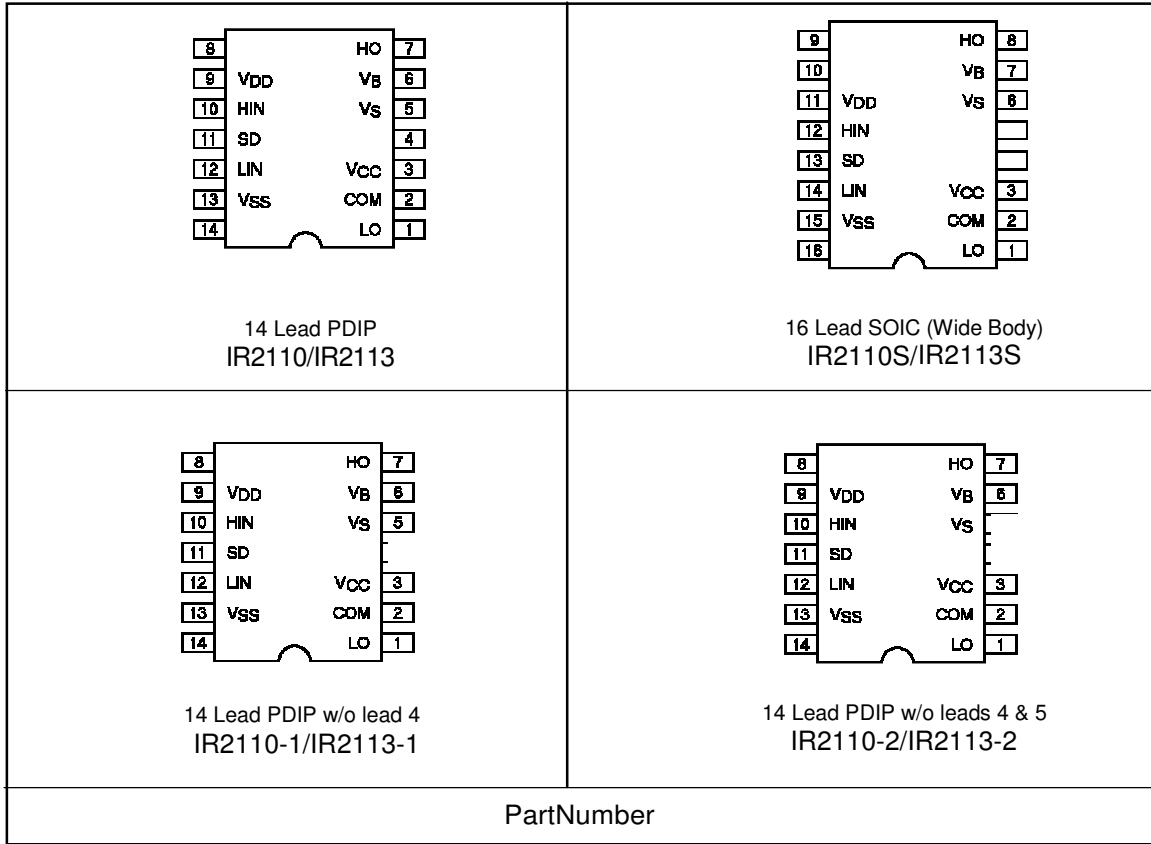
Functional Block Diagram



Lead Definitions

Symbol	Description
V _{DD}	Logic supply
HIN	Logic input for high side gate driver output (HO), in phase
SD	Logic input for shutdown
LIN	Logic input for low side gate driver output (LO), in phase
V _{SS}	Logic ground
V _B	High side floating supply
HO	High side gate drive output
V _S	High side floating supply return
V _{CC}	Low side supply
LO	Low side gate drive output
COM	Low side return

LeadAssignments



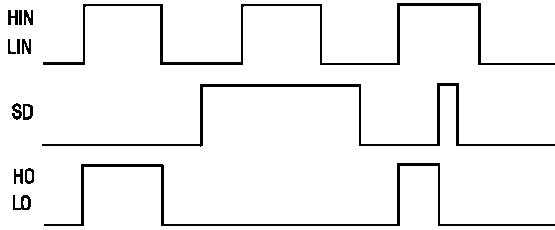


Figure 1. Input/Output Timing Diagram

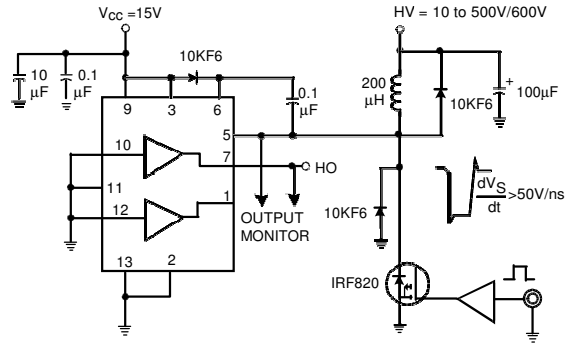


Figure 2. Floating Supply Voltage Transient Test Circuit

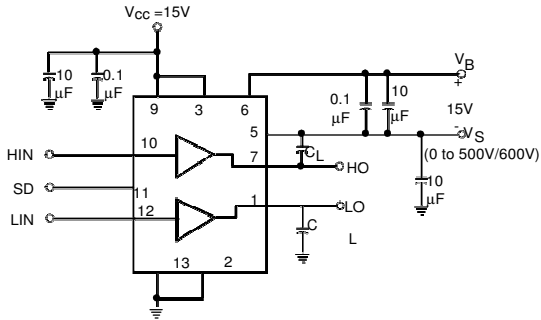


Figure 3. Switching Time Test Circuit

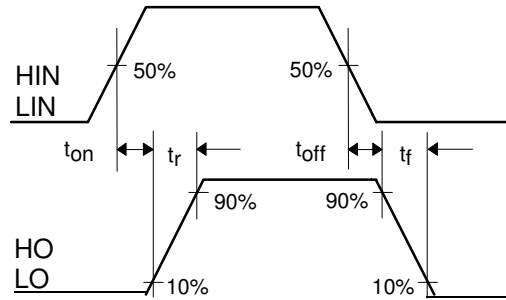


Figure 4. Switching Time Waveform Definition

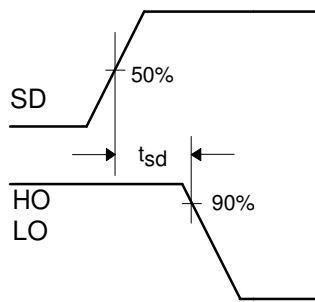


Figure 5. Shutdown Waveform Definitions

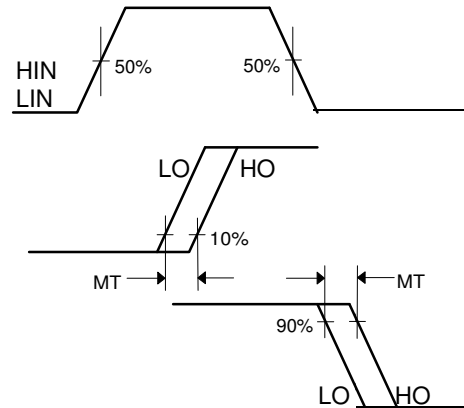


Figure 6. Delay Matching Waveform Definitions

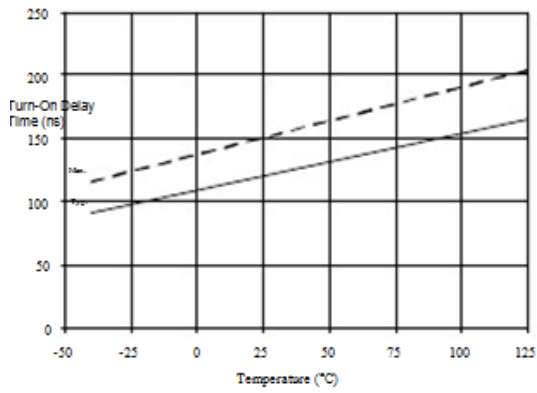


Figure 7A. Turn-On Time vs. Temperature

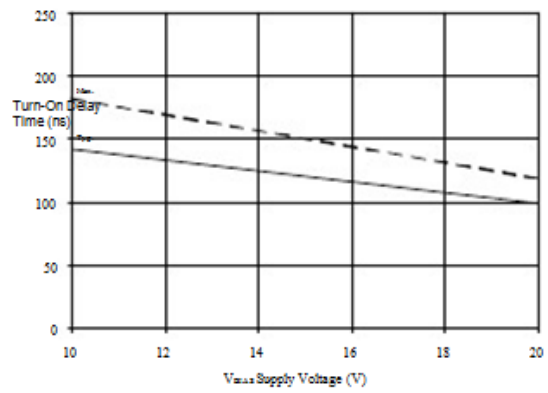


Figure 7B. Turn-On Time vs. Voltage

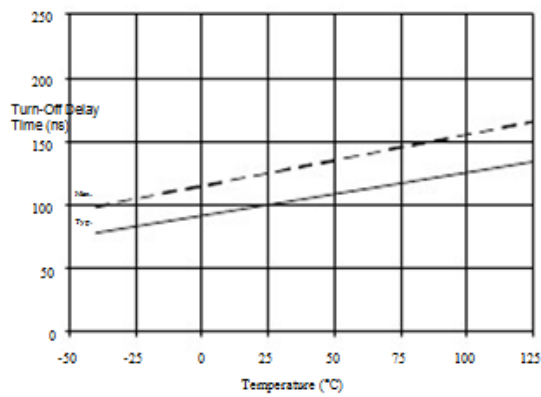


Figure 8A. Turn-Off Time vs. Temperature

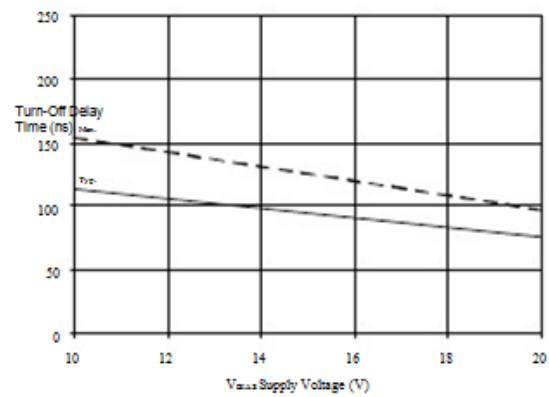


Figure 8B. Turn-Off Time vs. Voltage

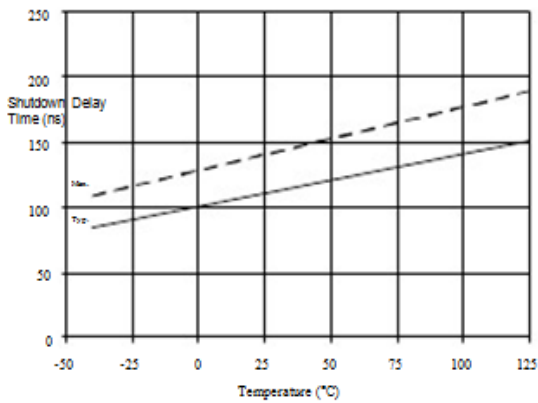


Figure 9A. Shutdown Time vs. Temperature

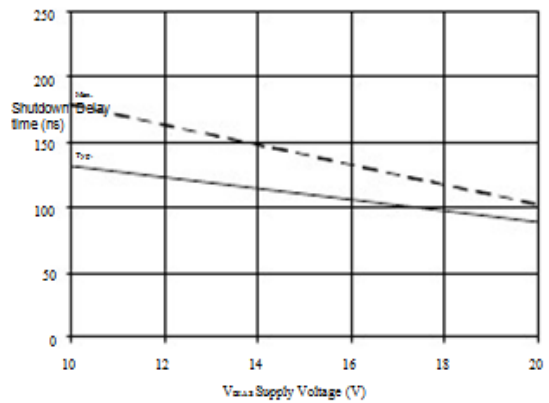


Figure 9B. Shutdown Time vs. Voltage

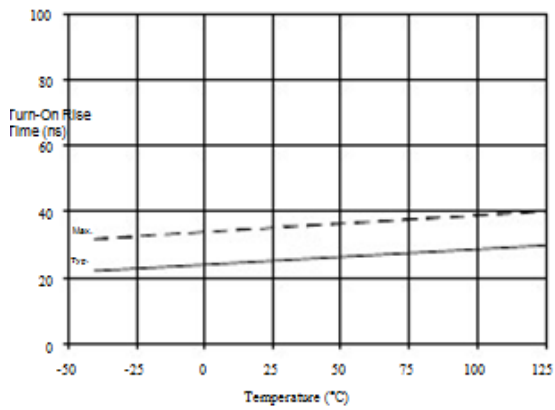


Figure 10A. Turn-On Rise Time vs. Temperature

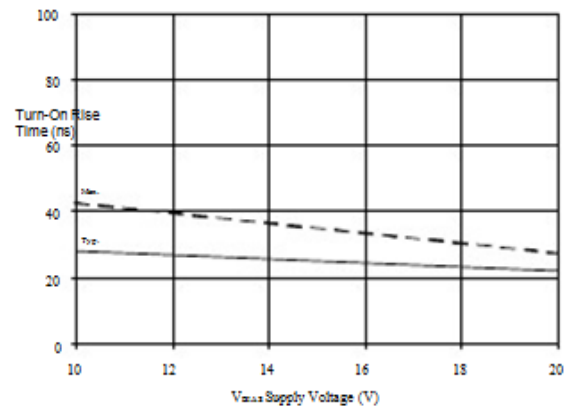


Figure 10B. Turn-On Rise Time vs. Voltage

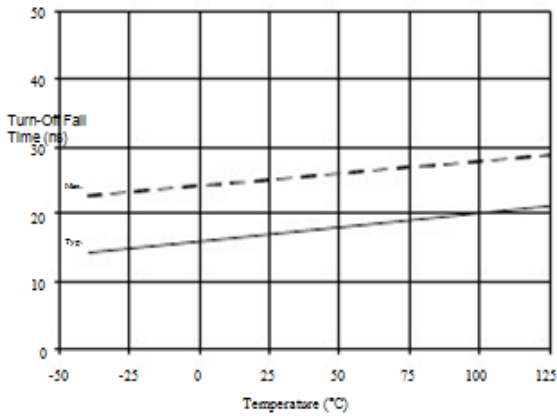


Figure 11A. Turn-Off Fall Time vs. Temperature

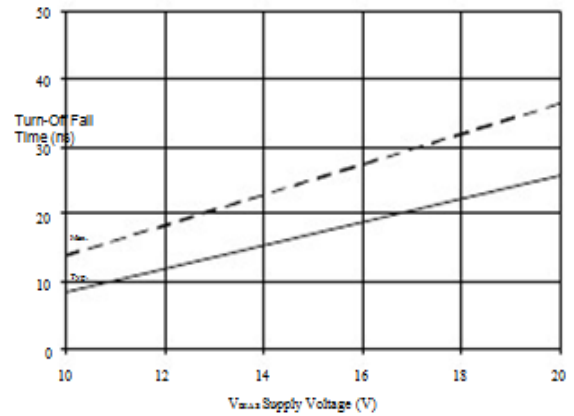


Figure 11B. Turn-Off Fall Time vs. Voltage

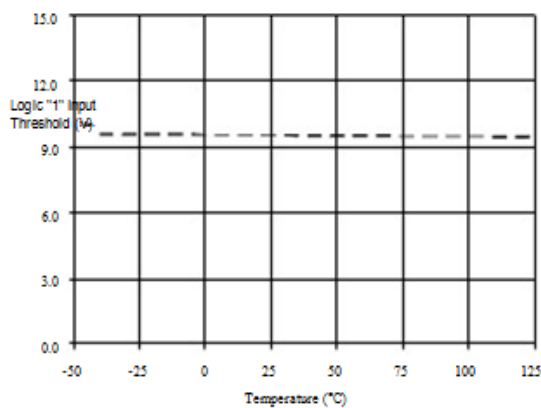


Figure 12A. Logic "1" Input Threshold vs. Temperature

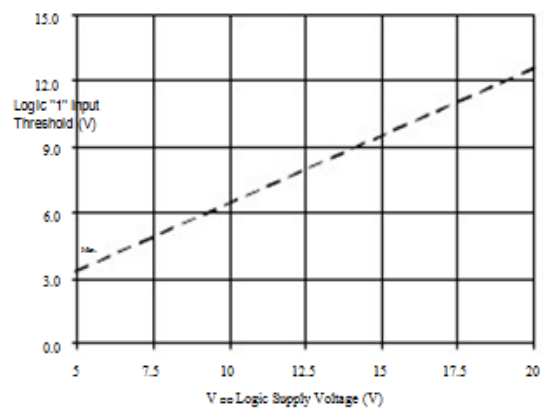


Figure 12B. Logic "1" Input Threshold vs. Voltage

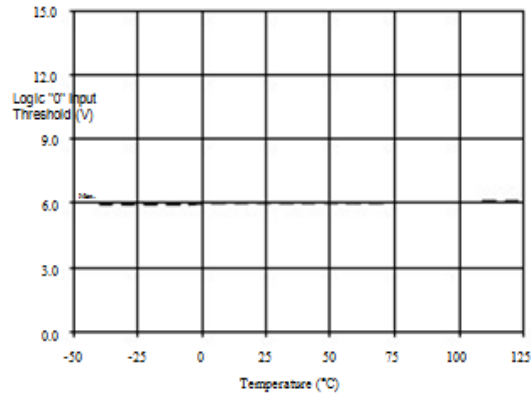


Figure 13A. Logic "0" Input Threshold vs. Temperature

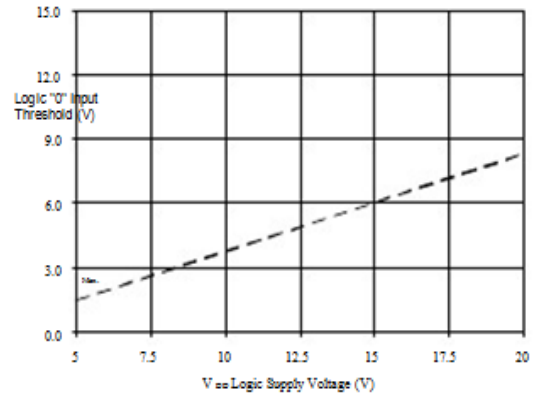


Figure 13B. Logic "0" Input Threshold vs. Voltage

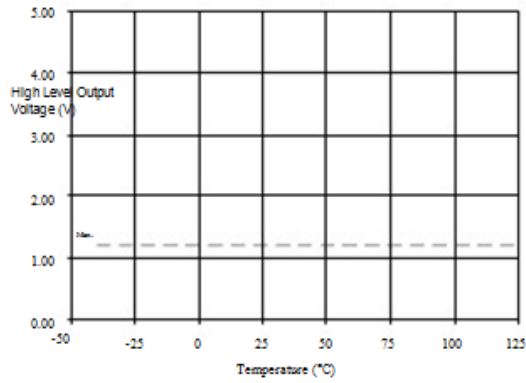


Figure 14A. High Level Output vs. Temperature

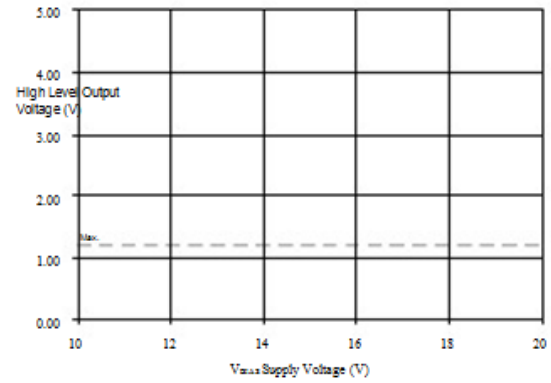


Figure 14B. High Level Output vs. Voltage

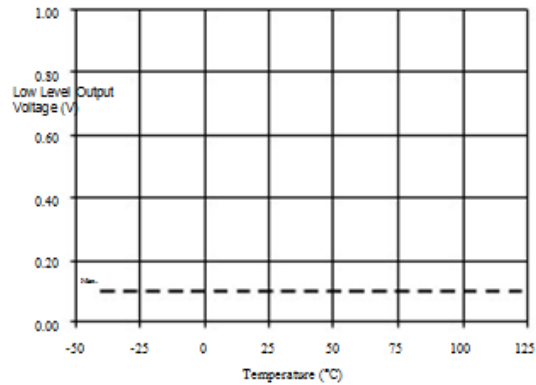


Figure 15A. Low Level Output vs. Temperature

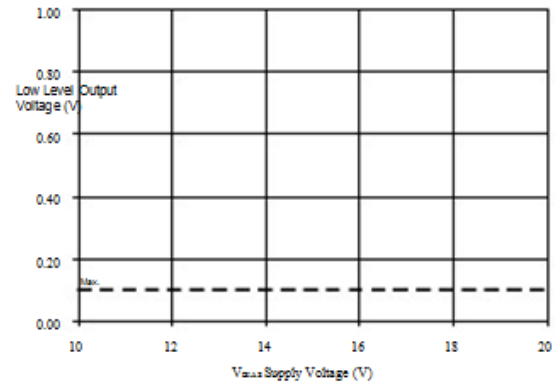


Figure 15B. Low Level Output vs. Voltage

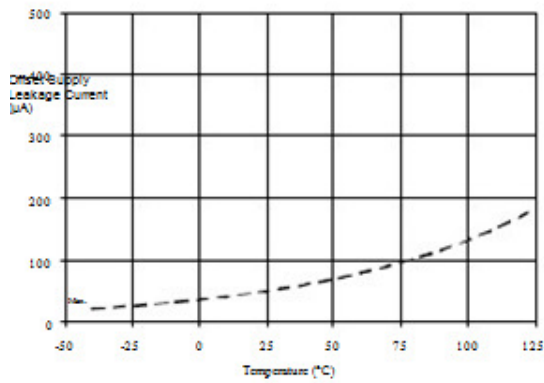


Figure 16A. Offset Supply Current vs. Temperature

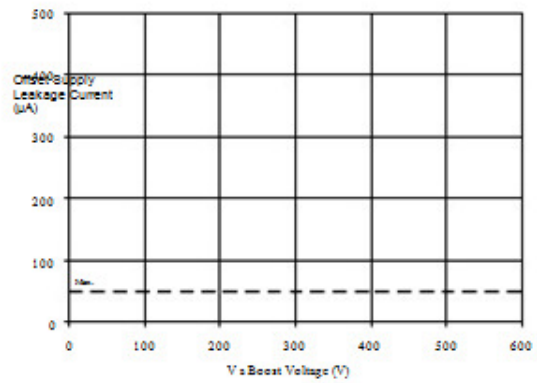


Figure 16B. Offset Supply Current vs. Voltage

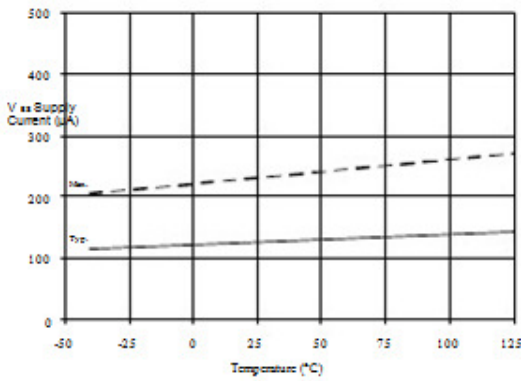


Figure 17A. VBS Supply Current vs. Temperature

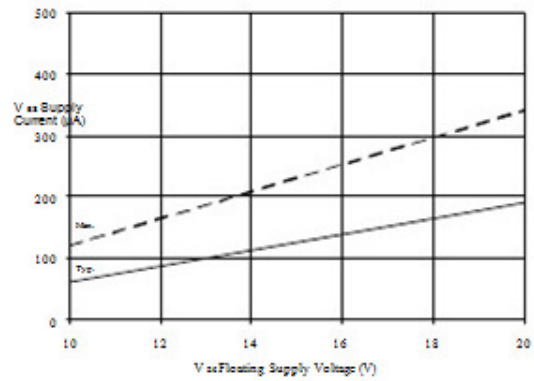


Figure 17B. VBS Supply Current vs. Voltage

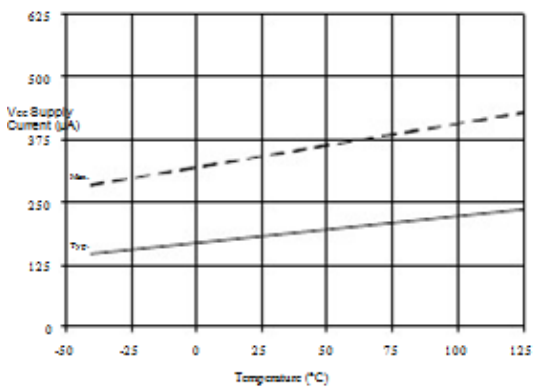


Figure 18A. VCC Supply Current vs. Temperature

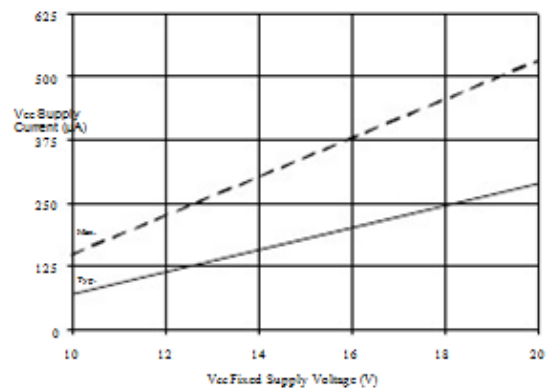


Figure 18B. V_{CC} Supply Current vs. Voltage

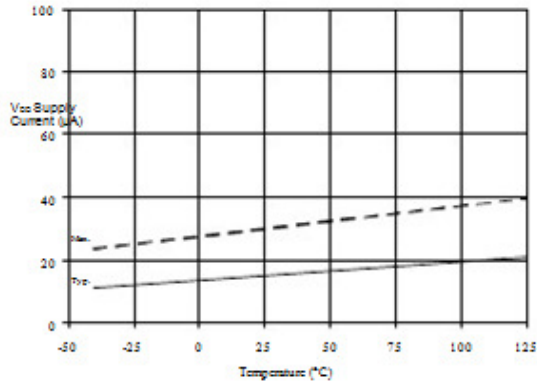


Figure 19A. VDD Supply Current vs. Temperature

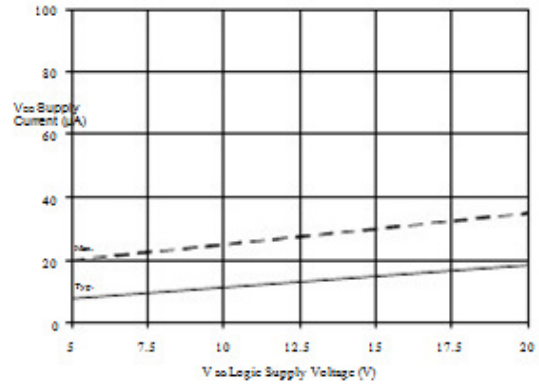


Figure 19B. VDD Supply Current vs. Voltage

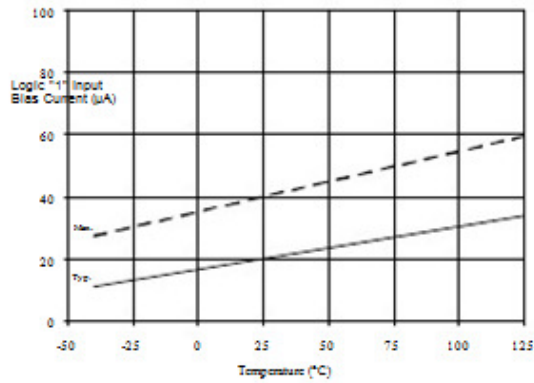


Figure 20A. Logic "1" Input Current vs. Temperature

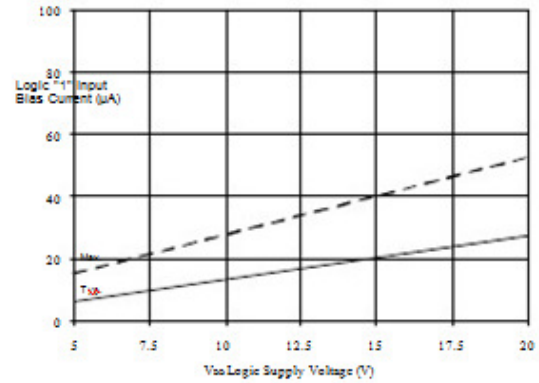


Figure 20B. Logic "1" Input Current vs. Voltage

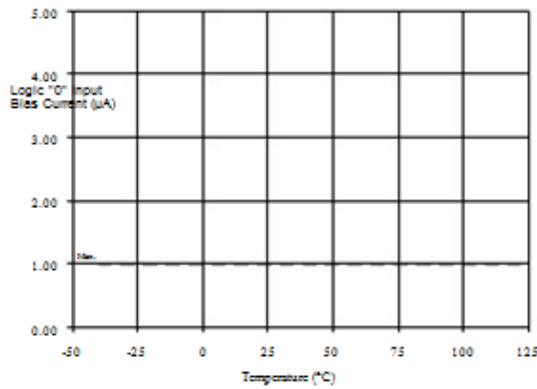


Figure 21A. Logic "0" Input Current vs. Temperature

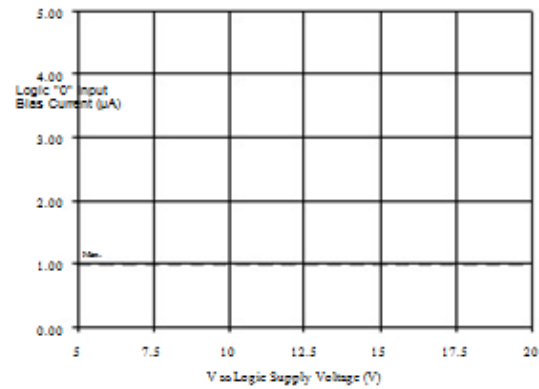


Figure 21B. Logic "0" Input Current vs. Voltage

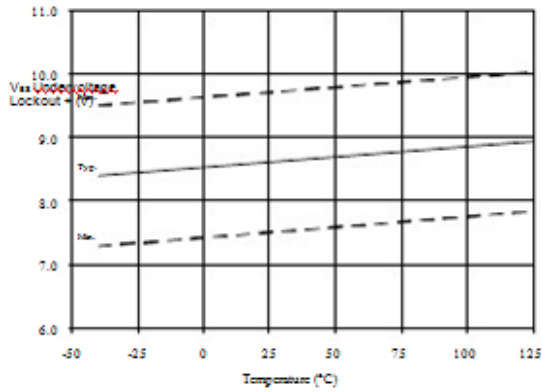


Figure 22. VBS Undervoltage (+) vs. Temperature

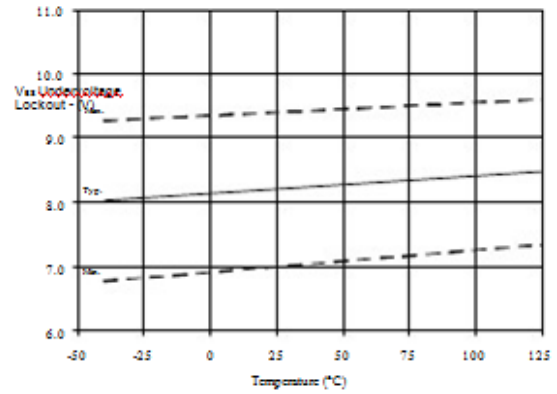


Figure 23. VBS Undervoltage (-) vs. Temperature

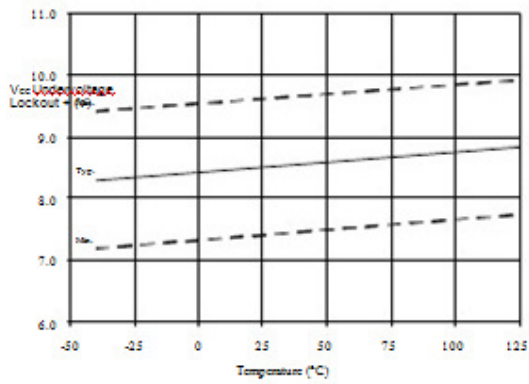


Figure 24. VCC Undervoltage (+) vs. Temperature

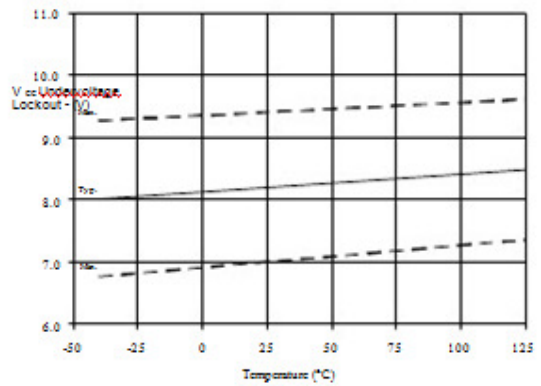


Figure 25. VCC Undervoltage (-) vs. Temperature

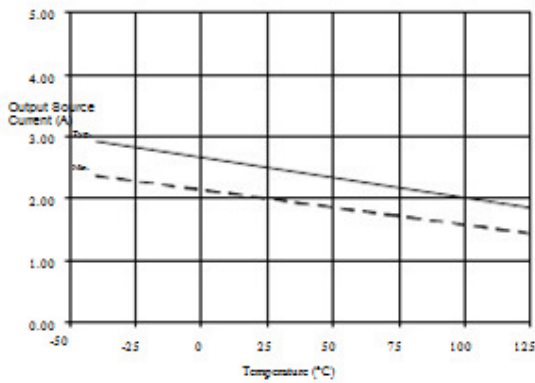


Figure 26A. Output Source Current vs. Temperature

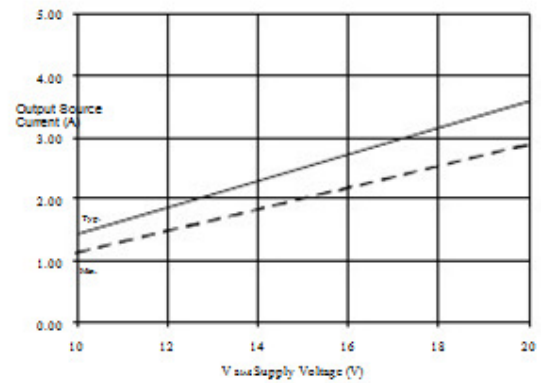


Figure 26B. Output Source Current vs. Voltage

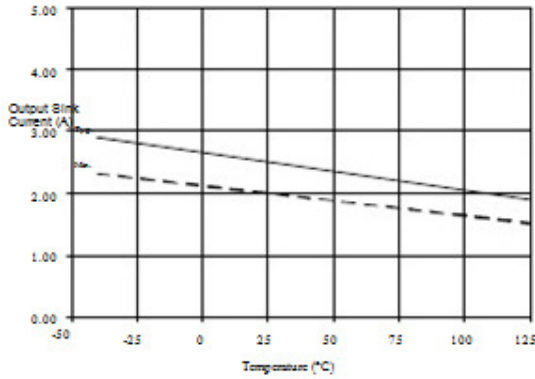


Figure 27A. Output Sink Current vs. Temperature

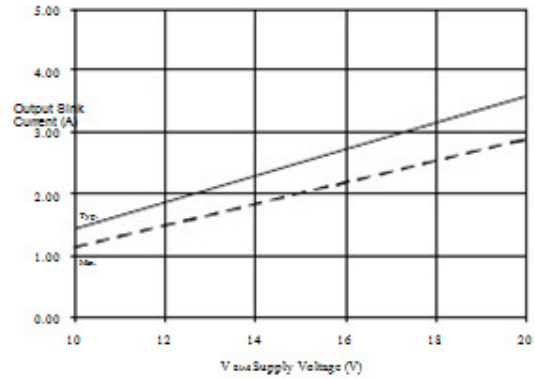


Figure 27B. Output Sink Current vs. Voltage

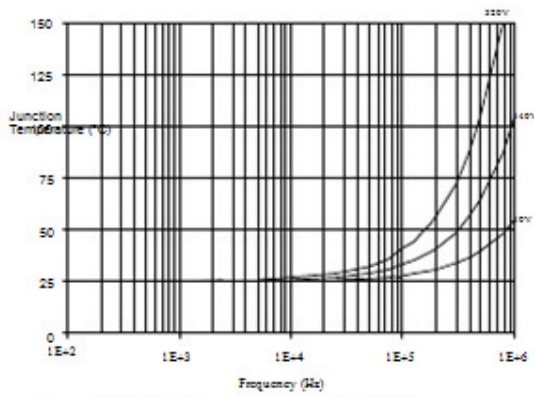


Figure 28. IR2113 TJ vs. Frequency (IRFBC20)
RGATE = 33Ω, VCC = 15V&

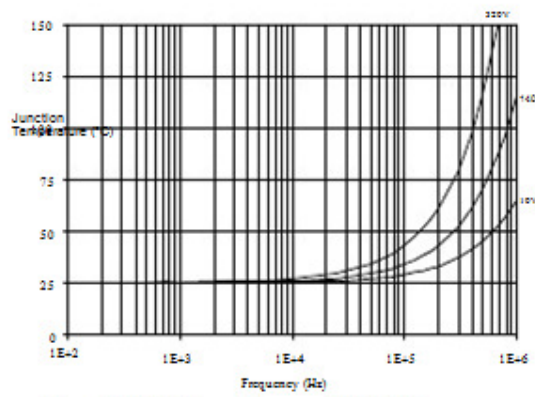


Figure 29. IR2113 TJ vs. Frequency (IRFBC30)
RGATE = 22Ω, VCC = 15V&

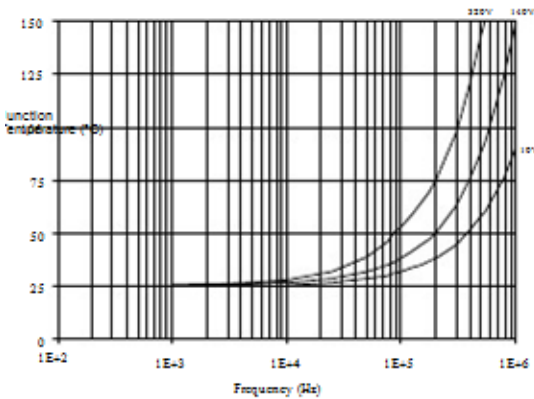


Figure 30. IR2113 TJ vs. Frequency (IRFBC40)
RGATE = 15Ω, VCC = 15V&

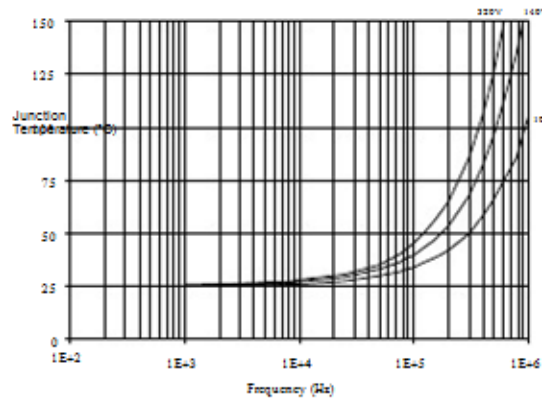


Figure 31. IR2113 TJ vs. Frequency (IRFPE50)
RGATE = 10Ω, VCC = 15V&

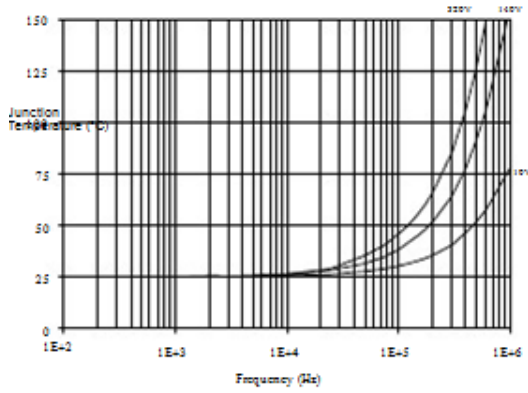


Figure 32. IR2113S TJ vs. Frequency (IRFBC20)
 RGATE = 33Ω, VCC = 15V&

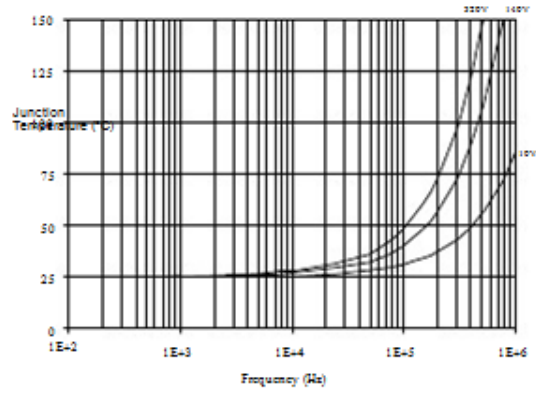


Figure 33. IR2113S TJ vs. Frequency (IRFBC30)
 RGATE = 22Ω, VCC = 15V&

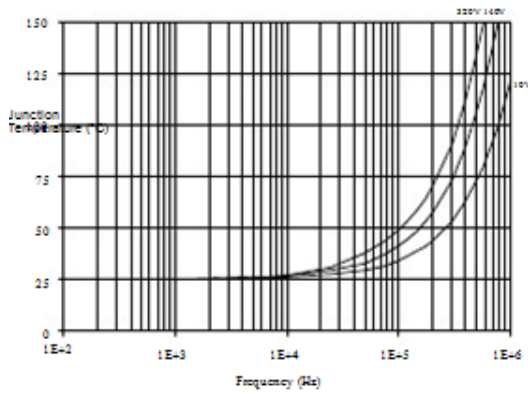


Figure 34. IR2113S TJ vs. Frequency (IRFBC40)
 RGATE = 15Ω, VCC = 15V&

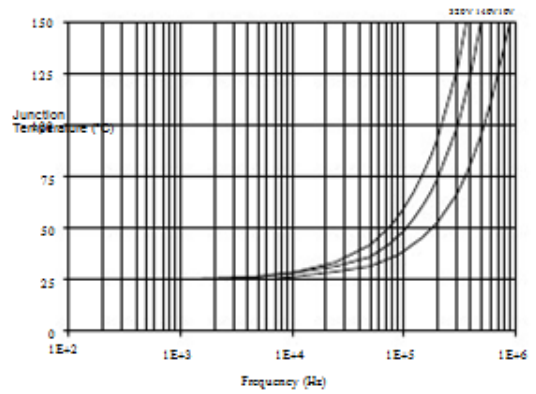


Figure 35. IR2113S TJ vs. Frequency (IRFPE50)
 RGATE = 10Ω, VCC = 15V&

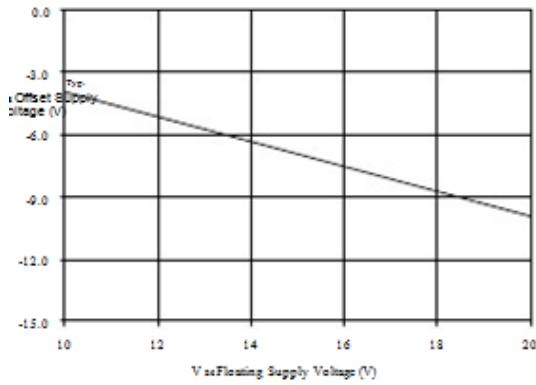


Figure 36. Maximum Vss Negative Offset vs. Vbs Supply Voltage

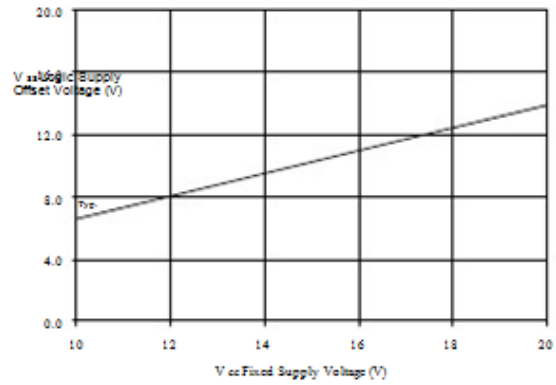
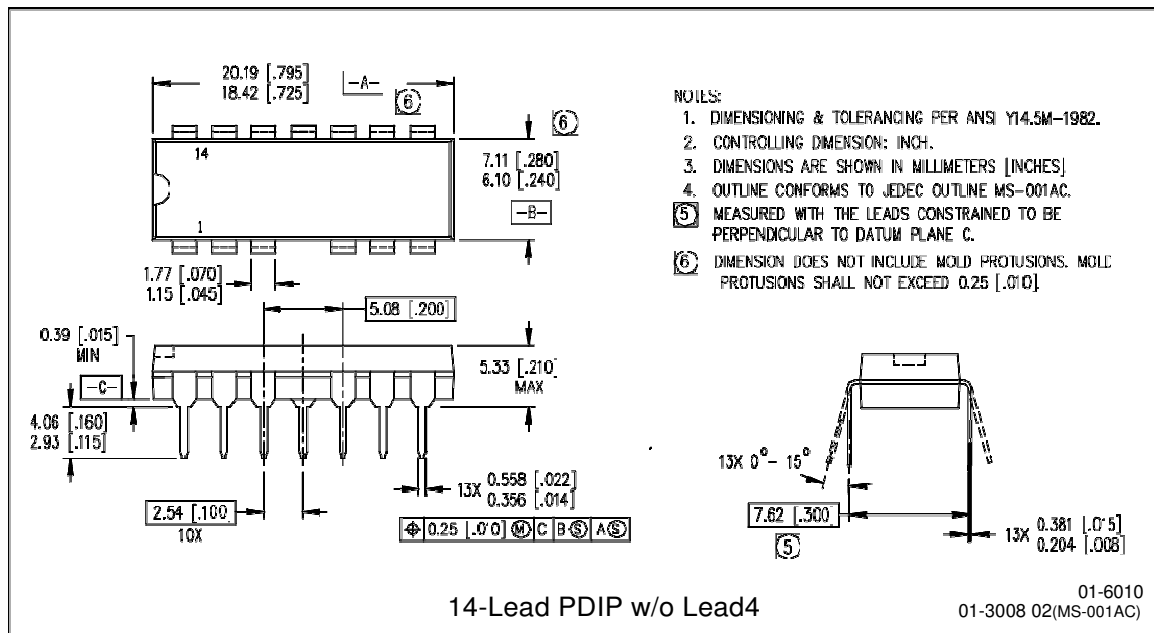
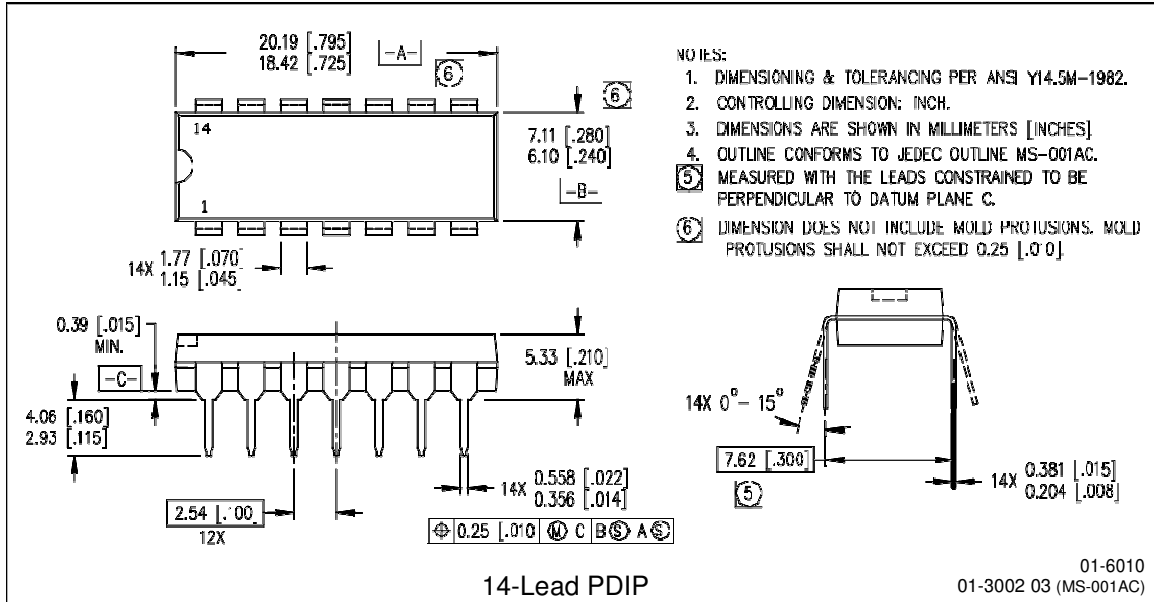
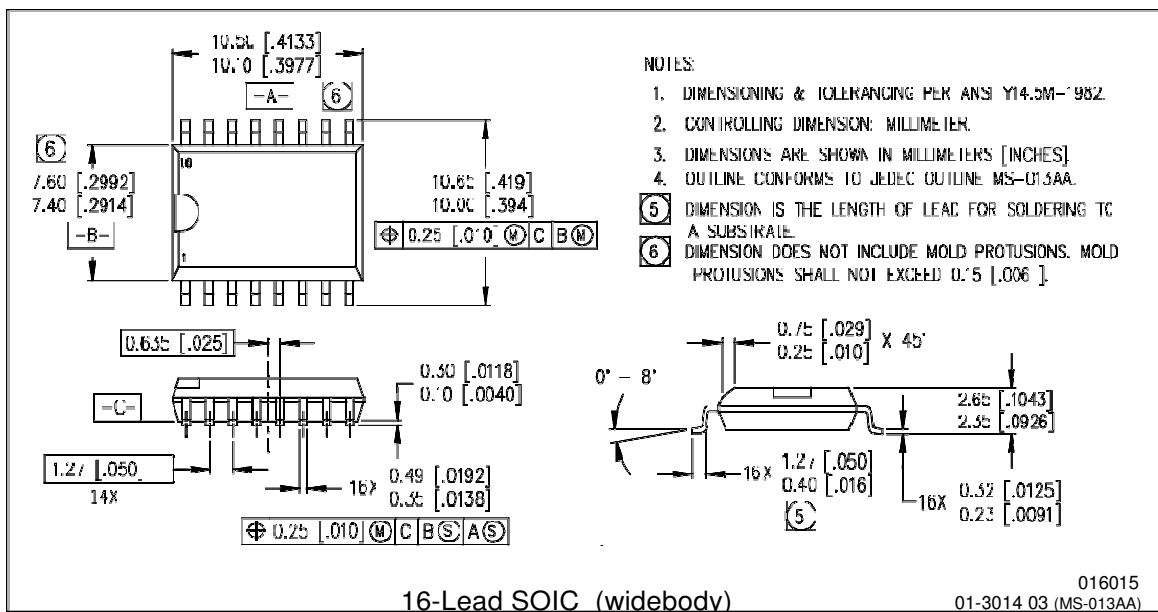
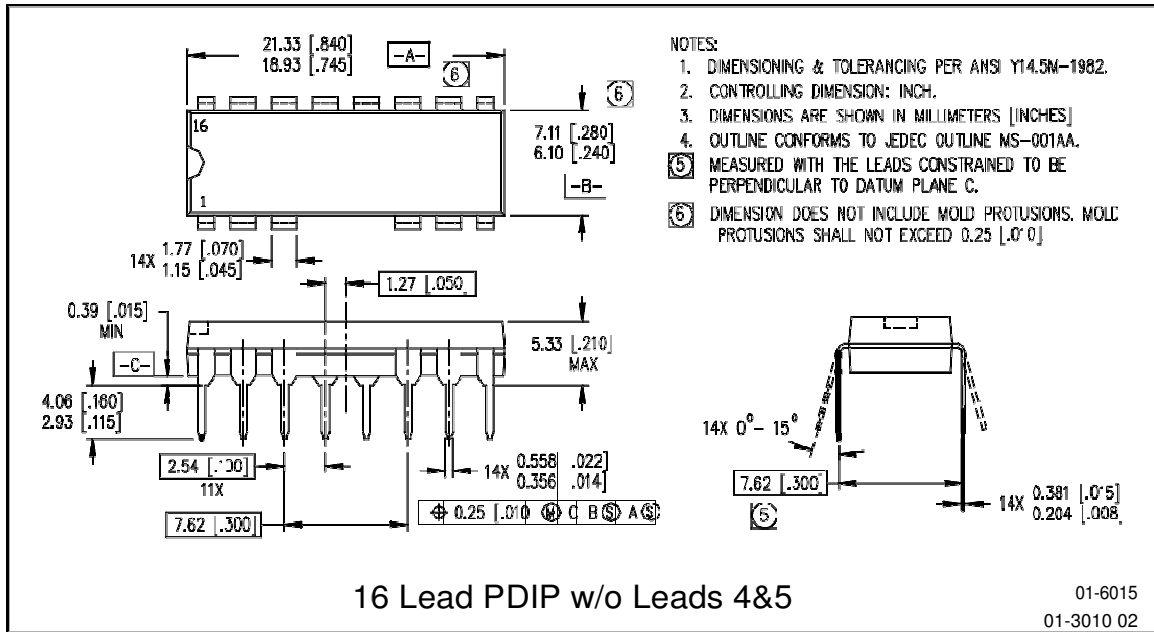


Figure 37. Maximum Vss Positive Offset vs. Vcc Supply Voltage

Case Outlines





6N137

HIGH SPEED COUPLER

6N137 INFRARED LED + PHOTO IC

The 6N137 consists of a high emitting diode and a one chip photo IC. This unit is an 8-lead DIP package.

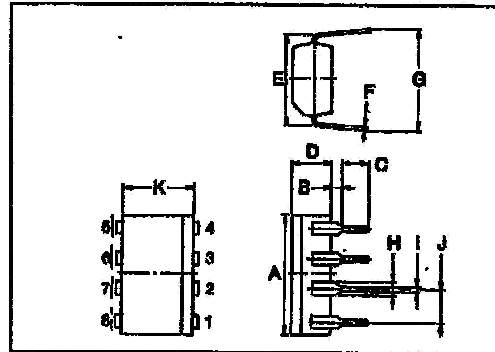
APPLICATIONS

- DIGITAL LOGIC ISOLATION
- TELE-COMMUNICATIONS
- ANALOG DATA EQUIPMENT CONTROL

FEATURES

- LSTTL/TTL compatible: 5V Supply.
- Ultra high speed; 75nS.
- Guaranteed performance over temperature.
- High isolation voltage: 2500V_{rms}.
- UL recognized.

T-41-81



1. NO CONNECTION
2. LED ANODE
3. LED CATHODE
4. NO CONNECTION
5. GND
6. OUTPUT (OPEN COLLECTOR)
7. ENABLE
8. VCC

SYMBOL	DIMENSIONS	MM
A	0.880 ± 0.010	0.66 ± 0.25
B	0.081	0.6
C	0.099 MIN	2.5 MIN
D	0.144	3.65
E	0.300	7.62 ± 0.25
F	0.098 ± 0.008	0.25 ± 0.1
G	0.309 ~ 0.348	7.85 ~ 8.90
H	0.047	1.2
I	0.020	0.5
J	0.100	2.54
K	0.282	6.4

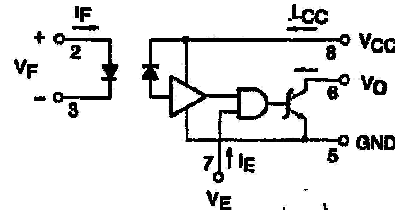
MAXIMUM RATINGS (T_a = 25°C)

CHARACTERISTIC	SYMBOL	RATING	UNIT
Forward Current	I _F	20	mA
A Pulse Forward Current (Note)	I _{FP}	40	mA
Reverse Voltage	V _R	5	V
Output Current	I _O	50	mA
Output Voltage	V _O	7	V
B Supply Voltage (1 Minute Maximum)	V _{CC}	7	V
Enable Input Voltage (Not to exceed V _{CC} by more than 500mV)	V _{EH}	5.5	V
Output Collector Power Dissipation	P _O	85	mW
Operating Temperature Range	T _{opr}	- 0 ~ 70	°C
Storage Temperature Range	T _{stg}	- 55 ~ 125	°C

Note: 50% duty cycle, 1ms pulse width.

A - LED B - DETECTOR

PIN CONFIGURATIONS (TOP VIEW)



OPTO-ELECTRICAL CHARACTERISTICS OVER RECOMMENDED TEMPERATURE (Ta = 0°C~70°C Unless otherwise noted)

CHARACTERISTIC	SYMBOL	TEST CONDITION	MIN.	TYP.*	MAX.	UNIT
High Level Output Current	IOH	VCC=5.5V, VO=5.5V IF=280μA, VE=2.0V	—	1	250	μA
Low Level Output Voltage	VOL	VCC=5.5V, IF=5mA VEH=2.0V, IOL(Sinking)=13mA	—	0.4	0.8	V
High Level Enable Current	IEH	VCC=5.5V, VE=2.0V	—	-1.0	—	mA
Low Level Enable Current	IEL	VCC=5.5V, VE=0.5V	—	-1.8	-2.0	mA
High Level Supply Current	ICCH	VCC=5.5V, IF=0, VE=0.5V	—	7	15	mA
Low Level Supply Current	ICCL	VCC=5.5V, IF=10mA, VE=0.5V	—	12	18	mA
Input-Output Insulation Leakage Current (Note)	IIO	45% Relative Humidity Ta=25°C, t=5s VIO=3000Vdc	—	—	1.0	μA
Resistance (Input-Output) (Note)	RIO	VIO=500V, Ta=25°C	—	10 ¹²	—	Ω
Capacitance (Input-Output) (Note)	CIO	f=1MHz, Ta=25°C	—	0.8	—	pF
Input Forward Voltage	VF	IF=10mA, Ta=25°C	—	1.85	1.75	V
Input Reverse Breakdown Voltage	BVR	IR=10μA, Ta=25°C	5	—	—	V
Input Capacitance	CIN	VF=0, f=1MHz	—	45	—	pF
Current Transfer Ratio	CTR	IF=5.0mA, RL=100Ω	—	1000	—	%

*All typical values are at VCC=5V, Ta=25°C.

Note: Pins 1, 2, 3 and 4 shorted together and Pins 5, 6, 7 and 8 shorted together.

SWITCHING CHARACTERISTICS (Ta = 25°C, VCC = 5V)

CHARACTERISTIC	SYMBOL	TEST CIRCUIT	TEST CONDITION	MIN.	TYP.	MAX.	UNIT
Propagation Delay Time to High Output Level	tPLH	1	RL=3500, CL=15pF IF=7.5mA	—	60	75	ns
Propagation Delay Time to Low Output Level	tPHL			—	60	75	ns
Output Rise-Fall Time (10-90%)	tr, tf	—	—	—	30	—	ns
Propagation Delay Time of Enable from VEH to VEL	tELH	2	RL=3500, CL=15pF IF=7.5mA, VEH=3.0V VEL=0.5V	—	25	—	ns
Propagation Delay Time of Enable from VEL to VEH	tEHL			—	25	—	ns
Common Mode Transient Immunity at Logic High Output Level	CMH	3	VCM=10V, RL=3500 VO(min.)=2V, IF=0mA	—	200	—	Vps
Common Mode Transient Immunity at Logic Low Output Level	CML		VCM=10V, RL=3500 VO(max.)=0.6V, IF=5mA	—	-500	—	Vps

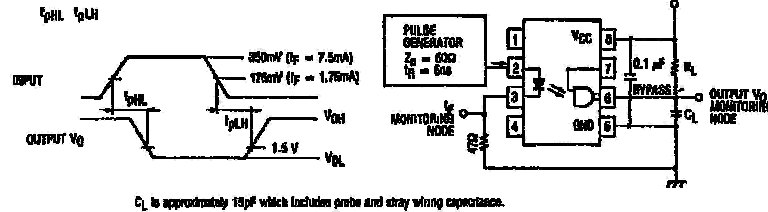
RECOMMENDED OPERATING CONDITIONS

CHARACTERISTIC	SYMBOL	MIN.	MAX.	UNIT
Input Current, Low Level Each Channel	I_{pL}	0	250	μA
Input Current, High Level Each Channel	I_{pH}	7	20	mA
High Level Enable Voltage	V_{EH}	2.0	V_{CC}	V
Low Level Enable Voltage (Output High)	V_{EL}	0	0.8	V
Supply Voltage, Output	V_{CC}	4.5	6.5	V
Fan Out (TTL Load)	N	—	8	
Operating Temperature	T_{opr}	0	70	$^{\circ}\text{C}$

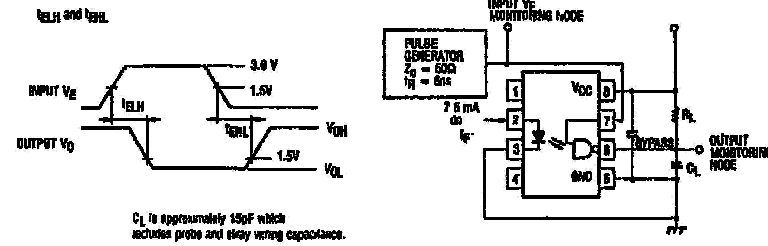
TRUTH TABLE

INPUT	ENABLE	OUTPUT
H	H	L
L	H	H
H	L	H
L	L	H

TEST CIRCUIT 1.

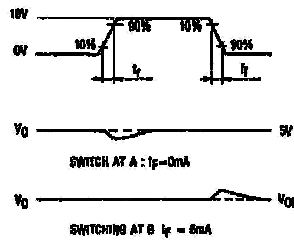


TEST CIRCUIT 2.

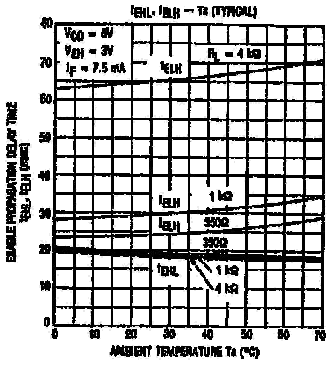
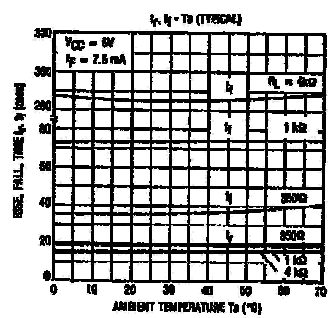
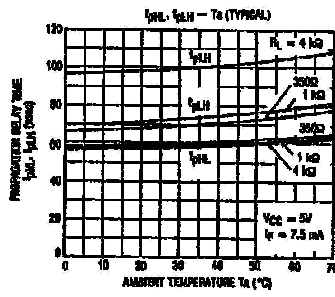
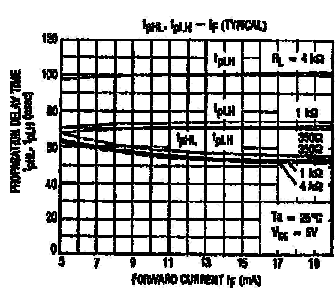
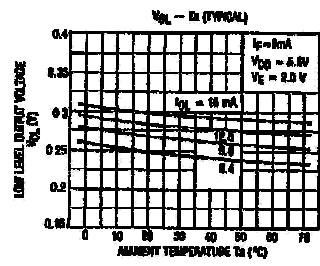
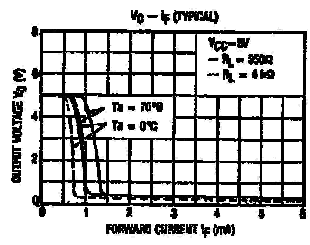
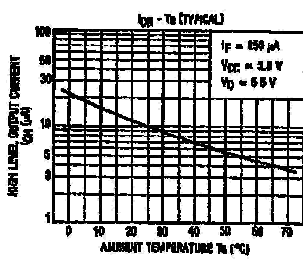
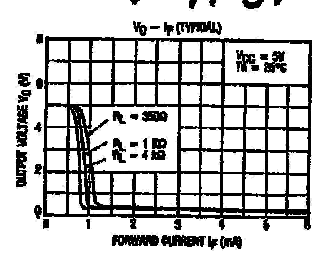
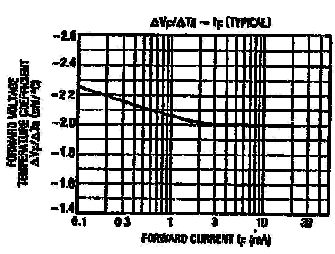
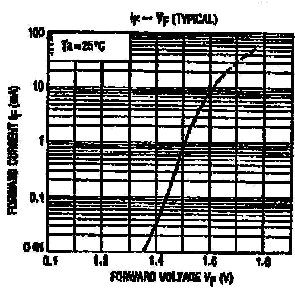


TEST CIRCUIT 3.

Transient Immunity and Typical Waveforms



T-41-81



Investigation on Transformation of Carbon Black to Carbon Nanotube using Arc Discharge Method

THESIS

Submitted in the partial fulfillment
of the requirements for the degree of

DOCTOR OF PHILOSOPHY

by

NEHA ARORA
[2012PHXF423P]

Under the Supervision of

PROF. NITI NIPUN SHARMA
Department of Mechanical Engineering
School of Automobile, Mechanical & Mechatronics Engineering
Manipal University, Jaipur – 303 007

Co- Supervision

PROF. S. S. ISLAM
Solid state Electronics Research Laboratory
Jamia Millia Islamia (A Central University), New Delhi – 110 025



BITS Pilani
Pilani | Dubai | Goa | Hyderabad

BIRLA INSTITUTE OF TECHNOLOGY & SCIENCE
PILANI – 333 031 (RAJASTHAN) INDIA

2017

Overall Conclusion and Future Scope

6.1 Overall Conclusion

In this chapter, an insight of the research work done along with major contributions as explained in this thesis and the future scope of this research work are provided. For this purpose, a complete detail of the thesis chapter wise conclusion is explained below.

1. From literature review we studied graphite is the mostly investigated precursor in synthesis of carbon nanotubes, the other precursor such as coal, hydrocarbons, fullerene and tire powder need further understanding and investigations. Since Carbon black is less perused in literature, the investigation on transformation of CB to CNT forms interesting premises of research and investigations.
2. Comprehensive literature review including carbon nanotubes, its synthesis method, effect of various parameters such as power supply, current, voltage, frequency, catalyst, atmosphere, pressure, various carbon precursors required in formation of carbon nanotubes have been presented chronologically. Understanding on most of these verticals are still half way through to clarity and all of them presents as beckoning problem to investigation. Keeping in view the time for completion of thesis and vitality in context to contribution, we identified gaps in research and correspondingly defined scope and problem statement within the scope. As a first problem at hand, in an attempt to synthesize carbon nanotubes from carbon black arc discharge set up needs to be designed.
3. We have designed the arc discharge chamber by considering mechanical design and electrical circuit design of DC and pulsed arc discharge setup for the custom built arc chamber in chapter 3. The objective of the design is to obtain a stable arc and a constant arc current across the electrode. With this scope we investigate the amenability of conversion of different grades of CB to nanotube using DC arc discharge set up designed.

4. From various grades of carbon black we have chosen five type of carbon black grade that comes under class of furnace carbon black type. The five types of CB as carbon precursor we did 30 experiments for each carbon black grade. The experiments were done with an objective to transform CB to CNT and were conducted using DC arc discharge for an arc current of 40 A for a duration of 60 sec in argon atmosphere. After completing each experiment, the deposited material from surface of cathode was collected. Out of 30 collected samples for each grade we did analysis for three randomly selected samples for each grade of CB.
5. FESEM and TEM analysis conform the presence of MWCNTs. It was observed N330 carbon black grade gets converted to Carbon nanotubes. The possible attribution for this conversion was the presence of four adsorption sites 90% of which has been graphitic planes.
6. We report the importance of sustained constant arc temperature in the synthesis of carbon nanotubes. We found that 1400-1600°C arc temperature range is critical for nanotube formation. If the temperature is outside this range, then very few or no CNTs are observed.

We have also investigated the role of arc current variation from 22 A to 40 A with the step of 4 A with respect to time using pulse arc discharge method. It was observed that the nanoparticle merged into multilayer sheet with scattered flower type structure distributed on top layer and converted into tube like structure of different diameter at 40 A for 60 sec.

6.2 Future Scope of the Work

No research concludes with an absolute end. Several areas of synthesis of MWCNT from different grades of carbon black need better understanding so it can be improved further. Synthesis of carbon nanotube using grade of carbon black as precursor is not reported in literature. We have developed a method for conversion of carbon black grade into CNTs by DC and pulsed arc discharge method.

From the perspective of present work, the following aspects can be studied and investigated further.

1. From various grades of carbon black we have chosen five type of furnace carbon black grade for conversion of CB to CNTs from industrial aspect. The effect of other types of carbon black can be further investigated.
2. We have designed the circuit for pulsed power supply to synthesize CNT using carbon black as precursor. We were in need of a frequency varying power supply. Due to high cost involved in customizing frequency varying power supply, we conducted experiment on single frequency pulsed power supply. The effect of variation of duty cycle is a scope for improvisation by modifying the arc discharge parameters for better yield.
3. Since a large number of experimental reports have been published in the last two decades to synthesize CNTs, this field still needs further experiments and theoretical investigations to establish a correlation between various synthesis parameters and nucleation of carbon nanotubes and help us better understand the growth mechanism of carbon nanotubes.
4. It is an effort towards understanding of maintaining constant temperature rather than constant current in arc discharge will yield to pathway for further advancement in the methodology of phase transformation of CB to MWCNTs. There is wide scope of application of CNT from CB in day-to-day life due to light weight and high strength material. This provides an opportunity in innovative applications for materials such as reinforcing filler in tyres. However, in order to realize these scopes, more research is required to find the solutions to the challenges.